Faculty of Pharmaceutical, Biomedical and Veterinary Sciences
Department Biomedical Sciences

Targeting multiple myeloma through protein kinase and ferroptosis therapeutics

Multipel myeloom bestrijden met eiwitkinase en ferroptose therapieën

Emilie Logie

Thesis submitted in fulfillment of the requirements for the degree of Doctor in Biomedical Sciences at the University of Antwerp

Promotor: Prof. Dr. Wim Vanden Berghe

Laboratory of Protein Science, Proteomics and Epigenetic Signaling (PPES)
Antwerp, 2021

Disclaimer

The author allows to consult and copy parts of this work for personal use. Further reproduction or transmission in any form or by any means, without the prior permission of the author is strictly forbidden.

Composition of the PhD Examination Committee

Promotor

Prof. dr. Wim Vanden Berghe

Laboratory of Protein Science, Proteomics and Epigenetic Signaling (PPES), Department of Biomedical Sciences, University of Antwerp

Internal members

Prof. dr. Vincent Timmerman (Chair)

Peripheral Neuropathy Research Group, Department of Biomedical Sciences, University of Antwerp

Prof. dr. Guy Caljon (Member)

Laboratory of Microbiology, Parasitology and Hygiene, Department of Biomedical Sciences, University of Antwerp

External members

Prof. Dr. Sébastien Anguille (Member)

Laboratory for Experimental Hematology (LEH), Department of Hematology, University of Antwerp

Prof. Dr. Axel Imhof (Member)

Biomedical Center, Chromatin Proteomics Group, Department of Molecular Biology, Faculty of Medicine, Ludwig-Maximilians-Universität München, Germany

Prof. Dr. Esteban Ballestar (Member)

Epigenetics and Immune Disease Group, Joseph Carreras Leukemia Research Institute (IJC), Barcelona, Spain

Table of Contents

Acknowledgements

Dear reader, welcome to the acknowledgements section of this PhD work. This is, arguably, the most critical part of this thesis as most of you will only read this part (for which you are forgiven, although you will be missing out on quite some juicy data). The past four years have been an intriguing journey, where I was able to meet amazing people, develop new skills, and do a lot of self-reflection. It goes without saying that I would not be standing here today without the help of so many wonderful and talented people, who have supported me throughout my PhD.

First, my thanks go out to my promotor, **Wim Vanden Berghe**, who offered me the opportunity to start my research at PPES. Wim, I can honestly say that you have made my 4-year PhD journey more than interesting. You have supported and stimulated me to learn new skills and undergo new experiences. Whether it was through international conferences, research stays, salsa dancing, or mojito tasting, your open-mindedness was always contagious. Sometimes your ideas were rather ambitious (quite like your rum-concentrations in your homemade mojitos), but you were there to listen to any concerns or counterpropositions I had. I truly wish you the best of luck with all your future endeavors with the epigenetics lab. One tip: be more cautious when taking you PhD students out kayaking, not everyone might like to see Van Eyck paintings up close…

I would also like to thank the members of the jury, **Prof. dr. Vincent Timmerman**, **Prof. dr. Guy Caljon**, **Prof. dr. Sébastien Anguille, Prof. dr. Axel Imhof**, and **Prof. dr. Esteban Ballestar** for their useful critiques and comments throughout my research project. It is always refreshing to discuss research findings from different angles, and I am certain that our discussions have allowed me to deliver a more qualitative thesis.

Of course, I am thankful to my fellow PPES-members and -colleagues for creating such an amazing and stimulating work environment. **Zainab**, thank you for making S4 a more cheerful place and sharing my passion for crisps and other snacks. **Joey,** your laid-back and stress-free attitude has always impressed me, I really don't know how you do it (I have to admit, quite jealously)! I wish you all the best with your work in Switzerland the coming months. **Niels**, without doubt, you have contributed to one of my most precious PPES memories: our secret Santa Christmas party and your *fascinating* gift-choice. The best of luck in Spain. **Herald**, thank you so much for all your help in the lab. Whether I once again spammed you with delivery orders or had any other technical questions, you were ready to help. **Eva** and **Karen**, your passion and commitment to the students is really commendable and have made PPES one of the favorite internship- and thesis places of

BMW and BIC students. Thank you for all your help, gossip and exquisite birthday treats (your bakes were the best!).

Hanne, your motivation and knowledge is astounding, and I am really happy that you have found your way to our lab. I don't know how you're able to manage all your students at once and oversee the construction works of your house. You truly are superwoman. **Xaveer,** please be more careful on your bike! You had me worried a few times. Thanks for encouraging the PPES group to share our expertise with other research groups. It really stimulated me to start new, scientific collaborations. **Ruben,** where to even begin to express my gratitude to you. Over the years, you have become one of my closest friends with whom I could always share my geeky comments, work frustrations, and worries with. You are truly an amazing person, friend and scientist who is always able to guide students through their, sometimes chaotic, thesis internships. My sincerest thanks for your valuable friendship.

My gratitude also goes out to my epigenetics-partners in crime: **Claudio, Claudia, and Claudina**. **Claudio**, it is with great honor that I now pass the title of senior biatch to you. Carry this title proudly! I don't think I have ever met anyone who is more qualified than you to be a researcher and teaching assistant. I know that you have had to face many prejudices on your way here, but believe me when I say: you are such a talented researcher with so many skills, I have no doubt in my mind that you will achieve any goal that you might set for yourself. Regardless, I will never take any brownie or cake from you that suspiciously smells a lot like vanilla. **Claudia**, you have already had to face many hurdles during your PhD but you have demonstrated such perseverance and determination, it is admiring. Not a lot of people would be able to do what you are doing, and I really want you to remember that. You are an inspiring, clever, and funny woman and I am sure you will make it far in life. You were always there to help and you were a great conversational partner, who I will miss dearly. All the best to you and your family. Please, keep me updated about your sister's corgi story – I really want to know how it will go! **Claudina**, it is unbelievable how many things you are juggling at once. You are a researcher in two research labs (with two Vanden Berghes, nonetheless!), you mentor students, perform PamGene experiments, write research projects, supervise Cuban PPES visitors, and manage you family all at the same time. Yet, despite all of this, you were there to give me feedback and were open to scientific discussions. I have learned so much from your comments and input, and I will take them with me for the rest of my life. Thank you so much for everything. Just remember to think about yourself once in a while. To my successor and newest PPES member, **Amber**: I wish you all the strength, luck, and perseverance the coming years during your PhD. God knows you will need it! Thanks for helping me with completing some of my papers, your help has meant the world to me. The PPES group is lucky to have such a hard-working and motivated student among its ranks.

Prior PPES members have helped me considerably during my PhD too: thank you, **Stijn, Jolien, Roberta, Dietmar, Farnaz, Chandra, Marie-Louise, Daisy, Martin,** and **An**. **Evi** and **Zoë,** you are one of the reasons why I started at PPES. Your mentorship during my bachelor and master thesis really stimulated my passion for research and have encouraged my decision to go for a PhD. **Mops,** thank you for all your life advice, jokes, and memorable quotes. **Ken,** you were really a lifesaver during the first two years of my PhD. You have guided me through the PPES protocols and taught me everything I needed to know to get started. Thank you for answering all my questions, helping me with the students and preparing me for the yearly Cuban PPES invasions. I would also like to offer special thanks to **Sylvia,** who, although no longer with us, continues to inspire me and many other students she has mentored over the course of her career. Thank you for always lending a sympathetic ear when I needed it.

My gratitude goes out to my external collaborators as well. Thank you Biomina-members **Nicolas, Bart,** and **Kris** for your help with my RNAseq analysis; Histone experts **Bart** and **Maarten** for all you hard work and input during our meetings. **Desirée** and **Marianne** for learning me epigenetic editing techniques in Groningen; **Lode** for analyzing my DNA methylation samples on your uHPLC-MS/MS setup at KUL; **Priyanka** and **Annemie** from PLASMANT to help me with the molecular modeling.

I really appreciated the exotic atmosphere that our many international exchange students from Cuba, Ecuador, Thailand, and Poland brought to our lab. Thank you **Julio, Elisabeth R., Elisabeth, Ivones, José, Idania, Gilberto, Carlos, Olivia, Rene, Beatrice, Yo, Hannah, Alicya,** and **Patrycja.**

My biggest thanks also to my friends and family for all the support you have offered me these past years. **Vincent** and **Sarah,** our boardgame sessions were my favorite way of getting my mind of work and failed experiments. Although you both have extremely busy schedules, you were always prepared to help if needed. **Yannick L.** and **Lauren,** your sincere enthusiasm always puts a smile on my face, even on though days. I thoroughly enjoyed our (minigolf) double dates and can't wait to see your *foute party* outfits for next year's corona-proof edition! **Jente** and **Maarten,** I don't think I ever met a couple who is so down to earth and honest in everything they do. Although we weren't able to see each other that much due to covid, I would like to thank you, Jente, for sharing your Animal Crossing experience with me. It made the obligatory lock downs much more interesting. To my wonderful, breakfast-loving, puppy-hyping, advice-giving bridesmaids **Laura, Julie, and Anouk**: thank you for standing by me through this challenging PhD journey. You were always there to cheer me up and to listen to my frustrations (usually with a donut or two, which is always a big plus). I consider myself very lucky to have you as my supportive friend group and I happily look forward to our future adventures. **Yannick J.,** I am convinced that you underestimate the impact of your hilarious hospital stories of teen pregnancies or madmen

escape attempts on my mood and outlook on life. Please, please, please, never change who you are and continue to color the world of the people around you. **Raf**, you are one crazy son of a gun, with an imagination that can compete with Ruben's. I sincerely hope that you treat your real-life pets better than your D&D pets. Thanks for all your original jokes and memes. All the best with your new job, I am sure you will be an amazing (and entertaining) teacher.

My sincerest gratitude to my in-laws, especially **Inès, Guy,** and **Cathérine**, who have always welcomed me with open arms. Your heart-warming kindness and unfailing emotional support mean the world to me.

I also would like to deeply thank my amazing parents, who have always encouraged and supported me. Your unconditional love and interest in everything I do have raised me up, time and time again when times got challenging. **Mom,** thanks for being such a wonderful, smart, and funny role model. **Dad,** thank you for always checking in on me and my experiments. It was encouraging to know that you were always rooting for me.

To my fantastic and fearless sister, **Sofie**: thanks for always putting things into perspective. You are, without doubt, the wisest and funniest person I know and I continuously appreciate your advice. The cuddles and walks with Steve provided me with much appreciated mental breaks.

Of course, my unconditional love and thanks go out to my biggest supporter and soulmate, **Emmanuel**. I could not have wished for a more perfect life-partner. You are always there to share my worries, to alleviate my (*occasionally*) high stress levels, and to listen to my frustrations. Without doubt, I would not have been standing here today without you in my life. Nothing was ever too much for you: from reading proofs of my article manuscripts to dragging me away from my computer when I was working too much. Your unconditional trust, love, and friendship mean the world to me and I am overjoyed to spend the rest of my life with you. I love you so much. Always.

List of Abbreviations

ABC	ATP-binding cassette
ACTB	B-actin
ASCT	Autologous stem cell transplantation
ATP	Adenosine triphosphate
AZA	Aza-2'cytidine
BCR	B-cell receptor
BM	Bone marrow
BTK	Bruton tyrosine kinase
CAR-T	Chimeric antigen receptor T-cell
CRAB	hyperCalcemia, Renal impairment, Anemia, and Bone lesions
CSC	Cancer stem cell
DAC	5-aza-2'-deoxycytidine
DDA	Data-dependent acquisition
DEG	Differentially expressed gene
DEX	Dexamethasone
DMP	Differentially methylated probe
DNMT	DNA methyltransferase
DNMTi	DNA methyltransferase inhibitor
EMDR	Environment-mediated drug resistance
EMT	Epithelial-mesenchymal transition
ER	Endoplasmic reticulum
FDR	False discovery rate
FOXA1	Forkhead box A1
GC	Glucocorticoid
GPX4	Glutathione peroxidase
HDAC	Histone deacetylase
HDACi	Histone deacetylase inhibitor
HSC	Hematopoietic stem cell
IBR	Ibrutinib
Ig	Immunoglobin
IMiD	Immunomodulatory imide drug
IMWG	International Myeloma Working Group
JHDM	Jumonji domain-containing histone demethylase
LC MS/MS	Liquid chromatography with tandem mass spectrometry
lncRNA	Long non-coding RNA
LOX	Lipoxygenase
LPC	Lymphoid progenitor cell
mAb	Monoclonal antibody

MDR	Multi-drug resistance
MGUS	Monoclonal gammopathy of undetermined significance
miRNA	microRNA
MM	Multiple myeloma
Nec	Necrostatin
NGS	Next-generation sequencing
PC	Plasma cell
P-gP	P-glycoprotein
PI	Proteasome inhibitor
PKI	Protein kinase inhibitor
PTK	Tyrosine protein kinase
PTM	Post-translational modification
PUFA	Polyunsaturated fatty acid
RCD	Regulated cell death
ROS	Reactive oxygen species
SFMDR	Soluble factor mediated drug resistance
SMM	Smoldering multiple myeloma
STS	Staurosporine
STK	Serine/threonine protein kinase
TET	Ten-eleven translocase
TME	Tumor microenvironment
TK	Tyrosine kinase
WA	Withaferin A
WABI	Biotinylated Withaferin A

Summary

Multiple myeloma (MM) is a B-cell malignancy characterized by the accumulation of a clone of malignant plasma cells in the bone marrow. Despite recent advances in treatment regimens, MM remains an incurable disease with conventional therapies, such as proteasome inhibitors, immunomodulatory drugs, corticosteroids, and alkylating agents only resulting in low remission rates and limited survival times. This treatment failure of existing anti-cancer drugs can be explained by the development of (acquired) multi-drug resistance, which renders cancer cells cross-resistant to structurally and functionally unrelated drugs. Due to the multifactorial nature of the molecular mechanisms involved in acquisition of therapy resistance, it remains challenging to develop effective, curative treatments for MM. Thus, there is an urgent need to explore novel therapeutic strategies to achieve complete and persistent tumor remission in MM patients. In this PhD thesis work, we explored kinase inhibition, treatment with natural compounds, and ferroptosis induction as alternative therapy strategies to overcome MM drug resistance.

In the first part of the results section (chapter 3 and 4), we investigated whether (natural) kinase inhibitors can be used to eliminate glucocorticoid-resistant MM cells. Protein kinase signaling is often dysregulated in malignant cells and significantly contributes to the development of drug resistance. In this way, inhibition of key protein kinases orchestrating drug resistance may offer clinical benefits for MM patients.

In chapter 3, we performed phosphopeptidome kinome activity profiling of therapy-resistant and -sensitive MM cells to identify key protein kinases that regulate therapy resistance. We found that Bruton tyrosine kinase (BTK), involved in B-cell receptor signaling, is constitutively hyperactivated in resistant cells. Pharmacological inhibition of BTK by the FDA-approved inhibitor ibrutinib (IBR) and the preclinical phytochemical Withaferin A (WA) revealed that WA is more effective than IBR in killing BTK-overexpressing glucocorticoid-resistant MM cells. We further demonstrated that WA reverses BTK overexpression and inhibits BTK activity through cysteine-dependent covalent targeting.

In chapter 4, we explored the kinase activity changes taking place in ferroptotic and apoptotic MM cells. In contrast to apoptosis, ferroptosis is a mode of regulated cell death characterized by an iron dependent rise in reactive oxygen species that propagate lipid peroxidation reactions. By comparing the kinome profiles of both cell death modalities, we aimed to identify pivotal protein kinases that regulate ferroptosis- and apoptosis-specific cell death. Because multi-drug resistance in MM is often mediated by apoptosis evasion, ferroptosis induction by means of kinase inhibition might serve as an alternative strategy to treat drug-resistant MM cells. We showed that both apoptosis and ferroptosis induction mainly results in inhibition of CMGC and AGC kinase families, which are reported to primarily regulate cell cycle progression, cell survival, and cell proliferation. In contrast to apoptotic cell death, ferroptosis is also able to target a significant number of tyrosine

kinases, including key players of the B-cell receptor signaling pathway, which may aid in finding novel (ferroptosis-based) kinase targets in MM.

In the second part of the results section (chapter 5 and 6), we evaluated whether therapy-resistant MM cells are sensitive to ferroptotic cell death. Given that MM tumors already exhibit high basal oxidative stress levels and an altered iron metabolism due to their increased proliferation capacity, ferroptosis induction might further be exploited to exhaust the tumoral anti-oxidant defense mechanisms and overcome multi-drug resistance. Moreover, we examined the involvement of nuclear events and epigenetic regulatory mechanisms in ferroptosis signaling as they largely remain unexplored.

In chapter 5, we combined RNA sequencing, LC-MS/MS, pyrosequencing, and EPIC BeadChip analysis to characterize epigenetic changes taking place in therapy-resistant and -sensitive MM cells treated with ferroptosis inducer RSL3. We found that MM1 multiple myeloma cells are sensitive to ferroptosis induction and epigenetic reprogramming by RSL3, irrespective of their glucocorticoid-sensitivity status. LC-MS/MS analysis revealed the formation of non-heme iron-histone complexes and altered expression of histone modifications associated with DNA repair and cellular senescence. In line with this observation, EPIC BeadChip measurements of significant DNA methylation changes in ferroptotic myeloma cells demonstrated an enrichment of CpG probes located in genes associated with cell cycle progression and senescence, such as NR4A2. Overall, our data show that ferroptotic cell death is associated with an epigenomic stress response that might advance the therapeutic applicability of ferroptotic compounds.

In chapter 6, we investigated the role of chromatin remodeler forkhead box A1 (FOXA1) in ferroptosis signaling. We found that FOXA1 expression is consistently upregulated upon ferroptosis induction in different *in vitro* and *in vivo* disease models. Remarkably, FOXA1 upregulation in ferroptotic myeloma cells did not alter hormone signaling or epithelial-to-mesenchymal transition, two key downstream signaling pathways of FOXA1. CUT&RUN genome-wide transcriptional binding site profiling showed that GPX4-inhibition by RSL3 triggered loss of binding of FOXA1 to pericentromeric regions in MM cells, suggesting that this transcription factor is possibly involved in genomic instability, DNA damage, or cellular senescence under ferroptotic conditions.

Altogether, the results of this thesis demonstrate that both kinase inhibition and ferroptosis induction are effective strategies to overcome glucocorticoid-therapy resistance in MM. Nevertheless, to fully exploit the therapeutic potential of protein kinase inhibitors and ferroptotic compounds, multiple hurdles still need to be overcome. For example, the kinase inhibitory effects of compounds included in this work are largely aspecific. To what extend does this affect their therapeutical applicability? Can they be included in combinational treatment regimens for MM patients? Also, ferroptotic-induced epigenetic changes seem to promote genome instability and cellular senescence in MM cells. Does this phenomenon of 'ferrosenescence' aid in completely eliminating drug-resistant MM clones or does it possibly promote cancer development? These issues, together with recommendation for future follow-up studies, are discussed in the final part of this thesis.

Samenvatting

Multipel myeloom (MM) is een kwaadaardige tumor van plasmacellen die ongecontroleerd prolifereren in het beenmerg. Ondanks de therapeutische vooruitgang die de afgelopen decennia geboekt is, blijft MM een ongeneeslijke ziekte waarbij behandelingen met conventionele kankertherapeutica, zoals proteasoominhibitoren, immuuntherapie, corticosteroïden, en alkylerende middelen slechts resulteren in lage remissiepercentages en beperkte toename in overlevingspercentages. De lage effectiviteit van bestaande anti-kanker geneesmiddelen is meestal te wijten aan de ontwikkeling van multi-drug resistentie, waarbij kankercellen resistent worden tegen structureel en functioneel ongerelateerde geneesmiddelen. Door de multifactoriële aard van de moleculaire mechanismen die betrokken zijn bij de verwerving van therapieresistentie, blijft het een uitdaging om effectieve, curatieve behandelingen voor MM te ontwikkelen. Daarom is er een dringende nood aan nieuwe therapeutische strategieën om volledige en persistente tumorremissie te bekomen bij MM patiënten. In deze doctoraatsthesis hebben we kinase inhibitie, behandeling met natuurlijke stoffen, en ferroptose inductie onderzocht als alternatieve behandelingsstrategieën om resistentie in MM te overwinnen.

In het eerste deel van de resultatensectie (hoofdstuk 3 en 4) hebben we onderzocht of (natuurlijke) kinase inhibitoren gebruikt kunnen worden om glucocorticoïd-resistente MM cellen te elimineren. Kinase signalering is vaak ontregeld in maligne cellen en draagt significant bij aan de ontwikkeling van therapieresistentie. Op deze manier kan inhibitie van belangrijke therapieresistentie-modulerende kinasen potentieel klinische voordelen bieden voor MM patiënten.

In hoofdstuk 3 hebben we de belangrijkste verschillen in kinase activiteit tussen glucocorticoïd-resistente en -gevoelige MM cellen gekarakteriseerd om kinasen te identificeren die betrokken zijn bij de regulatie van therapieresistentie. Onze data toont aan dat Bruton tyrosine kinase (BTK), betrokken bij B cel receptor signalering, constitutief geactiveerd is in resistente cellen. Farmacologische inhibitie van BTK door de FDA-goedgekeurde kinase inhibitor ibrutinib (IBR) en de beloftevolle anti-kanker drug Withaferin A (WA) toonde aan dat WA effectiever is in het doden van BTK-overexpresserende glucocorticoïd-resistente MM-cellen in vergelijking met IBR. WA is bovendien in staat om BTK-overexpressie te herstellen en BTK-activiteit te remmen door middel van cysteïne-afhankelijke covalente targeting.

In hoofdstuk 4 bestudeerden we veranderingen in kinase activiteit in ferroptotische en apoptotische MM cellen. In tegenstelling tot apoptose, is ferroptose een vorm van gereguleerde celdood die gekenmerkt wordt door een ijzerafhankelijke toename in reactieve zuurstofspecies die lipide peroxidatie reacties induceren. Door het kinoom van beide celdood modaliteiten te vergelijken, wilden we kinasen identificeren die cruciaal zijn

in de regulatie van ferroptose- en apoptose-specifieke celdood. Omdat MM tumoren vaak in staat zijn om drug-geïnduceerde apoptose celdood te ontwijken, zou ferroptose inductie door middel van kinase inhibitie kunnen dienen als een alternatieve strategie om resistente MM cellen te behandelen. Onze resultaten toonden aan dat zowel apoptose als ferroptose inductie in MM cellen voornamelijk gepaard gaat met inhibitie van CMGC en AGC kinasen, waarvan wordt gerapporteerd dat ze betrokken zijn bij celcyclus progressie, cel overleving en cel proliferatie. In tegenstelling tot apoptotische celdood, is ferroptose ook in staat om een aanzienlijk aantal tyrosine kinasen te inhiberen, inclusief enkele belangrijke spelers van de B cel receptor signalering, wat kan helpen bij het vinden van nieuwe (ferroptose gebaseerde) kinase doelwitten in MM.

In het tweede deel van de resultatensectie (hoofdstuk 5 en 6) bestudeerden we of therapieresistente MM cellen gevoelig zijn voor ferroptotische celdood. Aangezien MM tumoren als gevolg van hun verhoogde proliferatiesnelheid gebukt gaan onder hogere oxidatieve stress en veranderingen in hun ijzermetabolisme, zou ferroptose inductie verder gebruikt kunnen worden om de tumorale anti-oxidant mechanismen uit te putten en multi-drug resistentie te overwinnen. Daarnaast hebben we de betrokkenheid van epigenetische regulatiemechanismen bij ferroptose-signalering onderzocht, omdat deze tot op heden nog niet in kaart zijn gebracht.

In hoofdstuk 5 hebben we RNA sequencing, LC-MS/MS, pyrosequencing en EPIC BeadChip analyse gecombineerd om epigenetische veranderingen te karakteriseren in therapieresistente en -gevoelige MM cellen, behandeld met ferroptose inducer RSL3. We ontdekten dat MM1 multiple myeloma cellen gevoelig zijn voor ferroptose inductie en epigenetische herprogrammering door RSL3, ongeacht hun glucocorticoïd-gevoeligheid. LC-MS/MS analyse toonde aan dat ferroptose inductie leidt tot de vorming van non-heem ijzer-histon complexen en tot veranderingen in expressie van histon modificaties geassocieerd met DNA herstel en cellulaire senescentie. In lijn met deze observaties, demonstreerde onze EPIC BeadChip analyse dat significante ferroptose-afhankelijke veranderingen in DNA methylatie voornamelijk plaatsvinden in genen die geassocieerd zijn met celcyclus progressie en senescentie, zoals NR4A2. Deze gegevens suggereren dat ferroptotische celdood geassocieerd is met een algemene epigenetische stress respons die de therapeutische waarde van ferroptose inductoren zou kunnen bevorderen.

In hoofdstuk 6 bestudeerden we de rol van de chromatine remodeler forkhead box A1 (FOXA1) in ferroptose signalering. Uit onze resultaten blijkt dat FOXA1 expressie consistent toeneemt bij ferroptose inductie en dit in verschillende *in vitro* en *in vivo* ziektemodellen. Opmerkelijk is dat de ferroptose-afhankelijke toename in FOXA1 expressie geen invloed had op hormoon signalering of epitheliale-mesenchymale transitie, twee belangrijke doelwitten van FOXA1. CUT&RUN sequencing van transcriptionele binding sites toonde echter wel aan dat GPX4-inhibitie door RSL3 leidt tot vermindering van FOXA1 binding aan pericentromerische regio's in MM cellen, wat suggereert dat deze transcriptiefactor

betrokken is bij genomische instabiliteit, DNA schade, of cellulaire senescentie in ferroptotische condities.

De resultaten van dit proefschrift demonstreren dat zowel kinase inhibitie als ferroptose inductie effectieve strategieën zijn om glucocorticoïd-therapie resistentie in MM te overwinnen. Om het therapeutisch potentieel van proteïne kinase inhibitoren en ferroptotische inductoren ten volle te benutten, moeten er echter nog verschillende hindernissen overwonnen worden. Zo zijn de kinase inhiberende effecten van WA en IBR gedeeltelijk aspecifiek. In hoeverre heeft dit gevolgen voor hun therapeutische toepasbaarheid? Kunnen ze worden geïncludeerd in combinatietherapieën voor MM patiënten? Ook lijken ferroptose-geïnduceerde epigenetische veranderingen genoominstabiliteit en cellulaire senescentie in MM-cellen te bevorderen. Helpt dit fenomeen van 'ferrosenescentie' om therapie-resistente MM cellen te elimineren of bevordert het net de ontwikkeling van persistente en resistente MM subpopulaties? Deze vragen, samen met aanbevelingen voor toekomstige vervolgstudies, worden besproken in het laatste gedeelte van dit proefschrift.
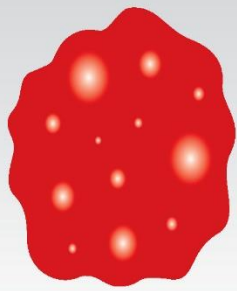
<u>INTRODUCTION</u>

CHAPTER 1:
Exploring the Pathogenesis and Current Treatment Landscape in Multiple Myeloma

CHAPTER 2:
Therapy Resistance in Multiple Myeloma: Past, Present, and Future

Introduction

Cancer refers to a vast group of diseases characterized by the uncontrollable growth of cells that invade and destroy surrounding healthy tissue. The aggressive nature of cancerous diseases is demonstrated in the World Health Organization (WHO) global mortality statistics reports, which state that one in six deaths in 2018 was a direct cause of cancer [1]. Due to its considerable clinical and social impact, ample research focusses on finding effective cancer treatments and cures. The past couple of decades are marked by significant advances in conventional cancer therapies, such as chemotherapy, radiotherapy, and surgery, and by a surge in the development of novel treatment strategies, including hormone - and immunotherapy [2, 3]. Yet, despite many promising breakthroughs and developments, the prevalence of drug- and therapy resistant cancers is increasing, eventually rendering many cancers incurable [4, 5]. This is also true for several hematological cancers, such as leukemia, lymphoma, or multiple myeloma (MM) [6-8]. In the latter example of MM, the disease is featured by a repeating pattern of remission and relapse periods where patients cycle through available treatment options, ultimately resulting in complete treatment failure [9-11]. Therefore, there is an urgent need for novel therapeutic approaches to overcome primary and acquired therapy resistance in MM. In order to enhance the use of conventional drugs and to design more effective treatments, an improved understanding of the molecular mechanisms mediating resistance is key. In this context, both genetic and epigenetic anomalies have been identified as drivers in both the development of the disease and of drug resistance. Indeed, several studies have demonstrated the potential of epigenetic drugs targeting aberrant DNA methylation and histone modifications in (pre)clinical settings of MM [12]. Alternatively, targeting tumor-specific deregulated signaling pathways within MM have also gained interest over the past years. Inhibitors of protein kinases (PKs), which are particularly prominent in signal transduction, are extensively being studied in clinical trials and have shown activity against MM [13]. Finally, knowing that many FDA-approved drugs are natural product derivatives, an extensive arsenal of plant-derived compounds has been explored to treat hematological cancers [14]. Of particular interest, broad-spectrum anti-cancer effects of the natural phytochemical Withaferin A (WA) have been reported in various of cancer types, involving reactive oxygen species (ROS)-mediated cytotoxicity, regulation of heat shock protein activity, induction of apoptosis and ferroptosis, and inhibition of PKs [15].

In the first introductory chapters, I will discuss the pathophysiology of MM, summarize the major causes of therapy resistance, and highlight promising treatment strategies to overcome drug resistance in this cancer type.

CHAPTER 1

Exploring the Pathogenesis and Current Treatment Landscape in Multiple Myeloma

Chapter 1 :

Exploring the Pathogenesis and Current Treatment Landscape in Multiple Myeloma

MM is a hematological malignancy that is characterized by the uncontrolled growth of terminally differentiated B-cells, which primarily reside in the bone marrow (BM) environment. The accumulation of these differentiated cells, the so-called plasma cells (PCs), directly leads to a host of problems including bone lesions, (recurrent) infections, anemia, hypercalcemia, renal failure, and fatigue. Although the exact causes or risk factors largely remain unknown, MM seems to be a progressive 'multi-step' disease that is often preceded by an age-progressive premalignant condition termed monoclonal gammopathy of undetermined significance (MGUS). Thanks to the introduction of autologous stem-cell transplantation and drugs such as thalidomide and bortezomib, the overall survival of MM patients has significantly increased. However, despite these remarkable therapeutic advancements, MM remains an incurable disease.

1.1 Pathophysiology of Multiple Myeloma

The human immune system is a complex network of specialized cells and proteins designed to defend the body against foreign invaders, such as bacteria, viruses, fungi and toxins. Typically, this system can be classified into two closely intertwined parts: the innate immunity, which serves as a non-specific first line of defense against common pathogens, and the adaptive immunity, which orchestrates a more customized, pathogen-specific immune reaction [16]. The latter system is primarily activated when the innate response is unable to eliminate the infectious treat and generates a slower, yet more accurate, immune response. To allow for its effective functioning, the adaptive immunity relies on the proliferation and differentiation of its key effector cells, the T- and B-lymphocytes, that are continuously replenished during hematopoiesis. B-cells are particularly important in the humoral mechanism of immunity within the adaptive immune response due to their ability to differentiate into specialized antibody-producing PCs.

In healthy individuals, B-lymphocytes undergo numerous rounds of proliferation and selection to ensure only functional (i.e. with a functional B-cell receptor (BCR)) cells are maintained (Figure 1). This developmental and selection process occurs within the BM and is initiated by a surge of early B-cell factor 1 (EBF1), transcription factor 3 (TF3), and paired box 5 (Pax5) expression in lymphoid progenitor cells (LPC), promoting their commitment to the B-lymphocyte lineage [17]. These committed cells, also known as pro-B-lymphocytes, subsequently undergo V(D)J rearrangement of the immunoglobin (Ig) heavy chain gene allowing for the production of monospecific B-cells. Only when this rearrangement is successful and functional Ig heavy chains are produced, the cells further differentiate into pre-B-lymphocytes [18]. After subsequent Ig light chain gene rearrangements, the

production and assembly of the complete membrane-associated Ig class M (IgM) BCR is started and immature B-lymphocytes are formed. At this stage, the B-cells are screened for auto-reactivity. If immature B-lymphocytes recognize ubiquitous self-antigens, they are either eliminated by clonal deletion or undergo receptor editing and change the specificity of their Ig molecule [18]. In their final maturation steps, the immature B-cells migrate towards secondary lymphoid organs, such as the lymph nodes or the spleen, traveling along a C-X-C motif chemokine ligand 13 (CXCL13). Here, they will co-express Ig-D on their membrane, which marks the end of the maturation process.
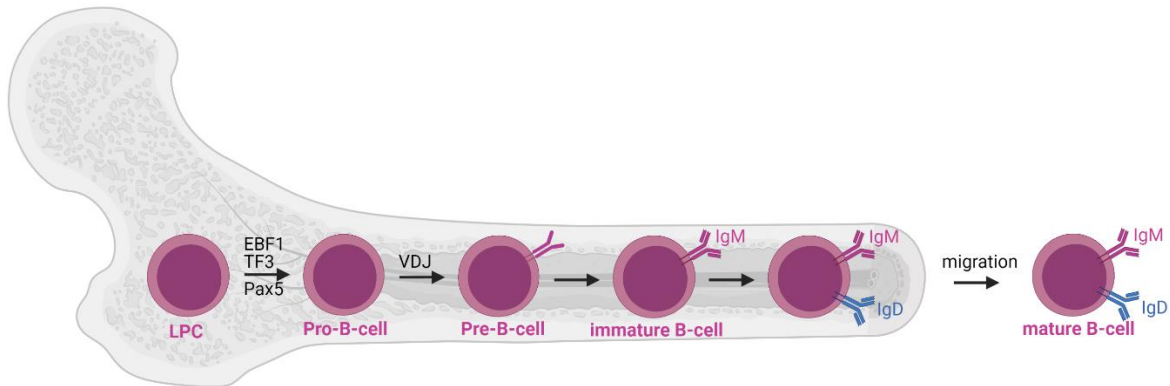

Figure 1: Differentiation of B-lymphocytes in the bone marrow. Mature B-cells originate from lymphoid progenitor cells (LPC) that undergo pro-B-cell, pre-B-cell, immature B-cell, and mature B-cell differentiation. Abbreviations: EBF1 = early B-cell factor, TF3 = transcription factor 3, Pax5 = paired box 5, VDJ = VDJ heavy chain rearrangement, IgM = immunoglobin class M, IgD = immunoglobin class D. Figure created with BioRender.com.

Mature, naïve B-cells circulate through the different secondary lymphoid organs until they are activated by exposure to an antigen. This activation initially results in the proliferation and differentiation of naïve B-cells in to low-affinity IgM-secreting PCs, which are only short lived and undergo apoptosis in situ (Figure 2) [19]. Supported by T helper lymphocytes, the activation process then causes naïve follicular B-cells to undergo proliferation, class switching, and somatic hypermutation in the germinal center sites of the secondary lymphoid organs. This results in the production of long-lived memory B-lymphocytes and terminally differentiated, long-lived PCs that are specialized in the secretion of high-affinity antibodies (Figure 2) [19]. These PCs live many months to years and typically home to the BM.

Throughout their entire maturation, PCs face two major developmental challenges. Firstly, they must be able to survive long-term to produce immunological memory for the infection against which they were generated [20]. The efficiency by which PCs are able to remove infectious triggers heavily relies on class switching and somatic hypermutation. These processes help create PCs which produce antibodies of different Ig isotypes with different functionalities and increase the binding affinity of the antibodies for the antigen. Mechanistically, both class switching and somatic hypermutation rely on double-strand breaks in the Ig loci. Although most breaks are repaired locally, they can also fuse with other breaks elsewhere in the genome, leading to aberrant chromosomal translocations

and DNA fusions, a molecular hallmark of MM [20, 21]. The second main challenge PCs face is the effective production of large quantities of antibody. This requires cessation of cell cycle progression, compaction of chromatin, silencing of cellular functions unnecessary for antibody production, and is strictly controlled by transcription factors (TFs), including X box protein 1s (XBP1s) [20]. Given that these TFs mostly regulate the expression of key survival and growth signals and stimulate genes required for Ig production, deregulation of these factors often contributes to myelomagenesis. Indeed, transgenic mice overexpressing XBP1s are known to develop a pathological syndrome that harbors several MM features [22].

Any derangement within PC development therefore increases the risk of triggering malignancy and often underlies the process of carcinogenesis. Most MM cells isolated from patients display mutations or chromosomal translocations caused by disruptions in class switching and somatic hypermutations, confirming that they are of post-germinal ancestry. However, the exact cell of origin of MM remains unknown [23]. As in other human cancers, it is likely that the disease is driven by a rare population of cells, termed MM cancer stem cells (CSCs), which are characterized by self-renewal capacity, clonogenic growth, and increased drug resistance [19, 24]. The presence of CSC might explain the high relapse rates in MM patients: even when all malignant PCs are eradicated by an anti-cancer drug, a small number of remaining CSC will guarantee the return of MM cells, possibly in a more aggressive and resistant form [25].
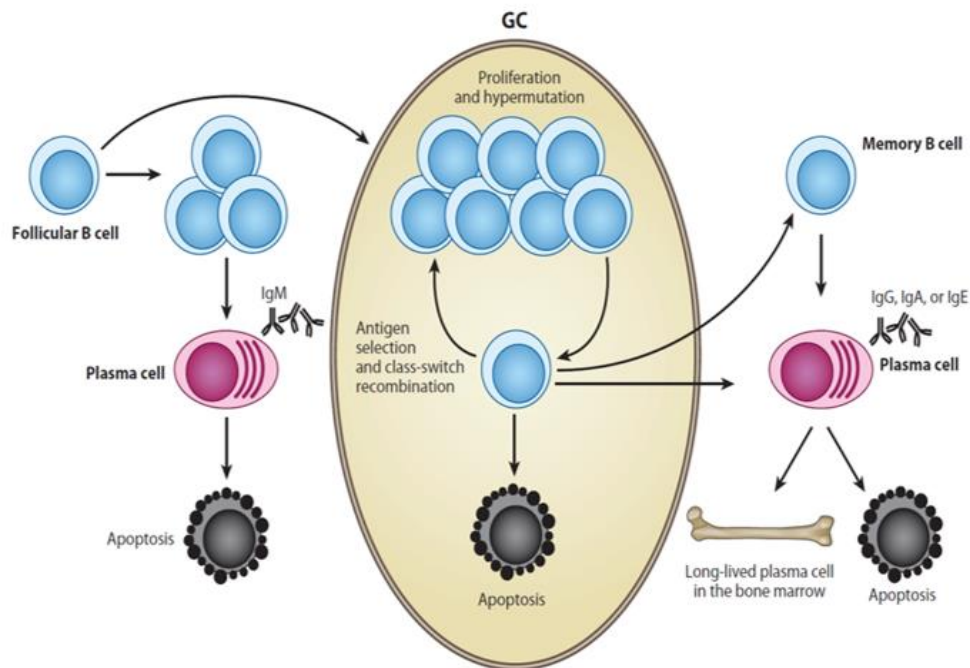
Figure 2: Schematic overview of the formation of long-lived plasma cells. Upon exposure to antigen, naïve B-cells differentiate into short-lived, low-affinity immunoglobulin M (IgM)-secreting plasma cells (left). Some of the activated B-lymphocytes subsequently form a germinal center (GC) initiating class switching and somatic hypermutation leading to the formation of memory B-cells and long-lived plasma cells (right). Adapted from [19].

Once a primary mutational event favors the growth of the MM cell of origin, clones of this cell proliferate and differentiate into pre-malignant PCs with various (epi)mutations that cause MGUS. MGUS is a pathological, asymptomatic state that is characterized by the infiltration of clonal PCs into the BM and the secretion of monoclonal protein (also known as myeloma protein), an abnormal antibody [21]. MM development is nearly always preceded by MGUS, with or without an intervening stage referred to as smoldering multiple myeloma (SMM) (Figure 3). On average, 1% of people diagnosed with MGUS will progress to MM each year [26]. In some cases, MM can evolve into an even more aggressive cancer and metastasize from the BM into the circulatory system (i.e. plasma cell leukemia).
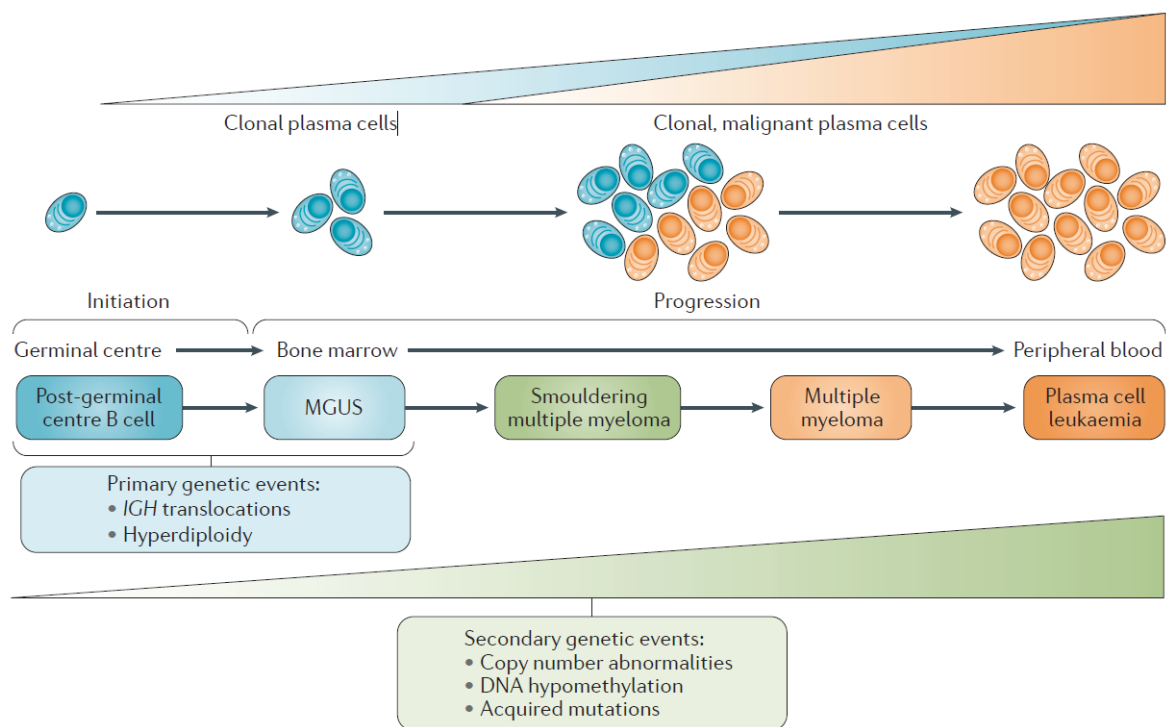
Figure 3: The development of multiple myeloma (MM). Typically, MM progression can be classified into two stages: the establishment of precursor disease states, including monoclonal gammopathy of undetermined significance (MGUS) and smoldering MM, and the progression to MM. The first stage is usually characterized by the occurrence of primary genetic events (e.g. chromosomal translocations involving the immunoglobulin genes), while secondary (epi)genetic alterations mostly appear in later disease stages. In some cases, MM can progress to bone marrow-independent diseases, such as plasma cell leukemia [21].

1.2 Epidemiology

In 2020, MM accounted for 1.8 % of all new cancer cases and for 2.1 % of cancer deaths worldwide [27]. Although the disease can affect people of all ages, MM is predominantly a disease of senior adults with the median age of diagnosis being 70 years [28]. Globally, the highest incidence of MM can be found in more-developed countries, including the United States, Western Europe, and Australia (Figure 4) [1]. The variety in incidence can probably be explained by a greater clinical awareness of the disease as well as by the availability of

better diagnostic tools in developed countries [21]. Interestingly, MM incidence is also 2-3 times higher in black individuals compared to Hispanic, Caucasian, and Asian individuals, and men are more likely to be affected by the disease than women [29].
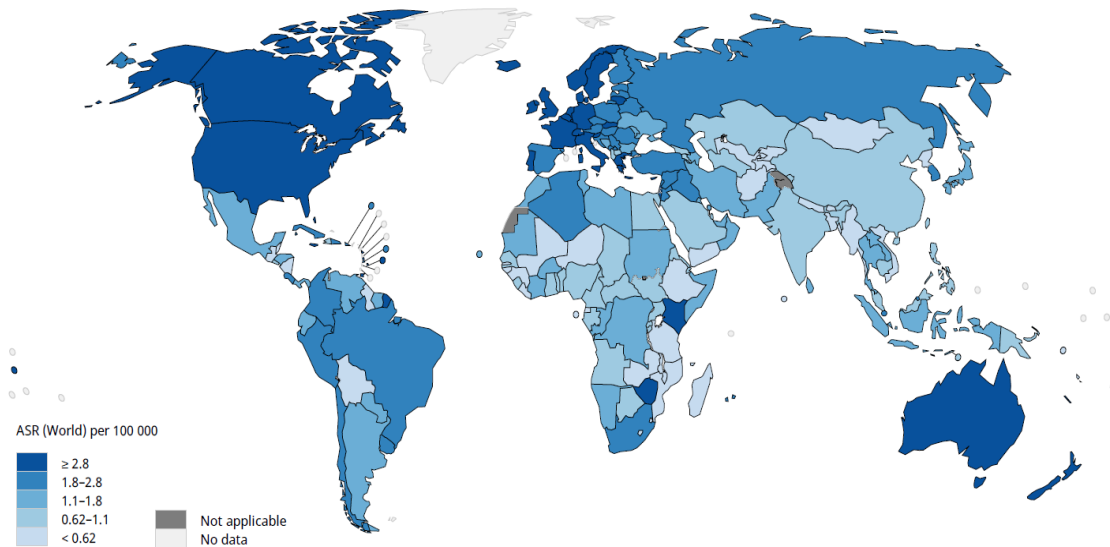
Figure 4: Global incidence of multiple myeloma in 2020. The incidence of multiple myeloma varies greatly and is generally higher in more-developed countries, such as Australia, Western Europe, and Northern America. Available from https://gco.iarc.fr/, accessed on February 24, 2021 [1].

1.3 Aetiology

Although the potential risk factors of MM have been evaluated in numerous studies, the precise cause of the disease remains unknown. Main risk factors include age, male gender, familial background, and MGUS history. Yet, certain environmental and occupational hazards have been associated with myelomagenesis as well [20, 21]. Some studies have reported an increased MM incidence in individuals exposed to higher levels of radiation [30], pesticides [31, 32], hair dyes [33], obesity [34], and immune dysfunction [35, 36], but little evidence thoroughly supports a true causal relationship with disease development [20]. A ruling hypothesis that has been proposed by several research groups states that the interindividual genetic variation governs the response to environmental triggers and may mediate some of the familial aggregation observed in MM [20].

1.3.1 Genetic Factors

MM is a clinically and biologically heterogeneous cancer where several genetic alterations have been proposed as driver mutations. A major genetic lesion identified in MM involves the chromosomal translocation of the enhancer of the immunoglobulin heavy locus (IGH), located on chromosome 14q32, and a limited set of recurrent partner genes, such as

encoding cyclin D1 (CCND1), fibroblast growth factor receptor 4 (FGFR3), and multiple myeloma SET domain (MMSET) [37]. Once these partner genes are placed under the control of the strong IGH enhancer, their expression will significantly increase and their corresponding pathways will be deregulated accordingly. The t(11;14) translocation, for example, is found in approximately 15-20 % of all MM patients and causes upregulation of the CCND1 gene, which codes for the cell cycle progression regulator cyclin D1 [19, 21, 38]. As a consequence of this translocation, the G1/S cell cycle transition is heavily perturbed in most MM patients and results in unregulated proliferation of myeloma cells [39]. Another translocation, t(4;14), alters MMSET and FGFR3 expression and is present in almost 15 % of patients. Patients harboring t(4;14) mutations have a significantly worse prognosis compared to other biological subgroups [40]. Both MMSET and FGFR3 possess potential oncogenic activity, although MMSET in particular seems to play a central role in MM pathogenesis. Known to have histone methyltransferase (HMT) activity, overexpression of MMSET often leads to global changes in histone methylation and promotes cell survival, DNA repair, and cell progression [41, 42].

Another frequently observed genetic aberration in MM cells is hyperdiploidy of the odd numbered chromosomes 3, 5, 7, 9, 11, 15, 19, and 21 [43]. The underlying mechanism of hyperdiploidy of these non-random selection of odd chromosomes is unknown. Interestingly, patients with hyperdiploidy are less likely to have primary IGH chromosomal translocations, though some patients with both genetic abnormalities have been reported [21].

Hyperdiploidy and chromosomal translocations seem to be crucial triggers of the early establishment of abnormal PCs, however, they are in itself not sufficient to drive the disease [44]. Secondary mutations in tumor suppressor or oncogenes are required to enhance the growth potential of abnormal PCs. The most frequently occurring mutations in MM patients are located in tumor protein 53 (TP53) (8 %), defective in sister chromatid joining (DIS3) (11 %), family with sequence similarity 46 member C (FAM46C) (11 %), neuroblastoma RAS viral oncogene (NRAS) (20 %), and Kirsten RAS oncogene (KRAS) (23 %) [21]. The heterogeneity in mutations between patients has consequences for potential therapies that target mutated proteins and should be considered when optimizing treatment schedules of the patient.

1.3.2 Epigenetic Factors

Next to genetic alterations, (reversible) epigenetic changes are one of the main drivers of MM pathogenesis. These are commonly found in later stages of MM and include altered DNA methylation, chromatin structure, histone modifications, and micro-RNA (miRNA) deregulation.

Through the covalent transfer of a methyl group to the C-5 position of the cytosine ring of DNA, DNA methylation alters the activity of genes without changing the DNA sequence itself. Methylation of DNA predominantly occurs in CpG dinucleotides (also known as CpG islands) of gene promotors and is associated with gene silencing. In MM, DNA methylation levels are highly variable between patients, although it usually follows a characteristic

pattern as the disease worsens [21, 45]. In the early transition phase, where patients progress from the MGUS stage to MM, global hypomethylation predominates whereas an increase in gene-specific hypermethylation occurs in later disease stages [45, 46]. Maximum DNA methylation is typically observed in patients with relapsed disease [46]. Genes that are inactivated by methylation during MM progression often have a role in tumor suppression and cell cycle regulation, such as cyclin-dependent kinase inhibitor 2A (CDKN2A) [47], cadherin-1 (CDH1) [48], and TGF beta receptor 2 (TGFBR2) [49]. Whole-exome sequencing has revealed that many MM patients carry mutations in two major determinants of DNA methylation: DNA methyltransferase 3A (DNMT3A) [45], responsible for *de novo* methylation marks, and ten-eleven translocation 2 (TET2) [50], which is involved in the enzymatic removal of methylation groups. These mutations alone, however, are insufficient to fully account for all DNA methylation aberrations observed in MM and their involvement in myelomagenesis remains uncertain [51]. Remarkably, patients harboring the t(4;14) translocation often show the most pronounced hypermethylation changes due to the overexpression of the MMSET gene, highlighting the interplay between DNA methylation and histone modifications [20].

Histone modifications themselves are also frequently altered during MM transformation. These covalent modifications, which include (but are not limited to) methylation, phosphorylation, acetylation, and ubiquitylation, are post-translational modifications (PTMs) of histone proteins. These are highly basic proteins, present in eukaryotic nuclei, that are responsible for the packaging and accessibility of the DNA. Any modification made to these structural proteins can affect gene expression by altering the chromatin structure or by recruiting epigenetic reader/writer enzymes. Histone (de)methylation changes are particularly frequent in MM and are also more prevalent in the late-stage disease [44]. In contrast to DNA methylation, some driver mutations in multiple chromatin-modifying and writer-reader-eraser enzymes have been identified as probable causes for global histone (de)methylation aberrations [51]. As mentioned, the MMSET protein is frequently upregulated in a specific subset of MM patients, and mainly catalyzes the addition of the active H3K36me2 mark [52, 53]. Knockdown or knockout of MMSET expression reduces growth of MM cells by inducing apoptosis and cell cycle arrest, and could be an interesting therapeutic target. A recent study has additionally demonstrated that H3K36 dimethylation by MMSET is crucial in the DNA repair process and in telomere protection, explaining why MM subclones carrying this mutation display a significant growth advantage [54]. MMSET can also impact a plethora of other histone modifications by enhancing the function of transcriptional repressors, including histone deacetylase 1 (HDAC1), HDAC2, sin3a, lysine-specific histone demethylase 1A (LSD1), and the HMT enhancer of zest homolog 2 (EZH2) [55]. Studies on several MM cell lines and primary patient samples have indeed shown a transcriptional upregulation and altered genomic distribution of EZH2 [56, 57]. As EZH2 is responsible for catalyzing the methylation of the repressive H3K27me3 mark, specific loci across the genome are typically silenced in MM patients compared to healthy individuals [58]. One of these loci is the miR-126 locus, coding for an miRNA responsible for targeting the c-Myc oncogene [59]. Independent of EZH2, several other miRNAs have also been reported to be abnormally expressed in MM [60]. miR-32 and miR-17-92, for example, are

often upregulated in MM samples and can impact the expression of suppressor of cytokine signaling 1 (SOCS-1), which regulates IL-6 mediated survival of MM cells [51].

1.4 Diagnosis and Clinical Representation

The diagnostic criteria for MM are frequently updated by the International Myeloma Working Group (IMWG) and are based on monoclonal protein levels, BM infiltration of clonal PCs, and myeloma defining events [61] (Table 1 & 2). These latter events are end-organ complications and are a direct cause of either a disruption of normal hematopoiesis (due to overgrowth of PCs in the BM) or an increase in blood viscosity (due to abnormal protein load). They consist of hyperCalcemia, Renal impairment, Anemia, and Bone lesions (CRAB). Additional symptoms often include fatigue, weight loss, bone pains, recurrent infections and abnormal bleedings [29]. The diagnostic work-up for a patient with suspected MM involves a full blood count and serum electrophoresis to detect abnormalities in blood cells and protein concentration, a urine test to evaluate kidney failure, and radiographic imaging to detect bone lesions [44].

Table 1: International Myeloma Working Group Criteria for the Diagnosis of Multiple Myeloma (from [61])

Feature	MGUS	SMM	MM
Monoclonal protein levels in serum	< 3 g per dl	≥ 3 g per dl	Monoclonal protein in serum and/or urine
Bone marrow infiltration	< 10 %	10 – 60 %	≥ 10
Symptomatology	No CRAB features	No CRAB features	Presence of CRAB features

MGUS, monoclonal gammopathy of undetermined significance; SMM, smoldering multiple myeloma; MM, multiple myeloma.

Table 2: CRAB features (from [61])

	Criteria
Hypercalcemia	Serum calcium > 0.25 mmol/L above upper limit of normal or > 2.75 mmol/L
Renal insufficiency	Glomerular filtration rate < 40 mL/min or serum creatinine > 177 µmol/L
Anemia	Hemoglobin 2.0 g/dl under lower limit of normal or < 10 g/dl
Bone Lesions	≥ one lesion detected by radiography, computed tomography or positron emission tomography

1.5 Current therapies

Once the diagnosis of MM has been confirmed, an effective treatment schedule needs to be determined for each patient. Due to the heterogeneity of the disease and the multitude of therapeutic options available, this remains one of the major challenges for physicians

[62]. Suboptimal treatment may lead to selection of resistant clones while only eradicating therapy-sensitive MM cells [63]. Thus, most patients receive a combination therapy where different agents with distinct and synergistic mechanisms of action are included to limit the development of drug resistance [63]. Several other factors also impact the management strategy of MM, including the eligibility for autologous hematopoietic stem cell transplantation (ASCT) (which is mainly determined by age of the patient), presence of co-morbidities, risk stratification and patient preference [21]. Currently used drugs in MM include chemotherapy, proteasome inhibitors, immunomodulatory drugs, monoclonal antibodies, histone deacetylase inhibitors, alkylating agents, and glucocorticoids (GCs).

1.5.1 Autologous Stem Cell Transplantation

In Europe, ASCT paired with induction therapy is the standard of care for first-line treatment in MM patients up to 65 years [64]. This procedure starts with a short-term (3-5 cycles) induction regimen aimed to produce a profound therapeutic response prior to ASCT, and usually comprises the administration of bortezomib, lenalidomide, and dexamethasone (VRd) [65]. Subsequently, patients receive growth factors to stimulate the growth of hematopoietic stem cells (HSCs) and to trigger their release into the blood stream. HSCs are then harvested by apheresis and returned to the donor once they received high-dose chemotherapy, which efficiently destroys MM cells within the BM (Figure 5).
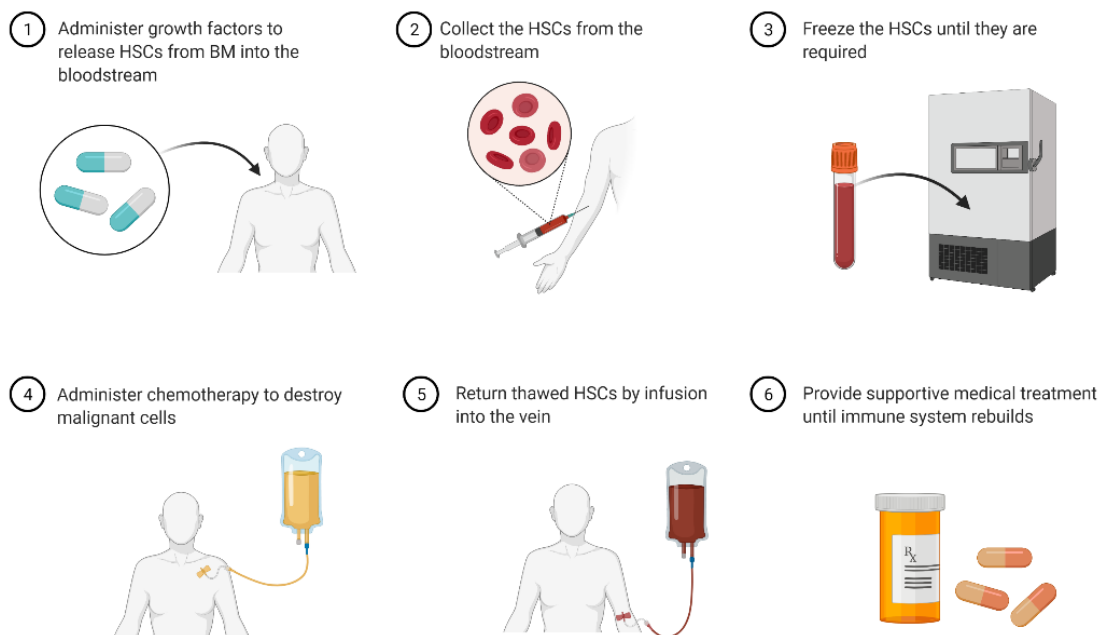
Figure 5: Overview of the autologous stem cell transplantation (ASCT) procedure in multiple myeloma patients. After administration of growth factors, hematopoietic stem cells (HSCs) are harvested and frozen (up to 10 years) until needed. Patients then receive high-doses of chemotherapy aimed to eradicate all malignant cells. Thawed HSCs are finally returned to the patient and supportive treatments are administered. Figure created with BioRender.com.

ASCT coupled with high-doses of chemotherapy improves overall survival and progression free survival, but rarely is a cure for MM [66]. The majority of patients relapse 18 to 36 months after their transplant is completed [67].

1.5.2 Chemotherapy

Patients not eligible for ASCT, either because of their age or the presence of co-morbidities, usually receive a treatment regimen that contains chemotherapeutic agents. These drugs aim to target rapidly proliferating cells, such as malignant MM cells, and include alkylating agents and topoisomerase inhibitors. Chemotherapy effectively reduces disease burden, and is characterized by a high response rate: some patients enter complete remission, but most enter a plateau phase with lower production of myeloma protein [29]. The two most currently used alkylating drugs in MM management are melphalan and cyclophosphamide [21]. Both compounds crosslink the DNA through the addition of alkyl groups at the guanine residue, which blocks DNA synthesis and ultimately leads to cell death [68]. Alternatively, compounds such as etoposide target DNA synthesis by inhibiting the topoisomerase II enzyme and induce apoptosis by causing DNA breakage [69].

1.5.3 Proteasome Inhibitors

Proteasome inhibitors (PIs) have proven to be quite successful in the treatment of MM. The ubiquitin-proteasome pathway plays a pivotal role in maintaining normal cellular homeostasis by regulating the degradation of eukaryotic proteins [70]. Misfolded or unfolded proteins (i.e. inactive proteins) in particular, are tagged with multiple molecules of ubiquitin and undergo degradation into short peptides by the proteasome protein complex. Given that MM cells typically produce and secrete large amounts of monoclonal proteins, they are extremely sensitive to any imbalance between load and capacity of the proteasome [21]. Therapies that further increase stress on protein turnover cause accumulation of misfolded proteins in the endoplasmic reticulum (ER) and stimulate multiple apoptotic pathways [71]. In 2003, the first FDA approved PI, bortezomib, was approved for the treatment of MM [71]. Two other agents, carfilzomib and ixazomib, have also secured regulatory approval for MM since then. Despite the encouraging clinical results obtained with bortezomib and other PIs, acquired and intrinsic resistance continue to hamper their therapeutic efficiency [72].

1.5.4 Immunomodulators

Immunomodulatory imide drugs (IMiDs) are an important class of MM drugs and remain a cornerstone in the current treatment of the disease (as they are included in the standard VRd regimen). They display a wide spectrum of effects on the immune system, including activation of natural killer cells [73], stimulation of IL-2 production in T cells [74], stimulation of cytokine secretion [75], and activation of dendritic cells [76]. Additionally, they are described to impact cell adhesion, lower angiogenesis and induce apoptosis [77].

Although their exact mechanism of action is not yet fully understood, their activity can partially be attributed to their ability to inhibit cereblon, which is part of an E3 ubiquitin ligase complex that ubiquitinylates and degrades several TFs [78]. Ultimately, this results in downregulation of the interferon regulatory factor 4 protein (IRF4) and triggers MM cytotoxicity [79, 80]. IMiDs currently approved for use in MM are thalidomide, lenalidomide, and pomalidomide

1.5.5 Immunotherapy

In 2015, the first regimens incorporating monoclonal antibodies (mAbs) in mono- or combination therapies for MM were approved by the FDA [81]. These antibodies bind to specific antigens overexpressed on the surface of malignant PCs and induce cell death by a variety of different mechanisms (Figure 6). Daratumumab and elotuzumab, for example, target transmembrane glycoproteins cluster of differentiation 38 (CD38) and signaling lymphocyte activation molecule family member 7 (SLAMF7) respectively, and have significantly improved the clinical outcome of MM patients [81, 82]. Unfortunately, the presence of certain cytogenetic abnormalities, such as t(4;14) and t(14;16), has been described to negatively impact therapy response to daratumumab and other mAbs [82].
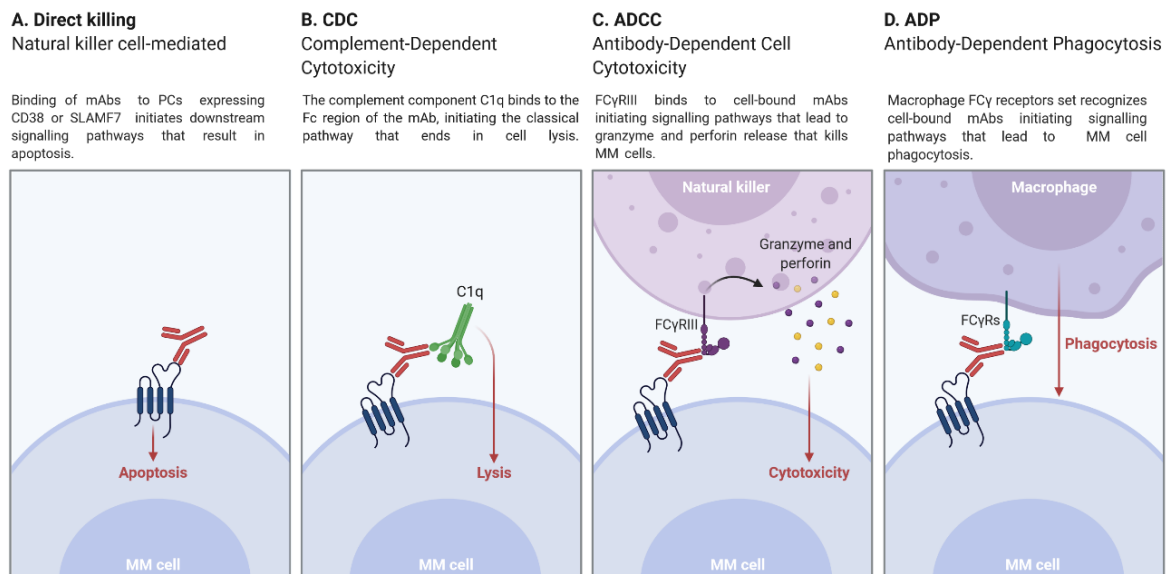
Figure 6: Mechanism of action of monoclonal antibodies (mAbs) targeting transmembrane glycoproteins overexpressed on multiple myeloma (MM). (**A**) mAbs can directly kill MM cells via induction of apoptosis or blockade of growth factor binding. (**B**) Complement-Dependent Cytotoxicity is initiated when complement component C1q binds to mAbs, resulting in lysis of MM tumor cells. (**C**) Natural killer cells recognize cell-bound mAbs via FcγRIII and attack MM cells. (**D**) mAb binding to MM cells triggers recognition and phagocytosis by macrophages. Figure created with BioRender.com.

Another form of immunotherapy being explored in MM is chimeric antigen receptor T-cells (CAR-T) therapy. This treatment technique uses the patient's own T-cells and alters them to produce CARs, artificial fusion proteins that specifically recognize and target antigen(s) present on the patient's malignant cells [83]. Recent successful clinical outcomes of CAR-T

therapy in relapsed or refractory MM patients have led to its FDA approval in March 2021 [83, 84]. In the pivotal KarMMa trial, for example, 72 % of the patients achieved a rapid and durable respone after CAR-T therapy, with a median duration of response of 11 months [84].

1.5.6 Glucocorticoids

Next to PIs and IMiDs, GCs form the backbone for MM treatment. Dexamethasone (DEX) in particular, is often paired with existing and novel agents to induce high clinical response rates [85]. Mechanistically, GCs mediate their therapeutic effects by 4 different mechanisms (Figure 7): (1) activation and nuclear translocation of the cytosolic glucocorticoid receptor (GR) promotes gene transcription modulation, (2) activation of the cytosolic GR promotes non-genomic effects through different signaling cascades, (3) activation of the membrane-bound GR promotes non-genomic effects, and (4) non-specific interaction with cellular membranes alters their physiochemical properties and activities [86]. The net effect of GC treatment is promotion of anti-inflammatory and immunosuppressive activity, and the induction of cell death in cancerous cells [85, 87]. The precise mechanism of action of GC-induced apoptosis has not yet been fully elucidated. Generally, it is believed that GCs activate apoptosis-inducing genes or inhibit survival genes [87].
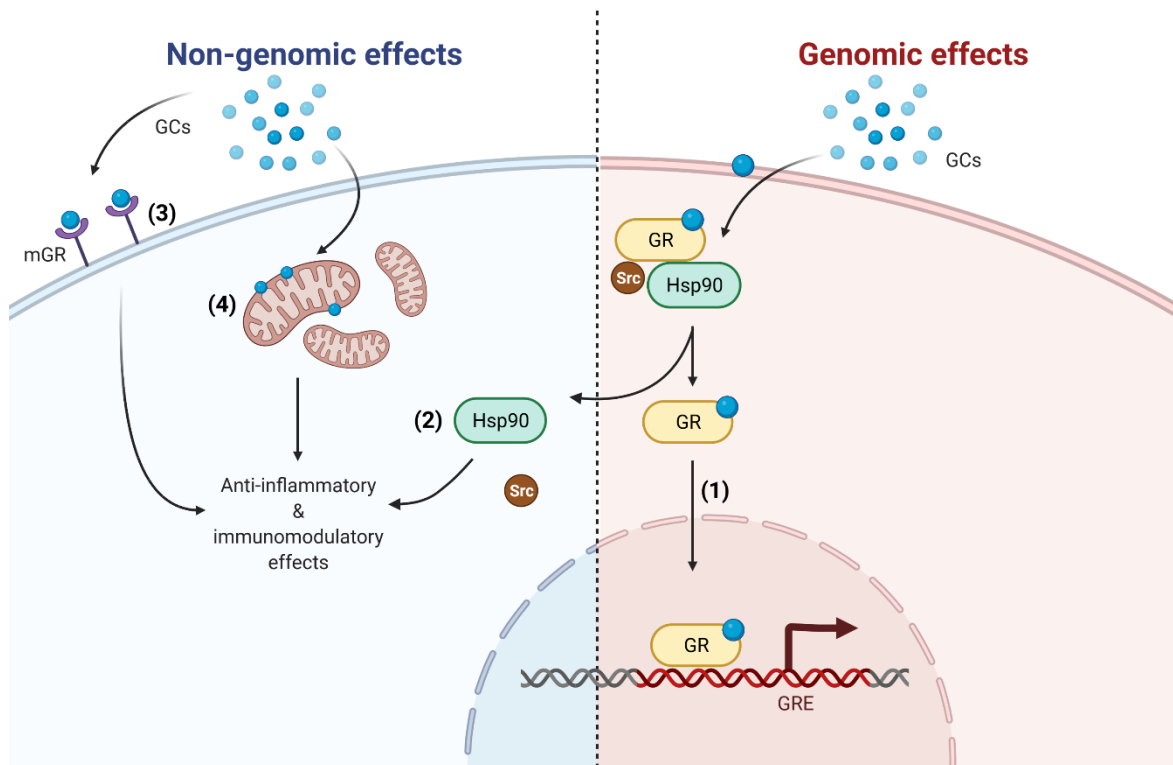
Figure 7: Overview of the genomic and non-genomic mechanism of glucocorticoids (GCs). (**1**) Lipophilic GCs pass through the cell membrane and bind to the cytosolic glucocorticoid receptor (GR). This results in a conformational change and promotes GR nuclear localization, binding to glucocorticoid response elements (GREs) in the DNA, and gene modulation. (**2**) GCs binding to the GR promotes the release of signaling molecules from the GR-multi-protein complex. (**3**) GCs binding

to membrane-bound GR (mGR) to exert their effects. (**4**) At high concentrations, GCs will intercalate with membranes and change their properties and activity. Adapted from [86] and created with BioRender.com.

1.5.7 **Epigenetic Drugs**

Targeting reversible epigenetic modifications is another attractive therapeutic strategy to kill malignant cells or to revert them to a more "normal" state [51]. Several (clinical) studies have addressed the potential of epigenetic modulating agents in MM, focusing especially on DNA methyltransferase inhibitors (DNMTi) and histone deacetylase inhibitors (HDACi) [88]. *In vitro* and *in vivo* experiments have demonstrated that two DNMTi compounds, 5-aza-2'cytidine (AZA) and 5-aza-2'-deoxycytidine (DAC), display anti-myeloma activity by inducing apoptosis and inhibiting cell cycle progression [89-91]. Both AZA and DAC are widely used therapies for myelodysplastic syndromes [92], but still await FDA approval for the treatment of MM. In contrast, the oral pan-HDACi Panobinostat has been approved as a third-line therapy in MM [93]. Panobinostat directly inhibits the enzymatic activity of HDACs, and results in an overall increase in histone acetylation and transcriptional activation. Additionally, it can promote hyperacetylation of non-histone proteins, such as tubulin, and increase cellular stress [94].

1.6. **References**

1. Bray F, Ferlay J, Soerjomataram I, Siegel RL, Torre LA, Jemal A. Global cancer statistics 2018: GLOBOCAN estimates of incidence and mortality worldwide for 36 cancers in 185 countries. CA Cancer J Clin. 2018;68(6):394-424.
2. Urruticoechea A, Alemany R, Balart J, Villanueva A, Vinals F, Capella G. Recent advances in cancer therapy: an overview. Curr Pharm Des. 2010;16(1):3-10.
3. Hideshima T, Anderson KC. Molecular mechanisms of novel therapeutic approaches for multiple myeloma. Nat Rev Cancer. 2002;2(12):927-37.
4. Housman G, Byler S, Heerboth S, Lapinska K, Longacre M, Snyder N, Sarkar S. Drug resistance in cancer: an overview. Cancers (Basel). 2014;6(3):1769-92.
5. Nikolaou M, Pavlopoulou A, Georgakilas AG, Kyrodimos E. The challenge of drug resistance in cancer treatment: a current overview. Clin Exp Metastasis. 2018;35(4):309-18.
6. Robak P, Drozdz I, Szemraj J, Robak T. Drug resistance in multiple myeloma. Cancer Treat Rev. 2018;70:199-208.
7. Klener P, Klanova M. Drug Resistance in Non-Hodgkin Lymphomas. Int J Mol Sci. 2020;21(6).
8. Hackl H, Astanina K, Wieser R. Molecular and genetic alterations associated with therapy resistance and relapse of acute myeloid leukemia. J Hematol Oncol. 2017;10(1):51.
9. Clinical Pathways to Address the Challenges of Treatment Resistance and Relapse in Multiple Myeloma. Journal of Clinical Pathways. 2017;3(7):49-55.
10. Hulin C, Hansen T, Heron L, Pughe R, Streetly M, Plate A, Perkins S, Morgan K, Tinel A, Rodrigues F, et al. Living with the burden of relapse in multiple myeloma from the patient and physician perspective. Leuk Res. 2017;59:75-84.
11. San-Miguel JF, Mateos M-V. Can multiple myeloma become a curable disease? Haematologica. 2011;96(9):1246-8.
12. Caprio C, Sacco A, Giustini V, Roccaro AM. Epigenetic Aberrations in Multiple Myeloma. Cancers (Basel). 2020;12(10).
13. Lind J, Czernilofsky F, Vallet S, Podar K. Emerging protein kinase inhibitors for the treatment of multiple myeloma. Expert Opin Emerg Drugs. 2019;24(3):133-52.
14. Lucas DM, Still PC, Perez LB, Grever MR, Kinghorn AD. Potential of plant-derived natural products in the treatment of leukemia and lymphoma. Curr Drug Targets. 2010;11(7):812-22.
15. Hassannia B, Logie E, Vandenabeele P, Vanden Berghe T, Vanden Berghe W. Withaferin A: From ayurvedic folk medicine to preclinical anti-cancer drug. Biochem Pharmacol. 2020;173:113602.
16. Janeway C, Travers P, Walport M, Shlomchik M. Immunobiology: The Immune System in Health and Disease: Garland Science; 2001.
17. Hagman J, Ramirez J, Lukin K. B lymphocyte lineage specification, commitment and epigenetic control of transcription by early B cell factor 1. Curr Top Microbiol Immunol. 2012;356:17-38.
18. Abbas A, Lichtman A. Basic immunology : functions and disorders of the immune system. 3rd edition ed: Philadelphia, PA : Saunders/Elsevier, c2009; 2009.
19. Anderson KC, Carrasco RD. Pathogenesis of myeloma. Annu Rev Pathol. 2011;6:249-74.
20. Boyle EM, Davies FE, Leleu X, Morgan GJ. Understanding the multiple biological aspects leading to myeloma. Haematologica. 2014;99(4):605-12.
21. Kumar SK, Rajkumar V, Kyle RA, van Duin M, Sonneveld P, Mateos MV, Gay F, Anderson KC. Multiple myeloma. Nat Rev Dis Primers. 2017;3:17046.
22. Carrasco DR, Sukhdeo K, Protopopova M, Sinha R, Enos M, Carrasco DE, Zheng M, Mani M, Henderson J, Pinkus GS, et al. The differentiation and stress response factor XBP-1 drives multiple myeloma pathogenesis. Cancer Cell. 2007;11(4):349-60.
23. Johnsen HE, Bogsted M, Schmitz A, Bodker JS, El-Galaly TC, Johansen P, Valent P, Zojer N, Van Valckenborgh E, Vanderkerken K, et al. The myeloma stem cell concept, revisited: from phenomenology to operational terms. Haematologica. 2016;101(12):1451-9.

24. Gao M, Kong Y, Yang G, Gao L, Shi J. Multiple myeloma cancer stem cells. Oncotarget. 2016;7(23):35466-77.
25. Dammacco F, Leone P, Silvestris F, Racanelli V, Vacca A. Chapter 9 - Cancer Stem Cells in Multiple Myeloma and the Development of Novel Therapeutic Strategies. In: Dammacco F, Silvestris F, editors. Oncogenomics: Academic Press; 2019. p. 121-37.
26. Zingone A, Kuehl WM. Pathogenesis of monoclonal gammopathy of undetermined significance and progression to multiple myeloma. Semin Hematol. 2011;48(1):4-12.
27. National Cancer Institute. https://seer.cancer.gov/statfacts/html/mulmy.html. Date accessed: 24/02/2021
28. Weinhold N, Ashby C, Rasche L, Chavan SS, Stein C, Stephens OW, Tytarenko R, Bauer MA, Meissner T, Deshpande S, et al. Clonal selection and double-hit events involving tumor suppressor genes underlie relapse in myeloma. Blood. 2016;128(13):1735-44.
29. Medical Masterclass c, Firth J. Haematology: multiple myeloma. Clin Med (Lond). 2019;19(1):58-60.
30. Ichimaru M, Ishimaru T, Mikami M, Matsunaga M. Multiple myeloma among atomic bomb survivors in Hiroshima and Nagasaki, 1950-76: relationship to radiation dose absorbed by marrow. J Natl Cancer Inst. 1982;69(2):323-8.
31. Khuder SA, Mutgi AB. Meta-analyses of multiple myeloma and farming. Am J Ind Med. 1997;32(5):510-6.
32. Burmeister LF. Cancer mortality in Iowa farmers, 1971-78. J Natl Cancer Inst. 1981;66(3):461-4.
33. Altekruse SF, Henley SJ, Thun MJ. Deaths from hematopoietic and other cancers in relation to permanent hair dye use in a large prospective study (United States). Cancer Causes Control. 1999;10(6):617-25.
34. Patel AV, Diver WR, Teras LR, Birmann BM, Gapstur SM. Body mass index, height and risk of lymphoid neoplasms in a large United States cohort. Leuk Lymphoma. 2013;54(6):1221-7.
35. Grulich AE, van Leeuwen MT, Falster MO, Vajdic CM. Incidence of cancers in people with HIV/AIDS compared with immunosuppressed transplant recipients: a meta-analysis. Lancet. 2007;370(9581):59-67.
36. Lindqvist EK, Goldin LR, Landgren O, Blimark C, Mellqvist UH, Turesson I, Wahlin A, Bjorkholm M, Kristinsson SY. Personal and family history of immune-related conditions increase the risk of plasma cell disorders: a population-based study. Blood. 2011;118(24):6284-91.
37. Morgan GJ, Walker BA, Davies FE. The genetic architecture of multiple myeloma. Nat Rev Cancer. 2012;12(5):335-48.
38. Gabrea A, Bergsagel PL, Chesi M, Shou Y, Kuehl WM. Insertion of excised IgH switch sequences causes overexpression of cyclin D1 in a myeloma tumor cell. Mol Cell. 1999;3(1):119-23.
39. Ely S, Di Liberto M, Niesvizky R, Baughn LB, Cho HJ, Hatada EN, Knowles DM, Lane J, Chen-Kiang S. Mutually exclusive cyclin-dependent kinase 4/cyclin D1 and cyclin-dependent kinase 6/cyclin D2 pairing inactivates retinoblastoma protein and promotes cell cycle dysregulation in multiple myeloma. Cancer Res. 2005;65(24):11345-53.
40. Chesi M, Bergsagel PL, Shonukan OO, Martelli ML, Brents LA, Chen T, Schrock E, Ried T, Kuehl WM. Frequent dysregulation of the c-maf proto-oncogene at 16q23 by translocation to an Ig locus in multiple myeloma. Blood. 1998;91(12):4457-63.
41. Brito JL, Walker B, Jenner M, Dickens NJ, Brown NJ, Ross FM, Avramidou A, Irving JA, Gonzalez D, Davies FE, et al. MMSET deregulation affects cell cycle progression and adhesion regulons in t(4;14) myeloma plasma cells. Haematologica. 2009;94(1):78-86.
42. Pei H, Zhang L, Luo K, Qin Y, Chesi M, Fei F, Bergsagel PL, Wang L, You Z, Lou Z. MMSET regulates histone H4K20 methylation and 53BP1 accumulation at DNA damage sites. Nature. 2011;470(7332):124-8.

43. Chng WJ, Kumar S, Vanwier S, Ahmann G, Price-Troska T, Henderson K, Chung TH, Kim S, Mulligan G, Bryant B, et al. Molecular dissection of hyperdiploid multiple myeloma by gene expression profiling. Cancer Res. 2007;67(7):2982-9.

44. Brigle K, Rogers B. Pathobiology and Diagnosis of Multiple Myeloma. Semin Oncol Nurs. 2017;33(3):225-36.

45. Heuck CJ, Mehta J, Bhagat T, Gundabolu K, Yu Y, Khan S, Chrysofakis G, Schinke C, Tariman J, Vickrey E, et al. Myeloma is characterized by stage-specific alterations in DNA methylation that occur early during myelomagenesis. J Immunol. 2013;190(6):2966-75.

46. Walker BA, Wardell CP, Chiecchio L, Smith EM, Boyd KD, Neri A, Davies FE, Ross FM, Morgan GJ. Aberrant global methylation patterns affect the molecular pathogenesis and prognosis of multiple myeloma. Blood. 2011;117(2):553-62.

47. Gonzalez-Paz N, Chng WJ, McClure RF, Blood E, Oken MM, Van Ness B, James CD, Kurtin PJ, Henderson K, Ahmann GJ, et al. Tumor suppressor p16 methylation in multiple myeloma: biological and clinical implications. Blood. 2007;109(3):1228-32.

48. Seidl S, Ackermann J, Kaufmann H, Keck A, Nosslinger T, Zielinski CC, Drach J, Zochbauer-Muller S. DNA-methylation analysis identifies the E-cadherin gene as a potential marker of disease progression in patients with monoclonal gammopathies. Cancer. 2004;100(12):2598-606.

49. de Carvalho F, Colleoni GW, Almeida MS, Carvalho AL, Vettore AL. TGFbetaR2 aberrant methylation is a potential prognostic marker and therapeutic target in multiple myeloma. Int J Cancer. 2009;125(8):1985-91.

50. Busque L, Patel JP, Figueroa ME, Vasanthakumar A, Provost S, Hamilou Z, Mollica L, Li J, Viale A, Heguy A, et al. Recurrent somatic TET2 mutations in normal elderly individuals with clonal hematopoiesis. Nat Genet. 2012;44(11):1179-81.

51. Issa ME, Takhsha FS, Chirumamilla CS, Perez-Novo C, Vanden Berghe W, Cuendet M. Epigenetic strategies to reverse drug resistance in heterogeneous multiple myeloma. Clin Epigenetics. 2017;9:17.

52. Martinez-Garcia E, Popovic R, Min DJ, Sweet SM, Thomas PM, Zamdborg L, Heffner A, Will C, Lamy L, Staudt LM, et al. The MMSET histone methyl transferase switches global histone methylation and alters gene expression in t(4;14) multiple myeloma cells. Blood. 2011;117(1):211-20.

53. Kuo AJ, Cheung P, Chen K, Zee BM, Kioi M, Lauring J, Xi Y, Park BH, Shi X, Garcia BA, et al. NSD2 links dimethylation of histone H3 at lysine 36 to oncogenic programming. Mol Cell. 2011;44(4):609-20.

54. de Krijger I, van der Torre J, Peuscher MH, Eder M, Jacobs JJL. H3K36 dimethylation by MMSET promotes classical non-homologous end-joining at unprotected telomeres. Oncogene. 2020;39(25):4814-27.

55. Ohguchi H, Hideshima T, Anderson KC. The biological significance of histone modifiers in multiple myeloma: clinical applications. Blood Cancer J. 2018;8(9):83.

56. Croonquist PA, Van Ness B. The polycomb group protein enhancer of zeste homolog 2 (EZH 2) is an oncogene that influences myeloma cell growth and the mutant ras phenotype. Oncogene. 2005;24(41):6269-80.

57. Pawlyn C, Bright MD, Buros AF, Stein CK, Walters Z, Aronson LI, Mirabella F, Jones JR, Kaiser MF, Walker BA, et al. Overexpression of EZH2 in multiple myeloma is associated with poor prognosis and dysregulation of cell cycle control. Blood Cancer J. 2017;7(3):e549.

58. Popovic R, Martinez-Garcia E, Giannopoulou EG, Zhang Q, Zhang Q, Ezponda T, Shah MY, Zheng Y, Will CM, Small EC, et al. Histone methyltransferase MMSET/NSD2 alters EZH2 binding and reprograms the myeloma epigenome through global and focal changes in H3K36 and H3K27 methylation. PLoS Genet. 2014;10(9):e1004566.

59. Min DJ, Ezponda T, Kim MK, Will CM, Martinez-Garcia E, Popovic R, Basrur V, Elenitoba-Johnson KS, Licht JD. MMSET stimulates myeloma cell growth through microRNA-mediated modulation of c-MYC. Leukemia. 2013;27(3):686-94.

60. Handa H, Murakami Y, Ishihara R, Kimura-Masuda K, Masuda Y. The Role and Function of microRNA in the Pathogenesis of Multiple Myeloma. Cancers (Basel). 2019;11(11).

61. Rajkumar SV, Dimopoulos MA, Palumbo A, Blade J, Merlini G, Mateos MV, Kumar S, Hillengass J, Kastritis E, Richardson P, et al. International Myeloma Working Group updated criteria for the diagnosis of multiple myeloma. Lancet Oncol. 2014;15(12):e538-48.

62. Ludwig H, Sonneveld P, Davies F, Blade J, Boccadoro M, Cavo M, Morgan G, de la Rubia J, Delforge M, Dimopoulos M, et al. European perspective on multiple myeloma treatment strategies in 2014. Oncologist. 2014;19(8):829-44.

63. Keats JJ, Chesi M, Egan JB, Garbitt VM, Palmer SE, Braggio E, Van Wier S, Blackburn PR, Baker AS, Dispenzieri A, et al. Clonal competition with alternating dominance in multiple myeloma. Blood. 2012;120(5):1067-76.

64. Engelhardt M, Terpos E, Kleber M, Gay F, Wasch R, Morgan G, Cavo M, van de Donk N, Beilhack A, Bruno B, et al. European Myeloma Network recommendations on the evaluation and treatment of newly diagnosed patients with multiple myeloma. Haematologica. 2014;99(2):232-42.

65. Durie BGM, Hoering A, Abidi MH, Rajkumar SV, Epstein J, Kahanic SP, Thakuri M, Reu F, Reynolds CM, Sexton R, et al. Bortezomib with lenalidomide and dexamethasone versus lenalidomide and dexamethasone alone in patients with newly diagnosed myeloma without intent for immediate autologous stem-cell transplant (SWOG S0777): a randomised, open-label, phase 3 trial. Lancet. 2017;389(10068):519-27.

66. Goldschmidt H, Ashcroft J, Szabo Z, Garderet L. Navigating the treatment landscape in multiple myeloma: which combinations to use and when? Ann Hematol. 2019;98(1):1-18.

67. Foundation IM. Understanding High-Dose Therapy with Stem Cell Rescue. 2018.

68. Thirumaran R, Prendergast GC, Gilman PB. Chapter 7 - Cytotoxic Chemotherapy in Clinical Treatment of Cancer. In: Prendergast GC, Jaffee EM, editors. Cancer Immunotherapy. Burlington: Academic Press; 2007. p. 101-16.

69. Pommier Y, Leo E, Zhang H, Marchand C. DNA Topoisomerases and Their Poisoning by Anticancer and Antibacterial Drugs. Chemistry & Biology. 2010;17(5):421-33.

70. Ito S. Proteasome Inhibitors for the Treatment of Multiple Myeloma. Cancers (Basel). 2020;12(2).

71. Nunes AT, Annunziata CM. Proteasome inhibitors: structure and function. Semin Oncol. 2017;44(6):377-80.

72. Niewerth D, Jansen G, Assaraf YG, Zweegman S, Kaspers GJ, Cloos J. Molecular basis of resistance to proteasome inhibitors in hematological malignancies. Drug Resist Updat. 2015;18:18-35.

73. Davies FE, Raje N, Hideshima T, Lentzsch S, Young G, Tai YT, Lin B, Podar K, Gupta D, Chauhan D, et al. Thalidomide and immunomodulatory derivatives augment natural killer cell cytotoxicity in multiple myeloma. Blood. 2001;98(1):210-6.

74. Schafer PH, Gandhi AK, Loveland MA, Chen RS, Man HW, Schnetkamp PP, Wolbring G, Govinda S, Corral LG, Payvandi F, et al. Enhancement of cytokine production and AP-1 transcriptional activity in T cells by thalidomide-related immunomodulatory drugs. J Pharmacol Exp Ther. 2003;305(3):1222-32.

75. Corral LG, Haslett PA, Muller GW, Chen R, Wong LM, Ocampo CJ, Patterson RT, Stirling DI, Kaplan G. Differential cytokine modulation and T cell activation by two distinct classes of thalidomide analogues that are potent inhibitors of TNF-alpha. J Immunol. 1999;163(1):380-6.

76. Costa F, Vescovini R, Bolzoni M, Marchica V, Storti P, Toscani D, Accardi F, Notarfranchi L, Dalla Palma B, Manferdini C, et al. Lenalidomide increases human dendritic cell maturation in multiple myeloma patients targeting monocyte differentiation and modulating mesenchymal stromal cell inhibitory properties. Oncotarget. 2017;8(32):53053-67.

77. Quach H, Ritchie D, Stewart AK, Neeson P, Harrison S, Smyth MJ, Prince HM. Mechanism of action of immunomodulatory drugs (IMiDS) in multiple myeloma. Leukemia. 2010;24(1):22-32.

78. Kortum KM, Zhu YX, Shi CX, Jedlowski P, Stewart AK. Cereblon binding molecules in multiple myeloma. Blood Rev. 2015;29(5):329-34.

79. Shaffer AL, Emre NC, Lamy L, Ngo VN, Wright G, Xiao W, Powell J, Dave S, Yu X, Zhao H, et al. IRF4 addiction in multiple myeloma. Nature. 2008;454(7201):226-31.

80. Mondala PK, Vora AA, Zhou T, Lazzari E, Ladel L, Luo X, Kim Y, Costello C, MacLeod AR, Jamieson CHM, et al. Selective antisense oligonucleotide inhibition of human IRF4 prevents malignant myeloma regeneration via cell cycle disruption. Cell Stem Cell. 2021.

81. Laubach JP, Paba Prada CE, Richardson PG, Longo DL. Daratumumab, Elotuzumab, and the Development of Therapeutic Monoclonal Antibodies in Multiple Myeloma. Clin Pharmacol Ther. 2017;101(1):81-8.

82. van de Donk N, Usmani SZ. CD38 Antibodies in Multiple Myeloma: Mechanisms of Action and Modes of Resistance. Front Immunol. 2018;9:2134.

83. Mikkilineni L, Kochenderfer JN. CAR T cell therapies for patients with multiple myeloma. Nat Rev Clin Oncol. 2021;18(2):71-84.

84. Information AP. Bristol Myers Squibb. March 2021.

85. Burwick N, Sharma S. Glucocorticoids in multiple myeloma: past, present, and future. Ann Hematol. 2019;98(1):19-28.

86. Stahn C, Lowenberg M, Hommes DW, Buttgereit F. Molecular mechanisms of glucocorticoid action and selective glucocorticoid receptor agonists. Mol Cell Endocrinol. 2007;275(1-2):71-8.

87. Greenstein S, Ghias K, Krett NL, Rosen ST. Mechanisms of glucocorticoid-mediated apoptosis in hematological malignancies. Clin Cancer Res. 2002;8(6):1681-94.

88. Fratta E, Montico B, Rizzo A, Colizzi F, Sigalotti L, Dolcetti R. Epimutational profile of hematologic malignancies as attractive target for new epigenetic therapies. Oncotarget. 2016;7(35):57327-50.

89. Wang W, Wang J, Chen M, Liang Y, Li Z, Zhang Z, Jing H. 5-Azacitidine Remolds the Methylation Status and Inhibits Growth in Multiple Myeloma. Blood. 2015;126(23):4817-.

90. Khouri J, Faiman BM, Grabowski D, Mahfouz RZ, Khan SN, Wei W, Valent J, Dean R, Samaras C, Jha BK, et al. DNA methylation inhibition in myeloma: Experience from a phase 1b study of low-dose continuous azacitidine in combination with lenalidomide and low-dose dexamethasone in relapsed or refractory multiple myeloma. Semin Hematol. 2021;58(1):45-55.

91. Zhou J, Shen Q, Lin H, Hu L, Li G, Zhang X. Decitabine shows potent anti-myeloma activity by depleting monocytic myeloid-derived suppressor cells in the myeloma microenvironment. J Cancer Res Clin Oncol. 2019;145(2):329-36.

92. Jabbour E, Short NJ, Montalban-Bravo G, Huang X, Bueso-Ramos C, Qiao W, Yang H, Zhao C, Kadia T, Borthakur G, et al. Randomized phase 2 study of low-dose decitabine vs low-dose azacitidine in lower-risk MDS and MDS/MPN. Blood. 2017;130(13):1514-22.

93. Yee AJ, Raje NS. Panobinostat and Multiple Myeloma in 2018. Oncologist. 2018;23(5):516-7.

94. Catley L, Weisberg E, Kiziltepe T, Tai YT, Hideshima T, Neri P, Tassone P, Atadja P, Chauhan D, Munshi NC, et al. Aggresome induction by proteasome inhibitor bortezomib and alpha-tubulin hyperacetylation by tubulin deacetylase (TDAC) inhibitor LBH589 are synergistic in myeloma cells. Blood. 2006;108(10):3441-9.

CHAPTER 2

Therapy Resistance in Multiple Myeloma:
Past, Present, and Future

Chapter 2:

Therapy Resistance in Multiple Myeloma: Past, Present, and Future

Despite the considerable number of treatment options, MM remains difficult to treat. Patients often relapse or become refractory after one or more successive treatment regimens, mostly due to (multiple) therapy resistance. Several mechanisms, which will be discussed in this chapter, contribute to the development of drug resistance. Some of these directly impact MM cells while others rather affect the BM environment. The development of novel treatment strategies therefore heavily relies on achieving a better understanding of the pathways involved in MM drug resistance. In this PhD thesis work, alternative therapy regimens, including kinase inhibition, treatment with natural compounds, and ferroptosis induction, have been explored to overcome MM drug resistance.

2.1. Causes of Therapy Resistance in Multiple Myeloma

Multi-drug resistance (MDR) is a phenomenon where cancer cells become cross-resistant to structurally and functionally unrelated drugs [1]. Development of MDR is typically multifactorial and is caused by (epi)-genetic alterations, a dysfunctional tumor microenvironment, dysregulation of apoptosis signaling pathways, abnormal drug transport and metabolism, the persistence of CSCs, tumor heterogeneity, and other specific mechanisms for mAb immunotherapy (Figure 1) [2]. These cellular and molecular alterations make that cancers are either inherently untreatable or acquire resistance to a wide variety of anticancer drugs.

2.1.1. Genetic and Epigenetic Alterations Influencing Drug Resistance

As discussed in Chapter 1, MM is characterized by the presence of various (epi)genetic changes. Some of these are associated with therapeutic failure, worse prognosis, and higher relapse rates. For example, patients harboring t(4;14) translocations and corresponding MMSET and FGFR3 overexpression have shorter overall survival times and display increased resistance to alkylating agents [3]. Alternatively, mutations in drug-target regions have also been attributed to specific drug resistances in MM. Missense mutations in the proteasome 20S subunit beta 5 (PSMB5) gene, for instance, drastically lower the effects of PI bortezomib, and have even been described to be responsible for resistance to next-generation PIs carfilzomib and ixazomib as well [4, 5]. Similar to bortezomib, these latter PIs interfere with the catalytic N-terminal threonine residue by occupying the PSMB5 substrate binding pocket. Point mutations in the PSMB5 gene severely impair PI binding but also reduce proteasome activity, explaining why the majority of bortezomib-resistant patients exhibit a compensatory PSMB5 upregulation [6]. Similarly, acquired resistance to IMiDs, such as lenalidomide or pomalidomide, is associated with mutations, copy number loss, and structural variations in the cereblon gene [7]. It is estimated that one-third of MM

patients carry cereblon mutations by the time they are refractory to pomalidomide therapy [7]. A final example highlighting the importance of genetic alterations in drug resistance can be found in GC-resistant MM. Chronic exposure to DEX in MM cells is reported to induce expression of a truncated GR mRNA carrying a 3' end deletion lacking a significant portion of the hormone binding domain [8].
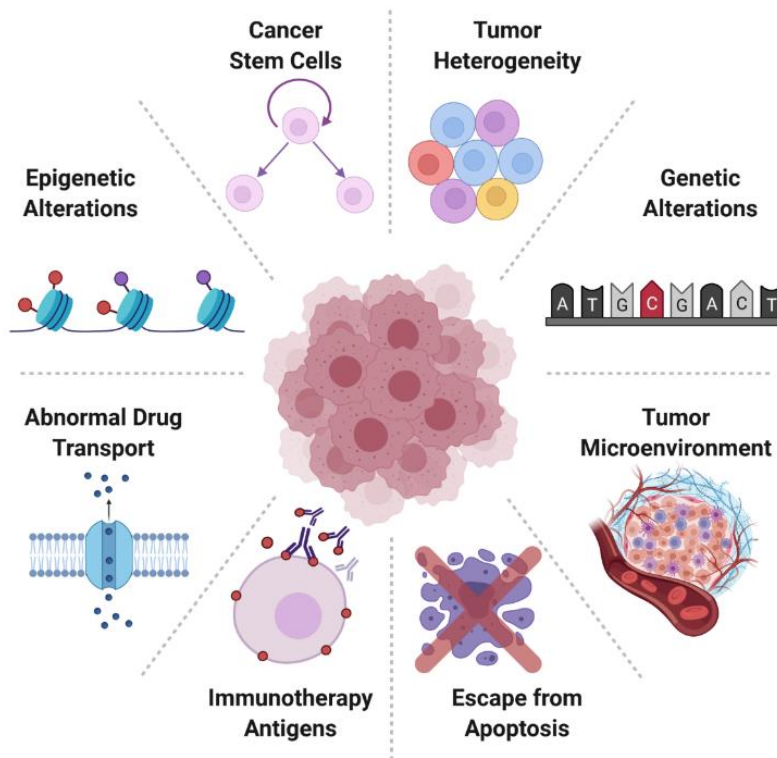
Figure 1: Mechanisms of multi-drug resistance of refractory and relapse multiple myeloma (MM). Adapted from [2] and created with BioRender.com.

DEX resistance has also been linked to epigenetic changes. Nojima and colleagues demonstrated that promotor hypermethylation of the Ras-related dexamethasone induced 1 (RASD1) gene correlated with reduced sensitivity to DEX treatment, which could be reversed by erasing DNA methylation marks with DAC [9]. In line with this observation, promotor hypermethylation of tumor suppressor genes, including glutathione peroxidase 3 (GPX3) and transforming growth factor beta (TGFB), may be involved in chemotherapy resistance [10, 11]. Next to hypermethylation, hypomethylation has been linked to drug resistance as well, especially when demethylation occurs in promotor regions of drug transporters. ATP-binding Cassette (ABC) solute transporters, such as ABCG2, are reported to be upregulated in MM patients as a results of global hypomethylation [12]. Given that these transporters are responsible for the efflux of xenobiotic and endogenous metabolites, they promote MDR by transporting commonly used MM drugs (i.e. PIs, IMiDs, alkylating agents,…) to the extracellular environment [13]. Finally, miRNAs and long non-coding RNAs (lncRNAs) are known to impact MDR development too by modulating expression of cell cycle related proteins, drug targets, drug-transporter proteins, and apoptosis signaling proteins [14, 15]. Although it remains challenging to link dysregulated

miRNAs directly to drug resistance, miR-137/197, miR-21, and miR-221/222 are reported to negatively modulate sensitivity to chemotherapy, GCs and PIs (reviewed in [16]). Their potential application as therapeutic targets, however, still needs to be further explored.

2.1.2. Intra-Tumor Heterogeneity

Beside the extensive inter-patient (epi)genomic heterogeneity, intra-tumor clonal heterogeneity poses a significant challenge to successful personalized therapy in myeloma [17-19]. Within a same tumor specimen, distinct tumor populations with different genomic and biological variations can coexist (Figure 2). Next-generation sequencing (NGS) and single cell sequencing techniques revealed the presence of two to six major myeloma subclones at presentation [20]. Currently, two hypotheses aim to explain the origin of the clonal mosaic observed in MM. The Darwinian model states that the occurrence of new mutations results in an improved adaptation of clones, outgrowing the previously dominant tumor clones [21]. In line with this theory, Melchor et al. observed clonal extinction and the emergence of new clones that acquire mutations during treatment [20]. In contrast, the branching evolution theory states that, during treatment, MM clones emerge from a common (drug-resistant) ancestor and that different clones dominate at the diagnosis and relapse of MM [22]. Both models of MM progression and evolution have considerable implications for diagnostic and therapeutic strategies in the clinic.
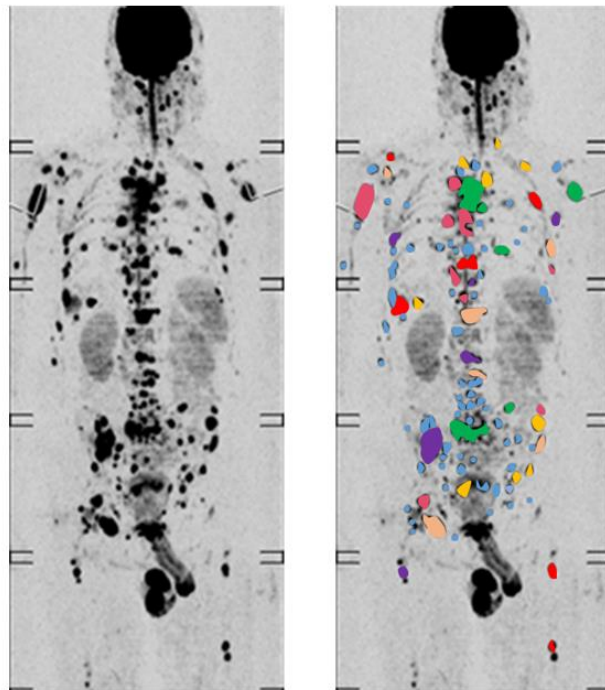

Figure 2: CT-image displaying the intra-tumor heterogeneity in multiple myeloma (MM). Colored spots indicate the presence of different focal lesions identified by multi-region sequencing of CT-guided fine needle aspirates [18].

2.1.3. Abnormal Drug Transport in MM

Of all identified efflux transporters, P-glycoprotein (P-gp) is the best characterized multidrug resistance protein [17, 23]. Similar to ABCG2, P-gp is an ABC solute transporter that is highly expressed in relapsed patients compared to non-treated MM patients [24]. This upregulation in P-gp expression significantly contributes to development of drug resistant cells by decreasing the intracellular accumulation of (chemo)therapeutic substances, hampering their therapeutic efficacy [17]. Most MM drugs, including lenalidomide, carfilzomib, and bortezomib, have been described as P-gp substrates [25-28]. Remarkably, a recent study investigating bortezomib resistance in MM cell lines demonstrated that P-gp inhibition did not enhance PI therapeutic efficacy [29]. This suggests that therapeutic targeting of P-gp overexpression might not be of clinical interest. However, further (pre)clinical experiments need to further confirm this hypothesis.

2.1.4. Persistence of Multiple Myeloma Cancer Stem Cells

The majority of malignant MM cells display a terminally differentiated and quiescent phenotype. This implies that a minor subpopulation of CSCs, which exhibit both self-renewal and differentiation properties, is responsible for tumor replenishment and relapse [30-32]. CSCs portray enhanced DNA damage repair mechanisms, overexpression of MDR efflux pumps, increased evasion from the immune system and cell death pathways, and greater cellular plasticity, explaining why they have been suggested as the main cells responsible for drug resistance development [2, 33]. It is hypothesized that both autonomous and tumor microenvironment (TME) signals trigger survival and self-renewal of CSCs [17, 33]. However, the MM CSCs theory remains somewhat controversial due to lack of real CSCs markers [10, 17]. Yet, in 2004, Matsui and colleagues were able to identify the absence of cell surface antigen syndecan-1 (CD138) expression as an important clonogenic marker in MM cell lines and BM-derived MM samples [34, 35]. Their experiments revealed that, in contrast to CD138$^+$ PCs, CD138$^-$ demonstrate a greater clonogenic and self-renewal potential *in vitro* [34]. Future functional assays of CD138$^-$ cells will have to confirm whether this cell population indeed actively contributes to MM drug resistance.

CSCs are believed to promote therapy resistance through several molecular mechanisms. Firstly, CSCs highly express members ABC transporter superfamily and are characterized by an increased drug efflux (cfr. Section 2.1.3) [36]. Secondly, the (drug) metabolism in CSCs differs from that in normal stem cells. Aldehyde dehydrogenase 1 (ALDH1), for example, is a detoxification enzyme that is frequently upregulated in MM CSCs [37]. ALDH enzymes are known to regulate multiple pathways that potentially contribute to carcinogenesis, such as ROS signaling and DNA damage, and have been associated with stem cell regulation [38]. Inhibition of ALDH1 might therefore be a promising therapeutic targets to eradicate MM CSCs. Indeed, a preliminary study in ALDH$^+$ MM cell demonstrated that the ALDH inhibitor disulfiram abolished MM clonogenicity and reduced tumor growth [39]. Other signaling pathways that govern self-renewal in MM CSCs and might be of interest as therapeutic targets include Hedgehog signaling (HH), Wnt signaling, and Notch signaling [40]. Aberrant

activity of these three pathways have been described in CSC populations, including in MM models [40-42]. Alternatively, inhibiting self-renewal of MM CSCs might be accomplished by drug-induced differentiation of the stem cell population [43]. Although further research is needed to test this differentiation strategy in MM, all-trans retinoic acid (ATRA)-induced stem cell differentiation in glioblastoma resulted in therapy-sensitizing effects *in vitro* and induced anti-tumor effects *in vivo* [44].

2.1.5. Apoptosis Evasion

Apoptosis is a form of regulated cell death that allows for the elimination of damaged or redundant cells through activation of major signaling pathways, such as NF-κB, PI3K/AKT, and the proteasome pathway. One of the major cancer hallmarks is the ability of tumor cells to evade apoptotic cell death through the upregulation of anti-apoptotic or pro-survival proteins [45]. These evasion mechanisms not only contribute to tumorigenesis but also protect cancer cells from drug-induced apoptosis [17]. Increased protein expression of anti-apoptotic factors B-cell lymphoma 2 (Bcl-2) and myeloid cell leukemia sequence 1 (Mcl-1) is associated with MM cell survival [46-49]. Overexpression of both proteins shifts the balance towards cell survival by sequestering pro-apoptotic proteins, such as Bcl-2-associated protein (Bax), and by subsequently inhibiting activation of caspase enzymes, the executioners of apoptosis. In MM, the synthesis of both Bcl-2 and Mcl-2 is often promoted by the constitutive activation of (non-)canonical NF-κB signaling [50]. Anti-MM drugs that target NF-κB-mediated overexpression of Bcl-2 and Mcl-1 might prove useful in overcoming drug resistance [51]. To date, however, no specific NF-κB inhibitor has been approved for treating MM. Alternatively, pro-survival signaling pathways, including NF-κB and PI3K/AKT signaling, can also be targeted by inhibition of upstream regulators. For example, inhibition of heat-shock protein 90 (Hsp90), a cytosolic ATP-dependent chaperone protein that stabilizes a plethora of polypeptides and protects them from proteolytic degradation [52, 53], successfully disturbs pro-survival signaling pathways [52, 54].

2.1.6. Tumor Microenvironment

MM homing to the BM is orchestrated by expression of cellular adhesion molecules, such as lymphocyte function associated antigen-1 (LFA-1) on MM cells and intercellular adhesion molecule-1 (ICAM1) on BM stromal cells [55]. Additionally, BM-secreted cytokines, including IL-6, insulin-like growth factor 1 (IGF-1), RANKL, TNF-α, vascular endothelial growth factor (VEGF), and stromal cell-derived factor 1 (SDF1) further modulate MM cell adhesion by upregulating cell surface adhesion molecules through stimulation of the NF-κB signaling pathway [14, 56]. This intricate crosstalk between the BM TME and MM cells is crucial in myelomagenesis and regulation of tumor growth and survival [57]. Furthermore, the TME can mediate *de novo* therapy resistance, a process known as environment-mediated drug resistance (EMDR), by protecting cancer cells from chemotherapy, radiotherapy or receptor-targeting drugs. Generally, EMDR can be

classified into two categories: soluble factor mediated drug resistance (SFMDR) and cell adhesion mediated drug resistance (CAMDR) [58]. SFMDR relies on the secretion of cytokines, chemokines and growth factors by BM stromal or MM cells. These soluble factors act on several cell targets and regulate crucial processes, such as cell migration, cell growth, angiogenesis, and apoptosis [58]. A key example of a soluble factor crucial for MM growth and survival, is IL-6. Paracrine and autocrine secretion of IL-6 by BM stromal and MM cells is associated with dexamethasone, bortezomib, and thalidomide resistance [59, 60]. Through activation of MAPK, JAK/STAT3, and PI3K/AKT signaling pathways, IL-6 protects tumor cells by upregulating of several anti-apoptotic proteins, including c-Myc. IL-6 also enhances secretion of angiogenic factors and stimulates tumor migration and invasion [61].

The second category, CAMDR, promotes MM survival and resistance to the cytotoxic effects of anti-cancer drugs through the interaction with stromal cells or other extracellular matrix components. Studies in cell lines and primary MM cells have demonstrated the involvement of CAMDR in doxorubicin, melphalan, and dexamethasone drug resistance [62, 63]. One of the pathways mediating CAMDR, is Notch signaling [64]. Notch activation enhances β1 integrin affinity for fibronectin and promotes drug resistance through perturbation of cell cycle progression, thereby lowering the efficacy of anti-cancer drugs targeting proliferating cells [65-67].

2.1.7. Other Mechanisms Contributing to mAb Therapy Resistance

Some MM patients are non-responsive to specific mAb treatment regimens. The underlying resistance mechanisms against mAbs are not fully understood but appear to be different from those observed in other anti-MM drugs [68]. Preclinical data from daratumumab resistance studies suggest that CD38 expression on MM cells is an important factor in predicting primary (but not acquired) resistance towards CD38-directed Abs [69, 70]. Additionally, mAb-induced cytotoxicity in MM cells could be impaired by overexpression of soluble or membrane-bound complement inhibitor proteins, including CD46, CD56, and CD59, that interfere with the effector functions of the mAbs [70]. *In vitro* experiments in MM cell lines could correlate low CD56 and CD59 expression with increased susceptibility to daratumumab [68]. However, these results could not be confirmed in primary MM cells or in the GEN501 and SIRIUS daratumumab phase II trials [68]. Finally, soluble forms of CD38 and SLAMF7 might also affect daratumumab and elotuzumab activity, respectively, by reducing specific binding to MM cells [71]. However, only a limited number of MM patients have displayed measurable levels of soluble CD38 and none of them were resistant to daratumumab treatment [69].

2.2. Overcoming Therapy Resistance with Novel Treatment Strategies

To overcome therapy resistance in MM, numerous efforts are being made to discover novel diagnostic, prognostic, and therapeutic biomarkers and to identify druggable targets that may improve current treatments [72, 73]. In this section, three promising therapeutic strategies for MM are discussed.

2.2.1. Targeting Protein Kinases in MM

Every living cell has to rely on efficient communication pathways for its survival. At any given moment, millions of different signaling cues reach the cell and these have to be processed efficiently in order to generate the appropriate response. This requires the presence of an accurate and fast communication network that is able to both distinguish and transmit these different kinds of information to the correct cellular compartment. One of the most important players in this vast network of signaling transduction are PKs. This family of proteins consists of more than 500 different kinases and plays a role in a plethora of vital cellular processes, including differentiation, cell death, cell mobility, cell cycle proliferation, and many more [74]. This diversity in function is also reflected at the gene level: almost 2% of all eukaryotic genes are translated in kinases, making them one of the largest eukaryotic gene families [75]. All eukaryotic kinases are able to convey cellular signals by catalyzing the transfer of γ-phosphate of a purine nucleotide triphosphate (i.e. adenosine triphosphate (ATP) or guanosine triphosphate (GTP)) to hydroxyl groups of their substrate (Figure 3a). In this reaction, protein alcohol and/or phenolic groups, present on serine/threonine and tyrosine protein residues respectively, serve as phosphate acceptors and help generate phosphate monoesters [74].

Regulating protein activity through phosphorylation and dephosphorylation offers many advantages [76]. Since the addition of phosphate groups only takes a few seconds, it allows for rapid signal transduction. Furthermore, it is easily reversible and does not require the synthesis of new proteins, making it a highly efficient manner of communication. The addition of phosphate groups to a protein significantly alters its properties. It can, for instance, impact enzymatic activity and function as a regulatory 'on/off switch'. A well-studied example of this phenomenon is the phosphorylation of AKT, a PK which relies on the phosphorylation of its Ser and Thr residues in order to execute its function as cell survival regulator [77]. Additionally, phosphorylation can affect cellular localization and protein-protein interactions, as demonstrated by the transcription factor nuclear factor-κB (NFκB) [78]. In unstimulated cells, NFκB is tethered to IκB inhibitory proteins and remains in its inactive, cytosolic form. Extracellular signals, such as inflammatory stimuli, trigger phosphorylation and dissociation of IκB proteins, and promote NFκB shuttling to the nucleus where it stimulates the transcription of target genes.

However, the process of phosphorylation (and dephosphorylation) is not always straightforward and often involves a signaling cascade wherein kinases interact with

multiple target proteins. These complex phospho-signaling networks are crucial in several cell signaling pathways, such as the AKT or MAPK survival pathways [79]. To date, 538 human kinases have been identified that are classified into 13 subcategories according to the Enzyme Commission. The major representative and most studied groups include protein tyrosine kinases, protein serine/threonine kinases and dual-specificity kinases, which can be further subclassified into receptor - and non-receptor kinases. Alternatively, PKs can be classified based on their conserved protein domains within the catalytic core into 11 groups, 133 families and 137 subfamilies [75, 80-82].

Structurally, all PKs are composed of 12 conserved subdomains that fold into a bi-lobed catalytic core (Figure 3b). The area between the lobes forms a cleft where the adenosine residue of ATP can interact with the kinase 'hinge' region [83]. Outside this active-site cleft, PKs also possess a conserved activation loop with characteristic DFG and APE motifs positioned and the start and the end of the loop, respectively [84]. The activation loop regulates PK activity and typically needs to be phosphorylated to assume an 'active' conformation and to allow for substrate binding [85].
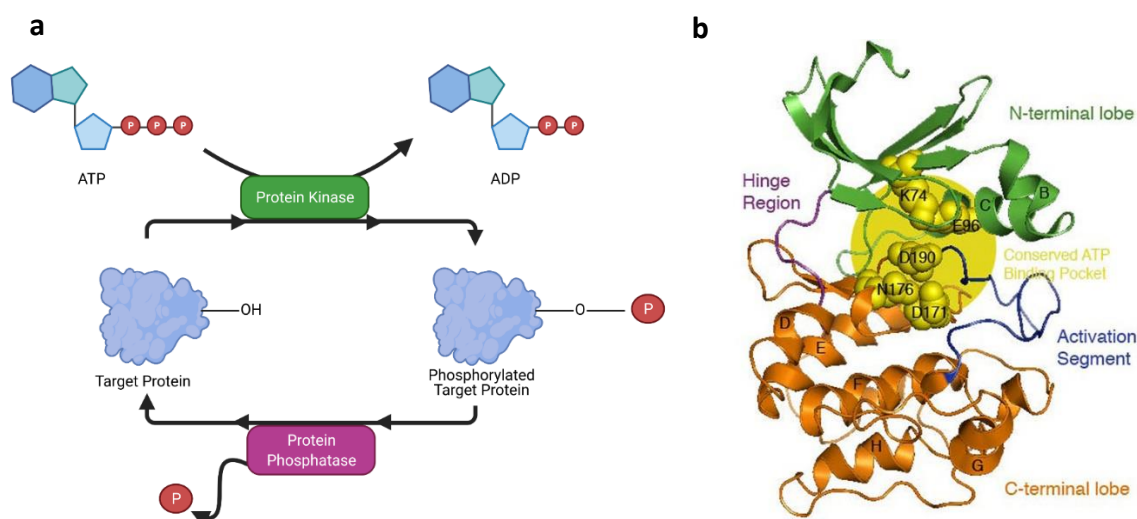
Figure 3: Structure and function of human protein kinases. (**a**) Mechanism of protein (de)phosphorylation by protein kinases and phosphatases. Phosphate groups are indicated as red circles. (**b**) Secondary structure of protein kinases [86]. The model shows an N-terminal (green) and C-terminal (orange) lobe joined together by a hinge region (magenta). The ATP binding pocket (yellow) is blocked by the activation segment (blue) unless the latter is activated by phosphorylation. Abbreviations: ATP = adenosine triphosphate, ADP = adenosine diphosphate. Figure created with BioRender.com.

Given their diverse cellular functions, it is not surprising that dysregulated expression or activity of PKs is involved in the pathogenesis numerous of diseases, including cancer [87]. Indeed, PKs represent the largest group of clinical drug targets in cancer and it is estimated that one quarter of all drug discovery efforts aim to target PKs [88, 89]. So far, 62 kinase inhibitors, targeting more than 20 different PKs, have been FDA-approved and have entered clinical practice in various types of solid and hematological cancers [89]. Based on their binding properties, small-molecule protein kinase inhibitors (PKIs) can be divided into 7 classes (summarized in Table 1 and Figure 4) [84]. Most FDA-approved PKIs to date are

type I inhibitors, ATP-competitive inhibitors that directly bind to the ATP binding pocket of active PKs. In contrast, type II inhibitors recognize the inactive conformation (i.e. activation loop not phosphorylated) of kinases. Type III and IV inhibitors modulate kinase activity in an allosteric manner, and only differ in their binding site relative to the ATP-binding pocket. Type V or bivalent inhibitors aim to target both the ATP-binding site and a unique, kinase-specific feature. Finally, type VI kinase inhibitors covalently bind to their targets.

Table 1: Classification of Protein Kinase Inhibitors (adapted from [89]).

| Inhibitor Type	Properties	FDA-approved drug example
Type I	Binds in and around the ATP-binding pocket of an active kinase	Erlotinib
Type II	Binds in and around the ATP-binding pocket of an inactive kinase	Imatinib
Type III	Allosteric inhibitor bound next to the ATP-binding pocket	Trametinib
Type IV	Allosteric inhibitor bound away from the ATP-binding pocket	N/A
Type V	Bivalent inhibitor spanning two kinase domain regions	N/A
Type VI	Covalent kinase inhibitor	Ibrutinib

N/A, not applicable
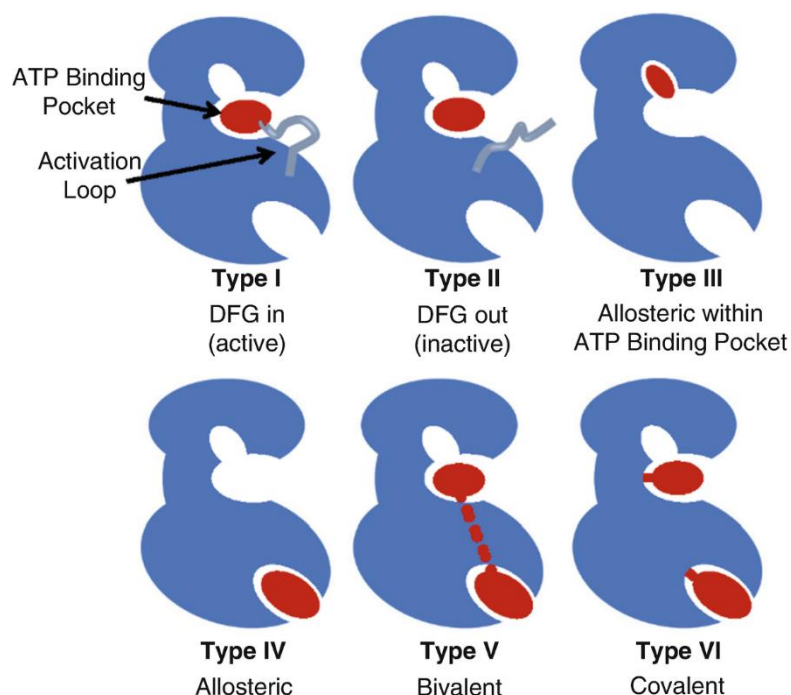
Figure 4: Binding properties of the different classes of protein kinase inhibitors. Red circles indicate the primary binding sites of the inhibitors. Abbreviations: ATP = adenosine triphosphate, DFG = Asp-Phe-Gly motif. From [90]

Despite the major impact of PKIs on the treatment of cancer, including hematological tumors, they have not been approved for use in MM [91]. So far, only two PKIs, namely perifosine and masitinib, have reached phase III MM trials and both trials were prematurely terminated due to failure in efficacy [88]. Nevertheless, encouraging preclinical data strengthens the therapeutic potential of PKIs in MM (summarized in [91]). For instance, a kinome expression profiling performed by de Boussac and colleagues found that 36 kinome-related genes were significantly linked with a prognostic value to MM [92]. Subsequent targeting of these identified PKs, including checkpoint kinase 1 (CHEK1), maternal embryonic leucin zipper kinase (MELK), and lymphokine-activate killer T-cell-originated protein kinase (PBK), significantly reduced the viability of different myeloma cell lines. Similarly, inhibition of other kinase signaling pathways has been reported to hamper MM proliferation and tumor growth (Table 2). Targeting of two pathways in particular, PI3K/AKT/mTOR and JAK/STAT, seem to be highly efficient in eliminating (therapy-resistant) myeloma cells [93, 94]. Both are often hyperactivated in MM and promote cell survival and cell cycle progression. Moreover, AKT and/or STAT3 overexpression and hyperphosphorylation is associated with therapy resistance and poor prognosis [95-100]. In the same way, Bruton tyrosine kinase (BTK), a protein involved in BCR signaling and B-cell survival, has been reported to be elevated in MM and to promote resistance to anti-myeloma drugs through upregulation of stemness genes [101-103]. A recent clinical trial investigating the administration of ibrutinib (IBR), a covalent BTK inhibitor, together with low doses of dexamethasone observed a significantly prolonged progression-free survival in patients receiving the highest dose of IBR [104].

Table 2: Protein kinase inhibitors displaying anti-myeloma activity.

Targeted Kinase	Tyrosine kinase inhibitors	References
IGF1R	Linsitinib, GSK1838705A, GTX-134, Masoprocol	[105-107]
KIT	Amuvatinib, Imatinib, Masitinib	[108-111]
MET	Cabozantinib, Tivantinib	[112-114]
FGFR	Dovitinib	[115, 116]
VEGFR	Nintedanib, Pazopanib, Semaxanib, Vatalanib	[117-122]
STAT3	Atiprimod	[123]
JAK1/2	Brevalin A, Farnesol, Piceatannol	[124-127]
BTK	Acalabrutinib, Ibrutinib	[128, 129]
FAK1	Asiatic acid	[130]
SRC	Dasatinib	[131, 132]
SYK	Fostamatinib	[133, 134]
PI3K	Alpelisib, Idelalisib,	[135-137]
AKT	Tricirbine, Afuresertib	[138-140]
mTOR	Everolimus, Sapanisertib, Cnicin	[141-143]
PIMK	LGB321	[144, 145]

2.2.2. Targeting MM with Natural Compounds: a Withaferin A Perspective

The majority of FDA-approved drugs are natural products and derivatives. Used for millennia in traditional ethnomedicine, herbal treatments are a promising alternative to existing therapies, with lower rates of adverse events and efficiency frequently comparable to that of conventional drugs. Several isolated herbal compounds, such as curcumin, resveratrol, and taxol have demonstrated significant anti-cancer effects and are in clinical use [146]. Combined with other anti-tumoral drugs, they also have the ability to attenuate therapy resistance and exert chemoprotective actions [147]. Therefore, the extensive arsenal of plant compounds is currently being explored and exploited for overcoming therapy resistance in MM [148].

A popular traditional ethnomedicinal herb displaying several anti-cancer properties is *Withania somnifera*, also known as Ashwagandha or Indian Winter Cherry. Roots and berries from this plant have been used for over 3000 years in Ayurvedic medicine and are described to remedy chronic fatigue, dehydration, rheumatism an ulcers [149]. *Withania somnifera* comprises over 35 chemical constituents of which the alkaloids, flavonoids, steroidal lactones and saponins are biologically active. However, the most potent bioactive compound isolated from *Withania somnifera* roots is the highly oxygenated lactone Withaferin A (WA). Studies show that most beneficial health effects of *Withania somnifera*, ranging from anti-inflammatory to anti-cancer effects, can be attributed to WA [150-153]. These effects are mostly accomplished via the covalent binding of WA with target proteins, resulting in a loss of activity of the latter [149]. Three sites in particular, namely the unsaturated A-ring at C3, the epoxide structure at position 5 and C24 in its E-ring, are especially prone to nucleophilic attacks and are often involved in Michael addition alkylation reactions (Figure 5) [149].
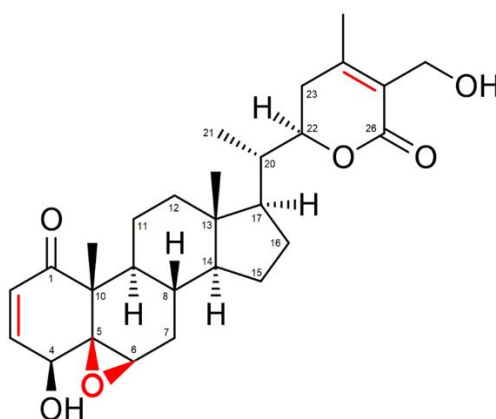

Figure 5: Structure of Withaferin A (WA). Regions prone to nucleophilic attacks are marked in red.

Pharmacokinetic studies in mice have shown that WA has a rapid oral absorption and reaches to peak plasma concentration of around 16.69 ± 4.02 ng/ml within 10 min after oral administration of *Withania somnifera* aqueous extract at a dose of 1000 mg/kg, which

is equivalent to 0.458 mg/kg of WA [154]. Following an intraperitoneal injection of WA in mice at a single 4 mg/kg dose, WA reached a maximum plasma concentration up to 2 µM with a half-life of around 1.4h. This shows that systemic achievable WA concentrations correspond with a pharmacologically therapeutic effective window. Moreover, one month intraperitoneal WA treatment (4mg/kg) in a breast cancer metastasis mouse model, showed dose-dependent inhibition of metastatic lung nodules with limited adverse toxicity, as evaluated by measuring fibrosis and/or necrosis of the pulmonary parenchyma [155]. Occasional reports on weight loss effects upon chronic WA treatment have recently been explained by WA-specific sensitization of leptin receptor signaling [155-157]. Furthermore, a toxicity study in rats identified no-observed-adverse-effects after oral administration of *Withania somnifera* extract with 3% WA at a dose of 2000mg/kg [158]. Recently, the safety and pharmacokinetics of root extract of *Withania somnifera*, containing 4.5% of WA w/w, was evaluated in a phase I trial in patients with advanced stage high-grade osteosarcoma. Up to 4800 mg extract, equivalent to 216 mg of WA per day, was well tolerated in patients without any dose limiting toxicity, revealing a good safety profile for oral administration applications of WA [159].

The anti-cancer activities of WA have been documented in a variety of cancers cells, such as glioblastoma, neuroblastoma, multiple myeloma, leukemia, breast, colon, ovarian, and head and neck cancer [157, 160, 161]. Accumulating reports have corroborated the tumor growth inhibition effect of WA in diverse mouse cancer models (Table 3). In addition, the combination treatment of WA with several therapeutic agents or modalities have been shown to improve efficacy of standard chemotherapy or to overcome drug resistance (Table 4). The molecular mechanism underlying the anti-tumor activity of WA is not completely understood, however, it seems to involve poly-pharmaceutical effects such as targeting cytoskeleton structure and proteasomal system, regulating heat shock protein activity, reactive oxygen species (ROS)-mediated cytotoxicity, inhibition of NF-κB and oncogenic pathways [149, 162, 163].

Table 3: Anti-cancer activities of Withaferin A in mice

Cancer	Animal model	Mechanism	References
Prostate	PC-3 xenograft in nude mice	PAR4-dependent apoptosis	[164]
Prostate	PC-3 xenograft in nude mice	Proteasome inhibition	[165]
Breast	MDA-MB-231 xenograft in nude mice	FOXO3a and Bim-dependent apoptosis	[166]
Breast	MDA-MB-231 xenograft in nude mice	Activation of ERK/RSK and CHOP/Elk1, upregulation of DR5	[167]
Pancreas	Panc-1 xenografts in nude mice	HSP90 inhibition, degradation of Akt and Cdk4	[168]
Medullary thyroid cancer	DRO 81-1 xenografts in nude mice	Inhibition RET proto-oncogen phosphorylation and activation	[169]
Cervical	CaSki xenograft in nude mice	Downregulation of HPV16 E6 and E7, induction of p53 protein levels	[170]

Mammary tumor	Spontaneous mouse mammary carcinoma model	Phosphorylation and disassembly of vimentin	[155]
Ovarian	A2780 xenograft in nude mice	ROS induction and autophagy	[171]
Uveal melanoma	92.1 xenograft in SCID mice	Inhibition of Akt, inhibition of c-MET activation	[172]
Mammary tumor	MMTV-neu mice	Suppression of glycolysis and TCA cycle, inhibition of self-renewal of cancer stem cells	[173, 174]
Ovarian	A2780 xenograft in nude mice	Inhibition of Notch-1, downregulation of cancer stem cells	[175]
Colon	HCT-116 xenograft in nude mice	Inhibition of STAT phosphorylation and activation	[176]
Skin	TPA skin cancer model	Suppression of AP-1 and inhibition of ACC1 gene	[177]
Pancreas	Panc-1 xenografts in nude mice	Mitochondrial dysfunction, ROS induction, PI3K/Akt inactivation	[178]
Colorectal	HCT-116 xenograft in nude mice	Akt inactivation, downregulation EMT markers	[179]
Ovarian	A270 intraperitoneal tumors in nude mice	Targeting cancer stem cells	[180]
Mammary tumor	Spontaneous mouse mammary carcinoma model	Inhibition of Ras-Mnk and PI3K/Akt, inhibition of eIF4E phosphorylation and protein translation, downregulation of c-FLIP	[181]
B-cell lymphoma	A20 allograft in Balb/c mice	HSP90 inhibition	[182]
T-cell ALL	Notch1-mutant T-ALL xenograft in NRG mice	eiIF2A-dependent translation inhibition	[161]
Neuroblastoma	IMR-32 xenograft in nude mice	GPX4 inhibition, HMOX1 activation	[157]

PAR4, prostate apoptosis response 4; FOXO3, Forkhead Box O3; ERK, extracellular-signal-regulated kinase;/RSK, ribosomal S6 kinase; CHOP, CCAAT-enhancer-binding protein homologous protein, DR5, death receptor 5; HSP90, heast shock protein 90; cdk4, cyclin-dependent kinases 4; ROS, reactive oxygene species; EMT, epithelial-mesenchymal transition; MET, mesenchymal epithelial transition; STAT3, signal transducer and activator of transcription 3; AP1, activator protein 1; ACC, acetyl-coa carboxylase; 3-WA, an analogue of WA; mTOR, mammalian target of rapamycin; FLIP, FLICE; fas-associated protein with death domain (FADD)-like IL-1β- converting enzyme; DBZ, γ-secretase inhibitors; ALL, Acute lymphoblastic leukemia; GPX4, glutathione peroxidase 4; HMOX1, heme oxygenase 1.

In context of B-cell malignancies, part of the anti-cancer activity of WA seems to be mediated by inhibition of NF-κB signaling (Figure 6a) [182-184]. As mentioned (cfr. Section 2.1.5. Apoptosis Evasion), this pathway is often constitutively active in MM and promotes evasion of apoptosis through the increased expression of anti-apoptotic proteins. Because of its importance in the regulation of cell survival, the activation of NF-κB is strictly regulated by its cytoplasmic inhibitor IκB. This inhibitor masks the nuclear localization signal of NF-κB, preventing nuclear translocation and subsequent activation of target genes [185]. Upon exposure to certain stimuli however, the IκB inhibitor is phosphorylated by the IκB-kinase (IKK) complex, composed of a regulatory subunit IKKγ (known as NEMO) and two

kinase subunits, IKKα and IKKβ, leading to proteasomal degradation and allowing activation of NF-κB responsive genes. Molecular docking studies demonstrate that WA is able to interfere with the NF-κB pathway by disrupting the formation of the IKK complex and by preventing subsequent IκB degradation [186]. Indeed, *in vitro* studies wherein ABC type diffuse large B-cell lymphoma cell lines were exposed to WA, NF-κB signaling was inhibited through the disruption of IKKγ unit [183]. Besides IKK, WA is able to target other PKs crucial for MM survival. Yco and colleagues demonstrated that WA induces dose-dependent cell death in therapy-resistant MM cell lines by preventing STAT3 dimerization and activation (Figure 6b) [187]. Within these models, WA specifically inhibits phosphorylation of STAT3 at Y705 and thereby blocks STAT3 nuclear translocation.

Table 4: Chemosensitisation effects of Withaferin a in combination treatments

Compound	Cancer cell	Chemosensitization Mechanism	References
WA + TRAIL	Renal cancer cells	Upregulation of DR5, downregulation of c-FLIP	[188]
WA + Sorafenib	Papillary and anaplastic cancer cells	Enhanced cell cycle arrest and apoptosis induction	[189]
WA + Doxorubicin	Epithelial ovarianc cancer cells	Induction of ROS and autophagy	[171]
WA + TRAIL	Breast cancer cells	Enhanced DR5 expression	[167]
WA + Cisplatin	Ovarian cancer cells	Enhanced suppression of cell migration suppression and downregulation of cancer stem cell markers	[175, 190]
WA + Oxaliplatin	Pancreatic cancer cells	Inactivation of PI3K/Akt and induction of oxidative stress	[178]
WA + Doxil	Ovarian cancer cells	Inhibition of ALDH1 and Notch1	[180]
WA + TTFields	Glioblastoma cells	Enhanced cell proliferation inhibition	[191]
WA + DBZ	T-ALL leukemia cells	Inhibition of eIF2A-dependent translation and Notch1 inhibition	[161]

TRAIL, TNF-related apoptosis-inducing ligand; DR5, death receptor 5; FLIP, FLICE (FADD-like IL-1β-converting enzyme)-inhibitory protein; ALDH1, aldehyde dehydrogenase; TTFields, tumor treating fields; GSI, γ-secretase inhibitor.

Although there are several examples demonstrating the interplay between WA and PKs, it sometimes remains uncertain whether any of the observed changes at the kinase level are a direct result of WA interaction or rather a secondary effect. A relevant illustration of the latter is the ability of WA to regulate the activity of HSPs [182], which are highly conserved molecular chaperones involved in the folding, transport, maintenance and assembly of key regulatory proteins like kinases [192]. By targeting and dissociating the CDC37-HSP90 complex, either via blocking the protein cleft of CDC37 [193] or via direct binding of HSP90 itself [168], WA downregulates HSP90 target proteins in B-cell lymphoma models, such as AKT and the IKK-complex (Figure 6c) [182].

Finally, the anti-proliferative effects of WA in MM have also been attributed to growth inhibition of both tumoral cells and CSCs [194]. WA treatment of MM-CSCs resulted in an altered cellular morphology and reduction of stemness markers, suggesting that WA

potentially reduces the self-renewal capacity of CSCs. Remarkably, higher concentrations (≥ 10 μM) of WA are significantly less toxic to normal hematopoietic stem cells compared to CSCs [194]. This indicates that WA portrays a degree of selectivity towards CSCs. However, further optimization might be required to retain or improve WA-CSC selectivity at lower concentrations as well.
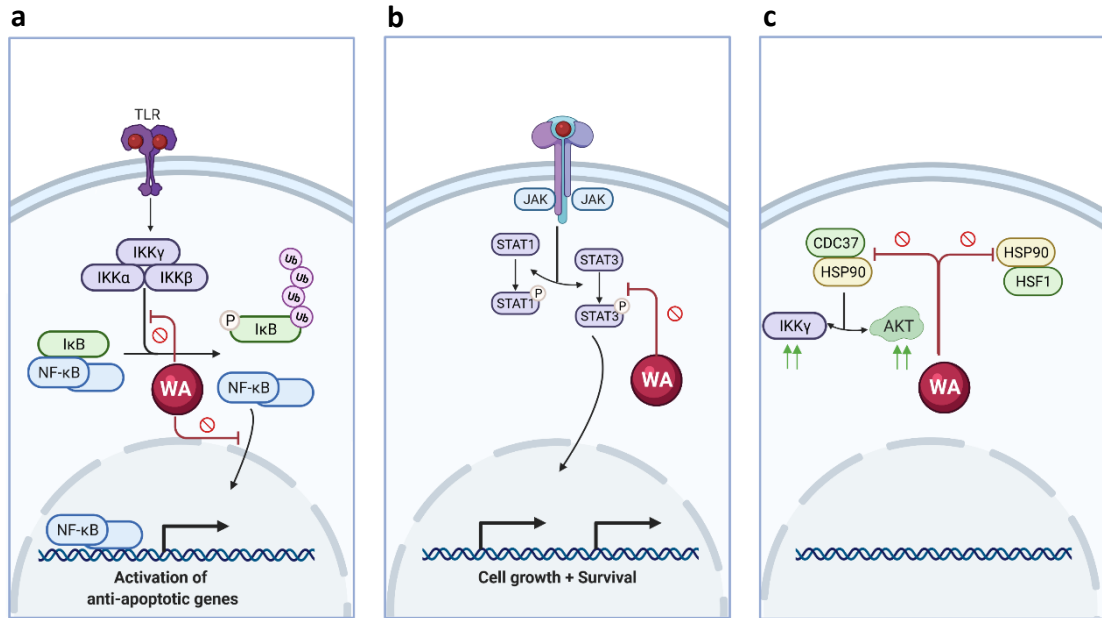

Figure 6: Overview of anti-proliferative effects of WA in B-cell malignancies. (**a**) WA inhibits NF-κB signaling; (**b**) Several kinase signaling pathways, such as AKT/mTOR and JAK/STAT, are regulated by WA. (**c**) WA mediates the heat shock response by inhibiting HSP90. Abbreviations: TLR = Toll-like receptor, IKK = IκB kinase, NF-κB = Nuclear Factor kappa B, WA = Withaferin A, JAK = Janus kinase, STAT = Signal Transducers and Activators of Transcription, PTEN = Phosphatase and Tensin Homolog, PDK1 = Phosphoinositide-dependent kinase-1, HSP90 = Heat Shock Protein 90, HSF1 = Heat Shock Factor 1. Figure created with BioRender.com.

2.2.3. Targeting MM with Ferroptotic Compounds

The majority of anti-cancer drugs within the field of clinical oncology aim to eradicate tumor cells through induction of apoptotic cell death [195]. However, as discussed above (cfr. Section 2.1.5), most cancers gradually acquire resistance to this mode of cell death by upregulating anti-apototic signals and downregulating pro-apoptotic proteins. To bypass treatment failure of apoptotic drugs, an alternative therapeutic strategy could be to explore other modes of cell death as well. Typically, cell death is classified into two classes: apoptosis or regulated cell death (RCD), and necrosis or unregulated cell death. As the name implies, the main difference between both cell death processes lies within their regulatory mechanisms. Apoptosis is a strictly controlled and regulated process, where the cell is carefully dismantled by caspase enzymes without eliciting an inflammatory response [196]. In contrast, necrosis is perceived to be accidentally triggered by environmental stresses and initiates cell swelling and bursting, which is accompanied by the uncontrolled release of pro-inflammatory cellular contents. Yet, research within the cell death field has revealed that this classic apoptosis-versus-necrosis paradigm is a serious oversimplification and does not capture the complexity of cell death process occurring within dying cells [197].

For example, genetic evidence and the discovery of necrosis inhibitors have demonstrated that signaling pathways for regulated necrosis also exist [198-201]. Regulated necrosis is a form of RCD where genetically defined processes orchestrate cytoplasmic granulation, organelle and/or cellular swelling, and eventually cause cellular leakage. Based on the nature of the cell death trigger and initiator mechanisms, regulated necrosis can be further subdivided into several new cell death subroutines (Figure 7) [197].
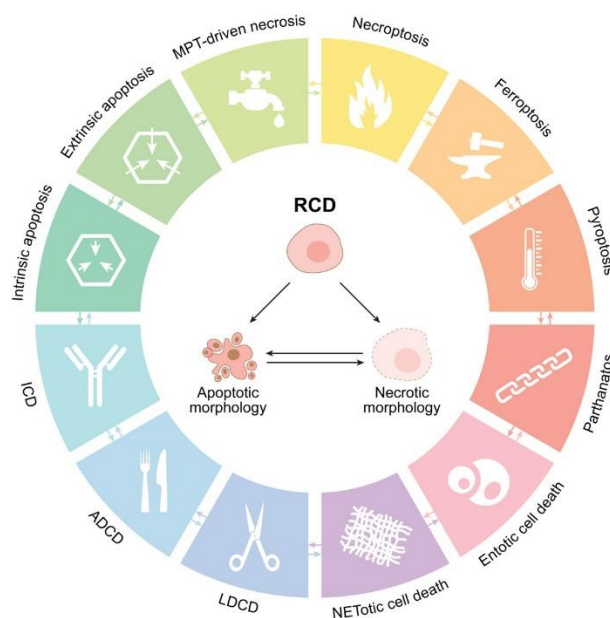
Figure 7: Overview of different modes of regulated cell death identified within mammalian cells. Abbreviations: LDCD = lysosome-dependent cell death, ADCD = autophagy-dependent cell death, ICD = immunogenic cell death, MPT = mitochondrial permeability transition [202].

One form of RCD, which might be of particular interest for MM therapy, is ferroptosis. This type of cell death is highly dependent on intracellular iron levels and is characterized by ROS-mediated lipid peroxidation [203]. Morphologically, ferroptosis is associated with a reduction in mitochondrial volume, an increase in mitochondrial membrane density, a ruptured outer membrane and perinuclear lipid droplet assembly followed by redistribution of lipid droplets [204]. Execution of ferroptosis heavily relies on the iron-catalyzed peroxidation of polyunsaturated fatty acids (PUFAs), which are mainly localized in mammalian cell membranes. The lipid peroxidation cascade can occur either by non-enzymatic free radical chain reaction or by enzyme catalysis (Figure 8). Non-enzymatic lipid peroxidation occurs when iron-triggered ROS, produced during Fenton and Fenton-like reactions (see reaction below), directly oxidize PUFAs.

$$Fe^{2+} + H_2O_2 \rightarrow Fe^{3+} + \bullet OH + OH^- \qquad \text{(Fenton reaction)}$$
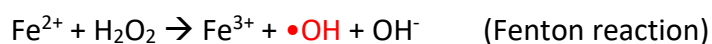
During the initial phases of non-enzymatic lipid peroxidation, free radicals - mainly hydroxyl radicals - will trigger the formation of lipid radicals (L•) by extracting hydrogen from PUFAs (Figure 8). The L• radicals thus produced will then rapidly react with molecular oxygen,

resulting in the production of lipid peroxyl radicals (LOO•) that will propagate the peroxidation reaction by removing another hydrogen atom from adjacent PUFAs to form a new L• and a lipide peroxide (LOOH). This auto-oxidation reaction will continue to amplify lipid radical concentrations, potentially leading to membrane destruction and cell death. Alternatively, propagation of lipid peroxidation can be terminated when two L• or LOO• interact with each other or when endogenous anti-oxidants (e.g. vitamin E) neutralize the radicals by donating electrons. Enzymatic lipid peroxidation is mediated by lipoxygenase (LOX), non-heme iron-containing enzymes that catalyze the oxygenation of PUFAs to generate lipid hydroperoxides (Figure 8) [205]. In humans, six functional LOX genes (ALOX15, ALOX15B, ALOX12, ALOX12B, ALOXE3, and ALOX5) encode six different LOX isoforms [206], of which the ALOX15 gene seems to be especially important for ferroptosis induction [207, 208]. Although the role of LOX in ferroptosis has been doubted in the past due to controversial results [209, 210], recent studies indicate that both non-enzymatic and enzymatic lipid peroxidation are crucial in ferroptosis [211]. How lipid peroxidation mechanistically triggers ferroptosis cell death remains elusive. It is hypothesized that peroxidation of the cell membrane impacts it structure and involves formation of lipid pore complexes [212], increased membrane permeability [213], loss of membrane integrity, and crosslinking and inactivation of essential proteins by toxic end products of lipid hydroperoxides (including 4-hydroxy-2-nonenals or malondialdehydes) [214].

Generally, ferroptosis is initiated when major cellular anti-oxidant or protective systems are depleted and can no longer detoxify reactive lipid peroxide species. Glutathione peroxidase 4 (GPX4) is one of those systems that is extremely important in suppressing iron-catalyzed lipid peroxidation in membranes [215]. Therefore, inhibition of GPX4 by small molecules (subsequently inducing ferroptotic cell death) is heavily being explored as a novel therapeutic strategy to eliminate cancer cells [215]. GPX4 inhibitors can be categorized into two classes [216]. The first class, also known as type I ferroptosis inducing compounds, include erastin and sulfasalazine and indirectly inhibit GPX4 activity by blocking the X_c^- cystine/glutamate antiporter. The X_c^- system orchestrates the intracellular import of cystine and is crucial for glutathione (GSH) synthesis. Given that GSH serves as a cofactor for GPX4, blocking the cellular cystine supply will result in accumulation of lipid ROS species and promotes ferroptotic cell death [206]. Type II ferroptosis inducing compounds, such as RSL3 and ML162, directly inhibit GPX4 activity through covalent interaction with the selenocysteine present in the active site of GPX4 [215]. Other types of ferroptosis inducers have been identified as well (reviewed in [217]) and target intracellular iron concentrations rather than GPX4 activity. Both class I and II compounds have demonstrated anti-cancer efficacy in different cancer models [215, 218-220]. Indeed, most cancer cells require higher intracellular iron levels and a higher lipid metabolism to accommodate for their increased proliferation speed [221]. This is also observed in MM cells, where malignant PCs are reported to have higher levels of iron than non-malignant cells, explaining why many MM patients suffer from anemia [222].
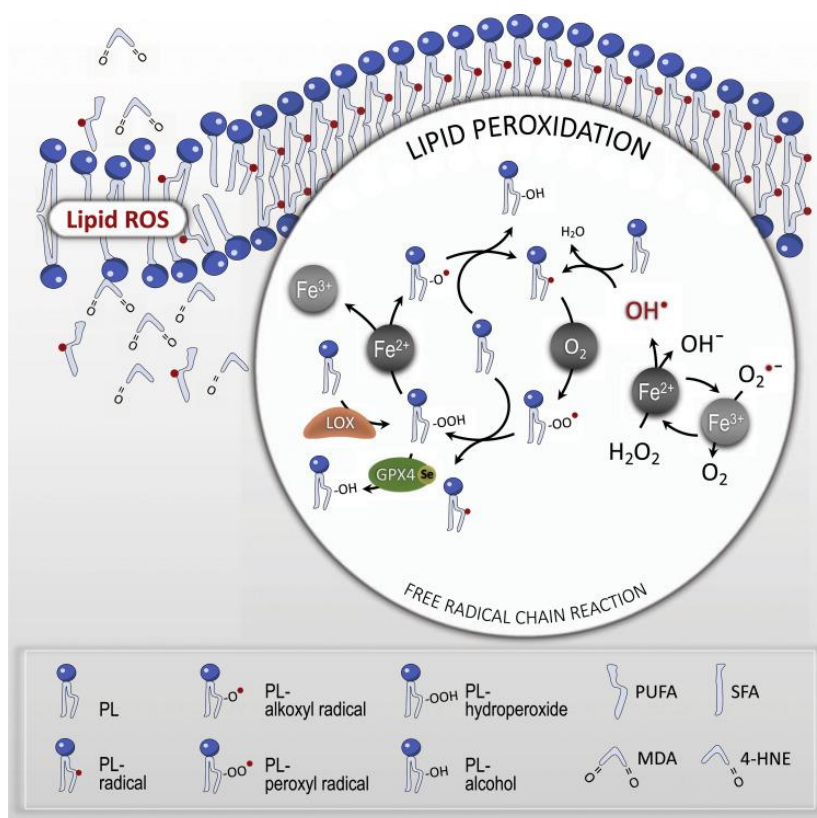
Figure 8: Lipid peroxidation cascade in ferroptosis. During Fenton reactions, ferrous iron (Fe^{2+}) is oxidized to ferric (Fe^{3+}) iron through reaction with hydrogen peroxide (H_2O_2), forming highly reactive hydroxyl radicals (•OH). In non-enzymatic lipid peroxidation or lipid autoxidation cascade, these •OH radicals will abstract hydrogen from polyunsaturated fatty acids (PUFAs) and generate a carbon-centered phospholipid (PL) and radical (PL•). This PL• will react with molecular oxygen to form phospholipid peroxyl radicals (PLOO•). The lipid peroxidation reaction is then further propagates via the interaction of this newly formed PLOO• with other PUFAs, forming a phospholipid hydroperoxide (PLOOH) and a new PL•, repeating the cycle. In enzymatic lipid peroxidation, lipoxygenase (LOX) enzymes will catalyze the dioxygenation fo PUFAs to generate PLOOH. PLOOH can then either react with Fe^{2+} and decompose to alkoxyl phospholipid radicals (PLO•), which will further propagate lipid peroxidation, or decompose to 4-hydroxynonenal (4-HNE) or malondialdehyde (MDA), which can potentially inactivate other cellular proteins through crosslinking reactions. Both reaction cascades can be halted by glutathione peroxidase 4 (GPX4) due to its ability to reduce reactive PL hydroperoxides to unreactive phospholipid alcohols (PL-OH). From [217].

Interestingly, several studies have suggested that therapy-resistant cancer cells are more susceptible to ferroptosis induction [223-226]. Tumors displaying mesenchymal and dedifferentiated characteristics are thought to heavily rely on GPX4 activity [223, 227]. GPX4 inhibition has also been associated with tumor relapse in melanoma xenografts model, highlighting its potential as a drug target [224]. To date, ferroptosis induction to overcome therapy resistance in MM or other B-cell malignancies has only sporadically been investigated. A study by Yang and colleagues showed that different MM and diffuse large B-cell lymphoma cell lines are sensitive to erastin-induced ferroptosis [215]. Similarly, a xenograft diffuse large B-cell lymphoma model recently portrayed sensitivity to imidazole ketone erastin [228]. Other compounds or plant extracts, including fingolimod, artesunate, dimethyl fumarate, and *Thymus vulgaris*, are also reported to possess anti-myeloma and -lymphoma activity through the induction of lipid peroxidation [229-232].

Remarkably, further increasing the intracellular iron load in MM cells also holds promise as a therapy sensitization strategy. For example, ferroptotic agents can potentially improve the efficacy of chemotherapeutic agents by augmenting Fe^{2+} levels and lipid ROS [233]. Likewise, iron supplementation or ferritin inhibition target the 26S proteasomal chymotrypsin-like activity and increase the susceptibility of MM cells to bortezomib treatment [234-236]. Finally, ferroptosis induction could potentially sensitize to existing anti-cancer therapy through epigenetic alterations. As mentioned, both myelomagenesis and MM therapy resistance are, in part, mediated through epigenetic alterations. Targeting or reverting these changes by changing intracellular Fe^{2+} levels with ferroptotic agents might therefore help in treating resistant tumor cells. The epigenetic machinery, iron metabolism, and oxidative stress are closely intertwined (Figure 9) [237-239]. For instance, •OH radicals produced during Fenton chemistry can react with methionine sulfoxide to produce methyl radicals and cause non-enzymatic methylation of cytosine residues in the DNA [240]. Surges in free Fe^{2+} could also potentially alter the activity of iron-dependent epigenetic enzymes, such as JmjC-domain-containing histone demethylases and TET enzymes [237, 239, 241]. In the same way, (lipid) ROS could alter the activity of epigenetic enzymes through inactivation of iron-sulfur center proteins, such as succinate dehydrogenase (SDH) [242, 243], which indirectly impacts activity of epigenetic proteins as well. When SDH is inhibited, for example, succinate is accumulated in the cytoplasm and causes product-level inhibition of 2-oxoglutarate-dependent epigenetic enzymes that release additional succinate upon activation [244, 245]. Finally, inhibition of the X_c^- system by type I ferroptosis inducers might trigger the activation of compensatory signaling pathways to counterbalance for cystine/cysteine loss. A major cellular pathway which can aid in cysteine supply is the transsulfuration pathway [239]. This pathway is mainly involved in the production of the methyldonor S-adenosyl-methionine (SAM) from methionine and homocysteine. However, in cysteine- or GSH-depleted conditions, homocysteine could also be utilized for cysteine production [246], which potentially lowers the availability of SAM methyldonors required for DNA and histone methylation [247]. Further research will have to determine whether this ferroptosis-epigenetic interplay can be utilized in anti-cancer treatments.
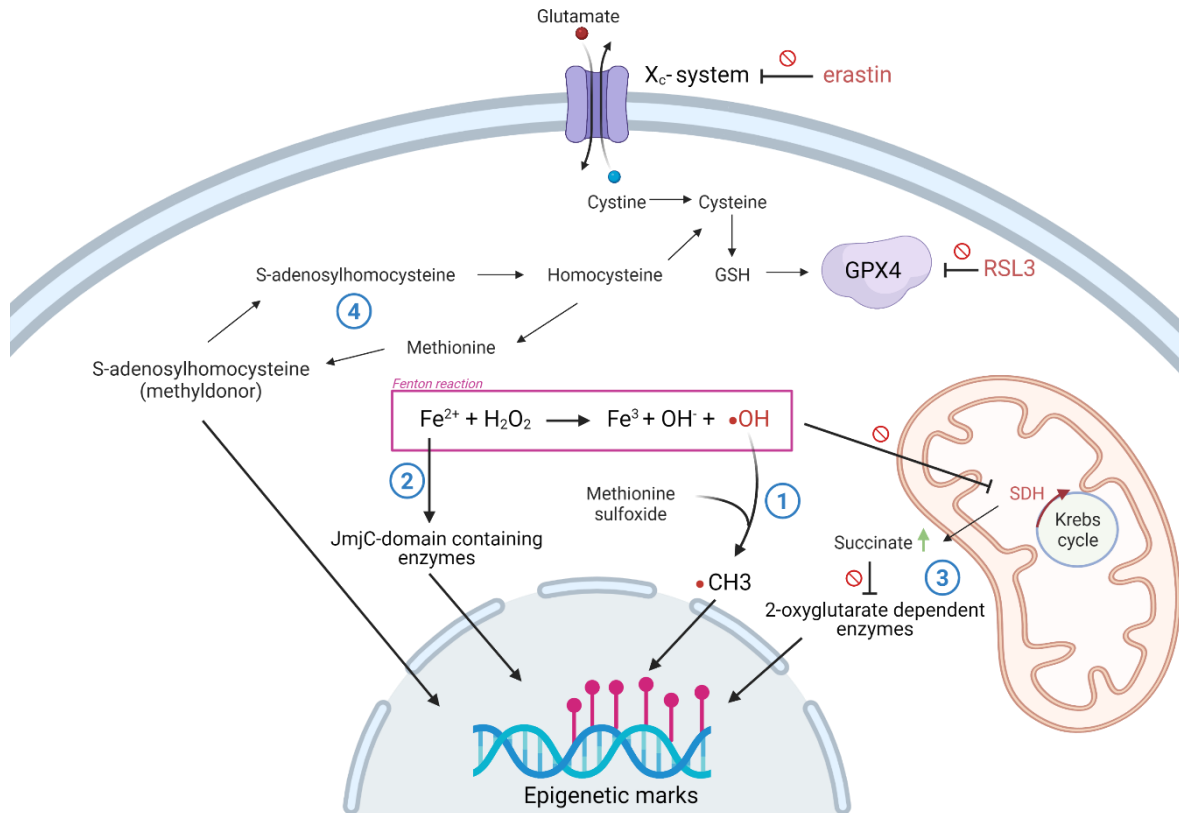
Figure 9: Ferroptosis-epigenetic cross-talk. (**1**) Hydroxyl radicals (•OH), produced during Fenton reactions, can react with methionine sulfoxide to create methyl radicals (•CH3) that can non-enzymatically methylate cytosine and guanine residues within the DNA. (**2**) Increases in intracellular iron levels might impact the activity of iron-dependent epigenetic enzymes, such as JmjC-domain containing enzymes. (**3**) Reactive oxygen species, including •OH or lipid peroxide species, can oxidize and inactive iron-sulfur center proteins, such as succinate dehydrogenase (SDH). Inactivation of these enzymes can impact epigenetic enzymes, which rely on Krebs cycle metabolites (e.g. succinate), through product level inhibition mechanisms. (**4**) Upon cysteine depletion, the transsulfuration pathway will interconverse homocysteine to cysteine as a compensatory mechanism. As a consequence, levels of S-adenosylhomocysteine, a methyldonor required for DNA and histone methylation, will drop due to limited conversion of homocysteine to methionine. Figure created with BioRender.com.

2.3. **References**

1. Kibria G, Hatakeyama H, Harashima H. Cancer multidrug resistance: mechanisms involved and strategies for circumvention using a drug delivery system. Arch Pharm Res. 2014;37(1):4-15.
2. Pinto V, Bergantim R, Caires HR, Seca H, Guimaraes JE, Vasconcelos MH. Multiple Myeloma: Available Therapies and Causes of Drug Resistance. Cancers (Basel). 2020;12(2).
3. Jaksic W, Trudel S, Chang H, Trieu Y, Qi X, Mikhael J, Reece D, Chen C, Stewart AK. Clinical outcomes in t(4;14) multiple myeloma: a chemotherapy-sensitive disease characterized by rapid relapse and alkylating agent resistance. J Clin Oncol. 2005;23(28):7069-73.
4. Allmeroth K, Horn M, Kroef V, Miethe S, Muller RU, Denzel MS. Bortezomib resistance mutations in PSMB5 determine response to second-generation proteasome inhibitors in multiple myeloma. Leukemia. 2021;35(3):887-92.
5. Barrio S, Stuhmer T, Da-Via M, Barrio-Garcia C, Lehners N, Besse A, Cuenca I, Garitano-Trojaola A, Fink S, Leich E, et al. Spectrum and functional validation of PSMB5 mutations in multiple myeloma. Leukemia. 2019;33(2):447-56.
6. Franke NE, Niewerth D, Assaraf YG, van Meerloo J, Vojtekova K, van Zantwijk CH, Zweegman S, Chan ET, Kirk CJ, Geerke DP, et al. Impaired bortezomib binding to mutant beta5 subunit of the proteasome is the underlying basis for bortezomib resistance in leukemia cells. Leukemia. 2012;26(4):757-68.
7. Gooding S, Ansari-Pour N, Towfic F, Ortiz Estevez M, Chamberlain PP, Tsai KT, Flynt E, Hirst M, Rozelle D, Dhiman P, et al. Multiple cereblon genetic changes are associated with acquired resistance to lenalidomide or pomalidomide in multiple myeloma. Blood. 2021;137(2):232-7.
8. Moalli PA, Pillay S, Weiner D, Leikin R, Rosen ST. A mechanism of resistance to glucocorticoids in multiple myeloma: transient expression of a truncated glucocorticoid receptor mRNA. Blood. 1992;79(1):213-22.
9. Nojima M, Maruyama R, Yasui H, Suzuki H, Maruyama Y, Tarasawa I, Sasaki Y, Asaoku H, Sakai H, Hayashi T, et al. Genomic screening for genes silenced by DNA methylation revealed an association between RASD1 inactivation and dexamethasone resistance in multiple myeloma. Clin Cancer Res. 2009;15(13):4356-64.
10. Issa ME, Takhsha FS, Chirumamilla CS, Perez-Novo C, Vanden Berghe W, Cuendet M. Epigenetic strategies to reverse drug resistance in heterogeneous multiple myeloma. Clin Epigenetics. 2017;9:17.
11. Kaiser MF, Johnson DC, Wu P, Walker BA, Brioli A, Mirabella F, Wardell CP, Melchor L, Davies FE, Morgan GJ. Global methylation analysis identifies prognostically important epigenetically inactivated tumor suppressor genes in multiple myeloma. Blood. 2013;122(2):219-26.
12. Turner JG, Gump JL, Zhang C, Cook JM, Marchion D, Hazlehurst L, Munster P, Schell MJ, Dalton WS, Sullivan DM. ABCG2 expression, function, and promoter methylation in human multiple myeloma. Blood. 2006;108(12):3881-9.
13. Tamaki A, Ierano C, Szakacs G, Robey RW, Bates SE. The controversial role of ABC transporters in clinical oncology. Essays Biochem. 2011;50(1):209-32.
14. Yang WC, Lin SF. Mechanisms of Drug Resistance in Relapse and Refractory Multiple Myeloma. Biomed Res Int. 2015;2015:341430.
15. Liu K, Gao L, Ma X, Huang JJ, Chen J, Zeng L, Ashby CR, Jr., Zou C, Chen ZS. Long non-coding RNAs regulate drug resistance in cancer. Mol Cancer. 2020;19(1):54.
16. Abdi J, Jian H, Chang H. Role of micro-RNAs in drug resistance of multiple myeloma. Oncotarget. 2016;7(37):60723-35.
17. Nass J, Efferth T. Drug targets and resistance mechanisms in multiple myeloma. Cancer Drug Resistance. 2018;1(2):87-117.
18. Rasche L, Kortum KM, Raab MS, Weinhold N. The Impact of Tumor Heterogeneity on Diagnostics and Novel Therapeutic Strategies in Multiple Myeloma. Int J Mol Sci. 2019;20(5).
19. Rasche L, Chavan SS, Stephens OW, Patel PH, Tytarenko R, Ashby C, Bauer M, Stein C, Deshpande S, Wardell C, et al. Spatial genomic heterogeneity in multiple myeloma revealed by multi-region sequencing. Nat Commun. 2017;8(1):268.

20. Melchor L, Brioli A, Wardell CP, Murison A, Potter NE, Kaiser MF, Fryer RA, Johnson DC, Begum DB, Hulkki Wilson S, et al. Single-cell genetic analysis reveals the composition of initiating clones and phylogenetic patterns of branching and parallel evolution in myeloma. Leukemia. 2014;28(8):1705-15.

21. Bahlis NJ. Darwinian evolution and tiding clones in multiple myeloma. Blood. 2012;120(5):927-8.

22. Weinhold N, Ashby C, Rasche L, Chavan SS, Stein C, Stephens OW, Tytarenko R, Bauer MA, Meissner T, Deshpande S, et al. Clonal selection and double-hit events involving tumor suppressor genes underlie relapse in myeloma. Blood. 2016;128(13):1735-44.

23. Sharom FJ. The P-glycoprotein efflux pump: how does it transport drugs? J Membr Biol. 1997;160(3):161-75.

24. Abraham J, Salama NN, Azab AK. The role of P-glycoprotein in drug resistance in multiple myeloma. Leuk Lymphoma. 2015;56(1):26-33.

25. Hawley TS, Riz I, Yang W, Wakabayashi Y, Depalma L, Chang YT, Peng W, Zhu J, Hawley RG. Identification of an ABCB1 (P-glycoprotein)-positive carfilzomib-resistant myeloma subpopulation by the pluripotent stem cell fluorescent dye CDy1. Am J Hematol. 2013;88(4):265-72.

26. Besse A, Stolze SC, Rasche L, Weinhold N, Morgan GJ, Kraus M, Bader J, Overkleeft HS, Besse L, Driessen C. Carfilzomib resistance due to ABCB1/MDR1 overexpression is overcome by nelfinavir and lopinavir in multiple myeloma. Leukemia. 2018;32(2):391-401.

27. Bellamy WT, Dalton WS, Kailey JM, Gleason MC, McCloskey TM, Dorr RT, Alberts DS. Verapamil reversal of doxorubicin resistance in multidrug-resistant human myeloma cells and association with drug accumulation and DNA damage. Cancer Res. 1988;48(22):6365-70.

28. Hofmeister CC, Yang X, Pichiorri F, Chen P, Rozewski DM, Johnson AJ, Lee S, Liu Z, Garr CL, Hade EM, et al. Phase I trial of lenalidomide and CCI-779 in patients with relapsed multiple myeloma: evidence for lenalidomide-CCI-779 interaction via P-glycoprotein. J Clin Oncol. 2011;29(25):3427-34.

29. Mynott RL, Wallington-Beddoe CT. Inhibition of P-Glycoprotein Does Not Increase the Efficacy of Proteasome Inhibitors in Multiple Myeloma Cells. ACS Pharmacology & Translational Science. 2021.

30. Drewinko B, Alexanian R, Boyer H, Barlogie B, Rubinow SI. The growth fraction of human myeloma cells. Blood. 1981;57(2):333-8.

31. Gao M, Kong Y, Yang G, Gao L, Shi J. Multiple myeloma cancer stem cells. Oncotarget. 2016;7(23):35466-77.

32. Lee LX, Li SC. Hunting down the dominating subclone of cancer stem cells as a potential new therapeutic target in multiple myeloma: An artificial intelligence perspective. World J Stem Cells. 2020;12(8):706-20.

33. Franqui-Machin R, Wendlandt EB, Janz S, Zhan F, Tricot G. Cancer stem cells are the cause of drug resistance in multiple myeloma: fact or fiction? Oncotarget. 2015;6(38):40496-506.

34. Matsui W, Huff CA, Wang Q, Malehorn MT, Barber J, Tanhehco Y, Smith BD, Civin CI, Jones RJ. Characterization of clonogenic multiple myeloma cells. Blood. 2004;103(6):2332-6.

35. Wu D, Zhang P, Li F, Shen Y, Chen H, Feng Y, He A, Wang F. CD138(-) multiple myeloma cells express high level of CHK1 which correlated to overall survival in MM patient. Aging (Albany NY). 2020;12(22):23067-81.

36. Vinogradov S, Wei X. Cancer stem cells and drug resistance: the potential of nanomedicine. Nanomedicine (Lond). 2012;7(4):597-615.

37. Reghunathan R, Bi C, Liu SC, Loong KT, Chung TH, Huang G, Chng WJ. Clonogenic multiple myeloma cells have shared stemness signature associated with patient survival. Oncotarget. 2013;4(8):1230-40.

38. Clark DW, Palle K. Aldehyde dehydrogenases in cancer stem cells: potential as therapeutic targets. Ann Transl Med. 2016;4(24):518.

39. Jin N, Zhu X, Cheng F, Zhang L. Disulfiram/copper targets stem cell-like ALDH(+) population of multiple myeloma by inhibition of ALDH1A1 and Hedgehog pathway. J Cell Biochem. 2018;119(8):6882-93.

40. Takebe N, Miele L, Harris PJ, Jeong W, Bando H, Kahn M, Yang SX, Ivy SP. Targeting Notch, Hedgehog, and Wnt pathways in cancer stem cells: clinical update. Nat Rev Clin Oncol. 2015;12(8):445-64.

41. Nefedova Y, Sullivan DM, Bolick SC, Dalton WS, Gabrilovich DI. Inhibition of Notch signaling induces apoptosis of myeloma cells and enhances sensitivity to chemotherapy. Blood. 2008;111(4):2220-9.

42. Peacock CD, Wang Q, Gesell GS, Corcoran-Schwartz IM, Jones E, Kim J, Devereux WL, Rhodes JT, Huff CA, Beachy PA, et al. Hedgehog signaling maintains a tumor stem cell compartment in multiple myeloma. Proc Natl Acad Sci U S A. 2007;104(10):4048-53.

43. Issa ME, Cretton S, Cuendet M. Targeting Multiple Myeloma Cancer Stem Cells with Natural Products - Lessons from Other Hematological Malignancies. Planta Med. 2017;83(9):752-60.

44. Campos B, Wan F, Farhadi M, Ernst A, Zeppernick F, Tagscherer KE, Ahmadi R, Lohr J, Dictus C, Gdynia G, et al. Differentiation therapy exerts antitumor effects on stem-like glioma cells. Clin Cancer Res. 2010;16(10):2715-28.

45. Hanahan D, Weinberg RA. Hallmarks of cancer: the next generation. Cell. 2011;144(5):646-74.

46. Wuilleme-Toumi S, Robillard N, Gomez P, Moreau P, Le Gouill S, Avet-Loiseau H, Harousseau JL, Amiot M, Bataille R. Mcl-1 is overexpressed in multiple myeloma and associated with relapse and shorter survival. Leukemia. 2005;19(7):1248-52.

47. Zhang B, Gojo I, Fenton RG. Myeloid cell factor-1 is a critical survival factor for multiple myeloma. Blood. 2002;99(6):1885-93.

48. Spets H, Stromberg T, Georgii-Hemming P, Siljason J, Nilsson K, Jernberg-Wiklund H. Expression of the bcl-2 family of pro- and anti-apoptotic genes in multiple myeloma and normal plasma cells: regulation during interleukin-6(IL-6)-induced growth and survival. Eur J Haematol. 2002;69(2):76-89.

49. Slomp A, Peperzak V. Role and Regulation of Pro-survival BCL-2 Proteins in Multiple Myeloma. Front Oncol. 2018;8:533.

50. Roy P, Sarkar UA, Basak S. The NF-kappaB Activating Pathways in Multiple Myeloma. Biomedicines. 2018;6(2).

51. Wong AH, Shin EM, Tergaonkar V, Chng WJ. Targeting NF-kappaB Signaling for Multiple Myeloma. Cancers (Basel). 2020;12(8).

52. Usmani SZ, Chiosis G. HSP90 inhibitors as therapy for multiple myeloma. Clin Lymphoma Myeloma Leuk. 2011;11 Suppl 1:S77-81.

53. Giulino-Roth L, van Besien HJ, Dalton T, Totonchy JE, Rodina A, Taldone T, Bolaender A, Erdjument-Bromage H, Sadek J, Chadburn A, et al. Inhibition of Hsp90 Suppresses PI3K/AKT/mTOR Signaling and Has Antitumor Activity in Burkitt Lymphoma. Mol Cancer Ther. 2017;16(9):1779-90.

54. Richardson PG, Mitsiades CS, Laubach JP, Lonial S, Chanan-Khan AA, Anderson KC. Inhibition of heat shock protein 90 (HSP90) as a therapeutic strategy for the treatment of myeloma and other cancers. Br J Haematol. 2011;152(4):367-79.

55. Teoh G, Anderson KC. Interaction of tumor and host cells with adhesion and extracellular matrix molecules in the development of multiple myeloma. Hematol Oncol Clin North Am. 1997;11(1):27-42.

56. Mirandola L, Apicella L, Colombo M, Yu Y, Berta DG, Platonova N, Lazzari E, Lancellotti M, Bulfamante G, Cobos E, et al. Anti-Notch treatment prevents multiple myeloma cells localization to the bone marrow via the chemokine system CXCR4/SDF-1. Leukemia. 2013;27(7):1558-66.

57. Hou J, Wei R, Qian J, Wang R, Fan Z, Gu C, Yang Y. The impact of the bone marrow microenvironment on multiple myeloma (Review). Oncol Rep. 2019.

58. Di Marzo L, Desantis V, Solimando AG, Ruggieri S, Annese T, Nico B, Fumarulo R, Vacca A, Frassanito MA. Microenvironment drug resistance in multiple myeloma: emerging new players. Oncotarget. 2016;7(37):60698-711.

59. Rosean TR, Tompkins VS, Tricot G, Holman CJ, Olivier AK, Zhan F, Janz S. Preclinical validation of interleukin 6 as a therapeutic target in multiple myeloma. Immunol Res. 2014;59(1-3):188-202.

60. Voorhees PM, Chen Q, Small GW, Kuhn DJ, Hunsucker SA, Nemeth JA, Orlowski RZ. Targeted inhibition of interleukin-6 with CNTO 328 sensitizes pre-clinical models of multiple myeloma to dexamethasone-mediated cell death. Br J Haematol. 2009;145(4):481-90.

61. Vacca A, Ria R, Ribatti D, Semeraro F, Djonov V, Di Raimondo F, Dammacco F. A paracrine loop in the vascular endothelial growth factor pathway triggers tumor angiogenesis and growth in multiple myeloma. Haematologica. 2003;88(2):176-85.

62. Damiano JS, Cress AE, Hazlehurst LA, Shtil AA, Dalton WS. Cell adhesion mediated drug resistance (CAM-DR): role of integrins and resistance to apoptosis in human myeloma cell lines. Blood. 1999;93(5):1658-67.

63. Noborio-Hatano K, Kikuchi J, Takatoku M, Shimizu R, Wada T, Ueda M, Nobuyoshi M, Oh I, Sato K, Suzuki T, et al. Bortezomib overcomes cell-adhesion-mediated drug resistance through downregulation of VLA-4 expression in multiple myeloma. Oncogene. 2009;28(2):231-42.

64. Colombo M, Mirandola L, Platonova N, Apicella L, Basile A, Figueroa AJ, Cobos E, Chiriva-Internati M, Chiaramonte R. Notch-directed microenvironment reprogramming in myeloma: a single path to multiple outcomes. Leukemia. 2013;27(5):1009-18.

65. Karsan A. Notch and integrin affinity: a sticky situation. Sci Signal. 2008;1(2):pe2.

66. Hodkinson PS, Elliott PA, Lad Y, McHugh BJ, MacKinnon AC, Haslett C, Sethi T. Mammalian NOTCH-1 activates beta1 integrins via the small GTPase R-Ras. J Biol Chem. 2007;282(39):28991-9001.

67. Hazlehurst LA, Damiano JS, Buyuksal I, Pledger WJ, Dalton WS. Adhesion to fibronectin via beta1 integrins regulates p27kip1 levels and contributes to cell adhesion mediated drug resistance (CAM-DR). Oncogene. 2000;19(38):4319-27.

68. Franssen LE, Stege CAM, Zweegman S, van de Donk N, Nijhof IS. Resistance Mechanisms Towards CD38-Directed Antibody Therapy in Multiple Myeloma. J Clin Med. 2020;9(4).

69. Nijhof IS, Casneuf T, van Velzen J, van Kessel B, Axel AE, Syed K, Groen RW, van Duin M, Sonneveld P, Minnema MC, et al. CD38 expression and complement inhibitors affect response and resistance to daratumumab therapy in myeloma. Blood. 2016;128(7):959-70.

70. Nijhof IS, Groen RW, Lokhorst HM, van Kessel B, Bloem AC, van Velzen J, de Jong-Korlaar R, Yuan H, Noort WA, Klein SK, et al. Upregulation of CD38 expression on multiple myeloma cells by all-trans retinoic acid improves the efficacy of daratumumab. Leukemia. 2015;29(10):2039-49.

71. van de Donk NW, Moreau P, Plesner T, Palumbo A, Gay F, Laubach JP, Malavasi F, Avet-Loiseau H, Mateos MV, Sonneveld P, et al. Clinical efficacy and management of monoclonal antibodies targeting CD38 and SLAMF7 in multiple myeloma. Blood. 2016;127(6):681-95.

72. Guang MHZ, McCann A, Bianchi G, Zhang L, Dowling P, Bazou D, O'Gorman P, Anderson KC. Overcoming multiple myeloma drug resistance in the era of cancer 'omics'. Leuk Lymphoma. 2018;59(3):542-61.

73. Yang HH, Ma MH, Vescio RA, Berenson JR. Overcoming drug resistance in multiple myeloma: the emergence of therapeutic approaches to induce apoptosis. J Clin Oncol. 2003;21(22):4239-47.

74. Wang Z, Cole PA. Catalytic mechanisms and regulation of protein kinases. Methods Enzymol. 2014;548:1-21.

75. Manning G, Whyte DB, Martinez R, Hunter T, Sudarsanam S. The protein kinase complement of the human genome. Science. 2002;298(5600):1912-34.

76. Fabbro D, Cowan-Jacob SW, Moebitz H. Ten things you should know about protein kinases: IUPHAR Review 14. Br J Pharmacol. 2015;172(11):2675-700.

77. Case N, Thomas J, Sen B, Styner M, Xie Z, Galior K, Rubin J. Mechanical regulation of glycogen synthase kinase 3beta (GSK3beta) in mesenchymal stem cells is dependent on Akt protein serine 473 phosphorylation via mTORC2 protein. J Biol Chem. 2011;286(45):39450-6.

78. Dejardin E, Deregowski V, Chapelier M, Jacobs N, Gielen J, Merville MP, Bours V. Regulation of NF-kappaB activity by I kappaB-related proteins in adenocarcinoma cells. Oncogene. 1999;18(16):2567-77.

79. Liu Z, Wang Y, Xue Y. Phosphoproteomics-based network medicine. FEBS J. 2013;280(22):5696-704.

80. Manning G, Plowman GD, Hunter T, Sudarsanam S. Evolution of protein kinase signaling from yeast to man. Trends Biochem Sci. 2002;27(10):514-20.

81. Hanks SK, Hunter T. Protein kinases 6. The eukaryotic protein kinase superfamily: kinase (catalytic) domain structure and classification. FASEB J. 1995;9(8):576-96.

82. Hanks SK, Quinn AM, Hunter T. The protein kinase family: conserved features and deduced phylogeny of the catalytic domains. Science. 1988;241(4861):42-52.

83. Traxler P, Furet P. Strategies toward the design of novel and selective protein tyrosine kinase inhibitors. Pharmacol Ther. 1999;82(2-3):195-206.

84. Zhang J, Yang PL, Gray NS. Targeting cancer with small molecule kinase inhibitors. Nat Rev Cancer. 2009;9(1):28-39.

85. Adams JA. Activation loop phosphorylation and catalysis in protein kinases: is there functional evidence for the autoinhibitor model? Biochemistry. 2003;42(3):601-7.

86. Izarzugaza JM, Hopcroft LE, Baresic A, Orengo CA, Martin AC, Valencia A. Characterization of pathogenic germline mutations in human protein kinases. BMC Bioinformatics. 2011;12 Suppl 4:S1.

87. Cohen P. The role of protein phosphorylation in human health and disease. The Sir Hans Krebs Medal Lecture. Eur J Biochem. 2001;268(19):5001-10.

88. Lind J, Czernilofsky F, Vallet S, Podar K. Emerging protein kinase inhibitors for the treatment of multiple myeloma. Expert Opin Emerg Drugs. 2019;24(3):133-52.

89. Roskoski R, Jr. Properties of FDA-approved small molecule protein kinase inhibitors: A 2021 update. Pharmacol Res. 2021;165:105463.

90. Martinez R, Defnet A, Shapiro P. Avoiding or Co-Opting ATP Inhibition: Overview of Type III, IV, V, and VI Kinase Inhibitors. Next Generation Kinase Inhibitors. 2020:29-59.

91. Abramson HN. Kinase inhibitors as potential agents in the treatment of multiple myeloma. Oncotarget. 2016;7(49):81926-68.

92. de Boussac H, Bruyer A, Jourdan M, Maes A, Robert N, Gourzones C, Vincent L, Seckinger A, Cartron G, Hose D, et al. Kinome expression profiling to target new therapeutic avenues in multiple myeloma. Haematologica. 2020;105(3):784-95.

93. Chong PSY, Chng WJ, de Mel S. STAT3: A Promising Therapeutic Target in Multiple Myeloma. Cancers (Basel). 2019;11(5).

94. Keane NA, Glavey SV, Krawczyk J, O'Dwyer M. AKT as a therapeutic target in multiple myeloma. Expert Opin Ther Targets. 2014;18(8):897-915.

95. Jung SH, Ahn SY, Choi HW, Shin MG, Lee SS, Yang DH, Ahn JS, Kim YK, Kim HJ, Lee JJ. STAT3 expression is associated with poor survival in non-elderly adult patients with newly diagnosed multiple myeloma. Blood Res. 2017;52(4):293-9.

96. Zhu YX, Shi CX, Bruins LA, Wang X, Riggs DL, Porter B, Ahmann JM, de Campos CB, Braggio E, Bergsagel PL, et al. Identification of lenalidomide resistance pathways in myeloma and targeted resensitization using cereblon replacement, inhibition of STAT3 or targeting of IRF4. Blood Cancer J. 2019;9(2):19.

97. Catlett-Falcone R, Landowski TH, Oshiro MM, Turkson J, Levitzki A, Savino R, Ciliberto G, Moscinski L, Fernandez-Luna JL, Nunez G, et al. Constitutive activation of Stat3 signaling confers resistance to apoptosis in human U266 myeloma cells. Immunity. 1999;10(1):105-15.

98. Tsubaki M, Takeda T, Ogawa N, Sakamoto K, Shimaoka H, Fujita A, Itoh T, Imano M, Ishizaka T, Satou T, et al. Overexpression of survivin via activation of ERK1/2, Akt, and NF-kappaB plays a central role in vincristine resistance in multiple myeloma cells. Leuk Res. 2015;39(4):445-52.

99. Zhang Y, Fu Y, Zhang F, Liu J. Destabilization of akt promotes the death of myeloma cell lines. Biomed Res Int. 2014;2014:190629.

100. Ramakrishnan V, Kimlinger T, Haug J, Painuly U, Wellik L, Halling T, Rajkumar SV, Kumar S. Anti-myeloma activity of Akt inhibition is linked to the activation status of PI3K/Akt and MEK/ERK pathway. PLoS One. 2012;7(11):e50005.

101. Bam R, Venkateshaiah SU, Khan S, Ling W, Randal SS, Li X, Zhang Q, van Rhee F, Barlogie B, Epstein J, et al. Role of Bruton's tyrosine kinase (BTK) in growth and metastasis of INA6 myeloma cells. Blood Cancer J. 2014;4:e234.

102. Yang Y, Shi J, Gu Z, Salama ME, Das S, Wendlandt E, Xu H, Huang J, Tao Y, Hao M, et al. Bruton tyrosine kinase is a therapeutic target in stem-like cells from multiple myeloma. Cancer Res. 2015;75(3):594-604.

103. Tai YT, Chang BY, Kong SY, Fulciniti M, Yang G, Calle Y, Hu Y, Lin J, Zhao JJ, Cagnetta A, et al. Bruton tyrosine kinase inhibition is a novel therapeutic strategy targeting tumor in the bone marrow microenvironment in multiple myeloma. Blood. 2012;120(9):1877-87.

104. Richardson PG, Bensinger WI, Huff CA, Costello CL, Lendvai N, Berdeja JG, Anderson LD, Jr., Siegel DS, Lebovic D, Jagannath S, et al. Ibrutinib alone or with dexamethasone for relapsed or relapsed and refractory multiple myeloma: phase 2 trial results. Br J Haematol. 2018;180(6):821-30.

105. Kuhn DJ, Berkova Z, Jones RJ, Woessner R, Bjorklund CC, Ma W, Davis RE, Lin P, Wang H, Madden TL, et al. Targeting the insulin-like growth factor-1 receptor to overcome bortezomib resistance in preclinical models of multiple myeloma. Blood. 2012;120(16):3260-70.

106. Mulvihill MJ, Cooke A, Rosenfeld-Franklin M, Buck E, Foreman K, Landfair D, O'Connor M, Pirritt C, Sun Y, Yao Y, et al. Discovery of OSI-906: a selective and orally efficacious dual inhibitor of the IGF-1 receptor and insulin receptor. Future Med Chem. 2009;1(6):1153-71.

107. Liang SB, Yang XZ, Trieu Y, Li Z, Zive J, Leung-Hagesteijn C, Wei E, Zozulya S, Coss CC, Dalton JT, et al. Molecular target characterization and antimyeloma activity of the novel, insulin-like growth factor 1 receptor inhibitor, GTx-134. Clin Cancer Res. 2011;17(14):4693-704.

108. Phillip CJ, Zaman S, Shentu S, Balakrishnan K, Zhang J, Baladandayuthapani V, Taverna P, Redkar S, Wang M, Stellrecht CM, et al. Targeting MET kinase with the small-molecule inhibitor amuvatinib induces cytotoxicity in primary myeloma cells and cell lines. J Hematol Oncol. 2013;6:92.

109. Dispenzieri A, Gertz MA, Lacy MQ, Geyer SM, Greipp PR, Rajkumar SV, Kimlinger T, Lust JA, Fonseca R, Allred J, et al. A phase II trial of imatinib in patients with refractory/relapsed myeloma. Leuk Lymphoma. 2006;47(1):39-42.

110. Heinrich MC, Griffith DJ, Druker BJ, Wait CL, Ott KA, Zigler AJ. Inhibition of c-kit receptor tyrosine kinase activity by STI 571, a selective tyrosine kinase inhibitor. Blood. 2000;96(3):925-32.

111. Druker BJ, Tamura S, Buchdunger E, Ohno S, Segal GM, Fanning S, Zimmermann J, Lydon NB. Effects of a selective inhibitor of the Abl tyrosine kinase on the growth of Bcr-Abl positive cells. Nat Med. 1996;2(5):561-6.

112. You WK, Sennino B, Williamson CW, Falcon B, Hashizume H, Yao LC, Aftab DT, McDonald DM. VEGF and c-Met blockade amplify angiogenesis inhibition in pancreatic islet cancer. Cancer Res. 2011;71(14):4758-68.

113. Yakes FM, Chen J, Tan J, Yamaguchi K, Shi Y, Yu P, Qian F, Chu F, Bentzien F, Cancilla B, et al. Cabozantinib (XL184), a novel MET and VEGFR2 inhibitor, simultaneously suppresses metastasis, angiogenesis, and tumor growth. Mol Cancer Ther. 2011;10(12):2298-308.

114. Munshi N, Jeay S, Li Y, Chen CR, France DS, Ashwell MA, Hill J, Moussa MM, Leggett DS, Li CJ. ARQ 197, a novel and selective inhibitor of the human c-Met receptor tyrosine kinase with antitumor activity. Mol Cancer Ther. 2010;9(6):1544-53.

115. Scheid C, Reece D, Beksac M, Spencer A, Callander N, Sonneveld P, Kalimi G, Cai C, Shi M, Scott JW, et al. Phase 2 study of dovitinib in patients with relapsed or refractory multiple myeloma with or without t(4;14) translocation. Eur J Haematol. 2015;95(4):316-24.

116. Trudel S, Li ZH, Wei E, Wiesmann M, Chang H, Chen C, Reece D, Heise C, Stewart AK. CHIR-258, a novel, multitargeted tyrosine kinase inhibitor for the potential treatment of t(4;14) multiple myeloma. Blood. 2005;105(7):2941-8.

117. Hilberg F, Roth GJ, Krssak M, Kautschitsch S, Sommergruber W, Tontsch-Grunt U, Garin-Chesa P, Bader G, Zoephel A, Quant J, et al. BIBF 1120: triple angiokinase inhibitor with sustained receptor blockade and good antitumor efficacy. Cancer Res. 2008;68(12):4774-82.

118. Kropff M, Kienast J, Bisping G, Berdel WE, Gaschler-Markefski B, Stopfer P, Stefanic M, Munzert G. An open-label dose-escalation study of BIBF 1120 in patients with relapsed or refractory multiple myeloma. Anticancer Res. 2009;29(10):4233-8.

119. Podar K, Tonon G, Sattler M, Tai YT, Legouill S, Yasui H, Ishitsuka K, Kumar S, Kumar R, Pandite LN, et al. The small-molecule VEGF receptor inhibitor pazopanib (GW786034B) targets both tumor and endothelial cells in multiple myeloma. Proc Natl Acad Sci U S A. 2006;103(51):19478-83.

120. Harris PA, Boloor A, Cheung M, Kumar R, Crosby RM, Davis-Ward RG, Epperly AH, Hinkle KW, Hunter RN, 3rd, Johnson JH, et al. Discovery of 5-[[4-[(2,3-dimethyl-2H-indazol-6-yl)methylamino]-2-

pyrimidinyl]amino]-2-methyl-b enzenesulfonamide (Pazopanib), a novel and potent vascular endothelial growth factor receptor inhibitor. J Med Chem. 2008;51(15):4632-40.

121. Fong TA, Shawver LK, Sun L, Tang C, App H, Powell TJ, Kim YH, Schreck R, Wang X, Risau W, et al. SU5416 is a potent and selective inhibitor of the vascular endothelial growth factor receptor (Flk-1/KDR) that inhibits tyrosine kinase catalysis, tumor vascularization, and growth of multiple tumor types. Cancer Res. 1999;59(1):99-106.

122. Wood JM, Bold G, Buchdunger E, Cozens R, Ferrari S, Frei J, Hofmann F, Mestan J, Mett H, O'Reilly T, et al. PTK787/ZK 222584, a novel and potent inhibitor of vascular endothelial growth factor receptor tyrosine kinases, impairs vascular endothelial growth factor-induced responses and tumor growth after oral administration. Cancer Res. 2000;60(8):2178-89.

123. Neri P, Tassone P, Shammas M, Yasui H, Schipani E, Batchu RB, Blotta S, Prabhala R, Catley L, Hamasaki M, et al. Biological pathways and in vivo antitumor activity induced by Atiprimod in myeloma. Leukemia. 2007;21(12):2519-26.

124. Liu Y, Chen XQ, Liang HX, Zhang FX, Zhang B, Jin J, Chen YL, Cheng YX, Zhou GB. Small compound 6-O-angeloylplenolin induces mitotic arrest and exhibits therapeutic potentials in multiple myeloma. PLoS One. 2011;6(7):e21930.

125. Lee JH, Kim C, Kim SH, Sethi G, Ahn KS. Farnesol inhibits tumor growth and enhances the anticancer effects of bortezomib in multiple myeloma xenograft mouse model through the modulation of STAT3 signaling pathway. Cancer Lett. 2015;360(2):280-93.

126. Alas S, Bonavida B. Inhibition of constitutive STAT3 activity sensitizes resistant non-Hodgkin's lymphoma and multiple myeloma to chemotherapeutic drug-mediated apoptosis. Clin Cancer Res. 2003;9(1):316-26.

127. Schmeel FC, Schmeel LC, Kim Y, Schmidt-Wolf IG. Piceatannol exhibits selective toxicity to multiple myeloma cells and influences the Wnt/ beta-catenin pathway. Hematol Oncol. 2014;32(4):197-204.

128. Wu J, Zhang M, Liu D. Acalabrutinib (ACP-196): a selective second-generation BTK inhibitor. J Hematol Oncol. 2016;9:21.

129. Honigberg LA, Smith AM, Sirisawad M, Verner E, Loury D, Chang B, Li S, Pan Z, Thamm DH, Miller RA, et al. The Bruton tyrosine kinase inhibitor PCI-32765 blocks B-cell activation and is efficacious in models of autoimmune disease and B-cell malignancy. Proc Natl Acad Sci U S A. 2010;107(29):13075-80.

130. Zhang J, Ai L, Lv T, Jiang X, Liu F. Asiatic acid, a triterpene, inhibits cell proliferation through regulating the expression of focal adhesion kinase in multiple myeloma cells. Oncol Lett. 2013;6(6):1762-6.

131. Wildes TM, Procknow E, Gao F, Dipersio JF, Vij R. Dasatinib in relapsed or plateau-phase multiple myeloma. Leuk Lymphoma. 2009;50(1):137-40.

132. Jungkunz-Stier I, Zekl M, Stuhmer T, Einsele H, Seggewiss-Bernhardt R. Modulation of natural killer cell effector functions through lenalidomide/dasatinib and their combined effects against multiple myeloma cells. Leuk Lymphoma. 2014;55(1):168-76.

133. Koerber RM, Held SAE, Heine A, Kotthoff P, Daecke SN, Bringmann A, Brossart P. Analysis of the anti-proliferative and the pro-apoptotic efficacy of Syk inhibition in multiple myeloma. Exp Hematol Oncol. 2015;4:21.

134. Braselmann S, Taylor V, Zhao H, Wang S, Sylvain C, Baluom M, Qu K, Herlaar E, Lau A, Young C, et al. R406, an orally available spleen tyrosine kinase inhibitor blocks fc receptor signaling and reduces immune complex-mediated inflammation. J Pharmacol Exp Ther. 2006;319(3):998-1008.

135. Azab F, Vali S, Abraham J, Potter N, Muz B, de la Puente P, Fiala M, Paasch J, Sultana Z, Tyagi A, et al. PI3KCA plays a major role in multiple myeloma and its inhibition with BYL719 decreases proliferation, synergizes with other therapies and overcomes stroma-induced resistance. Br J Haematol. 2014;165(1):89-101.

136. Ikeda H, Hideshima T, Fulciniti M, Perrone G, Miura N, Yasui H, Okawa Y, Kiziltepe T, Santo L, Vallet S, et al. PI3K/p110{delta} is a novel therapeutic target in multiple myeloma. Blood. 2010;116(9):1460-8.

137. Lannutti BJ, Meadows SA, Herman SE, Kashishian A, Steiner B, Johnson AJ, Byrd JC, Tyner JW, Loriaux MM, Deininger M, et al. CAL-101, a p110delta selective phosphatidylinositol-3-kinase inhibitor for the treatment of B-cell malignancies, inhibits PI3K signaling and cellular viability. Blood. 2011;117(2):591-4.

138. Gursel DB, Connell-Albert YS, Tuskan RG, Anastassiadis T, Walrath JC, Hawes JJ, Amlin-Van Schaick JC, Reilly KM. Control of proliferation in astrocytoma cells by the receptor tyrosine kinase/PI3K/AKT signaling axis and the use of PI-103 and TCN as potential anti-astrocytoma therapies. Neuro Oncol. 2011;13(6):610-21.

139. Dumble M, Crouthamel MC, Zhang SY, Schaber M, Levy D, Robell K, Liu Q, Figueroa DJ, Minthorn EA, Seefeld MA, et al. Discovery of novel AKT inhibitors with enhanced anti-tumor effects in combination with the MEK inhibitor. PLoS One. 2014;9(6):e100880.

140. Spencer A, Yoon SS, Harrison SJ, Morris SR, Smith DA, Brigandi RA, Gauvin J, Kumar R, Opalinska JB, Chen C. The novel AKT inhibitor afuresertib shows favorable safety, pharmacokinetics, and clinical activity in multiple myeloma. Blood. 2014;124(14):2190-5.

141. Yee AJ, Hari P, Marcheselli R, Mahindra AK, Cirstea DD, Scullen TA, Burke JN, Rodig SJ, Hideshima T, Laubach JP, et al. Outcomes in patients with relapsed or refractory multiple myeloma in a phase I study of everolimus in combination with lenalidomide. Br J Haematol. 2014;166(3):401-9.

142. Maiso P, Liu Y, Morgan B, Azab AK, Ren P, Martin MB, Zhang Y, Liu Y, Sacco A, Ngo H, et al. Defining the role of TORC1/2 in multiple myeloma. Blood. 2011;118(26):6860-70.

143. Johrer K, Obkircher M, Neureiter D, Parteli J, Zelle-Rieser C, Maizner E, Kern J, Hermann M, Hamacher F, Merkel O, et al. Antimyeloma activity of the sesquiterpene lactone cnicin: impact on Pim-2 kinase as a novel therapeutic target. J Mol Med (Berl). 2012;90(6):681-93.

144. Garcia PD, Langowski JL, Wang Y, Chen M, Castillo J, Fanton C, Ison M, Zavorotinskaya T, Dai Y, Lu J, et al. Pan-PIM kinase inhibition provides a novel therapy for treating hematologic cancers. Clin Cancer Res. 2014;20(7):1834-45.

145. Keane NA, Reidy M, Natoni A, Raab MS, O'Dwyer M. Targeting the Pim kinases in multiple myeloma. Blood Cancer J. 2015;5:e325.

146. Majolo F, de Oliveira Becker Delwing LK, Marmitt DJ, Bustamante-Filho IC, Goettert MI. Medicinal plants and bioactive natural compounds for cancer treatment: Important advances for drug discovery. Phytochemistry Letters. 2019;31:196-207.

147. Lin S-R, Chang C-H, Hsu C-F, Tsai M-J, Cheng H, Leong MK, Sung P-J, Chen J-C, Weng C-F. Natural compounds as potential adjuvants to cancer therapy: Preclinical evidence. Br J Pharmacol. 2020;177(6):1409-23.

148. Pojero F, Poma P, Spano V, Montalbano A, Barraja P, Notarbartolo M. Targeting multiple myeloma with natural polyphenols. Eur J Med Chem. 2019;180:465-85.

149. Vanden Berghe W, Sabbe L, Kaileh M, Haegeman G, Heyninck K. Molecular insight in the multifunctional activities of Withaferin A. Biochem Pharmacol. 2012;84(10):1282-91.

150. Sun GY, Li R, Cui J, Hannink M, Gu Z, Fritsche KL, Lubahn DB, Simonyi A. Withania somnifera and Its Withanolides Attenuate Oxidative and Inflammatory Responses and Up-Regulate Antioxidant Responses in BV-2 Microglial Cells. Neuromolecular Med. 2016;18(3):241-52.

151. Khedgikar V, Ahmad N, Kushwaha P, Gautam J, Nagar GK, Singh D, Trivedi PK, Mishra PR, Sangwan NS, Trivedi R. Preventive effects of Withaferin A isolated from the leaves of an Indian medicinal plant Withania somnifera (L.): comparisons with 17-beta-estradiol and alendronate. Nutrition. 2015;31(1):205-13.

152. Jayaprakasam B, Zhang Y, Seeram NP, Nair MG. Growth inhibition of human tumor cell lines by withanolides from Withania somnifera leaves. Life Sci. 2003;74(1):125-32.

153. Chandrasekaran S, Veronica J, Sundar S, Maurya R. Alcoholic Fractions F5 and F6 from Withania somnifera Leaves Show a Potent Antileishmanial and Immunomodulatory Activities to Control Experimental Visceral Leishmaniasis. Front Med (Lausanne). 2017;4:55.

154. Patil D, Gautam M, Mishra S, Karupothula S, Gairola S, Jadhav S, Pawar S, Patwardhan B. Determination of Withaferin A and withanolide A in mice plasma using high-performance liquid chromatography-

tandem mass spectrometry: application to pharmacokinetics after oral administration of Withania somnifera aqueous extract. J Pharm Biomed Anal. 2013;80:203-12.

155. Thaiparambil JT, Bender L, Ganesh T, Kline E, Patel P, Liu Y, Tighiouart M, Vertino PM, Harvey RD, Garcia A, et al. Withaferin A inhibits breast cancer invasion and metastasis at sub-cytotoxic doses by inducing vimentin disassembly and serine 56 phosphorylation. Int J Cancer. 2011;129(11):2744-55.

156. Lee J, Liu J, Feng X, Salazar Hernandez MA, Mucka P, Ibi D, Choi JW, Ozcan U. Withaferin A is a leptin sensitizer with strong antidiabetic properties in mice. Nat Med. 2016;22(9):1023-32.

157. Hassannia B, Wiernicki B, Ingold I, Qu F, Van Herck S, Tyurina YY, Bayir H, Abhari BA, Angeli JPF, Choi SM, et al. Nano-targeted induction of dual ferroptotic mechanisms eradicates high-risk neuroblastoma. J Clin Invest. 2018;128(8):3341-55.

158. Patel SB, Rao NJ, Hingorani LL. Safety assessment of Withania somnifera extract standardized for Withaferin A: Acute and sub-acute toxicity study. J Ayurveda Integr Med. 2016;7(1):30-7.

159. Pires N, Gota V, Gulia A, Hingorani L, Agarwal M, Puri A. Safety and pharmacokinetics of Withaferin-A in advanced stage high grade osteosarcoma: A phase I trial. J Ayurveda Integr Med. 2020;11(1):68-72.

160. Samadi AK. Potential Anticancer Properties and Mechanisms of Action of Withanolides. Enzymes. 2015;37:73-94.

161. Sanchez-Martin M, Ambesi-Impiombato A, Qin Y, Herranz D, Bansal M, Girardi T, Paietta E, Tallman MS, Rowe JM, De Keersmaecker K, et al. Synergistic antileukemic therapies in NOTCH1-induced T-ALL. Proc Natl Acad Sci U S A. 2017;114(8):2006-11.

162. Chirumamilla CS, Perez-Novo C, Van Ostade X, Vanden Berghe W. Molecular insights into cancer therapeutic effects of the dietary medicinal phytochemical Withaferin A. Proc Nutr Soc. 2017;76(2):96-105.

163. Lee IC, Choi BY. Withaferin-A--A Natural Anticancer Agent with Pleitropic Mechanisms of Action. Int J Mol Sci. 2016;17(3):290.

164. Srinivasan S, Ranga RS, Burikhanov R, Han SS, Chendil D. Par-4-dependent apoptosis by the dietary compound Withaferin A in prostate cancer cells. Cancer Res. 2007;67(1):246-53.

165. Yang H, Shi G, Dou QP. The tumor proteasome is a primary target for the natural anticancer compound Withaferin A isolated from "Indian winter cherry". Mol Pharmacol. 2007;71(2):426-37.

166. Stan SD, Hahm ER, Warin R, Singh SV. Withaferin A causes FOXO3a- and Bim-dependent apoptosis and inhibits growth of human breast cancer cells in vivo. Cancer Res. 2008;68(18):7661-9.

167. Nagalingam A, Kuppusamy P, Singh SV, Sharma D, Saxena NK. Mechanistic elucidation of the antitumor properties of Withaferin a in breast cancer. Cancer Res. 2014;74(9):2617-29.

168. Yu Y, Hamza A, Zhang T, Gu M, Zou P, Newman B, Li Y, Gunatilaka AA, Zhan CG, Sun D. Withaferin A targets heat shock protein 90 in pancreatic cancer cells. Biochem Pharmacol. 2010;79(4):542-51.

169. Samadi AK, Mukerji R, Shah A, Timmermann BN, Cohen MS. A novel RET inhibitor with potent efficacy against medullary thyroid cancer in vivo. Surgery. 2010;148(6):1228-36; discussion 36.

170. Munagala R, Kausar H, Munjal C, Gupta RC. Withaferin A induces p53-dependent apoptosis by repression of HPV oncogenes and upregulation of tumor suppressor proteins in human cervical cancer cells. Carcinogenesis. 2011;32(11):1697-705.

171. Fong MY, Jin S, Rane M, Singh RK, Gupta R, Kakar SS. Withaferin A synergizes the therapeutic effect of doxorubicin through ROS-mediated autophagy in ovarian cancer. PLoS One. 2012;7(7):e42265.

172. Samadi AK, Cohen SM, Mukerji R, Chaguturu V, Zhang X, Timmermann BN, Cohen MS, Person EA. Natural withanolide Withaferin A induces apoptosis in uveal melanoma cells by suppression of Akt and c-MET activation. Tumour Biol. 2012;33(4):1179-89.

173. Hahm ER, Lee J, Kim SH, Sehrawat A, Arlotti JA, Shiva SS, Bhargava R, Singh SV. Metabolic alterations in mammary cancer prevention by Withaferin A in a clinically relevant mouse model. J Natl Cancer Inst. 2013;105(15):1111-22.

174. Kim SH, Singh SV. Mammary cancer chemoprevention by Withaferin A is accompanied by in vivo suppression of self-renewal of cancer stem cells. Cancer Prev Res (Phila). 2014;7(7):738-47.

175. Kakar SS, Ratajczak MZ, Powell KS, Moghadamfalahi M, Miller DM, Batra SK, Singh SK. Withaferin a alone and in combination with cisplatin suppresses growth and metastasis of ovarian cancer by targeting putative cancer stem cells. PLoS One. 2014;9(9):e107596.

176. Choi BY, Kim BW. Withaferin-A Inhibits Colon Cancer Cell Growth by Blocking STAT3 Transcriptional Activity. J Cancer Prev. 2015;20(3):185-92.

177. Li W, Zhang C, Du H, Huang V, Sun B, Harris JP, Richardson Q, Shen X, Jin R, Li G, et al. Withaferin A suppresses the up-regulation of acetyl-coA carboxylase 1 and skin tumor formation in a skin carcinogenesis mouse model. Mol Carcinog. 2016;55(11):1739-46.

178. Li X, Zhu F, Jiang J, Sun C, Wang X, Shen M, Tian R, Shi C, Xu M, Peng F, et al. Synergistic antitumor activity of Withaferin A combined with oxaliplatin triggers reactive oxygen species-mediated inactivation of the PI3K/AKT pathway in human pancreatic cancer cells. Cancer Lett. 2015;357(1):219-30.

179. Suman S, Das TP, Sirimulla S, Alatassi H, Ankem MK, Damodaran C. Withaferin-A suppress AKT induced tumor growth in colorectal cancer cells. Oncotarget. 2016;7(12):13854-64.

180. Kakar SS, Worth CA, Wang Z, Carter K, Ratajczak M, Gunjal P. DOXIL when combined with Withaferin A (WFA) targets ALDH1 positive cancer stem cells in ovarian cancer. J Cancer Stem Cell Res. 2016;4.

181. ur Rasool R, Rah B, Amin H, Nayak D, Chakraborty S, Rawoof A, Mintoo MJ, Yousuf K, Mukherjee D, Kumar LD, et al. Dual modulation of Ras-Mnk and PI3K-AKT-mTOR pathways: A Novel c-FLIP inhibitory mechanism of 3-AWA mediated translational attenuation through dephosphorylation of eIF4E. Sci Rep. 2016;6:18800.

182. McKenna MK, Gachuki BW, Alhakeem SS, Oben KN, Rangnekar VM, Gupta RC, Bondada S. Anti-cancer activity of Withaferin A in B-cell lymphoma. Cancer Biol Ther. 2015;16(7):1088-98.

183. Jackson SS, Oberley C, Hooper CP, Grindle K, Wuerzberger-Davis S, Wolff J, McCool K, Rui L, Miyamoto S. Withaferin A disrupts ubiquitin-based NEMO reorganization induced by canonical NF-kappaB signaling. Exp Cell Res. 2015;331(1):58-72.

184. Malara N, Foca D, Casadonte F, Sesto MF, Macrina L, Santoro L, Scaramuzzino M, Terracciano R, Savino R. Simultaneous inhibition of the constitutively activated nuclear factor kappaB and of the interleukin-6 pathways is necessary and sufficient to completely overcome apoptosis resistance of human U266 myeloma cells. Cell Cycle. 2008;7(20):3235-45.

185. Oeckinghaus A, Ghosh S. The NF-kappaB family of transcription factors and its regulation. Cold Spring Harb Perspect Biol. 2009;1(4):a000034.

186. Grover A, Shandilya A, Punetha A, Bisaria VS, Sundar D. Inhibition of the NEMO/IKKbeta association complex formation, a novel mechanism associated with the NF-kappaB activation suppression by Withania somnifera's key metabolite Withaferin A. BMC Genomics. 2010;11 Suppl 4:S25.

187. Yco LP, Mocz G, Opoku-Ansah J, Bachmann AS. Withaferin A Inhibits STAT3 and Induces Tumor Cell Death in Neuroblastoma and Multiple Myeloma. Biochem Insights. 2014;7:1-13.

188. Lee TJ, Um HJ, Min do S, Park JW, Choi KS, Kwon TK. Withaferin A sensitizes TRAIL-induced apoptosis through reactive oxygen species-mediated up-regulation of death receptor 5 and down-regulation of c-FLIP. Free Radic Biol Med. 2009;46(12):1639-49.

189. Cohen SM, Mukerji R, Timmermann BN, Samadi AK, Cohen MS. A novel combination of Withaferin A and sorafenib shows synergistic efficacy against both papillary and anaplastic thyroid cancers. Am J Surg. 2012;204(6):895-900; discussion -1.

190. Kakar SS, Jala VR, Fong MY. Synergistic cytotoxic action of cisplatin and Withaferin A on ovarian cancer cell lines. Biochem Biophys Res Commun. 2012;423(4):819-25.

191. Chang E, Pohling C, Beygui N, Patel CB, Rosenberg J, Ha DH, Gambhir SS. Synergistic inhibition of glioma cell proliferation by Withaferin A and tumor treating fields. J Neurooncol. 2017;134(2):259-68.

192. Karnitz LM, Felts SJ. Cdc37 regulation of the kinome: when to hold 'em and when to fold 'em. Sci STKE. 2007;2007(385):pe22.

193. Grover A, Shandilya A, Agrawal V, Pratik P, Bhasme D, Bisaria VS, Sundar D. Hsp90/Cdc37 chaperone/co-chaperone complex, a novel junction anticancer target elucidated by the mode of action of herbal drug Withaferin A. BMC Bioinformatics. 2011;12 Suppl 1:S30.

194. Issa ME, Cuendet M. Withaferin A induces cell death and differentiation in multiple myeloma cancer stem cells. Medchemcomm. 2017;8(1):112-21.

195. Pistritto G, Trisciuoglio D, Ceci C, Garufi A, D'Orazi G. Apoptosis as anticancer mechanism: function and dysfunction of its modulators and targeted therapeutic strategies. Aging (Albany NY). 2016;8(4):603-19.

196. Fink SL, Cookson BT. Apoptosis, pyroptosis, and necrosis: mechanistic description of dead and dying eukaryotic cells. Infect Immun. 2005;73(4):1907-16.

197. Vanden Berghe T, Linkermann A, Jouan-Lanhouet S, Walczak H, Vandenabeele P. Regulated necrosis: the expanding network of non-apoptotic cell death pathways. Nat Rev Mol Cell Biol. 2014;15(2):135-47.

198. Holler N, Zaru R, Micheau O, Thome M, Attinger A, Valitutti S, Bodmer JL, Schneider P, Seed B, Tschopp J. Fas triggers an alternative, caspase-8-independent cell death pathway using the kinase RIP as effector molecule. Nat Immunol. 2000;1(6):489-95.

199. Teng X, Degterev A, Jagtap P, Xing X, Choi S, Denu R, Yuan J, Cuny GD. Structure-activity relationship study of novel necroptosis inhibitors. Bioorg Med Chem Lett. 2005;15(22):5039-44.

200. Cho YS, Challa S, Moquin D, Genga R, Ray TD, Guildford M, Chan FK. Phosphorylation-driven assembly of the RIP1-RIP3 complex regulates programmed necrosis and virus-induced inflammation. Cell. 2009;137(6):1112-23.

201. Degterev A, Huang Z, Boyce M, Li Y, Jagtap P, Mizushima N, Cuny GD, Mitchison TJ, Moskowitz MA, Yuan J. Chemical inhibitor of nonapoptotic cell death with therapeutic potential for ischemic brain injury. Nat Chem Biol. 2005;1(2):112-9.

202. Galluzzi L, Vitale I, Aaronson SA, Abrams JM, Adam D, Agostinis P, Alnemri ES, Altucci L, Amelio I, Andrews DW, et al. Molecular mechanisms of cell death: recommendations of the Nomenclature Committee on Cell Death 2018. Cell Death Differ. 2018;25(3):486-541.

203. Dixon SJ, Lemberg KM, Lamprecht MR, Skouta R, Zaitsev EM, Gleason CE, Patel DN, Bauer AJ, Cantley AM, Yang WS, et al. Ferroptosis: an iron-dependent form of nonapoptotic cell death. Cell. 2012;149(5):1060-72.

204. Chen X, Comish PB, Tang D, Kang R. Characteristics and Biomarkers of Ferroptosis. Front Cell Dev Biol. 2021;9:637162.

205. Stoyanovsky DA, Tyurina YY, Shrivastava I, Bahar I, Tyurin VA, Protchenko O, Jadhav S, Bolevich SB, Kozlov AV, Vladimirov YA, et al. Iron catalysis of lipid peroxidation in ferroptosis: Regulated enzymatic or random free radical reaction? Free Radic Biol Med. 2019;133:153-61.

206. Kuhn H, Banthiya S, van Leyen K. Mammalian lipoxygenases and their biological relevance. Biochim Biophys Acta. 2015;1851(4):308-30.

207. Seiler A, Schneider M, Forster H, Roth S, Wirth EK, Culmsee C, Plesnila N, Kremmer E, Radmark O, Wurst W, et al. Glutathione peroxidase 4 senses and translates oxidative stress into 12/15-lipoxygenase dependent- and AIF-mediated cell death. Cell Metab. 2008;8(3):237-48.

208. Yang WS, Kim KJ, Gaschler MM, Patel M, Shchepinov MS, Stockwell BR. Peroxidation of polyunsaturated fatty acids by lipoxygenases drives ferroptosis. Proc Natl Acad Sci U S A. 2016;113(34):E4966-75.

209. Shah R, Shchepinov MS, Pratt DA. Resolving the Role of Lipoxygenases in the Initiation and Execution of Ferroptosis. ACS Cent Sci. 2018;4(3):387-96.

210. Zilka O, Shah R, Li B, Friedmann Angeli JP, Griesser M, Conrad M, Pratt DA. On the Mechanism of Cytoprotection by Ferrostatin-1 and Liproxstatin-1 and the Role of Lipid Peroxidation in Ferroptotic Cell Death. ACS Cent Sci. 2017;3(3):232-43.

211. Anthonymuthu TS, Tyurina YY, Sun WY, Mikulska-Ruminska K, Shrivastava IH, Tyurin VA, Cinemre FB, Dar HH, VanDemark AP, Holman TR, et al. Resolving the paradox of ferroptotic cell death: Ferrostatin-1 binds to 15LOX/PEBP1 complex, suppresses generation of peroxidized ETE-PE, and protects against ferroptosis. Redox Biol. 2021;38:101744.

212. Riegman M, Sagie L, Galed C, Levin T, Steinberg N, Dixon SJ, Wiesner U, Bradbury MS, Niethammer P, Zaritsky A, et al. Ferroptosis occurs through an osmotic mechanism and propagates independently of cell rupture. Nat Cell Biol. 2020;22(9):1042-8.

213. Agmon E, Solon J, Bassereau P, Stockwell BR. Modeling the effects of lipid peroxidation during ferroptosis on membrane properties. Sci Rep. 2018;8(1):5155.

214. Zhong H, Yin H. Role of lipid peroxidation derived 4-hydroxynonenal (4-HNE) in cancer: focusing on mitochondria. Redox Biol. 2015;4:193-9.

215. Yang WS, SriRamaratnam R, Welsch ME, Shimada K, Skouta R, Viswanathan VS, Cheah JH, Clemons PA, Shamji AF, Clish CB, et al. Regulation of ferroptotic cancer cell death by GPX4. Cell. 2014;156(1-2):317-31.

216. Cao JY, Dixon SJ. Mechanisms of ferroptosis. Cell Mol Life Sci. 2016;73(11-12):2195-209.

217. Hassannia B, Vandenabeele P, Vanden Berghe T. Targeting Ferroptosis to Iron Out Cancer. Cancer Cell. 2019;35(6):830-49.

218. Sun X, Ou Z, Xie M, Kang R, Fan Y, Niu X, Wang H, Cao L, Tang D. HSPB1 as a novel regulator of ferroptotic cancer cell death. Oncogene. 2015;34(45):5617-25.

219. Basuli D, Tesfay L, Deng Z, Paul B, Yamamoto Y, Ning G, Xian W, McKeon F, Lynch M, Crum CP, et al. Iron addiction: a novel therapeutic target in ovarian cancer. Oncogene. 2017;36(29):4089-99.

220. Xu T, Ding W, Ji X, Ao X, Liu Y, Yu W, Wang J. Molecular mechanisms of ferroptosis and its role in cancer therapy. J Cell Mol Med. 2019;23(8):4900-12.

221. Li D, Li Y. The interaction between ferroptosis and lipid metabolism in cancer. Signal Transduct Target Ther. 2020;5(1):108-.

222. VanderWall K, Daniels-Wells TR, Penichet M, Lichtenstein A. Iron in multiple myeloma. Crit Rev Oncog. 2013;18(5):449-61.

223. Viswanathan VS, Ryan MJ, Dhruv HD, Gill S, Eichhoff OM, Seashore-Ludlow B, Kaffenberger SD, Eaton JK, Shimada K, Aguirre AJ, et al. Dependency of a therapy-resistant state of cancer cells on a lipid peroxidase pathway. Nature. 2017;547(7664):453-7.

224. Hangauer MJ, Viswanathan VS, Ryan MJ, Bole D, Eaton JK, Matov A, Galeas J, Dhruv HD, Berens ME, Schreiber SL, et al. Drug-tolerant persister cancer cells are vulnerable to GPX4 inhibition. Nature. 2017;551(7679):247-50.

225. Tsoi J, Robert L, Paraiso K, Galvan C, Sheu KM, Lay J, Wong DJL, Atefi M, Shirazi R, Wang X, et al. Multi-stage Differentiation Defines Melanoma Subtypes with Differential Vulnerability to Drug-Induced Iron-Dependent Oxidative Stress. Cancer Cell. 2018;33(5):890-904 e5.

226. Wu J, Minikes AM, Gao M, Bian H, Li Y, Stockwell BR, Chen ZN, Jiang X. Intercellular interaction dictates cancer cell ferroptosis via NF2-YAP signalling. Nature. 2019;572(7769):402-6.

227. Lee J, You JH, Kim MS, Roh JL. Epigenetic reprogramming of epithelial-mesenchymal transition promotes ferroptosis of head and neck cancer. Redox Biol. 2020;37:101697.

228. Zhang Y, Tan H, Daniels JD, Zandkarimi F, Liu H, Brown LM, Uchida K, O'Connor OA, Stockwell BR. Imidazole Ketone Erastin Induces Ferroptosis and Slows Tumor Growth in a Mouse Lymphoma Model. Cell Chem Biol. 2019;26(5):623-33 e9.

229. A NA, ME FH, Naqishbandi AM, Efferth T. Induction of Apoptosis, Autophagy and Ferroptosis by Thymus vulgaris and Arctium lappa Extract in Leukemia and Multiple Myeloma Cell Lines. Molecules. 2020;25(21).

230. Schmitt A, Xu W, Bucher P, Grimm M, Konantz M, Horn H, Zapukhlyak M, Berning P, Brandle M, Jarboui MA, et al. Dimethyl fumarate induces ferroptosis and impairs NF-kappaB/STAT3 signaling in DLBCL. Blood. 2021.

231. Wang N, Zeng GZ, Yin JL, Bian ZX. Artesunate activates the ATF4-CHOP-CHAC1 pathway and affects ferroptosis in Burkitt's Lymphoma. Biochem Biophys Res Commun. 2019;519(3):533-9.

232. Zhong Y, Tian F, Ma H, Wang H, Yang W, Liu Z, Liao A. FTY720 induces ferroptosis and autophagy via PP2A/AMPK pathway in multiple myeloma cells. Life Sci. 2020;260:118077.

233. Zuo S, Yu J, Pan H, Lu L. Novel insights on targeting ferroptosis in cancer therapy. Biomark Res. 2020;8:50.

234. Campanella A, Santambrogio P, Fontana F, Frenquelli M, Cenci S, Marcatti M, Sitia R, Tonon G, Camaschella C. Iron increases the susceptibility of multiple myeloma cells to bortezomib. Haematologica. 2013;98(6):971-9.

235. Bordini J, Galvan S, Ponzoni M, Bertilaccio MT, Chesi M, Bergsagel PL, Camaschella C, Campanella A. Induction of iron excess restricts malignant plasma cells expansion and potentiates bortezomib effect in models of multiple myeloma. Leukemia. 2017;31(4):967-70.

236. Bordini J, Morisi F, Cerruti F, Cascio P, Camaschella C, Ghia P, Campanella A. Iron Causes Lipid Oxidation and Inhibits Proteasome Function in Multiple Myeloma Cells: A Proof of Concept for Novel Combination Therapies. Cancers (Basel). 2020;12(4).

237. Cao LL, Liu H, Yue Z, Liu L, Pei L, Gu J, Wang H, Jia M. Iron chelation inhibits cancer cell growth and modulates global histone methylation status in colorectal cancer. Biometals. 2018;31(5):797-805.

238. Pan ZY, Tan CP, Rao LS, Zhang H, Zheng Y, Hao L, Ji LN, Mao ZW. Recoding the Cancer Epigenome by Intervening in Metabolism and Iron Homeostasis with Mitochondria-Targeted Rhenium(I) Complexes. Angew Chem Int Ed Engl. 2020;59(42):18755-62.

239. Cyr AR, Domann FE. The redox basis of epigenetic modifications: from mechanisms to functional consequences. Antioxid Redox Signal. 2011;15(2):551-89.

240. Kawai K, Li YS, Song MF, Kasai H. DNA methylation by dimethyl sulfoxide and methionine sulfoxide triggered by hydroxyl radical and implications for epigenetic modifications. Bioorg Med Chem Lett. 2010;20(1):260-5.

241. Wang Y, Yu L, Ding J, Chen Y. Iron Metabolism in Cancer. Int J Mol Sci. 2018;20(1).

242. Flint DH, Tuminello JF, Emptage MH. The inactivation of Fe-S cluster containing hydro-lyases by superoxide. J Biol Chem. 1993;268(30):22369-76.

243. Ye H, Rouault TA. Human iron-sulfur cluster assembly, cellular iron homeostasis, and disease. Biochemistry. 2010;49(24):4945-56.

244. Yang M, Pollard PJ. Succinate: a new epigenetic hacker. Cancer Cell. 2013;23(6):709-11.

245. Cramer-Morales KL, Heer CD, Mapuskar KA, Domann FE. Succinate Accumulation Links Mitochondrial MnSOD Depletion to Aberrant Nuclear DNA Methylation and Altered Cell Fate. J Exp Pathol (Wilmington). 2020;1(2):60-70.

246. Lu SC. Regulation of glutathione synthesis. Curr Top Cell Regul. 2000;36:95-116.

247.Lertratanangkoon K, Wu CJ, Savaraj N, Thomas ML. Alterations of DNA methylation by glutathione depletion. Cancer Lett. 1997;120(2):149-56.

THESIS OUTLINE

&

RESEARCH OBJECTIVES

Thesis Outline and Research Objectives

As outlined in the introductory chapters, multiple myeloma (MM) is a heterogenous disease hallmarked by treatment failure of existing anti-cancer drugs. Due to the multifactorial nature of the molecular mechanisms involved in acquisition of therapy resistance, it remains challenging to develop effective, curative treatment regimens for MM. Thus, there is an urgent need to explore novel therapeutic strategies to achieve complete and persistent tumor remission in MM patients.

In this thesis, we aimed to characterize the mechanism of action and efficacy of (natural) protein kinase inhibitors and ferroptosis-inducing compounds in MM. In particular, the following two research questions are discussed in the results section of this PhD work:

Part 1 - Do protein kinase inhibitors hold promise in treating drug-resistant multiple myeloma cells?
Protein kinases (PKs) are enzymes that promote rapid signal transduction of extra- and intracellular stimuli by phosphorylating their substrate proteins. Many malignancies, including MM, display aberrant kinase signaling, which results in development of therapy resistance and improved cell survival. Protein kinase inhibitors (PKIs) have therefore received growing pharmacological interest over the past decades and have shown promising therapeutic responses in B-cell malignancies. To this end, we examined whether inhibition of key PKs might aid in eliminating therapy-resistant MM cells.

In **chapter 3**, we performed phosphopeptidome kinome activity profiling of glucocorticoid-resistant and -sensitive MM cells to identify key PKs that regulate therapy resistance. We subsequently explored whether certain PKIs, such as Withaferin a and ibrutinib, effectively target GC-resistant cells and could offer clinical benefits for MM patients by further elucidating their mechanism of action.

In **chapter 4**, we explored the kinase activity changes taking place in ferroptotic and apoptotic MM cells. By comparing the kinome profiles of both cell death modalities, we aimed to identify pivotal PKs that regulate ferroptosis- and apoptosis-specific cell death. Because multi-drug resistance in MM is often mediated by their ability to evade apoptosis, ferroptosis induction by means of PKI might serve as an alternative strategy to treat drug-resistant MM cells.

Part 2 - Can ferroptosis-induced epigenetic changes overcome therapy-resistance in multiple myeloma?
Ferroptosis is a non-apoptotic mode of regulated cell death characterized by an iron dependent rise in reactive oxygen species that propagate lipid peroxidation reactions. Given that MM tumors already exhibit high basal oxidative stress levels and an altered iron metabolism due to their increased proliferation capacity, ferroptosis induction might

further be exploited to exhaust the tumoral anti-oxidant defense mechanisms and overcome multi-drug resistance. In the second part of the results section, we investigated whether MM cells are sensitive to ferroptosis induction. Moreover, we examined the involvement of nuclear events and epigenetic regulatory mechanisms in ferroptosis signaling as they largely remain unexplored.

In **chapter 5**, we combined RNA sequencing, LC-MS/MS, pyrosequencing, and EPIC BeadChip analysis to characterize epigenetic changes taking place in therapy-resistant and -sensitive MM cells treated with ferroptosis inducer RSL3.

In **chapter 6**, we investigated the role of chromatin remodeler forkhead box A1 (FOXA1) in ferroptosis signaling. Ferroptotic MM cells were subjected to RNA and CUT&RUN sequencing to characterize FOXA1 expression profiles and downstream targets in different ferroptosis models.
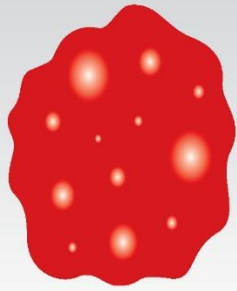
RESULTS

CHAPTER 3:
Covalent Cysteine Targeting of Bruton Tyrosine Kinase (BTK) Family by Withaferin-A Reduces Survival of Glucocorticoid Resistant Multiple Myeloma MM1 Cells

CHAPTER 4:
Unraveling the Kinase Signature of Ferroptotic Multiple Myeloma Cells

CHAPTER 5:
Ferroptosis Induction in Multiple Myeloma Cells Triggers an Epigenomic Stress Response Associated with DNA Repair and Cellular Senescence

CHAPTER 6:
Characterizing the Role of Chromatin Remodeler FOXA1 in Ferroptotic Cell Death

Chapter 3

Covalent Cysteine Targeting of Bruton Tyrosine Kinase (BTK) Family by Withaferin-A Reduces Survival of Glucocorticoid Resistant Multiple Myeloma MM1 Cells

Chapter 3:

Covalent Cysteine Targeting of Bruton Tyrosine Kinase (BTK) Family by Withaferin-A Reduces Survival of Glucocorticoid Resistant Multiple Myeloma MM1 Cells

Emilie Logie[1†], Chandra S Chirumamilla[1†], Claudina Perez-Novo[1], Priyanka Shaw[2], Ken Declerck[1], Ajay Palagani[1], Savithri Rangarajan[3], Bart Cuypers[4], Nicolas De Neuter[4], Fazil Mobashar Hussain Urf Turabe[5], Navin Kumar Verma[5], Annemie Bogaerts[2], Kris Laukens [4], Fritz Offner[6], Pieter Van Vlierberghe[7], Xaveer van Ostade[1], Wim Vanden Berghe[1]*

1. Laboratory of Protein Science, Proteomics and Epigenetic Signaling (PPES) and Integrated Personalized and Precision Oncology Network (IPPON), Department of Biomedical Sciences, University of Antwerp, Campus Drie Eiken, Universiteitsplein 1, Wilrijk, Belgium
2. Plasma Lab for Applications in Sustainability and Medicine Antwerp (PLASMANT), Department of Chemistry, University of Antwerp, Wilrijk, Belgium
3. PamGene International B.V., 's Hertogenbosch, , The Netherlands
4. Biomedical Informatics Network Antwerp (Biomina), Department of Informatics, University of Antwerp, Wilrijk, Belgium
5. Lymphocyte Signaling Research Laboratory, Lee Kong Chian School of Medicine, Nanyang Technological University Singapore, 1308232, Singapore
6. Hematology, Department of internal medicine, Ghent University, Ghent, Belgium
7. Department of Biomolecular Medicine, Ghent University, Ghent, Belgium

† These authors contributed equally to this work
* Corresponding author: wim.vandenberghe@uantwerpen.be

Conflict of Interest: The authors declare no conflict of interest.

Abstract

Multiple myeloma (MM) is a hematological malignancy characterized by the uncontrolled growth of plasma cells. The major barrier in treating MM is the occurrence of primary and acquired therapy resistance to anti-cancer drugs. Often, this therapy resistance is associated with constitutive hyperactivation of tyrosine kinase signaling. Novel covalent kinase inhibitors, such as the clinically approved Bruton tyrosine kinase (BTK) inhibitor ibrutinib (IBR) and the preclinical phytochemical Withaferin A (WA), have therefore gained pharmaceutical interest. Remarkably, WA is more effective than IBR in killing BTK-overexpressing glucocorticoid (GC)-resistant MM1R cells. To further characterize the kinase inhibitor profiles of WA and IBR in GC-resistant MM cells, we applied phosphopeptidome- and transcriptome-specific tyrosine kinome profiling. In contrast to IBR, WA was found to reverse BTK overexpression in GC-resistant MM1R cells. Furthermore, WA-induced cell death involves covalent cysteine targeting of Hinge-6 domain type tyrosine kinases of the kinase cysteinome classification, including inhibition of the hyperactivated BTK. Covalent interaction between WA and BTK could further be confirmed by biotin-based affinity purification and confocal microscopy. Similarly, molecular modeling suggests WA preferably targets conserved cysteines in the Hinge-6 region of the kinase cysteinome classification, favoring inhibition of multiple B-cell receptor (BCR) family kinases. Altogether, we show that promiscuous inhibition of multiple BTK family tyrosine kinases by WA represents a highly effective strategy to overcome GC-therapy resistance in MM.

Keywords: Withaferin A; BTK; multiple myeloma; therapy resistance; glucocorticoids; ibrutinib
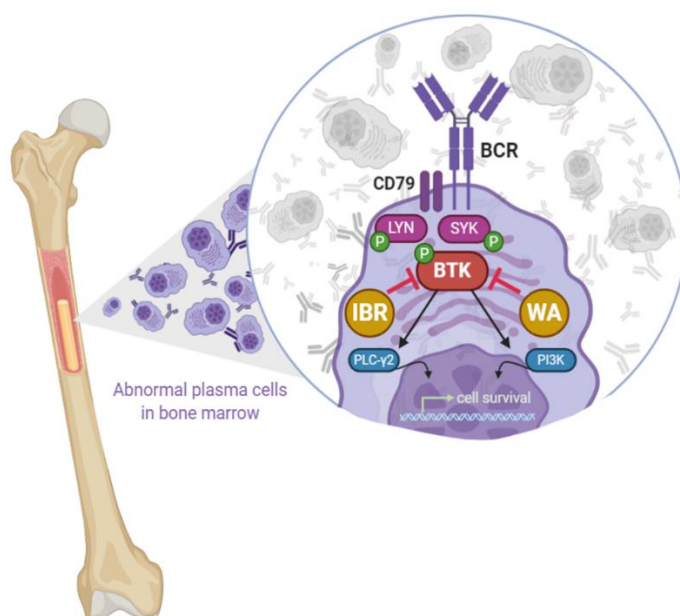
3.1. Introduction

MM is a hematological malignancy of terminally differentiated plasma cells and is currently the second most common adult blood cancer [1]. MM often results in the development of end-organ diseases, such as anemia, hypercalcemia, renal insufficiency, and bone lesions, making it an illness of considerable clinical and social impact [2,3]. In recent years, important therapeutical advancements in the field of MM have been made, increasing life expectancy of patients with six to ten years [4,5]. These novel therapies have mostly been developed on the basis of an improved understanding of the biology of myeloma cells and their interaction with the bone marrow (BM) environment [6] and include proteasome inhibitors [7], immunomodulatory drugs [8], GCs [9], monoclonal antibodies [10], and histone deacetylase inhibitors [11]. However, MM still remains an incurable disease as the majority of patients eventually relapse and become refractory to existing therapies [12]. Acquisition of resistance to anti-cancer drugs therefore remains the main barrier in treating MM [4,13].

One of the cellular pathways mediating drug resistance in many B-cell malignancies is the B-cell receptor (BCR) signaling pathway [14]. Under physiological conditions, the BCR is activated upon ligation of antigen and promotes survival, function and development of B-cells [15]. After initial antigen binding, the immune receptor tyrosine activation motif domains CD79A and CD79B are phosphorylated by Src family kinases Lyn and Syk, and recruit other adaptor proteins and tyrosine kinases (TK), a key example being Bruton tyrosine kinase (BTK) [16]. BTK ultimately orchestrates activation of downstream effectors of BCR signaling, such as nuclear factor-κB (NF-κB) and nuclear factor of activated T cells (NFAT), through phospholipase C (PLC)-γ2 and phosphoinositide 3-kinase (PI3K) phosphorylation [14]. In MM, BTK is often constitutively activated thereby modulating survival signals and therapy resistance [17-20]. As a result, BTK kinase inhibitors have received growing pharmacological interest and have already shown promising therapeutic responses in B-cell malignancies in the clinic [21]. More particularly, the covalent binding BTK inhibitor IBR has shown to be a potent anti-cancer drug in chronic lymphocytic leukemia (CLL), mantle cell lymphoma, diffuse large B-cell lymphoma, and MM by interfering with B-cell homing, survival and microenvironment-mediated drug resistance [17,18,22-25]. Suppression of BTK hyperactivation is also key to therapeutic efficacy of GCs in B-cell leukemias, where IBR has been shown to improve GC therapy response [26-29]. In clinical trials of MM, combination therapies investigating IBR efficiency demonstrated encouraging responses and a manageable safety profile [30,31].

Although preliminary clinical data revealed the beneficial effects and acceptable safety profile of IBR in MM, clinical studies in other B-cell malignancies have linked IBR use with adverse effects, including diarrhea, fatigue, nausea, and rashes [32,33]. More importantly, IBR therapy is associated with a significant increase in the occurrence of ventricular arrhythmias and sudden cardiac death [34,35]. The underlying mechanisms of these severe side effects are not well understood but could be partially explained by the off-targets interaction of IBR with interleukin-2-inducible T-cell kinase (ITK), epidermal growth factor (EGFR), and PI3 [36]. Another pressing issue that has arisen since IBR has been applied in

the clinic, is the development of therapy resistance (reviewed in [37]). Nearly one third of patients diagnosed with B-cell malignancies display primary resistance against IBR therapy, while many others acquire resistance over time. These major issues accompanying therapeutic use of IBR have sparked the development of second and third generation BTK inhibitors (e.g. acalabrutinib), characterized by a higher selectivity and potency profiles [38]. Unfortunately, acquired resistance to these novel BTK inhibitors has already been described in some B-cell malignancies as well [39]. As a result, alternative treatment strategies to suppress BTK hyperactivation in therapy resistant hematological malignancies are currently being investigated in high-throughput combinatorial screenings of clinically approved and preclinical investigational compound libraries [40]. Given that nearly half of the agents used in cancer therapy today are either natural products or derivatives thereof, novel BTK-targeting lead compounds might be identified from this vast arsenal of chemically active structures [41-43]. Interestingly, Withaferin A, a withanolide phytochemical isolated from *Withania somnifera,* is one of the top investigational compounds prioritized for IBR combination therapy to target chronic active BCR signaling [40].

WA reveals broad spectrum therapeutic activities in several (drug resistant) cancer cell types [44], including B-cell lymphoma and MM [45-47]. Of particular interest, some of the anti-tumor effects of WA have been attributed to its ability to covalently target kinase activity [48-52]. Accordingly, innovative phosphopeptidome kinome activity profiling, RNA sequencing, in silico docking simulations, and chemo-affinity approaches were combined in this study to characterize BTK hyperactivation and tyrosine kinase (TK) inhibitor therapy response of WA and IBR in GC-resistant MM cells.

3.2. Results

3.2.1. GC Therapy resistance in Multiple Myeloma is Associated with Hyperactivation of Tyrosine Kinases

GC therapy sensitive MM1S and resistant MM1R cell lines derived from a single MM patient have previously been described as cell models to study etiology of GC therapy resistance and to evaluate novel classes of chemotherapeutic drugs [53,54]. To investigate the vulnerability of GC-resistant MM1R cells for specific clinical TK inhibitor drugs, we compared the tyrosine kinome activity profiles of GC-resistant MM1R and GC-sensitive MM1S cell lysates by means of a Tyrosine protein kinase (PTK)-specific phosphopeptide array (PamChip), containing 144 conserved peptides corresponding to TK specific substrates [55,56]. Overall, TK activity was consistently higher in MM1R cells compared to MM1S cells (Figure 1a, Supplementary Figure S1). Identification of the 20 most significant differential hyperphosphorylated peptides (adjusted p-value (FDR) < 0.01) in MM1R compared to MM1S predicted hyperactivation of multiple (non) receptor TK in MM1R, such as SYK, DDR, ABL, ZAP70, FAK2, BRK, BTK, ITK and FGR (Figures 1b). Subsequent MetaCore pathway analysis showed that the hyperactivated kinases in MM1R cells are involved in cell

proliferation, cell cycle regulation, cell adhesion, cancer, therapy resistance, immune response, T-cell receptor signaling and BCR signaling (Supplementary Figure S2).

To investigate whether the observed TK hyperactivation is also reflected at the transcriptome level, RNA sequencing analysis of basal gene expression in MM1S and MM1R cells was conducted. Results were analyzed with the R-package DESeq2 [57], using a selection criteria of a minimal FDR < 0.01. Upon comparing gene expression patterns in both cell lines, 1383 differentially expressed genes (DEG) (logFC > 1 or logFC < -1) could be identified (Figure 1c). Interestingly, from all hyperactivated TK in MM1R cells listed before, BTK was identified as the strongest upregulated TK in GC-resistant MM1R cells (Figure 1d) and is included in the top 20 most significant DEG (Table 1). Upregulation of BTK in MM1R cells was validated by qPCR and Western blot analysis (Figure 1e-f), and is in line with previous observations [17,58]. Taken together, these findings suggest that BCR signaling and BTK in MM1R cells may represent an attractive target to kill GC-resistant MM1R cells.

Table 1: Overview of top 20 most significantly differentially expressed genes (logFC>1 or logFC<-1) between GC-resistant MM1R and GC-sensitive MM1S cells.

	Symbol	Gene ID	Name	Log2FC	p-adj.
ECM and cell-cell adhesion	RELN*	5649	Reelin	2.9	7.4E-160
	PLXNB2	23654	Plexin B2	1.8	7.1E-96
	PODXL2*	50512	Podocalyxin like 2	2.6	6.8E-83
	ESAM	90952	Endothelial cell adhesion molecule	2.0	1.7E-80
	PRKX*	5613	Protein kinase X-linked	1.1	8.1E-79
	ACP5	54	Acid Phosphatase 5, tartrate resistant	4.8	2.0E-77
GPCR signaling	GNG7	2788	G protein subunit gamma 7	1.5	5.7E-99
	UTS2R	2837	Urotensin 2 receptor	1.9	5.4E-77
BCR signaling	**BTK***	**695**	**Bruton tyrosine kinase**	**2.8**	**1.5E-216**
	TNFRSF8	943	TNF receptor superfamily member 8	3.7	6.9E-93
	CD52	1043	CD52 molecule	3.5	5.6E-83
mRNA/protein stability	CTAG2	30848	Cancer/testis antigen 2	8.5	4.0E-168
	LINC01518	101929397	Long Intergenic Non-Protein Coding RNA 1518	7.9	1.4E-147
	CMTR1	23070	Cap methyltransferase 1	-1.1	9.6E-115
	TMEM25	84866	Transmembrane protein 25	4.8	6.0E-79
Cell cycle regulation	CDKN2A	1029	Cyclin dependent kinase inhibitor 2A	9.4	1.7E-210
Cytoskeleton	TUBB4A	10382	Tubulin beta 4A class IVa	3.6	6.1E-165
Inflammation	NLRP11	204801	NLR family pyrin domain containing 11	4.9	1.2E-220
Transmembrane transport	SLC38A5	92745	Solute carrier family 38 member 5	1.8	1.7E-92
	ABCG2*	9429	ATP binding cassette subfamily G member 2	5.6	2.0E-84

*Genes associated with therapy resistance. Abbreviations: ECM, extracellular matrix; GPCR, G-protein coupled receptor; BCR,B-cell receptor.

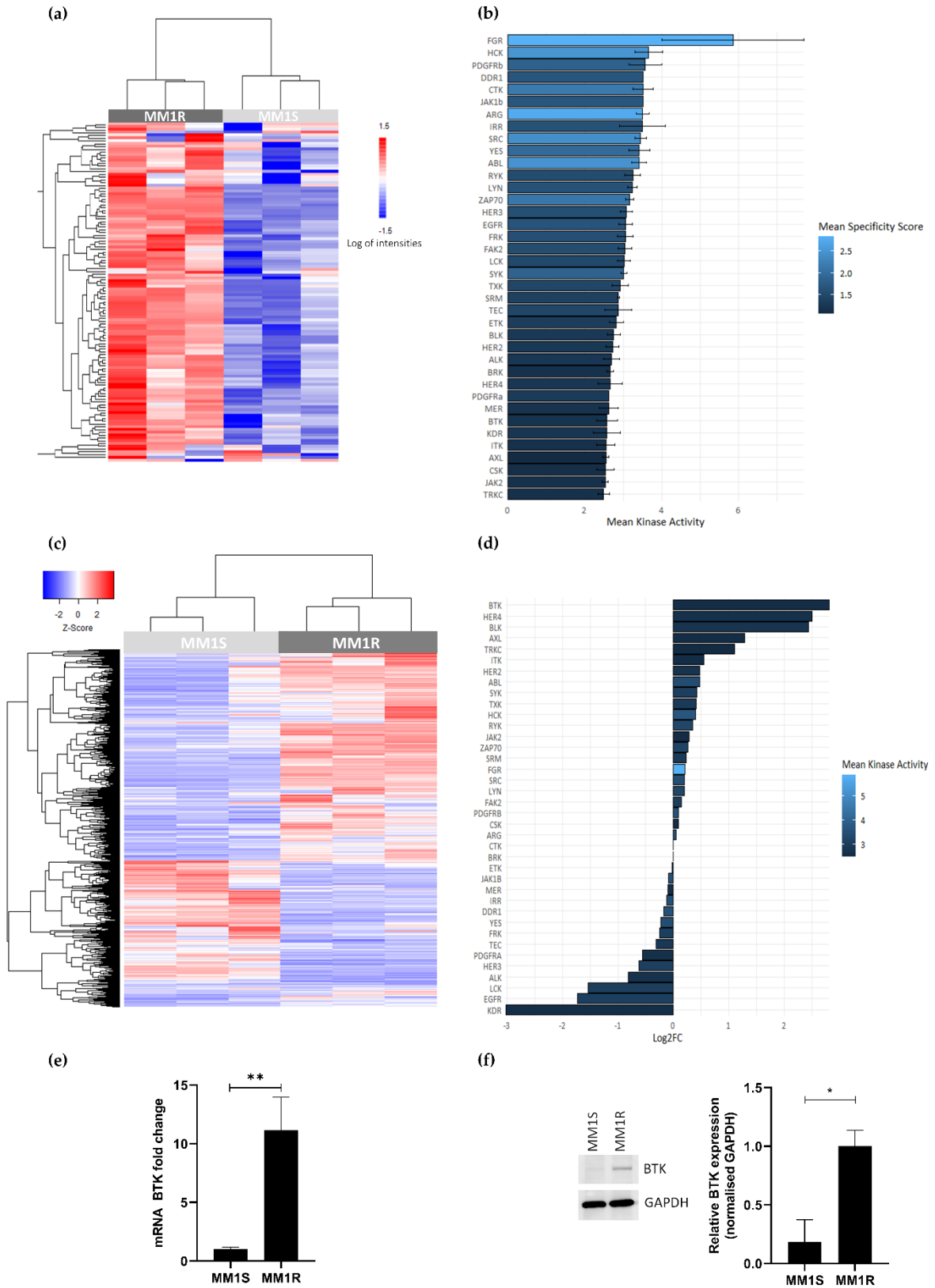*Figure 1:* (**a**) Heatmap showing phosphorylation intensities of peptides serving as substrates for tyrosine kinases. Figure shows hyperphosphorylated (red) or hypo-phosphorylated (blue) peptides in MM1R (*n*=3) and MM1S (*n*=3) samples. (**b**)

Ranking of hyperactivated kinases in MM1R versus MM1S cells based on the top 20 significant differentially phosphorylated peptides. Fill color of the bars is based on the kinase specificity score, indicating the specificity of differences in kinase activity with respect to the amount of peptides used for predicting the corresponding kinase (**c**) Heatmap representation of differentially expressed genes (logFC >|1|, p<0.01) in MM1R versus MM1S cells as determined by RNA sequencing. n=3 biologically independent replicates per cell line. (**d**) Ranking of the top overexpressed kinases in MM1R versus MM1S cells based on their log2 fold change as determined by RNA sequencing. Fill colors of the bars are a measure for kinase activity as measured via the PTK-specific phosphopeptide array. (**e**) Relative BTK mRNA levels in MM1R and MM1S cells. Data are plotted as the mean ± s.d., n=3 biologically independent replicates (**p = 0.0035, unpaired t-test). (**f**) Western immunoblot detection and quantification of basal BTK and GAPDH protein levels in MM1R and MM1S cells. Data are plotted as the mean ± s.d., n=3 biologically independent replicates (*p = 0.0385, unpaired t-test).

3.2.2. The Tyrosine Kinase Inhibitor Profile of Withaferin A and Ibrutinib Show a High Degree of Similarity

Taking into account the hyperactivation of BCR-BTK kinase signaling in MM1R cells (see 2.1.), we next tested their sensitivity for the clinically approved BTK inhibitor IBR as well as WA, a top prioritized investigational phytotherapeutic compound identified in a high-throughput drug screening against chronic BCR signaling [40]. MM1R cells were treated for 24 h with different concentrations of WA or IBR kinase inhibitors and the relative % cell survival/cell death was evaluated by MTT assay. Both compounds were effective in killing GC-resistant MM1R cells in a dose-dependent manner, although WA is the more potent cell death inducer (IC50 = 1.7 µM), since its IC50 was > 10 times lower than the one of IBR (IC50 = 27.9 µM) (Figure 2a). Remarkably, both WA and IBR also induce cell death in GC-sensitive MM1S cells lacking BTK overexpression, although IC50 values were higher compared to MM1R cells (IC50$_{WA}$ = 1.9 µM, IC50$_{IBR}$ = 49.3 µM) (Figure 2a).

To explore the mode of action of these compounds, we measured corresponding cellular changes in TK activities by phosphopeptidome based tyrosine kinome profiling of MM1R cells exposed to either WA (1 µM) or IBR (1 µM). Similarly, and as mentioned above, cell lysates of treated cells were analyzed through PTK-specific phospho-peptide arrays after which the top activated or inhibited kinases were identified based on the significant differences in phospho-intensities of the PTK peptide substrates. We found that WA and IBR both inhibited most of the hyperactivated kinases in MM1R cells, with largely overlapping, though promiscuous, TK inhibitor profiles (Figure 2b, annotation of heatmap rows can be found in Supplementary Figure S3). At the level of BCR signaling, clear inhibition of BTK kinase activity can be observed in presence of IBR, as expected, and WA (Figure 2c-d). Besides BTK, multiple BCR signaling kinases such as ZAP70, BLK, FLT3, TEC, and SYK, are also targeted by both WA and IBR (Figure 2c). In line with previous studies which already revealed that IBR can trigger off-target BCR-BTK independent kinase inhibitor (side) effects [59], we also identified additional IBR-responsive TK in MM1R cells (Figure 2c, Supplementary Figure S3). Of special note, whereas most binding affinities of IBR have been determined in vitro (Supplementary Figure S4), we provide the first cell-based integrated tyrosine kinome activity map in MM1R cells in the presence of the IBR inhibitor. Although WA inhibits similar BCR family kinases as IBR, variations in kinase inhibitor specificity/potency of WA in comparison to IBR treatment may explain differences in therapeutic efficacy of both compounds in MM1R cells (Figure 2a and 2d).
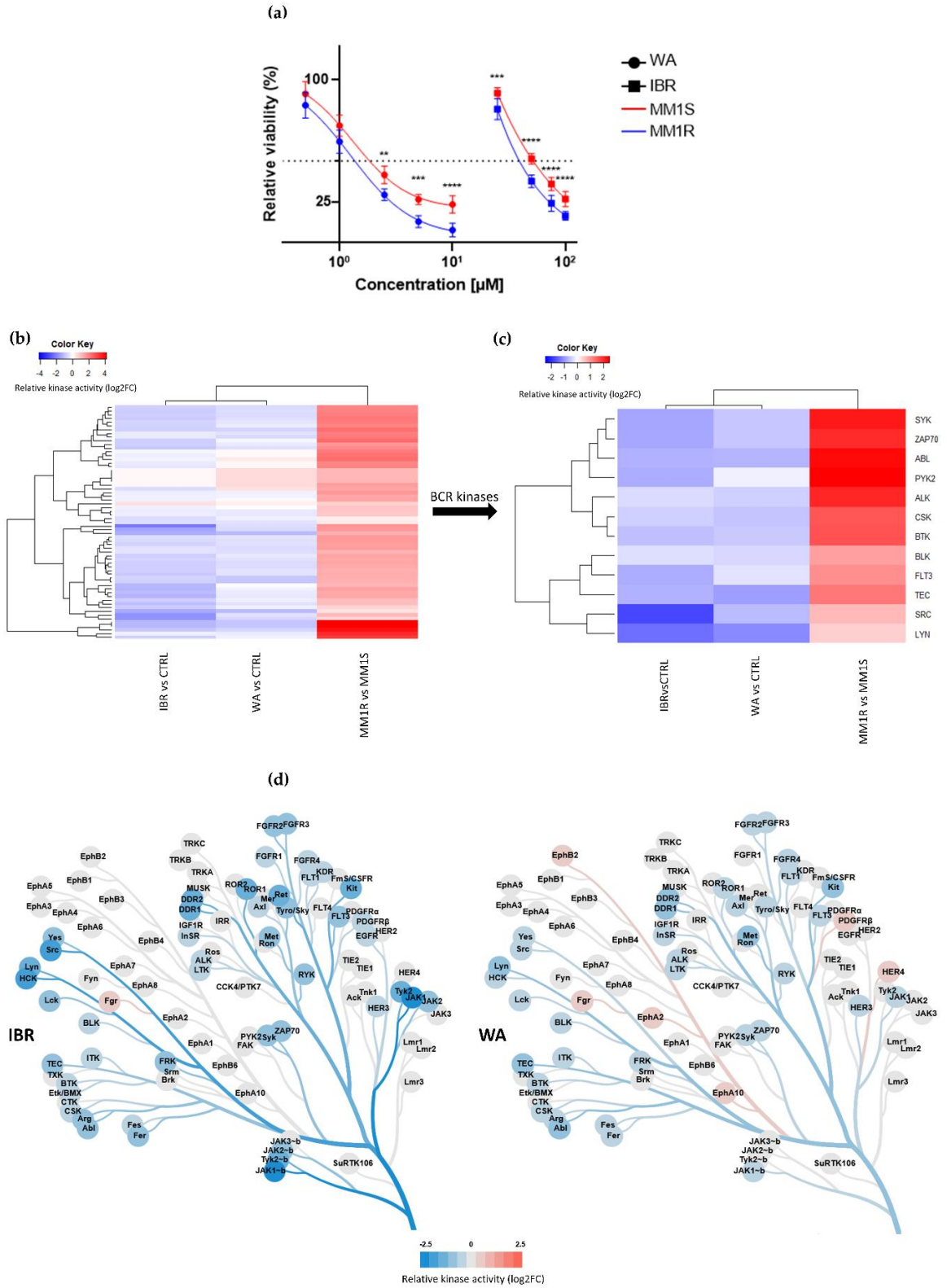
Figure 2: (**a**) Relative cell viability of MM1 cells upon 24 h exposure to increasing concentrations of IBR or WA. Data are plotted as the mean ± s.d., n=3 biologically independent replicates. (**p < 0.01, ***p < 0.001 ****p < 0.0001, ANOVA). (**b**) Heatmap representation of hyperactivated or inhibited kinases in MM1R versus MM1S cells, or following 15 min IBR or WA treatment, n=3 biologically independent replicates per treatment group. (**c**) Close-up heatmap representation of

figure 2b showing inhibited BCR-related kinases in MM1R versus MM1S, or following 15 min IBR or WA treatment, n=3 biologically independent replicates per treatment group. (**d**) Kinase trees displaying the tyrosine kinase targets of IBR (left) and WA (right). Kinases trees were generated with the CORAL web tool (http://phanstiel-lab.med.unc.edu/CORAL/).

3.2.3. WA Inhibits BCR-BTK Kinase Activity by Transcriptional Downregulation and Covalent Cysteine-Dependent Targeting of BTK

To further characterize how WA decreases BTK kinase activity in MM1R cells, we next checked whether WA treatment is changing BTK mRNA and protein expression levels. Panther pathway enrichment analysis of RNA sequencing data from WA-treated MM1R cells already revealed that DEGs are significantly enriched in B-cell activation (Figure 3a). More particularly, WA significantly decreased BTK mRNA expression (Log2FC = -0.525, FDR = 0.023). This was further confirmed by qPCR and Western immunoblot experiments. As can be observed from Figure 3b-3c, WA was able to lower BTK expression in a time-dependent manner, both at the mRNA and protein level. Similar WA-specific changes could also be observed in U266 cells, another GC-resistant multiple myeloma cell line sensitive to WA treatment (Figure 3b-3c, Supplementary Figure S5). In line with previous studies [60-62], we did not observe any changes in BTK expression after IBR treatment of MM1R cells indicating that IBR mainly targets BTK (hyper)phosphorylation and not total BTK protein levels (Supplementary Figure S6).

Since WA contains several reactive nucleophilic groups which can covalently bind to kinase sulfhydryl groups of cysteines through Michael addition [48,63,64], we also evaluated potential covalent binding of WA to BTK by pull-down experiments with biotinylated WA (WABI). Pull-down experiments with WABI in MM1R cells indeed confirmed cysteine-dependent binding to BTK, which can be blocked by excess amounts (1mM) of the reducing agent dithiothreitol (DTT) (Figure 4a). Along the same line, covalent WA-BTK interaction could be confirmed in U266 cells (Figure 4b). The biological relevance of this covalent interaction could further be validated in wash-out experiments where MM1R cells were exposed to increasing concentrations of WA for 15min, after which it was washed away with PBS. Although WA cells were only briefly treated with WA, cell viability of MM1R cells was still affected in a dose-dependent manner 24 h post treatment (Supplementary Figure S7). The growth inhibition remains the strongest in the unwashed cells, suggesting contribution of non-covalent interactions of WA as well. H-bond and van de waals interactions between WA and target molecules, such as Hsp90, have indeed been reported to contribute to the anti-cancer mechanism of WA [65]. Alternatively, covalent binding by WA maybe weaker than a normal covalent binding and become reversed by washout experiments [66-68] Finally, by confocal microscopy, we were also able to demonstrate colocalization of BTK and WABI in MM1R cells (Figure 4c).
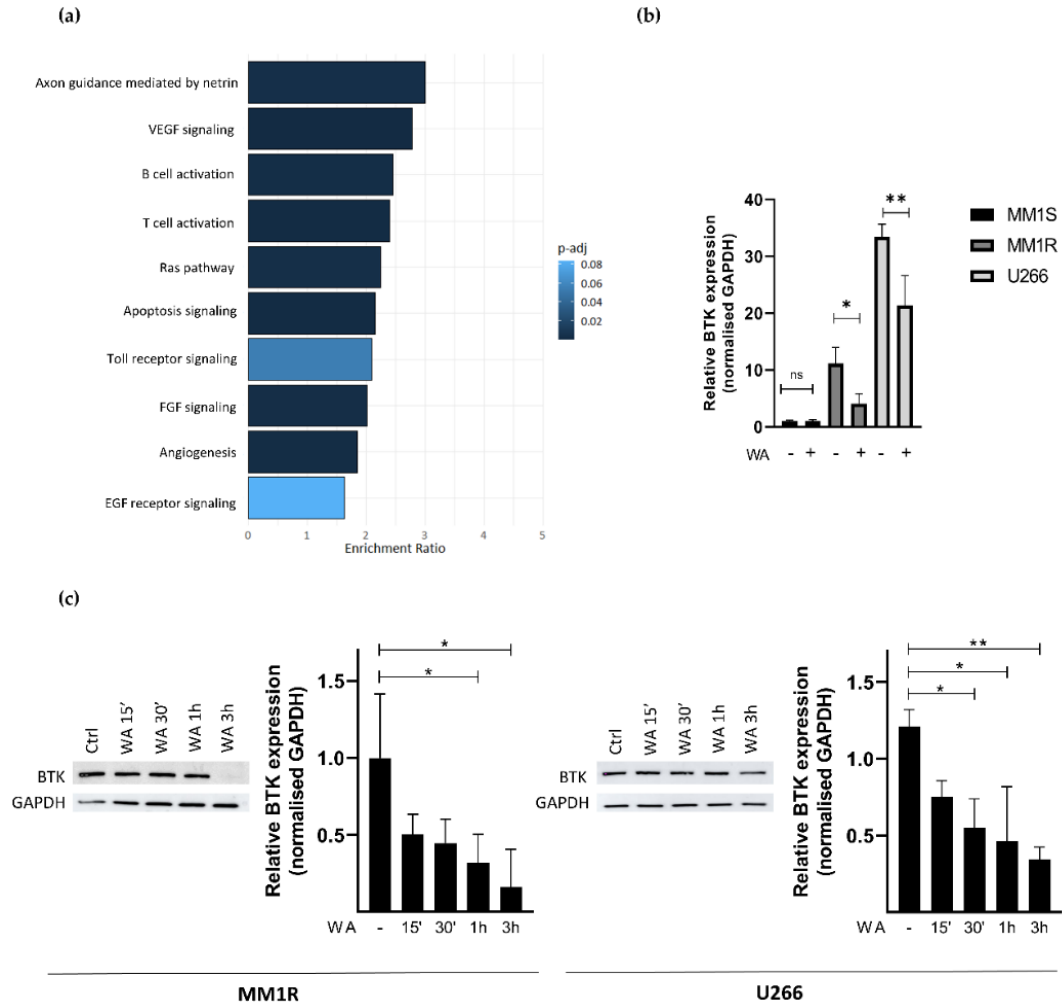
Figure 3: (**a**) Panther pathway enrichment analysis of significant (FDR < 0.05) differentially expressed genes of WA-treated MM1R cells as determined by RNA sequencing. (**b**) Relative BTK mRNA levels of MM1R, MM1S and U266 cells treated with WA for 3 hr. Data are plotted as the mean ± s.d., *n*=3 biologically independent replicates (*p = 0.0453, **p = 0.0015, ANOVA) (**c**) Western blot detection and quantification of BTK and GAPDH expression levels after WA treatment in MM1R and U266 cells. Data are plotted as the mean ± s.d., *n*=3 biologically independent replicates. (*p < 0.05, **p < 0.01, ANOVA).
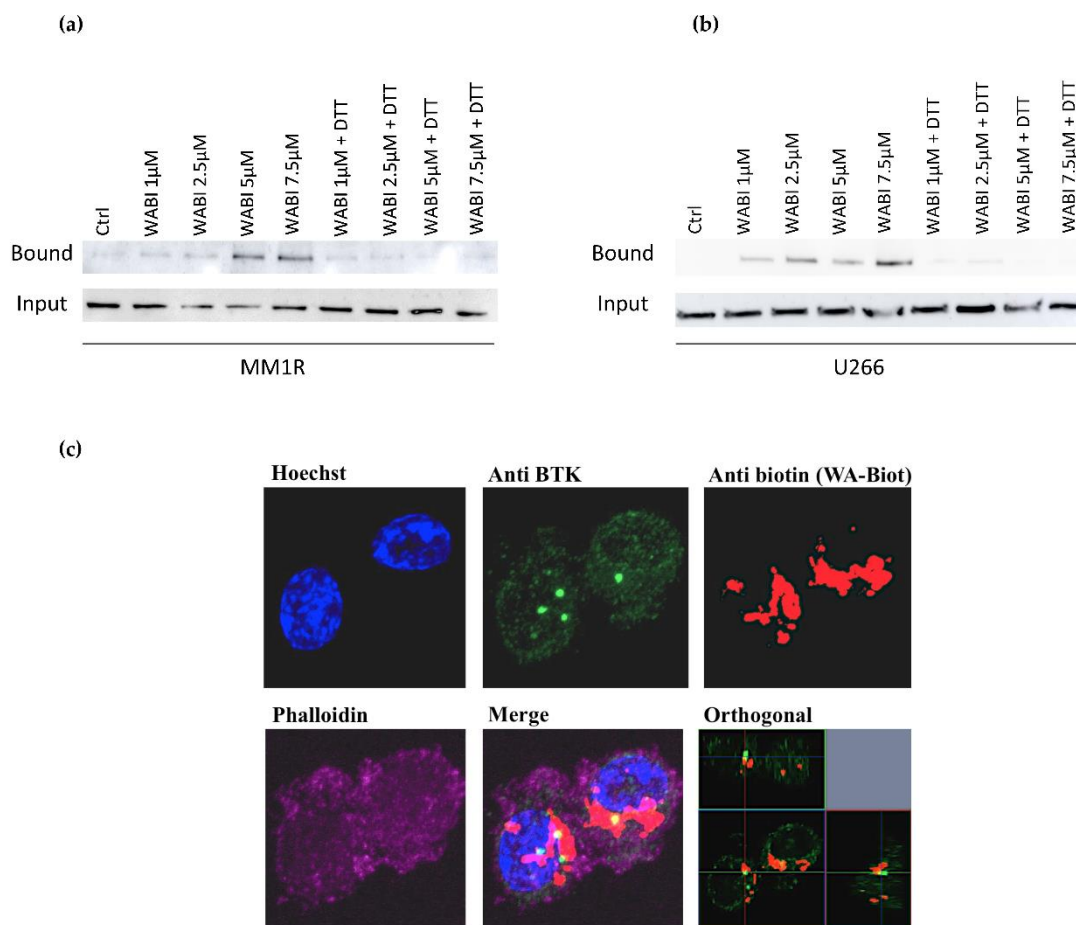
Figure 4: (**a**) Western immunoblot detection of BTK levels before and after pulldown with biotinylated WA (WABI), following 2 h WABI treatment in MM1R in the presence or absence of excess thiol donor DTT (1 mM). (**b**) Western immunoblot detection of BTK levels before and after pulldown with biotinylated WA (WABI), following 2 h WABI treatment in U266 cells in the presence or absence of excess thiol donor DTT (1 mM). (**c**) Confocal imaging of colocalization of BTK expression and WABI localization in MM1R cells.

3.2.4. Covalent C481 Targeting of BTK by WA in Hinge-6 Domain of the Protein Kinase Cysteinome Classification Reduces Survival of GC-Resistant MM1 cells

Human protein kinases are composed of two highly conserved domains, namely catalytic and regulatory domains. It has been shown that the catalytic domain can be further classified based on the positions of the gate keeper amino acids and cysteines hosted in the catalytic pocket [69-72]. Based on the positions of cysteines present across the human kinome, Leproult et al. reclassified the human kinome into a cysteinome according to the cysteine positions relative to the ATP binding pocket (Table 2) [69,73]. Interestingly, most kinases inhibited by WA treatment, including BTK, BLK and EGFR, were found to be highly enriched in Hinge-6 domain type kinases (Table 2). Multiple sequence alignment of these Hinge-6 domain orthologs revealed the presence of a conserved glycine-cysteine motif, suggesting that WA covalently binds to this site within its TK targets (Figure 5a). Through

molecular docking studies, we found that the conserved cysteine site within BTK (Cys481) is indeed accessible and favorable (-4,93 kcal/mol) for WA binding (Supplementary Table 1). The docking results predict that covalent bond formation occurs via the C_4-OH group of WA and the Cys481 residue of BTK and that this interaction is further stabilized via hydrogen bond formation with surrounding Leu482, Tyr485 and Gly480 amino acids (Figure 5b-c). Given that IBR also covalently targets the Cys481 residue of BTK, these results suggest that WA interacts with BTK in a similar manner as IBR [63]. By using the NanoBRET Target Engagement Intracellular Kinase assay, where the affinity of WA for BTK can be analyzed by competitive displacement of a fluorescent NanoBRET Tracer bound to BTK, we could further confirm that WA is able to displace the WT BTK protein but not the mutated C481S BTK protein in HEK-293 cells (Figure 5d). This suggest that the Cys481 residue of BTK is the main binding site of WA. Furthermore, we show that silencing of endogenous WT BTK reduces MM1R cell viability and can be rescued upon overexpression of C481S BTK. (Figure 5e, Supplementary Figure S8). Of special note, C481S BTK overexpression cannot completely rescue WA induced cell death in MM1R, confirming that WA kinase effects on cell viability are not limited to BTK alone and may involve additional hinge 6 domain type kinase targets of the cysteinome classification in MM1R cells. Along the same line, GC-sensitive MM1S cells lacking BTK overexpression are also sensitive to WA treatment, through promiscuous covalent cysteine targeting of alternative cell survival tyrosine kinases expressed in MM1S cells (Supplementary Figure S9a-c).

Table 2: Kinase cysteinome classification. Summarized from [73]. Bold highlighted kinases represent the main tyrosine kinase targets of Withaferin A.

Site	Subsite	Representative kinases
Gate keeper region	GK	MOK
	GK + 1	SgK494
	GK - 1	MAP2K4, MKK3, MAP2K6, KHS1, KHS2, GCK
DFG region	DFG + 1	MAP3K8, MOS, MAP3K4, PINK1
	DFG + 2	PKCz, PKCi, AKT1, AKT2, AKT3, PKCg, SGK1F, SGK2
	DFG -1	PBK, TGFbR2, CDKL3, CDKL2, PRP4, MNK2, MNK1
Glycine rich loop region	Glycineloop	WNK4, WNK1, WNK2, WNK3, HER3
	Glycineloop 1	ZAK
	Glycineloop 2	SgK496, MEKK1, PLK2, PLK3, PLK1, RSK1
	Glycineloop 3	SgK493
	Glycineloop5	FGFR1, FGFR2, FGFR3, FGFR4
Hinge binding region	Hinge 1	FGFR4, TTK, MAPKAPK2, MAPKAPK3
	Hinge 2	IKKa, IKKb, LKB1, NEK4, Wee1, SLK, FLT4, KDR
	Hinge 3	Ron, FGR, SgK494, Kit, CSFR, FLT3
	Hinge 4	SgK110, BubR1, LKB1, TBK1
	Hinge 5	PINK1, EphB3
	Hinge 6	MAP2K7**, TEC, TXK, ITK, BTK, BMX, BLK, HER2, EGFR, HER4,** JAK3
	Hinge 7	JNK1, JNK2, JNK3
Roof region	Roof sheet	HER3
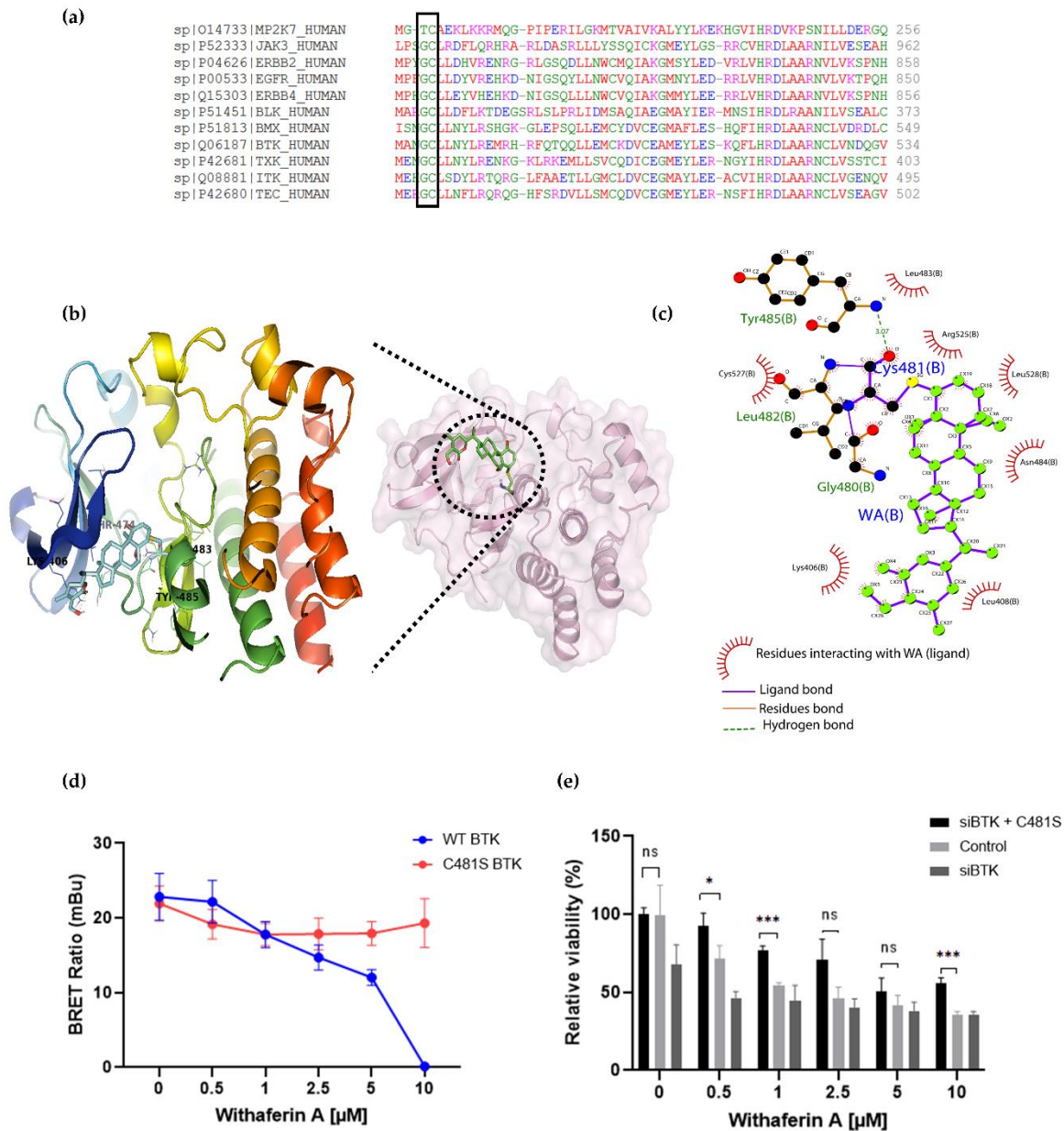
Figure 5: (**a**) Multiple sequence alignment of Hinge 6 domain type kinases. The conserved GC-motif between different orthologs is indicated. Alignment was performed with Clustal Omega (https://www.ebi.ac.uk/Tools/msa/clustalo/). (**b**) Crystal structure of BTK (PBD id: 6TFP) in complex with WA (PubChem CID: 26537). (**c**) Interaction between WA and BTK structure visualized using Ligplot [74] showing covalent bond formation of the C4-OH group of WA with the SH group of Cys481 from BTK. (**d**) Inhibition of wild-type (WT) BTK and mutated (C481S) BTK by WA in HEK-293 cells. Data are plotted as mean ± s.d., n=3 biologically independent replicates. (**e**) Relative viability of MM1R cells treated for 24 h with increasing concentrations of WA, upon BTK silencing (siBTK) in presence or absence of C481S BTK overexpression. Data are plotted as mean ± s.d., n=3 biologically independent replicates (ns = $p > 0.05$, *$p = 0.0309$, ***$p < 0.0001$, ANOVA).

3.3. Discussion

A common feature of many B-cell malignancies is their ability to develop therapy resistance through increased BCR signaling and BTK activity. Along the same line, increased BCR signaling has been shown to reduce therapeutic efficacy of GCs in B-cell leukemias [26-29]. Although MM cells are typically lacking active BCR, BTK overexpression and signaling has been associated with increased therapy resistance in the disease [18,75]. Accordingly, we compared the anti-cancer effect of the clinically approved BTK kinase inhibitor IBR and the preclinical phytotherapeutic kinase inhibitor WA to kill GC therapy resistant MM cells via suppression of BTK hyperactivation. Phosphopeptidome based tyrosine kinome profiling confirmed hyperactivation of multiple BCR family kinases besides other receptor TK families (FGFR, PDGFR, DDR) in GC therapy resistant MM1R cells. Furthermore, hyperactivated BCR kinases could completely be suppressed with both kinase inhibitors, WA and IBR. Nonetheless, kinase tree representations of both kinase inhibitor profiles revealed quantitative and qualitative differences in specificity and potency, which may underlie the differences in potency of WA and IBR to kill GC-resistant MM cells. Biotin affinity-purification experiments confirmed a cysteine-dependent covalent interaction between WA and BTK, similar to IBR-BTK Cys481 binding [63]. This is supported by molecular modeling studies which revealed favorable covalent WA binding to the conserved Cys481 residue in BTK. In addition, NanoBRET Target Engagement Intracellular Kinase assays confirm WA dependent inhibition of WT BTK kinase activity which is lost upon C481S mutation. Interestingly, most kinases inhibited by WA treatment, including BTK, BLK and EGFR, belong to the Hinge-6 domain type kinases, according to the kinase cysteinome classification. The latter suggests broad redundant kinase inhibitory effects of WA through covalent cysteine targeting. Accordingly, BTK silencing experiments could only partially mimic therapeutic cell death effects of WA in MM1R, whereas overexpression of the C481S kinase mutant could only partially protect against WA. Similarly, cancer therapeutic effects of WA could also be observed in GC sensitive MM1S cells which lack BTK overexpression, through covalent targeting of alternative cell survival kinases expressed in MM1S. As such, the therapeutic efficacy of WA against different cancer cell types may strongly depend on its promiscuous nucleophilic cysteine reactivity towards the cellular repertoire of hyperactivated tyrosine cell survival kinases. Additionally, the anti-cancer effects of WA may also partially rely on its non-covalent interactions with target proteins. H-bond interactions with terminal hydroxyl groups of WA were shown to be sufficient to deform protein complexes through naïve hindrance [65]. Alternatively, the covalent interaction of WA may be weaker than that of the normal covalent bond and be reversible in washout experiments [76]. Taunton and coworkers demonstrated that drug efficacy could be optimized by finetuning warhead residence time and exploiting the intrinsic reversibility of the reaction moiety [66,77]. In this respect, partially reversible covalent binding characteristics of WA may promote more promiscuous tyrosine kinase targeting than IBR and explain the higher efficacy of WA than IBR in overcoming MM drug resistance. Finally, WA-mediated inhibition of BTK kinase activity was also accompanied with a time-dependent decrease in BTK mRNA and protein expression, not observed for IBR, suggesting

that WA targets BTK hyperactivation at multiple levels [62]. For example, WA might indirectly decrease BTK activity by reducing kinase protein levels by inhibition of Sp1-dependent transcription [78], by post-transcriptional microRNA silencing mechanisms [53,79], or by decreasing kinase stability via heat shock chaperone proteins [45,47].

Although WA clearly suppresses hyperactivated BTK family kinases signaling, some limitations of our study need to be acknowledged. Most notably, mainly GC therapy resistant MM cell models were studied here. Further preclinical in vitro and in vivo studies are required to fully appreciate therapeutic efficacy of WA to overcome multi-drug resistance by covalent inhibition of hinge 6 cysteine domain BTK family kinases. In addition, small qualitative and/or quantitative variations in specificity/potency observed for the promiscuous BCR TK inhibitor profiles of WA and IBR may not be sufficient to explain the large difference in therapeutic efficacy of WA as compared to IBR, against GC-resistant MM cell lines. Of special note, whereas nM concentrations of IBR are effective against B-cell lymphoma cancer cells, much higher µM concentrations seem to be required to kill BTK overexpressing MM cells [17,80-83], presumably because of the presence of highly redundant BCR/NFKB survival pathways (PI3K/Akt/mTOR/Syk) in MM which compensate for pharmacological BTK inhibition [37]. Yet, despite the presence of these compensatory pathways, complete silencing of BTK expression is cytotoxic to MM1R cells, emphasizing BTK's involvement in myeloma cell survival. This is in line with previous observations made in BTK KO mouse models, where complete loss of BTK expression resulted in a more significant decrease in splenic B-cell numbers compared to mice harboring BTK mutations [84]. Because BTK also possesses crucial shuttling and scaffold activities, complete silencing of BTK is likely more detrimental to B-cells due to additional loss of non-kinase functions [85].

Furthermore, covalent cysteine binding of WA has also been reported to Ser/Thr kinases [86] and phosphatases [87] which were not included in our phosphopeptidome screening approach. Indeed, in addition to BTK, BCR signaling is fine-tuned by Ser/Thr kinases (for example IKK2, PKC) [15,88] and phosphatases (i.e. SHIP1, PTEN) [89,90]. Finally, chemoproteomic strategies have identified additional WA non-kinase target proteins, which may further strengthen the potential cancer therapeutic efficacy of WA [45,91]. Therefore, functional silencing approaches with shRNA libraries will be informative to further distinguish druggable key cancer targets from adverse off targets to defeat therapy resistance in MM by WA [87,92]. Further research determining the safety and pharmacokinetic profile of WA is needed as well. Preliminary (pre)clinical toxicology studies of WA in different cancer models revealed that WA administration is generally well tolerated with limited to no adverse toxicity reported [93-95]. Yet, no toxicology data of WA have been collected in B-cell malignancies, such as MM.

3.4. Materials and Methods

3.4.1. Cell Culture and Cell Viability Assays
GC-sensitive MM1S (CRL-2974) and GC-resistant MM1R MM cell lines (CRL-2975) have been described previously and were purchased from ATCC [53]. GC-resistant U266 cells

were kindly provided by dr. Eva Lion, Head of Tumor Immunology Group of the Laboratory of Experimental Hematology (University of Antwerp). Cells were cultivated in RPMI-1640 supplemented with 10% Fetal Bovine Serum (E.U Approved; South American Origin) and 1% Penicillin/Streptomycin Solution (Invitrogen). The cell lines were additionally supplemented with 1% MEM Non-Essential Amino Acids and 1% Sodium Pyruvate (Invitrogen). Each cell line was maintained at 37°C in 5% CO_2 and 95% air atmosphere and 95–98% humidity. Cell viability was assessed by colorimetric assay with 3-(4, 5-dimethylthiozol-2-yl)-2, 5-diphenyltetrazolium bromide (MTT) (Sigma Aldrich, St. Louis, MO, US) as previously described [53].

3.4.2. Cell Lysis and Peptide Array Based TK Activity Profiling

WA or BTK treated (15 min) and untreated MM1S and MM1R cells (n = 3 biologically independent samples per cell line per treatment) were lysed in M-PER lysis buffer containing 1:100 Halt's protease and phosphatase inhibitors (Pierce). The lysates were collected and centrifuged at >13,000 rpm for 15 min at 4 °C. The supernatants were transferred to pre-chilled Eppendorf tubes and flash frozen immediately on dry ice. Protein concentrations were determined by the BCA method (Pierce,Thermo Scientific) [96]. Cellular kinase activities were measured by TK-specific phosphopeptide arrays (PamChip, PamGene International B.V. the Netherlands) according to the manufacturer's protocol as previously described [56,97]. The differences in peptide phosphorylation signal intensity between different experimental setups were analyzed in a linear mixed model by using BioNavigator 6.3 software integrated with R (Bioconductor) for statistical analysis (paired two-sided t-test and unpaired t-tests). FDR were calculated using Benjamini-Hochberg method (adjusted p-values <0.05) [55]. The upstream kinases were correlated with the identified PTK specific phosphopeptide fingerprints according to the human (phospho)protein reference database [98-101]. Peptide lists showing differential phosphorylation intensities were further cross compared with phosphorylation specific datasets of the kinexus kinase predictor [102]. The ranking of the kinases was based upon scoring penalties of sensitivity and specificity of observed peptide phosphorylation changes in the tested experimental conditions. Significance of the upstream kinase scoring functions were calculated by the Fisher's exact test. Pathway enrichment of differentially phosphorylated protein IDs was analyzed via Metacore and Ingenuity Pathway Analysis (IPA) software [103].

3.4.3. RNA Extraction and RNA Sequencing

The RNeasy Mini Kit (Qiagen, Venlo, Netherlands) was used to extract total RNA from untreated or WA exposed MM1S and MM1R cells (n = 3 biologically independent samples per cell line per treatment) according to the manufacturer's protocol. Isolated, pure total RNA was then quantified and qualified using the Epoch[TM] Microplate Spectrophotometer (BioTek, US). RNA samples were stored at -80 °C and subsequently shipped to BGI (BGI Group, Bejing, China) where RNA integrity was determined using the 2100 Bioanalyzer system (Agilent Technologies, USA). All 12 samples with acceptable quality level (RNA content >80ng/μL, 28s/18s ≥ 1.0 and RIN ≥ 7.0) were included for sequencing library

preparation. Prepared libraries were 2 X 50 bp pair-end sequenced using the BGISEQ-500 platform (BGI Group, China). RNAseq data have been deposited in the NCBI GEO database (GSE162475).

Quality of the RNA sequencing reads was assessed using FastQC (v0.11.5) [104]. STAR (v2.7.3a) [105] was subsequently used to map reads to the human reference genome build 37 (hg19) and to generate a read count table summarizing the counts per gene. Finally, differential gene expression analysis was performed using the DESeq2 package [57] and pathway analysis was performed with Panther [106].

3.4.4. cDNA Conversion Quantitative Real-time PCR

Total RNA (1 μg) extracted from each sample was converted into cDNA with the Go Script reverse transcription system (Promega, Madison, Wisconsin, USA) following the manufacturer's protocol. Next, qPCR analysis was carried out using the GoTaq qPCR Master Mix (Promega) according to manufacturer's instructions. In brief, a 25 μl reaction volume mix per sample was prepared containing 12.5 μl GoTaq qPCR Master Mix, 0.4 μM forward and reverse primer, and nuclease-free water. The following PCR program was applied on the Rotor-Gene Q qPCR machine of Qiagen: 95°C for 2 min, 40 cycli denaturation (95°C, 15 s) and annealing/extension (60°C, 30 s), and dissociation (60–95°C). Each sample was run in triplicate. The median value of the triplicates was taken to calculate the ΔΔCt-values using GAPDH as the normalization gene. Primers sequences are listed in Supplementary Table 2.

3.4.5. Antibodies and Reagents

WA was purchased from Alta Vista Phytochemicals (Hyderabad, India) and biotinylation of WA was performed by Dr. P. Van der Veken (WA-BT; Universiteit Antwerpen, Belgium). Both formulations were stored as 20mM stocks in DMSO at -20°C as previously described [48,107]. IBR (IMBRUVICA®) stock solutions were obtained from Pharmacyclics (Sunnyville-CA, USA). Antibodies BTK (3533) and GAPDH (2118S) were obtained from Cell Signaling Technology (Danvers, Massachusetts, USA).

3.4.6. Cell Viability after WA washout

After 15 min treatment of MM1R cells with increasing concentrations of WA (with or without DTT), cells were washed extensively with PBS (3 x 5 min) and left to grow for an additional 24 hr in WA-free supplemented RPMI-1640 medium. Once incubation was complete, cell viability was determined by colorimetric MTT assay as described above. MM1R cells continuously treated with WA for 24 hr were included to allow for a direct comparison of covalent and non-covalent effects on cell viability.

3.4.7. Protein Extraction and Western Immunoblot Analysis

For Western immunoblot analyses, cell pellets were lysed in 0.5 ml RIPA buffer (150 mM NaCl, 0.1% Triton X-100, 0.1% SDS, 50 mM Tris-HCl pH 8) supplemented with protease inhibitors (Complete Mini®, Roche). Soluble protein extracts were obtained after 15 min incubation on ice followed by brief sonication and centrifugation at 16 g for 20 min at 4°C.

Samples were separated by sodium dodecyl sulfate-polyacrylamidegel electrophoresis (SDS-PAGE) and transferred onto nitrocellulose membranes (Hybond C, Amersham) following standard protocols. After blocking, membranes were incubated overnight at 4°C with the primary antibodies, followed by dye-conjugated secondary antibodies (polyclonal goat anti-rabbit HRP, #P0448, Dako). Bound complexes were detected with the Amersham Imager 680 (Cytiva) and quantified by Image J software [108].

3.4.8. WA-biotin Based Affinity Purification

WA-BT affinity purification and co-precipitation was performed as previously described [48]. In short, MM1R and U266 cells were seeded in 10 cm culture dishes and incubated for 24 hours at 37°C. Cells were treated with biotinylated WA (1 µM, 2.5 µM, 5 µM or 7.5 µM as indicated) or left untreated for 2 hours. Cells were then lysed in 1 ml lysis buffer (5 mM Tris pH 7.6, 1% Triton-X100 and 5 mM EDTA, supplemented with Complete™ protease inhibitor cocktail) and incubated with Neutravidin beads overnight. Beads were centrifuged for 5 min at 500 g after which the supernatant was removed. Beads were subsequently washed 5 times with lysis buffer. Total protein lysates, or coprecipitates, were separated by SDS–PAGE and electrotransferred onto a nitrocellulose membrane. Blots were probed using the appropriate antibodies and the immunoreactive proteins were detected using the Amersham Imager 680 (Cytiva).

3.4.9. Immunofluorescence Confocal Microscopy

After treatment with WABI, MM1R cells were fixed in 4% (v/v) formaldehyde. Cells were stained with Rhodamine-Phalloidin (Molecular Probes, Thermo Fisher Scientific Inc.) to visualize the cellular morphology, Hoechst 33258 (Sigma-Aldrich) to visualize the nucleus and Streptavidin-Alexa Fluor555 (Molecular Probes, Thermo Fisher Scientific Inc.) to visualize biotinylated WA. To determine WABI colocalization with specific proteins (BTK), WABI-treated MM1R cells were immunostained with primary (anti rabbit BTK, Cell Signaling Technology, mAb#8547) and corresponding labelled secondary antibodies (anti-rabbit Alexa Fluor-488, Molecular Probes, Thermo Fisher Scientific Inc.). Cells were then placed on glass slides and mounted with coverslips using Fluoromount™ (Sigma-Aldrich). Confocal imaging was carried out by a laser-scanning microscope equipped with a Plan-Apochromat 63X/1.40 Oil DIC objective lens and excitation wavelengths 405, 488, 561 and 640 nm (Zeiss LSM 800, Carl Zeiss, Germany). At least 20 different microscopic fields were analyzed for each sample using ZEN imaging software (Carl Zeiss). ZEN lite™ (Carl Zeiss, Germany) was used to perform image reconstruction and presentation.

3.4.10. Covalent Docking of WA with BTK

In silico molecular docking studies of the BTK protein (PDB id:6TFP) with WA (PubChem CID: 26537) were performed as previously described [109]. Briefly, BTK and WA structures were energy minimized with Swiss-PdbViewer (v4.1) [110] and UCSF Chimera [111] respectively. Molecular docking and calculation of the docking scores was performed with Autodock4 (v4.2.6). The obtained docking solutions were evaluated based on their scoring and the generated poses were clustered based on the cluster ranks of the ligand. Finally, the

clusters were differentiated based on the covalent bond lengths and prime energies. Final docking results were visualized with LIGPLOT (v.4.5.3) [74] and PyMOL (v.2.4) [112] software.

3.4.11. Cell Transfections and BRET Measurements

BTK- and BTK(C481S)-NanoLuc® Fusion Vectors were purchased from Promega and used in BRET target engagement experiments. HEK-293 cells were transfected with the NanoLuc® Fusion Vectors using FuGENE HD (Promega) according to the manufacturer's protocol. Briefly, Fusion Vectors were diluted into transfection carrier DNA (Promega) at a mass ratio of 1:10 after which FuGENE HD was added at a ratio of 1:3. The FuGENE HD complexes were then added to HEK-293 cells (1:20 ratio) at a density of 2×10^5 per mL. Subsequently, cells were plated onto white, 96-well plates (Corning) at a density of 2×10^4 cells/well and left to incubate for 24 hr at 37 °C and 5 % CO_2. After incubation, cells were equilibrated for 2 hr with the NanoBRET Tracer Reagent (K11, Promega) and increasing concentrations of WA (0.5-10 µM). To measure BRET, NanoBRET NanoGlo Substrate and Extracellular NanoLuc Inhibitor (Promega) was added according to the manufacturer's protocol, and filtered luminescence was measured on a GloMax Discover luminometer equipped with 450 nm BP filter and 600 nm LP filter. milliBRET units (mBU) were calculated by multiplying raw BRET values by 1000 and plotted with GraphPad Prism.

3.4.12. Nucleofection of siBTK and C481S BTK

The BTK(C481S)-NanoLuc® Fusion Vector was purchased from Promega and siBTK was purchased from GE-Healthcare Bio-sciences (Accell Human BTK siRNA, EQ-003107-00-0005, 29121299, sequence supplied in Table S3). MM1R cells were transfected with siBTK alone or siBTK combined with BTK(C481S) using the Nucleofector IIb device (Lonza, Switzerland) according to the manufacturer's instructions. In short, 2.10^6 MM1R cells were resuspended in supplemented nucleofector solution after which 300 nM siBTK was added with or without 2 µg BTK(C481S). To each nucleofection reaction, an additional 2 µg of pmaxGFP™ Vector was added as an internal positive control (transfection efficiency = 51.3 ± 2.4 %). Resuspended cells were subsequently transferred to a cuvette and transfected using the O-020 nucleofector program. After nucleofection, pre-equilibrated medium was added and cells were transferred to a 96-well plate at a density of 80.000 cells/well. Eight hours post transfection, transfection efficiency and GFP expression were assessed with fluorescence microscopy. If GFP signal was present, cells were treated with increasing concentrations of WA and cell viability was measured after 24 hrs using the MTT colorimetric method. BTK mRNA expression of nucleofected cells was further confirmed by quantitative real-time PCR.

3.5. Supplementary Material

Peptide ID	Significance code	MM1R	MM1S
VGFR2_1046_1058	ooooo		
CD79A_181_193			
PGFRB_1014_1028	oooo		
EFS_246_258			
SRC8_CHICK_492_504			
K2C6B_53_65			
DYR1A_212_224			
SRC8_CHICK_476_488	ooo		
RASA1_453_465			
CTNB1_79_91			
EGFR_1103_1115			
VGFR2_944_956			
P85A_600_612			
JAK2_563_577			
EPHA2_765_777			
VGFR2_1052_1064			
PLCG1_1246_1258			
EPHB1_921_933			
PDPK1_369_381			
FER_707_719			
EPHA1_774_786			
ERBB4_1277_1289			
41_654_666			
ENOG_37_49			
STAT4_714_726			
VGFR1_1040_1052			
LAT_194_206			
ODBA_340_352			
LAT_249_261			
FRK_380_392	oo		
EPHA7_607_619			
VGFR3_1061_1073			
PRRX2_202_214			
KSYK_518_530			
PLCG1_776_788			
FGFR3_753_765			
DCX_109_121			
VGFR1_1235_1247			
ZAP70_485_497			
LCK_387_399			
FGFR1_761_773			
PDPK1_2_14			
RET_1022_1034			
SRC8_CHICK_470_482			
EGFR_1165_1177			
VGFR1_1326_1338			
PGFRB_572_584			
PAXI_111_123			
CBL_693_705			
CALM_95_107			
PGFRB_1002_1014			
EPOR_361_373			
PLCG1_764_776			
PGFRB_771_783			
INSR_992_1004			
PGFRB_709_721			
FES_706_718			
PAXI_24_36			
FGFR2_762_774			
NTRK2_696_708			
MK10_216_228			
PGFRB_768_780			
EPHB1_771_783			
MBP_198_210			
VINC_815_827			
JAK1_1015_1027			
TEC_512_524			
TNNT1_2_14			
VGFR1_1320_1332_C1320S/			
CDK2_8_20	o		
FAK2_572_584			
EPHB4_583_595			
FAK1_569_581			
RB_804_816			
EPOR_419_431			
B3AT_39_51			
VGFR2_989_1001			
CRK_214_226			
PECA1_706_718			
MBP_259_271			
ANXA1_14_26			
ERBB2_1241_1253			
DYR1A_312_324			
ERBB2_870_882			
VGFR1_1162_1174			
ART_004_EAIYAAPFAKKKXC			
MET_1227_1239			
EGFR_1190_1202			
RON_1353_1365			
C1R_199_211			
MK12_178_190			
RON_1346_1358			
PP2AB_297_309			
PRGR_786_798			
RAF1_332_344			
EGFR_1118_1130			
CD3Z_116_128			
ACHD_383_395			
ERBB4_1181_1193			
VGFR2_1168_1180			
K2C8_425_437			
TYRO3_679_691			
RBL2_99_111			
CDK7_157_169			
MK14_173_185	.		
PTN11_539_551			
NCF1_313_325			
EPHA4_589_601			
VGFR2_1207_1219_C1208S			
INSR_1348_1360			
MK07_211_223			
ANXA2_17_29			
MK01_180_192			
EGFR_1062_1074			
ZBT16_621_633			
CD3Z_146_158			
NTRK1_489_501			
VGFR1_1206_1218			
EPHA2_581_593			
ART_003_EAI(pY)AAPFAKKKX(			
EGFR_908_920			

1.5

-1.5

Log of intensities

Figure S1 (previous page): Heatmap showing phosphorylation intensities of peptides serving as substrates for tyrosine kinases. Figure shows hyperphosphorylated (red) or hypo phosphorylated (blue) peptides in MM1R (n=3) and MM1S (n=3) samples ranked by the p-value resulting from a t-test. The significance is indicated using a significance code: ooooo: p< 0.00001, oooo: p < 0.0001, ooo: p < 0.001, oo: p < 0.001, o: p < 0.05.

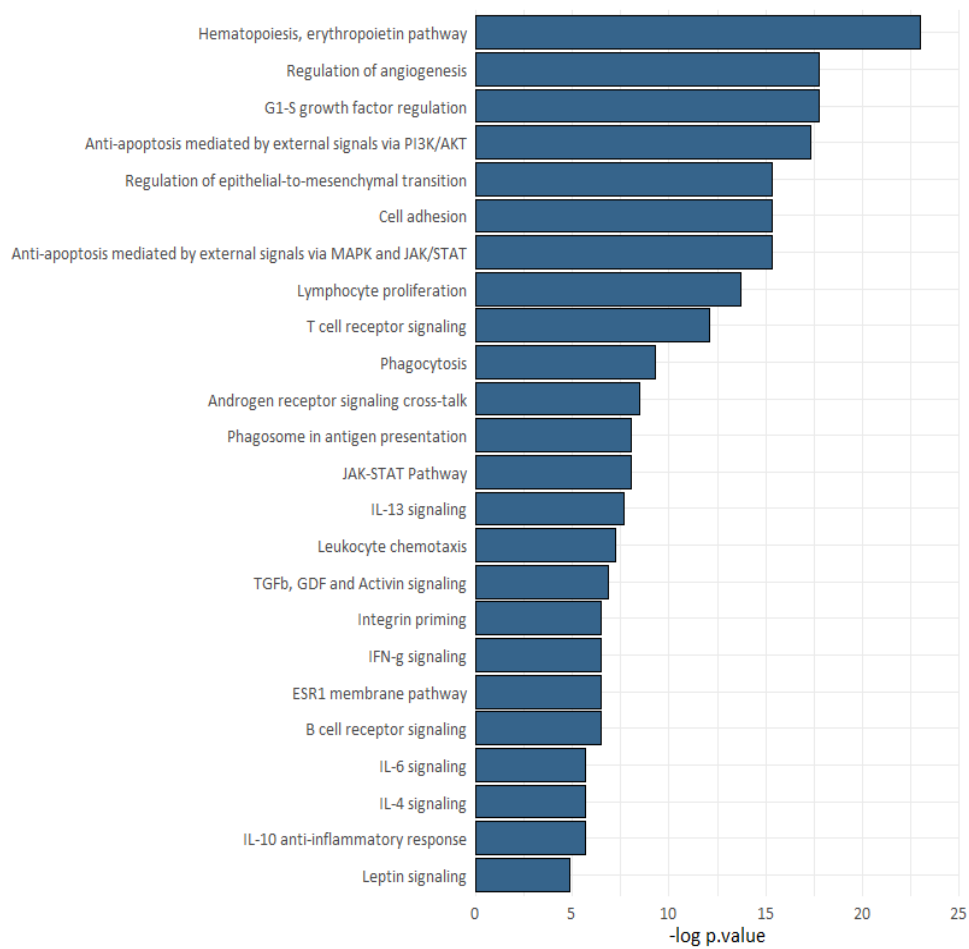*Figure S2:* MetaCore pathway analysis of differentially phosphorylated protein peptides (p<0.05) in MM1R versus MM1S cells.
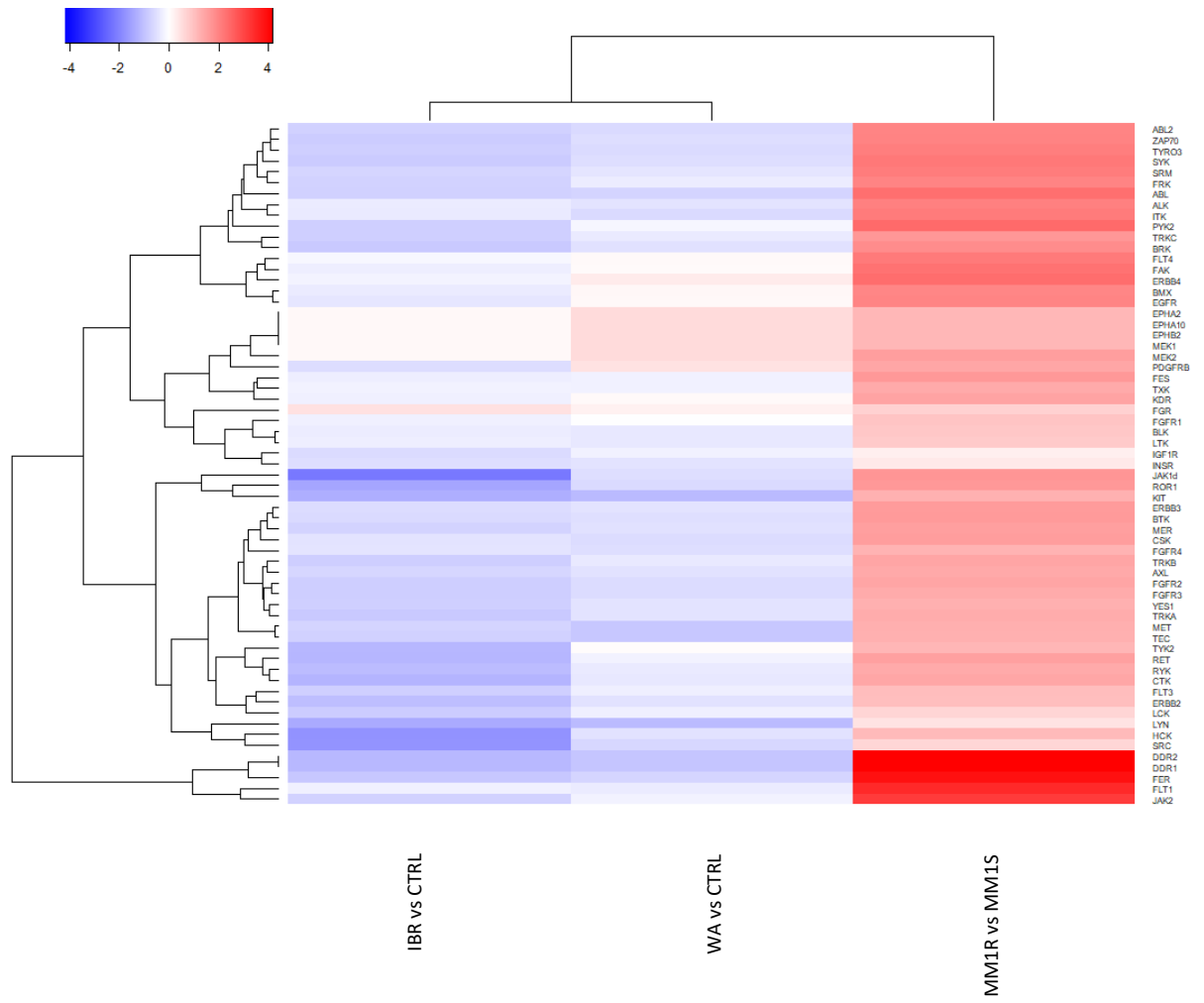
Figure S3: Row-annotated heatmap representation of hyperactivated or inhibited kinases in MM1R versus MM1S cells, or following 15 min IBR or WA treatment of MM1R cells, *n*=3 biologically independent samples per treatment group.
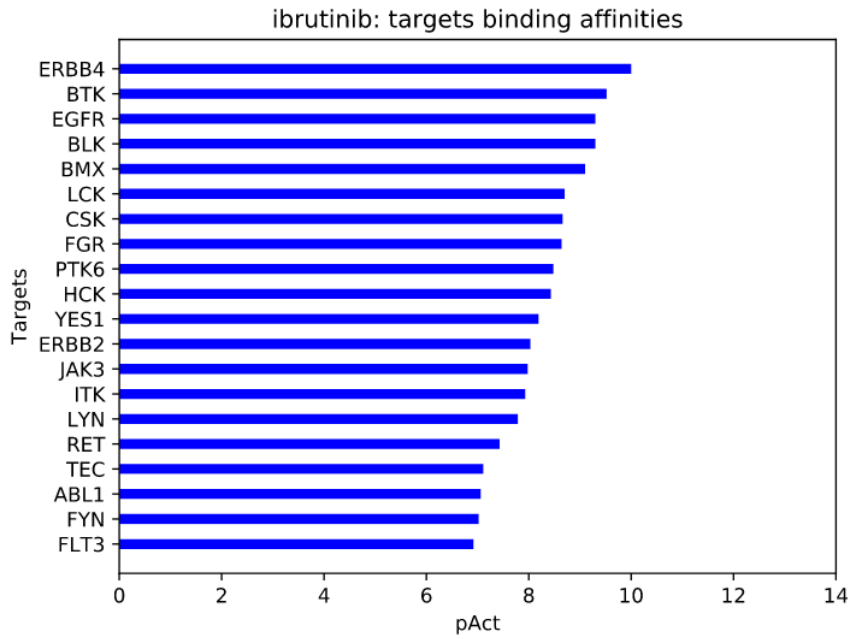
Figure S4: Target binding affinities of Ibrutinib. Binding affinities of Ibrutinib to its targets are shown as pAct (-Log(IC50/Ki/EC50,…)). Bars show the target interactions confirmed by ChEMBL/PubChem/papers. Graph was generated using the drug network map tool of the UC San Diego Abagyan Lab (http://ruben.ucsd.edu/dnet/).
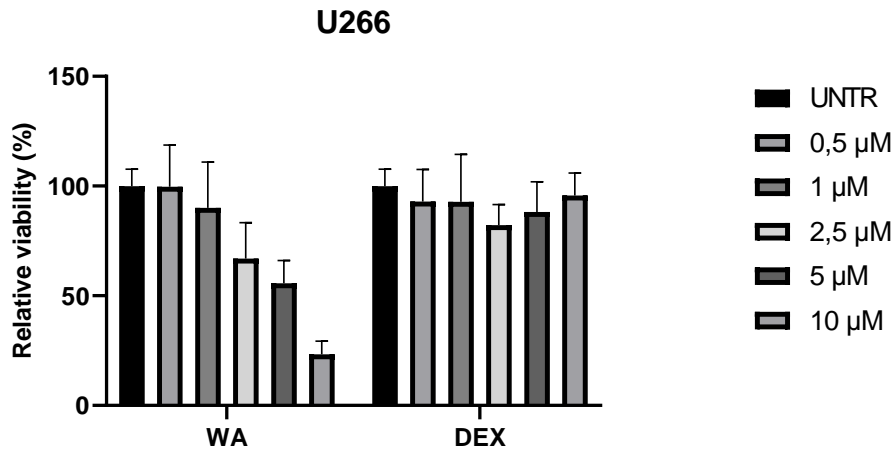

Figure S5: Relative viability (%) of U266 cells after 24 h treatment with WA or DEX. Data are plotted as the mean ± s.d., *n*=3 biologically independent samples.
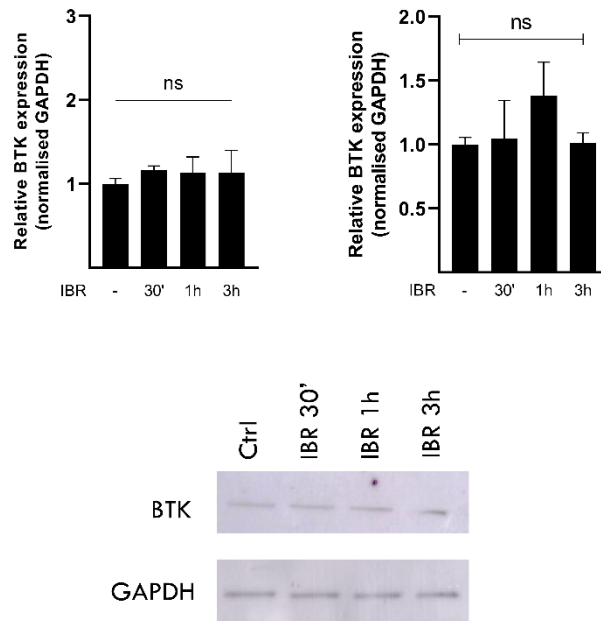
Figure S6: Relative BTK mRNA (upper left) and protein levels (upper right and lower panel) of MM1R cells treated with 1 μM IBR for the indicated timepoints. Data are plotted as mean ± s.d., n=3 biologically independent replicates (ns = p > 0.05, ANOVA).
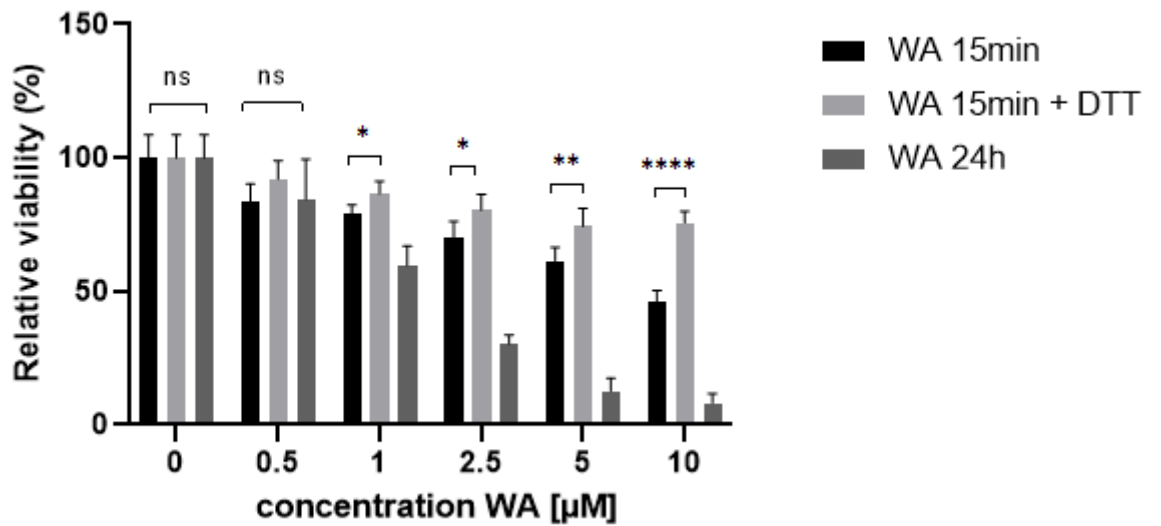
Figure S7: Relative viability of MM1R cells treated with increasing concentrations of WA 24 hrs post treatment. Cells were incubated with WA for 15 min (with or without DTT) after which WA was washed away or continuously for 24 hrs. Data are plotted as mean ± s.d., *n*=3 biologically independent replicates (ns = p > 0.05, *p < 0.05, **p < 0.01, ****p < 0.0001, ANOVA).
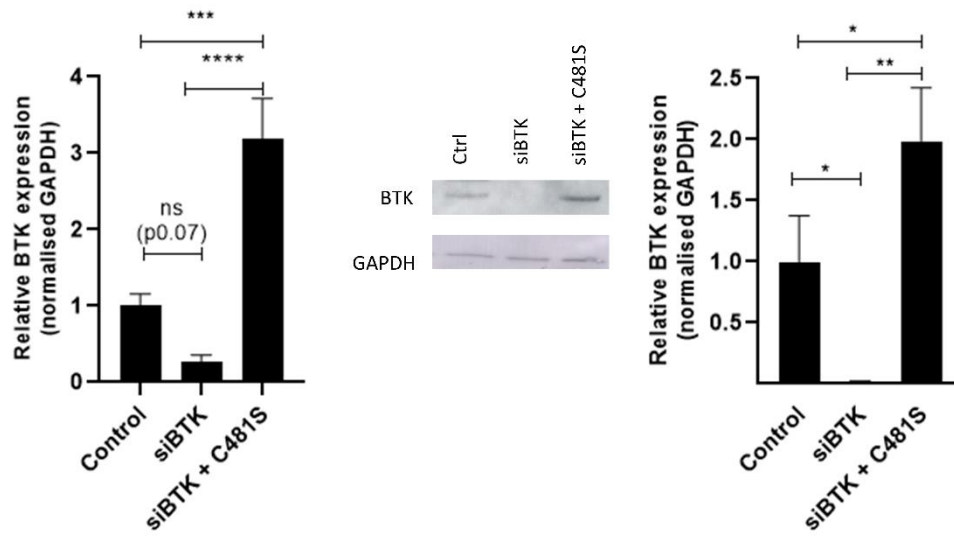
Figure S8: Relative BTK mRNA (left) and protein (right) expression of siBTK-transfected MM1R cells with or without the C481S BTK mutant. Data are plotted as mean ± s.d., n=3 biologically independent replicates (ns = p > 0.05, *p < 0.05, **p < 0.01, ****p < 0.0001, ANOVA).
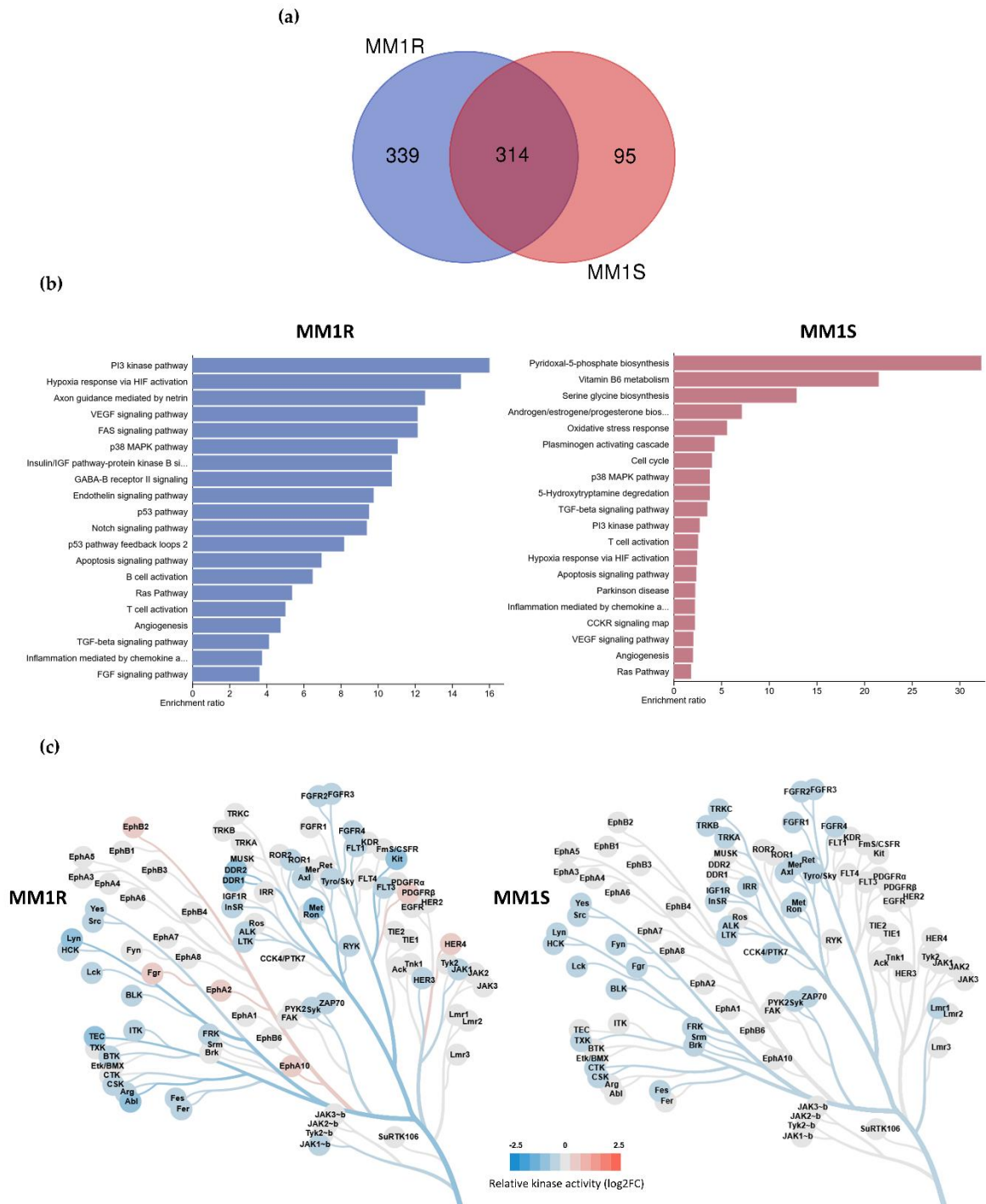
Figure S9: The biological targets of WA treatment strongly depends on cellular context. (**a**) Venn diagram showing the number of significantly differentially expressed genes (p < 0.05, logFC < |1|) in MM1R and MM1S cells after WA treatment. (**b**) Panther pathway analysis of significantly differentially expressed genes in MM1R only (left) and MM1S only (right). (**c**) Kinase trees displaying relative changes in kinase activities upon WA treatment in MM1R cells (left) and MM1S cell (right). Kinase trees were generated with the CORAL web tool (http://phanstiel-lab.med.unc.edu/CORAL/)

Table S1: Summary of binding energy and distance of the covalent bond of Cys481 with WA as predicted by covalent docking.

BTK interaction site	PDB ID	Binding energy	Bond length	No. of hydrogen bonds	Amino acid interaction
Cys481	6TFP	-4.93 kcal/mol	1.4 Å	3	Tyr485, Leu482, Gly480

Table S2: Overview of qPCR primers used in this study

Target		Primer Sequence	Gene accession number
BTK	Forward	GTC CCA CCT TCC AAG TCC TG	ENSG00000010671
	Reverse	GCC TCT TCT CCC ACG TTC AA	
GAPDH	Forward	GCT CTC TGC TCC TCC TGT TC	ENSG00000111640
	Reverse	ACG ACC AAA TCC GTT GAC TC	

Table S3: Overview of siRNA sequences used in this study

Target	Target Sequence	siRNA sequence
BTK	UUU UGA UGU GGG AAA UUU A	TAA ATT TCC CAC ATC AAA A

3.6. References

1. Siegel, R.L.; Miller, K.D.; Jemal, A. Cancer statistics, 2020. CA Cancer J Clin 2020, 70, 7-30, doi:10.3322/caac.21590.
2. Ferlay, J.; Soerjomataram, I.; Dikshit, R.; Eser, S.; Mathers, C.; Rebelo, M.; Parkin, D.M.; Forman, D.; Bray, F. Cancer incidence and mortality worldwide: sources, methods and major patterns in GLOBOCAN 2012. Int J Cancer 2015, 136, E359-386, doi:10.1002/ijc.29210.
3. Hussein, M.A. Multiple myeloma: most common end-organ damage and management. J Natl Compr Canc Netw 2007, 5, 170-178, doi:10.6004/jnccn.2007.0017.
4. Robak, P.; Drozdz, I.; Szemraj, J.; Robak, T. Drug resistance in multiple myeloma. Cancer Treat Rev 2018, 70, 199-208, doi:10.1016/j.ctrv.2018.09.001.
5. Rajkumar, S.V. Myeloma today: Disease definitions and treatment advances. Am J Hematol 2016, 91, 90-100, doi:10.1002/ajh.24236.
6. Yang, W.C.; Lin, S.F. Mechanisms of Drug Resistance in Relapse and Refractory Multiple Myeloma. Biomed Res Int 2015, 2015, 341430, doi:10.1155/2015/341430.
7. Ito, S. Proteasome Inhibitors for the Treatment of Multiple Myeloma. Cancers (Basel) 2020, 12, doi:10.3390/cancers12020265.
8. Abe, Y.; Ishida, T. Immunomodulatory drugs in the treatment of multiple myeloma. Jpn J Clin Oncol 2019, 49, 695-702, doi:10.1093/jjco/hyz083.
9. Burwick, N.; Sharma, S. Glucocorticoids in multiple myeloma: past, present, and future. Ann Hematol 2019, 98, 19-28, doi:10.1007/s00277-018-3465-8.
10. Thanendrarajan, S.; Davies, F.E.; Morgan, G.J.; Schinke, C.; Mathur, P.; Heuck, C.J.; Zangari, M.; Epstein, J.; Yaccoby, S.; Weinhold, N., et al. Monoclonal antibody therapy in multiple myeloma: where do we stand and where are we going? Immunotherapy 2016, 8, 367-384, doi:10.2217/imt.15.118.
11. Imai, Y.; Hirano, M.; Kobayashi, M.; Futami, M.; Tojo, A. HDAC Inhibitors Exert Anti-Myeloma Effects through Multiple Modes of Action. Cancers (Basel) 2019, 11, doi:10.3390/cancers11040475.
12. Kumar, S.K.; Therneau, T.M.; Gertz, M.A.; Lacy, M.Q.; Dispenzieri, A.; Rajkumar, S.V.; Fonseca, R.; Witzig, T.E.; Lust, J.A.; Larson, D.R., et al. Clinical course of patients with relapsed multiple myeloma. Mayo Clin Proc 2004, 79, 867-874, doi:10.4065/79.7.867.
13. Issa, M.E.; Takhsha, F.S.; Chirumamilla, C.S.; Perez-Novo, C.; Vanden Berghe, W.; Cuendet, M. Epigenetic strategies to reverse drug resistance in heterogeneous multiple myeloma. Clin Epigenetics 2017, 9, 17, doi:10.1186/s13148-017-0319-5.
14. Shain, K.H.; Tao, J. The B-cell receptor orchestrates environment-mediated lymphoma survival and drug resistance in B-cell malignancies. Oncogene 2014, 33, 4107-4113, doi:10.1038/onc.2013.379.
15. Woyach, J.A.; Johnson, A.J.; Byrd, J.C. The B-cell receptor signaling pathway as a therapeutic target in CLL. Blood 2012, 120, 1175-1184, doi:10.1182/blood-2012-02-362624.
16. Takata, M.; Sabe, H.; Hata, A.; Inazu, T.; Homma, Y.; Nukada, T.; Yamamura, H.; Kurosaki, T. Tyrosine kinases Lyn and Syk regulate B cell receptor-coupled Ca2+ mobilization through distinct pathways. EMBO J 1994, 13, 1341-1349.
17. Tai, Y.T.; Chang, B.Y.; Kong, S.Y.; Fulciniti, M.; Yang, G.; Calle, Y.; Hu, Y.; Lin, J.; Zhao, J.J.; Cagnetta, A., et al. Bruton tyrosine kinase inhibition is a novel therapeutic strategy targeting tumor in the bone marrow microenvironment in multiple myeloma. Blood 2012, 120, 1877-1887, doi:10.1182/blood-2011-12-396853.
18. Yang, Y.; Shi, J.; Gu, Z.; Salama, M.E.; Das, S.; Wendlandt, E.; Xu, H.; Huang, J.; Tao, Y.; Hao, M., et al. Bruton tyrosine kinase is a therapeutic target in stem-like cells from multiple myeloma. Cancer Res 2015, 75, 594-604, doi:10.1158/0008-5472.CAN-14-2362.
19. Wang, W.; Wei, R.; Liu, S.; Qiao, L.; Hou, J.; Gu, C.; Yang, Y. BTK induces CAM-DR through regulation of CXCR4 degradation in multiple myeloma. Am J Transl Res 2019, 11, 4139-4150.

20. Murray, M.Y.; Zaitseva, L.; Auger, M.J.; Craig, J.I.; MacEwan, D.J.; Rushworth, S.A.; Bowles, K.M. Ibrutinib inhibits BTK-driven NF-kappaB p65 activity to overcome bortezomib-resistance in multiple myeloma. Cell Cycle 2015, 14, 2367-2375, doi:10.1080/15384101.2014.998067.

21. Young, R.M.; Staudt, L.M. Targeting pathological B cell receptor signalling in lymphoid malignancies. Nat Rev Drug Discov 2013, 12, 229-243, doi:10.1038/nrd3937.

22. Dasmahapatra, G.; Patel, H.; Dent, P.; Fisher, R.I.; Friedberg, J.; Grant, S. The Bruton tyrosine kinase (BTK) inhibitor PCI-32765 synergistically increases proteasome inhibitor activity in diffuse large-B cell lymphoma (DLBCL) and mantle cell lymphoma (MCL) cells sensitive or resistant to bortezomib. Br J Haematol 2013, 161, 43-56, doi:10.1111/bjh.12206.

23. Herman, S.E.; Gordon, A.L.; Hertlein, E.; Ramanunni, A.; Zhang, X.; Jaglowski, S.; Flynn, J.; Jones, J.; Blum, K.A.; Buggy, J.J., et al. Bruton tyrosine kinase represents a promising therapeutic target for treatment of chronic lymphocytic leukemia and is effectively targeted by PCI-32765. Blood 2011, 117, 6287-6296, doi:10.1182/blood-2011-01-328484.

24. Herman, S.E.; Sun, X.; McAuley, E.M.; Hsieh, M.M.; Pittaluga, S.; Raffeld, M.; Liu, D.; Keyvanfar, K.; Chapman, C.M.; Chen, J., et al. Modeling tumor-host interactions of chronic lymphocytic leukemia in xenografted mice to study tumor biology and evaluate targeted therapy. Leukemia 2013, 27, 2311-2321, doi:10.1038/leu.2013.131.

25. Yang, Y.; Shaffer, A.L., 3rd; Emre, N.C.; Ceribelli, M.; Zhang, M.; Wright, G.; Xiao, W.; Powell, J.; Platig, J.; Kohlhammer, H., et al. Exploiting synthetic lethality for the therapy of ABC diffuse large B cell lymphoma. Cancer Cell 2012, 21, 723-737, doi:10.1016/j.ccr.2012.05.024.

26. Franco, L.M.; Gadkari, M.; Howe, K.N.; Sun, J.; Kardava, L.; Kumar, P.; Kumari, S.; Hu, Z.; Fraser, I.D.C.; Moir, S., et al. Immune regulation by glucocorticoids can be linked to cell type-dependent transcriptional responses. J Exp Med 2019, 216, 384-406, doi:10.1084/jem.20180595.

27. Kruth, K.A.; Fang, M.; Shelton, D.N.; Abu-Halawa, O.; Mahling, R.; Yang, H.; Weissman, J.S.; Loh, M.L.; Muschen, M.; Tasian, S.K., et al. Suppression of B-cell development genes is key to glucocorticoid efficacy in treatment of acute lymphoblastic leukemia. Blood 2017, 129, 3000-3008, doi:10.1182/blood-2017-02-766204.

28. Shi, Y.; Wang, G.; Muhowski, E.M.; McCaw, L.; Wang, C.; Bjarnason, G.; Woyach, J.A.; Spaner, D.E. Ibrutinib reprograms the glucocorticoid receptor in chronic lymphocytic leukemia cells. Leukemia 2019, 33, 1650-1662, doi:10.1038/s41375-019-0381-4.

29. Manzoni, D.; Catallo, R.; Chebel, A.; Baseggio, L.; Michallet, A.S.; Roualdes, O.; Magaud, J.P.; Salles, G.; Ffrench, M. The ibrutinib B-cell proliferation inhibition is potentiated in vitro by dexamethasone: Application to chronic lymphocytic leukemia. Leuk Res 2016, 47, 1-7, doi:10.1016/j.leukres.2016.05.003.

30. Chari, A.; Larson, S.; Holkova, B.; Cornell, R.F.; Gasparetto, C.; Karanes, C.; Matous, J.V.; Niesvizky, R.; Valent, J.; Lunning, M., et al. Phase 1 trial of ibrutinib and carfilzomib combination therapy for relapsed or relapsed and refractory multiple myeloma. Leuk Lymphoma 2018, 59, 2588-2594, doi:10.1080/10428194.2018.1443337.

31. Richardson, P.G.; Bensinger, W.I.; Huff, C.A.; Costello, C.L.; Lendvai, N.; Berdeja, J.G.; Anderson, L.D., Jr.; Siegel, D.S.; Lebovic, D.; Jagannath, S., et al. Ibrutinib alone or with dexamethasone for relapsed or relapsed and refractory multiple myeloma: phase 2 trial results. Br J Haematol 2018, 180, 821-830, doi:10.1111/bjh.15058.

32. Chi, J.; Park, J.; Saif, M.W. Ibrutinib-Induced Vasculitis in a Patient with Metastatic Colon Cancer Treated in Combination with Cetuximab. Case Rep Oncol Med 2020, 2020, 6154213, doi:10.1155/2020/6154213.

33. Burger, J.A.; Tedeschi, A.; Barr, P.M.; Robak, T.; Owen, C.; Ghia, P.; Bairey, O.; Hillmen, P.; Bartlett, N.L.; Li, J., et al. Ibrutinib as Initial Therapy for Patients with Chronic Lymphocytic Leukemia. N Engl J Med 2015, 373, 2425-2437, doi:10.1056/NEJMoa1509388.

34. Guha, A.; Derbala, M.H.; Zhao, Q.; Wiczer, T.E.; Woyach, J.A.; Byrd, J.C.; Awan, F.T.; Addison, D. Ventricular Arrhythmias Following Ibrutinib Initiation for Lymphoid Malignancies. J Am Coll Cardiol 2018, 72, 697-698, doi:10.1016/j.jacc.2018.06.002.

35. Salem, J.E.; Manouchehri, A.; Bretagne, M.; Lebrun-Vignes, B.; Groarke, J.D.; Johnson, D.B.; Yang, T.; Reddy, N.M.; Funck-Brentano, C.; Brown, J.R., et al. Cardiovascular Toxicities Associated With Ibrutinib. J Am Coll Cardiol 2019, 74, 1667-1678, doi:10.1016/j.jacc.2019.07.056.

36. Barf, T.; Covey, T.; Izumi, R.; van de Kar, B.; Gulrajani, M.; van Lith, B.; van Hoek, M.; de Zwart, E.; Mittag, D.; Demont, D., et al. Acalabrutinib (ACP-196): A Covalent Bruton Tyrosine Kinase Inhibitor with a Differentiated Selectivity and In Vivo Potency Profile. J Pharmacol Exp Ther 2017, 363, 240-252, doi:10.1124/jpet.117.242909.

37. George, B.; Chowdhury, S.M.; Hart, A.; Sircar, A.; Singh, S.K.; Nath, U.K.; Mamgain, M.; Singhal, N.K.; Sehgal, L.; Jain, N. Ibrutinib Resistance Mechanisms and Treatment Strategies for B-Cell lymphomas. Cancers (Basel) 2020, 12, doi:10.3390/cancers12051328.

38. Wu, J.; Liu, C.; Tsui, S.T.; Liu, D. Second-generation inhibitors of Bruton tyrosine kinase. J Hematol Oncol 2016, 9, 80, doi:10.1186/s13045-016-0313-y.

39. Woyach, J.; Huang, Y.; Rogers, K.; Bhat, S.A.; Grever, M.R.; Lozanski, A.; Doong, T.-J.; Blachly, J.S.; Lozanski, G.; Jones, D., et al. Resistance to Acalabrutinib in CLL Is Mediated Primarily By BTK Mutations. Blood 2019, 134, 504-504, doi:10.1182/blood-2019-127674.

40. Mathews Griner, L.A.; Guha, R.; Shinn, P.; Young, R.M.; Keller, J.M.; Liu, D.; Goldlust, I.S.; Yasgar, A.; McKnight, C.; Boxer, M.B., et al. High-throughput combinatorial screening identifies drugs that cooperate with ibrutinib to kill activated B-cell-like diffuse large B-cell lymphoma cells. Proc Natl Acad Sci U S A 2014, 111, 2349-2354, doi:10.1073/pnas.1311846111.

41. Lucas, D.M.; Still, P.C.; Perez, L.B.; Grever, M.R.; Kinghorn, A.D. Potential of plant-derived natural products in the treatment of leukemia and lymphoma. Curr Drug Targets 2010, 11, 812-822, doi:10.2174/138945010791320809.

42. Newman, D.J.; Cragg, G.M. Natural Products as Sources of New Drugs over the Nearly Four Decades from 01/1981 to 09/2019. J Nat Prod 2020, 83, 770-803, doi:10.1021/acs.jnatprod.9b01285.

43. Atanasov, A.G.; Zotchev, S.B.; Dirsch, V.M.; International Natural Product Sciences, T.; Supuran, C.T. Natural products in drug discovery: advances and opportunities. Nat Rev Drug Discov 2021, 10.1038/s41573-020-00114-z, doi:10.1038/s41573-020-00114-z.

44. Hassannia, B.; Logie, E.; Vandenabeele, P.; Vanden Berghe, T.; Vanden Berghe, W. Withaferin A: From ayurvedic folk medicine to preclinical anti-cancer drug. Biochem Pharmacol 2020, 173, 113602, doi:10.1016/j.bcp.2019.08.004.

45. Dom, M.; Offner, F.; Vanden Berghe, W.; Van Ostade, X. Proteomic characterization of Withaferin A-targeted protein networks for the treatment of monoclonal myeloma gammopathies. J Proteomics 2018, 179, 17-29, doi:10.1016/j.jprot.2018.02.013.

46. Issa, M.E.; Cuendet, M. Withaferin A induces cell death and differentiation in multiple myeloma cancer stem cells. Medchemcomm 2017, 8, 112-121, doi:10.1039/c6md00410e.

47. McKenna, M.K.; Gachuki, B.W.; Alhakeem, S.S.; Oben, K.N.; Rangnekar, V.M.; Gupta, R.C.; Bondada, S. Anti-cancer activity of Withaferin A in B-cell lymphoma. Cancer Biol Ther 2015, 16, 1088-1098, doi:10.1080/15384047.2015.1046651.

48. Heyninck, K.; Lahtela-Kakkonen, M.; Van der Veken, P.; Haegeman, G.; Vanden Berghe, W. Withaferin A inhibits NF-kappaB activation by targeting cysteine 179 in IKKbeta. Biochem Pharmacol 2014, 91, 501-509, doi:10.1016/j.bcp.2014.08.004.

49. Hahm, E.R.; Lee, J.; Singh, S.V. Role of mitogen-activated protein kinases and Mcl-1 in apoptosis induction by Withaferin A in human breast cancer cells. Mol Carcinog 2014, 53, 907-916, doi:10.1002/mc.22050.

50. Grogan, P.T.; Sleder, K.D.; Samadi, A.K.; Zhang, H.; Timmermann, B.N.; Cohen, M.S. Cytotoxicity of Withaferin A in glioblastomas involves induction of an oxidative stress-mediated heat shock

response while altering Akt/mTOR and MAPK signaling pathways. Invest New Drugs 2013, 31, 545-557, doi:10.1007/s10637-012-9888-5.

51. Mandal, C.; Dutta, A.; Mallick, A.; Chandra, S.; Misra, L.; Sangwan, R.S.; Mandal, C. Withaferin A induces apoptosis by activating p38 mitogen-activated protein kinase signaling cascade in leukemic cells of lymphoid and myeloid origin through mitochondrial death cascade. Apoptosis 2008, 13, 1450-1464, doi:10.1007/s10495-008-0271-0.

52. Oh, J.H.; Lee, T.J.; Kim, S.H.; Choi, Y.H.; Lee, S.H.; Lee, J.M.; Kim, Y.H.; Park, J.W.; Kwon, T.K. Induction of apoptosis by Withaferin A in human leukemia U937 cells through down-regulation of Akt phosphorylation. Apoptosis 2008, 13, 1494-1504, doi:10.1007/s10495-008-0273-y.

53. Palagani, A.; Op de Beeck, K.; Naulaerts, S.; Diddens, J.; Sekhar Chirumamilla, C.; Van Camp, G.; Laukens, K.; Heyninck, K.; Gerlo, S.; Mestdagh, P., et al. Ectopic microRNA-150-5p transcription sensitizes glucocorticoid therapy response in MM1S multiple myeloma cells but fails to overcome hormone therapy resistance in MM1R cells. PLoS One 2014, 9, e113842, doi:10.1371/journal.pone.0113842.

54. Greenstein, S.; Krett, N.L.; Kurosawa, Y.; Ma, C.; Chauhan, D.; Hideshima, T.; Anderson, K.C.; Rosen, S.T. Characterization of the MM.1 human multiple myeloma (MM) cell lines: a model system to elucidate the characteristics, behavior, and signaling of steroid-sensitive and -resistant MM cells. Exp Hematol 2003, 31, 271-282, doi:10.1016/s0301-472x(03)00023-7.

55. Hilhorst, R.; Houkes, L.; van den Berg, A.; Ruijtenbeek, R. Peptide microarrays for detailed, high-throughput substrate identification, kinetic characterization, and inhibition studies on protein kinase A. Anal Biochem 2009, 387, 150-161, doi:10.1016/j.ab.2009.01.022.

56. Chirumamilla, C.S.; Fazil, M.; Perez-Novo, C.; Rangarajan, S.; de Wijn, R.; Ramireddy, P.; Verma, N.K.; Vanden Berghe, W. Profiling Activity of Cellular Kinases in Migrating T-Cells. Methods Mol Biol 2019, 1930, 99-113, doi:10.1007/978-1-4939-9036-8_13.

57. Love, M.I.; Huber, W.; Anders, S. Moderated estimation of fold change and dispersion for RNA-seq data with DESeq2. Genome Biol 2014, 15, 550, doi:10.1186/s13059-014-0550-8.

58. Chauhan, D.; Auclair, D.; Robinson, E.K.; Hideshima, T.; Li, G.; Podar, K.; Gupta, D.; Richardson, P.; Schlossman, R.L.; Krett, N., et al. Identification of genes regulated by dexamethasone in multiple myeloma cells using oligonucleotide arrays. Oncogene 2002, 21, 1346-1358, doi:10.1038/sj.onc.1205205.

59. Berglof, A.; Hamasy, A.; Meinke, S.; Palma, M.; Krstic, A.; Mansson, R.; Kimby, E.; Osterborg, A.; Smith, C.I. Targets for Ibrutinib Beyond B Cell Malignancies. Scand J Immunol 2015, 82, 208-217, doi:10.1111/sji.12333.

60. Cheng, S.; Ma, J.; Guo, A.; Lu, P.; Leonard, J.P.; Coleman, M.; Liu, M.; Buggy, J.J.; Furman, R.R.; Wang, Y.L. BTK inhibition targets in vivo CLL proliferation through its effects on B-cell receptor signaling activity. Leukemia 2014, 28, 649-657, doi:10.1038/leu.2013.358.

61. Patel, V.; Balakrishnan, K.; Bibikova, E.; Ayres, M.; Keating, M.J.; Wierda, W.G.; Gandhi, V. Comparison of Acalabrutinib, A Selective Bruton Tyrosine Kinase Inhibitor, with Ibrutinib in Chronic Lymphocytic Leukemia Cells. Clin Cancer Res 2017, 23, 3734-3743, doi:10.1158/1078-0432.CCR-16-1446.

62. Chu, Y.; Lee, S.; Shah, T.; Yin, C.; Barth, M.; Miles, R.R.; Ayello, J.; Morris, E.; Harrison, L.; Van de Ven, C., et al. Ibrutinib significantly inhibited Bruton's tyrosine kinase (BTK) phosphorylation,in-vitro proliferation and enhanced overall survival in a preclinical Burkitt lymphoma (BL) model. Oncoimmunology 2019, 8, e1512455, doi:10.1080/2162402X.2018.1512455.

63. Pan, Z.; Scheerens, H.; Li, S.-J.; Schultz, B.E.; Sprengeler, P.A.; Burrill, L.C.; Mendonca, R.V.; Sweeney, M.D.; Scott, K.C.K.; Grothaus, P.G., et al. Discovery of Selective Irreversible Inhibitors for Bruton's Tyrosine Kinase. ChemMedChem 2007, 2, 58-61, doi:https://doi.org/10.1002/cmdc.200600221.

64. Vanden Berghe, W.; Sabbe, L.; Kaileh, M.; Haegeman, G.; Heyninck, K. Molecular insight in the multifunctional activities of Withaferin A. Biochem Pharmacol 2012, 84, 1282-1291, doi:10.1016/j.bcp.2012.08.027.

65. Grover, A.; Shandilya, A.; Agrawal, V.; Pratik, P.; Bhasme, D.; Bisaria, V.S.; Sundar, D. Hsp90/Cdc37 chaperone/co-chaperone complex, a novel junction anticancer target elucidated by the mode of action of herbal drug Withaferin A. BMC Bioinformatics 2011, 12 Suppl 1, S30, doi:10.1186/1471-2105-12-S1-S30.

66. Bradshaw, J.M.; McFarland, J.M.; Paavilainen, V.O.; Bisconte, A.; Tam, D.; Phan, V.T.; Romanov, S.; Finkle, D.; Shu, J.; Patel, V., et al. Prolonged and tunable residence time using reversible covalent kinase inhibitors. Nat Chem Biol 2015, 11, 525-531, doi:10.1038/nchembio.1817.

67. Lee, C.U.; Grossmann, T.N. Reversible covalent inhibition of a protein target. Angew Chem Int Ed Engl 2012, 51, 8699-8700, doi:10.1002/anie.201203341.

68. Serafimova, I.M.; Pufall, M.A.; Krishnan, S.; Duda, K.; Cohen, M.S.; Maglathlin, R.L.; McFarland, J.M.; Miller, R.M.; Frodin, M.; Taunton, J. Reversible targeting of noncatalytic cysteines with chemically tuned electrophiles. Nat Chem Biol 2012, 8, 471-476, doi:10.1038/nchembio.925.

69. Leproult, E.; Barluenga, S.; Moras, D.; Wurtz, J.M.; Winssinger, N. Cysteine mapping in conformationally distinct kinase nucleotide binding sites: application to the design of selective covalent inhibitors. J Med Chem 2011, 54, 1347-1355, doi:10.1021/jm101396q.

70. Chaikuad, A.; Koch, P.; Laufer, S.A.; Knapp, S. The Cysteinome of Protein Kinases as a Target in Drug Development. Angewandte Chemie International Edition 2018, 57, 4372-4385, doi:https://doi.org/10.1002/anie.201707875.

71. Liu, Y.; Gray, N.S. Rational design of inhibitors that bind to inactive kinase conformations. Nat Chem Biol 2006, 2, 358-364, doi:10.1038/nchembio799.

72. Zhang, J.; Yang, P.L.; Gray, N.S. Targeting cancer with small molecule kinase inhibitors. Nat Rev Cancer 2009, 9, 28-39, doi:10.1038/nrc2559.

73. Liu, Q.; Sabnis, Y.; Zhao, Z.; Zhang, T.; Buhrlage, S.J.; Jones, L.H.; Gray, N.S. Developing irreversible inhibitors of the protein kinase cysteinome. Chem Biol 2013, 20, 146-159, doi:10.1016/j.chembiol.2012.12.006.

74. Laskowski, R.A.; Swindells, M.B. LigPlot+: multiple ligand-protein interaction diagrams for drug discovery. J Chem Inf Model 2011, 51, 2778-2786, doi:10.1021/ci200227u.

75. Gu, C.; Peng, H.; Lu, Y.; Yang, H.; Tian, Z.; Yin, G.; Zhang, W.; Lu, S.; Zhang, Y.; Yang, Y. BTK suppresses myeloma cellular senescence through activating AKT/P27/Rb signaling. Oncotarget 2017, 8, 56858-56867, doi:10.18632/oncotarget.18096.

76. Zhao, Z.; Bourne, P.E. Progress with covalent small-molecule kinase inhibitors. Drug Discov Today 2018, 23, 727-735, doi:10.1016/j.drudis.2018.01.035.

77. Rao, S.; Gurbani, D.; Du, G.; Everley, R.A.; Browne, C.M.; Chaikuad, A.; Tan, L.; Schroder, M.; Gondi, S.; Ficarro, S.B., et al. Leveraging Compound Promiscuity to Identify Targetable Cysteines within the Kinome. Cell Chem Biol 2019, 26, 818-829 e819, doi:10.1016/j.chembiol.2019.02.021.

78. Prasanna, K.S., P.; Bharathi, P. Salimath. Withaferin A suppresses the expression of vascular endothelial growth factor in Ehrlich ascites tumor cells via Sp1 transcription factor. Current Trends in Biotechnology and Pharmacy 2010, 1, 138-148.

79. Bottoni, A.; Rizzotto, L.; Lai, T.H.; Liu, C.; Smith, L.L.; Mantel, R.; Reiff, S.; El-Gamal, D.; Larkin, K.; Johnson, A.J., et al. Targeting BTK through microRNA in chronic lymphocytic leukemia. Blood 2016, 128, 3101-3112, doi:10.1182/blood-2016-07-727750.

80. Terzi, H.E., M. In vitro comparison of cytotoxic effects of bortezomib resistant U266 myeloma cell line (U266/VELR) on combination of ibrutinib with carfilzomib and lenalidomid drugs. Cumhuriyet Medical Journal 2019, 41.

81. Kraus, J.; Kraus, M.; Liu, N.; Besse, L.; Bader, J.; Geurink, P.P.; de Bruin, G.; Kisselev, A.F.; Overkleeft, H.; Driessen, C. The novel beta2-selective proteasome inhibitor LU-102 decreases phosphorylation of I kappa B and induces highly synergistic cytotoxicity in combination with ibrutinib in multiple myeloma cells. Cancer Chemother Pharmacol 2015, 76, 383-396, doi:10.1007/s00280-015-2801-0.

82. Ma, J.; Gong, W.; Liu, S.; Li, Q.; Guo, M.; Wang, J.; Wang, S.; Chen, N.; Wang, Y.; Liu, Q., et al. Ibrutinib targets microRNA-21 in multiple myeloma cells by inhibiting NF-kappaB and STAT3. Tumour Biol 2018, 40, 1010428317731369, doi:10.1177/1010428317731369.

83. Rushworth, S.A.; Bowles, K.M.; Barrera, L.N.; Murray, M.Y.; Zaitseva, L.; MacEwan, D.J. BTK inhibitor ibrutinib is cytotoxic to myeloma and potently enhances bortezomib and lenalidomide activities through NF-kappaB. Cell Signal 2013, 25, 106-112, doi:10.1016/j.cellsig.2012.09.008.

84. Lindvall, J.M.; Blomberg, K.E.; Berglof, A.; Yang, Q.; Smith, C.I.; Islam, T.C. Gene expression profile of B cells from Xid mice and Btk knockout mice. Eur J Immunol 2004, 34, 1981-1991, doi:10.1002/eji.200324051.

85. Roman-Garcia, S.; Merino-Cortes, S.V.; Gardeta, S.R.; de Bruijn, M.J.W.; Hendriks, R.W.; Carrasco, Y.R. Distinct Roles for Bruton's Tyrosine Kinase in B Cell Immune Synapse Formation. Front Immunol 2018, 9, 2027, doi:10.3389/fimmu.2018.02027.

86. Chirumamilla, C.S.; Perez-Novo, C.; Van Ostade, X.; Vanden Berghe, W. Molecular insights into cancer therapeutic effects of the dietary medicinal phytochemical Withaferin A. Proc Nutr Soc 2017, 76, 96-105, doi:10.1017/S0029665116002937.

87. Grossman, E.A.; Ward, C.C.; Spradlin, J.N.; Bateman, L.A.; Huffman, T.R.; Miyamoto, D.K.; Kleinman, J.I.; Nomura, D.K. Covalent Ligand Discovery against Druggable Hotspots Targeted by Anti-cancer Natural Products. Cell Chem Biol 2017, 24, 1368-1376 e1364, doi:10.1016/j.chembiol.2017.08.013.

88. Shinohara, H.; Yasuda, T.; Aiba, Y.; Sanjo, H.; Hamadate, M.; Watarai, H.; Sakurai, H.; Kurosaki, T. PKC beta regulates BCR-mediated IKK activation by facilitating the interaction between TAK1 and CARMA1. J Exp Med 2005, 202, 1423-1431, doi:10.1084/jem.20051591.

89. Mohammad, D.K.; Nore, B.F.; Smith, C.I.E. Terminating B cell receptor signaling. Oncotarget 2017, 8, 109857-109858, doi:10.18632/oncotarget.22986.

90. Franks, S.E.; Cambier, J.C. Putting on the Brakes: Regulatory Kinases and Phosphatases Maintaining B Cell Anergy. Front Immunol 2018, 9, 665, doi:10.3389/fimmu.2018.00665.

91. Dom, M.; Vanden Berghe, W.; Van Ostade, X. Broad-spectrum antitumor properties of Withaferin A: a proteomic perspective. RSC Med. Chem. 2020, 11, 30-50.

92. Widodo, N.; Priyandoko, D.; Shah, N.; Wadhwa, R.; Kaul, S.C. Selective killing of cancer cells by Ashwagandha leaf extract and its component Withanone involves ROS signaling. PLoS One 2010, 5, e13536, doi:10.1371/journal.pone.0013536.

93. Pires, N.; Gota, V.; Gulia, A.; Hingorani, L.; Agarwal, M.; Puri, A. Safety and pharmacokinetics of Withaferin-A in advanced stage high grade osteosarcoma: A phase I trial. J Ayurveda Integr Med 2020, 11, 68-72, doi:10.1016/j.jaim.2018.12.008.

94. Patel, S.B.; Rao, N.J.; Hingorani, L.L. Safety assessment of Withania somnifera extract standardized for Withaferin A: Acute and sub-acute toxicity study. J Ayurveda Integr Med 2016, 7, 30-37, doi:10.1016/j.jaim.2015.08.001.

95. Thaiparambil, J.T.; Bender, L.; Ganesh, T.; Kline, E.; Patel, P.; Liu, Y.; Tighiouart, M.; Vertino, P.M.; Harvey, R.D.; Garcia, A., et al. Withaferin A inhibits breast cancer invasion and metastasis at sub-cytotoxic doses by inducing vimentin disassembly and serine 56 phosphorylation. Int J Cancer 2011, 129, 2744-2755, doi:10.1002/ijc.25938.

96. Smith, P.K.; Krohn, R.I.; Hermanson, G.T.; Mallia, A.K.; Gartner, F.H.; Provenzano, M.D.; Fujimoto, E.K.; Goeke, N.M.; Olson, B.J.; Klenk, D.C. Measurement of protein using bicinchoninic acid. Anal Biochem 1985, 150, 76-85, doi:10.1016/0003-2697(85)90442-7.

97. Hilhorst, R.; Houkes, L.; Mommersteeg, M.; Musch, J.; van den Berg, A.; Ruijtenbeek, R. Peptide microarrays for profiling of serine/threonine kinase activity of recombinant kinases and lysates of cells and tissue samples. Methods Mol Biol 2013, 977, 259-271, doi:10.1007/978-1-62703-284-1_21.

98. Folkvord, S.; Flatmark, K.; Dueland, S.; de Wijn, R.; Groholt, K.K.; Hole, K.H.; Nesland, J.M.; Ruijtenbeek, R.; Boender, P.J.; Johansen, M., et al. Prediction of response to preoperative

chemoradiotherapy in rectal cancer by multiplex kinase activity profiling. Int J Radiat Oncol Biol Phys 2010, 78, 555-562, doi:10.1016/j.ijrobp.2010.04.036.

99. Maat, W.; el Filali, M.; Dirks-Mulder, A.; Luyten, G.P.; Gruis, N.A.; Desjardins, L.; Boender, P.; Jager, M.J.; van der Velden, P.A. Episodic Src activation in uveal melanoma revealed by kinase activity profiling. Br J Cancer 2009, 101, 312-319, doi:10.1038/sj.bjc.6605172.

100. Safaei, J.; Manuch, J.; Gupta, A.; Stacho, L.; Pelech, S. Prediction of 492 human protein kinase substrate specificities. Proteome Sci 2011, 9 Suppl 1, S6, doi:10.1186/1477-5956-9-S1-S6.

101. Versele, M.; Talloen, W.; Rockx, C.; Geerts, T.; Janssen, B.; Lavrijssen, T.; King, P.; Gohlmann, H.W.; Page, M.; Perera, T. Response prediction to a multitargeted kinase inhibitor in cancer cell lines and xenograft tumors using high-content tyrosine peptide arrays with a kinetic readout. Mol Cancer Ther 2009, 8, 1846-1855, doi:10.1158/1535-7163.MCT-08-1029.

102. Kinexus | PhosphoNET. Available online: http://www.phosphonet.ca/ , Accessed on 21st May 2019.

103. IPA Q. Ingenuity pathway analysis. Available online: http://www.ingenuity.com/products/ipa, Accessed on 15th September 2020.

104. Andrews, S. FastQC: a quality control tool for high throughput sequence data. Babraham Bioinformatics, Babraham Institute, Cambridge, United Kingdom: 2010.

105. Dobin, A.; Davis, C.A.; Schlesinger, F.; Drenkow, J.; Zaleski, C.; Jha, S.; Batut, P.; Chaisson, M.; Gingeras, T.R. STAR: ultrafast universal RNA-seq aligner. Bioinformatics 2013, 29, 15-21, doi:10.1093/bioinformatics/bts635.

106. Thomas, P.D.; Campbell, M.J.; Kejariwal, A.; Mi, H.; Karlak, B.; Daverman, R.; Diemer, K.; Muruganujan, A.; Narechania, A. PANTHER: a library of protein families and subfamilies indexed by function. Genome Res 2003, 13, 2129-2141, doi:10.1101/gr.772403.

107. Szarc vel Szic, K.; Op de Beeck, K.; Ratman, D.; Wouters, A.; Beck, I.M.; Declerck, K.; Heyninck, K.; Fransen, E.; Bracke, M.; De Bosscher, K., et al. Pharmacological levels of Withaferin A (Withania somnifera) trigger clinically relevant anticancer effects specific to triple negative breast cancer cells. PLoS One 2014, 9, e87850, doi:10.1371/journal.pone.0087850.

108. Schindelin, J.; Arganda-Carreras, I.; Frise, E.; Kaynig, V.; Longair, M.; Pietzsch, T.; Preibisch, S.; Rueden, C.; Saalfeld, S.; Schmid, B., et al. Fiji: an open-source platform for biological-image analysis. Nat Methods 2012, 9, 676-682, doi:10.1038/nmeth.2019.

109. Heyninck, K.; Sabbe, L.; Chirumamilla, C.S.; Szarc Vel Szic, K.; Vander Veken, P.; Lemmens, K.J.A.; Lahtela-Kakkonen, M.; Naulaerts, S.; Op de Beeck, K.; Laukens, K., et al. Withaferin A induces heme oxygenase (HO-1) expression in endothelial cells via activation of the Keap1/Nrf2 pathway. Biochem Pharmacol 2016, 109, 48-61, doi:10.1016/j.bcp.2016.03.026.

110. Guex, N.; Peitsch, M.C. SWISS-MODEL and the Swiss-PdbViewer: an environment for comparative protein modeling. Electrophoresis 1997, 18, 2714-2723, doi:10.1002/elps.1150181505.

111. Pettersen, E.F.; Goddard, T.D.; Huang, C.C.; Couch, G.S.; Greenblatt, D.M.; Meng, E.C.; Ferrin, T.E. UCSF Chimera--a visualization system for exploratory research and analysis. J Comput Chem 2004, 25, 1605-1612, doi:10.1002/jcc.20084.

112. Schrödinger, L. The PyMOL Molecular Graphics System.

113. Dayalan Naidu, S.; Dinkova-Kostova, A.T. KEAP1, a cysteine-based sensor and a drug target for the prevention and treatment of chronic disease. Open Biol 2020, 10, 200105, doi:10.1098/rsob.200105.

114. Kobayashi, M.; Li, L.; Iwamoto, N.; Nakajima-Takagi, Y.; Kaneko, H.; Nakayama, Y.; Eguchi, M.; Wada, Y.; Kumagai, Y.; Yamamoto, M. The antioxidant defense system Keap1-Nrf2 comprises a multiple sensing mechanism for responding to a wide range of chemical compounds. Mol Cell Biol 2009, 29, 493-502, doi:10.1128/MCB.01080-08.

CHAPTER 4

Unraveling the Kinase Signature of Ferroptotic Multiple Myeloma Cells

Chapter 4

Unraveling the Kinase Signature of Ferroptotic Multiple Myeloma Cells

Emilie Logie[1], Claudina Perez Novo[1], Amber Driesen[1], Pieter Van Vlierberghe[2], Wim Vanden Berghe[1]*

1. Laboratory of Protein Science, Proteomics and Epigenetic Signaling (PPES) and Integrated Personalized and Precision Oncology Network (IPPON), Department of Biomedical Sciences, University of Antwerp, Campus Drie Eiken, Universiteitsplein 1, Wilrijk, Belgium
2. Department of Biomolecular Medicine, Ghent University, Ghent, Belgium

* Corresponding author: wim.vandenberghe@uantwerpen.be

Conflict of Interest: The authors declare no conflict of interest.

Abstract

Through phosphorylation of their substrate proteins, protein kinases are crucial for quickly transducing cellular signals and orchestrating key biological processes, including cell death and survival. Recent studies have revealed that kinases are also involved in ferroptosis, an iron-dependent mode of cell death associated with toxic lipid peroxidation. Given that ferroptosis is currently being explored as an alternative strategy to eliminate apoptosis-resistant tumor cells, further characterization of ferroptosis-dependent kinase changes might aid in identifying novel druggable targets for protein kinase inhibitors in context of cancer treatment. To this end, we performed a phosphopeptidome based kinase activity profiling of glucocorticoid-resistant multiple myeloma cells treated with either the apoptosis inducer staurosporine (STS) or the ferroptosis inducer RSL3 and compared their kinome activity signatures. Our data demonstrate that both cell death mechanisms inhibit the activity of kinases classified into the CMGC and AGC kinase families, with STS showing a broader spectrum of serine/threonine kinase inhibition. In contrast, RSL3 targeted a significant number of tyrosine kinases, including key players of the B-cell receptor signaling pathway. Remarkably, additional kinase profiling of the anti-cancer agent Withaferin A (WA) revealed considerable overlap with ferroptosis and apoptosis kinome activity, explaining why Withaferin A can induce mixed ferroptotic and apoptotic cell death features. Altogether, we show that apoptotic and ferroptotic cell death induce different kinase signaling changes and that kinome profiling might become a valid approach to stratify cell death chemosensitization modalities of novel anti-cancer agents.

Keywords: ferroptosis; kinase; staurosporine; multiple myeloma; Withaferin a; apoptosis
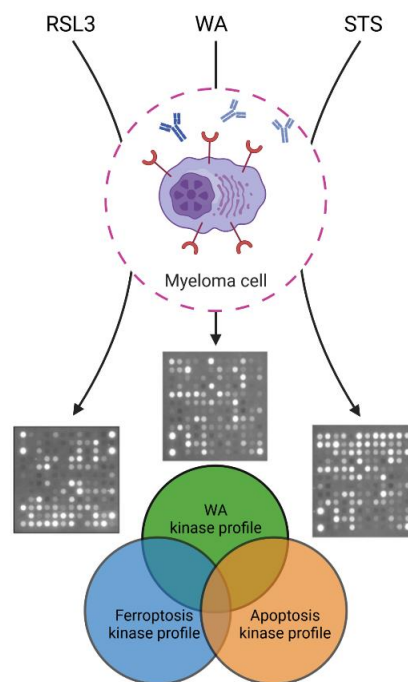
4.1. Introduction

Protein kinases (PKs) are enzymes that modify their substrate proteins by catalyzing the transfer of γ-phosphate from ATP to serine, threonine, and tyrosine residues. This process, known as protein phosphorylation, results in a functional change of the target protein and allows for a rapid signal transduction in response to intra- and extracellular triggers. Phosphorylation of proteins is considered to be one of the most crucial post-translational modifications and is required for proper regulation of various cellular functions, including metabolism [1, 2], cell cycle regulation [3, 4], differentiation [5, 6], and cell death and survival [7-9]. Thus, it is not surprising that perturbed phosphorylation events or dysregulation of PKs often results in a diseased state, such as cancer. In multiple myeloma (MM), a hematological malignancy characterized by the uncontrolled proliferation of plasma cells, several kinases, including AKT and B-cell receptor signaling (BCR) kinases, are known to be involved in tumorigenesis and therapy resistance [10-13]. Targeting these malfunctioning kinases with protein kinase inhibitors (PKIs) could therefore offer significant clinical benefits to patients suffering from MM [14, 15] or other cancer types [16]. Presently, 62 PKIs have been FDA-approved for clinical use and have had a major impact on the treatment of cancer worldwide [17]. However, no inhibitors have been approved for use in MM to date, mainly due to issues with drug efficacy [18]. Finding novel, targetable PKs in context of MM might aid in overcoming therapy resistance and curing the disease altogether.

Ferroptosis is a non-apoptotic mode of regulated cell death (RCD) that is orchestrated by an iron-dependent overproduction of lipid peroxides [19]. In the field of oncology, ferroptosis is currently being explored as a novel way to eradicate apoptosis-resistant cancer cells [20]. Different from apoptosis and other cell death modalities, ferroptosis does not depend on caspases or receptor-interacting protein 1, but heavily relies on the cysteine, lipid, and iron metabolism to promote cell death [21-23]. Taking into account that the majority of cancer types, including MM, are characterized by an increased iron uptake [24], an altered (cysteine) metabolism [25], and higher oxidative stress levels [26] compared to their healthy counterparts, ferroptosis-inducing agents might further destabilize these cellular processes to achieve complete tumor suppression [27]. However, the key signaling processes and determinants of ferroptotic cell death still largely remain elusive and need to be more extensively studied before the therapeutic use of ferroptotic kinase inhibitor compounds can fully be appreciated. Accumulating evidence indicates that PKs, such as AMPK and ATM, are involved in regulating ferroptosis [28, 29]. Recent studies have even reported that PKI sorafenib is able to trigger ferroptosis in a variety of cell lines [30]. To this end, PKIs that inhibit a subset of kinases and subsequently induce ferroptotic cell death might hold promise as novel anti-cancer agents in therapy-resistant tumors, such as MM. Consequently, we performed phosphopeptidome kinase activity profiling of glucocorticoid (GC)-resistant multiple myeloma cells treated with either apoptotic or ferroptotic compounds to obtain cell death-specific inhibitory kinome activity signatures. This approach allows us to directly compare apoptosis- and ferroptosis-dependent kinase activity changes and to identify ferroptosis-specific kinases based on the differential

peptide phosphorylation patterns. Finally, we also compared the kinome activity profile of natural anti-cancer agent Withaferin A (WA) with the apoptotic and ferroptotic signatures to predict its cell death modality in MM cells.

4.2. Results

4.2.1. Both Apoptotic and Ferroptotic Cell Death are Associated with a Progressive Inhibition of Protein Kinase Activity

Staurosporine (STS) is a reversible broad spectrum protein kinase inhibitor that is widely used to induce apoptotic cell death in tumor models, including MM [31]. To characterize ferroptosis-dependent kinase signaling changes in GC-resistant myeloma cells and compare them with apoptosis-dependent kinase changes, we analyzed the peptide phosphorylation profiles of STS-treated apoptotic and RSL3-treated ferroptotic MM1R cells. Both treatments steadily decreased cell viability of MM1R cells after ≥ 3 hour treatment (Figure 1a) and were accompanied by either an increase in lipid peroxidation in ferroptotic cells or PARP-1 cleavage in apoptotic cells (Figure 1b-c). In line with these observations, phosphorylation intensities of Ser/Thr kinase (STK) peptide substrates was markedly decreased after ≥ 3 hour STS and RSL3 treatment (Figure 2). A similar trend could be observed for the tyrosine kinase (PTK) peptide substrates in RSL3-treated MM1R cells but not in STS-treated cells (Figure 2), suggesting that PTKs play a more pronounced role in ferroptotic cell death.
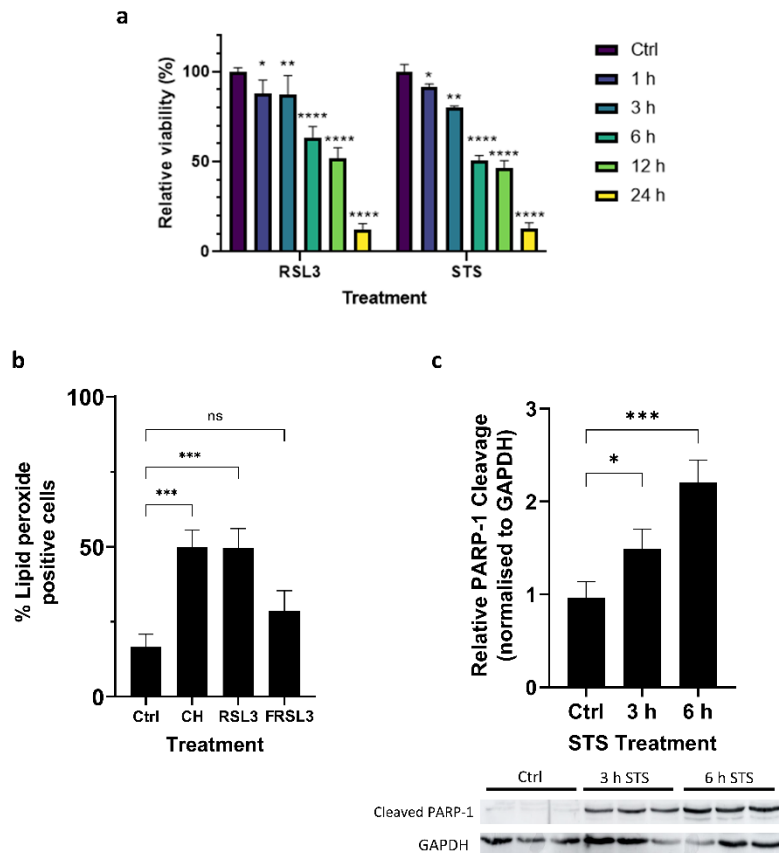
Figure 1 (previous page): (**a**) Relative cell viability (%) of MM1R cells treated with 5 µM RSL3 (left) or 1 µM STS (right). (**b**) % of RSL3-treated MM1R cells undergoing a fluorescence shift from red (590 nm) to green (510 nm) as a consequence of increased lipid peroxidation. Cumene hydroperoxide (CH) is included as a positive control, while untreated controls and cells pre-treatment with ferroptosis inhibitor ferrostatin-1 and RSL3 (FRSL3) are included as a negative controls. (**c**) Western blot detection and quantification of PARP-1 cleavage and GAPDH expression levels in MM1R cells treated with 5 µM STS for 3 and 6 hrs. All data are presented as the mean ± s.d., *n*=3 biologically independent samples per treatment (*p < 0.05, **p < 0.01, ***p < 0.001, ****p < 0.0001, ANOVA).

Figure 2: Heatmap visualization of individual phosphorylation intensities, represented as normalized z-scores, of peptides on serine/threonine kinase (STK) (upper panel) or tyrosine kinase (PTK) (lower panel) chips which serve as substrates for

serine/threonine or tyrosine kinases, respectively. Higher z-scores (yellow) indicate kinase activation while lower z-scores (dark blue) indicate kinase inhibition. MM1R cells were treated with either 5 µM RSL3 or 1 µM STS for increasing timepoints, as indicated by the figure legend.

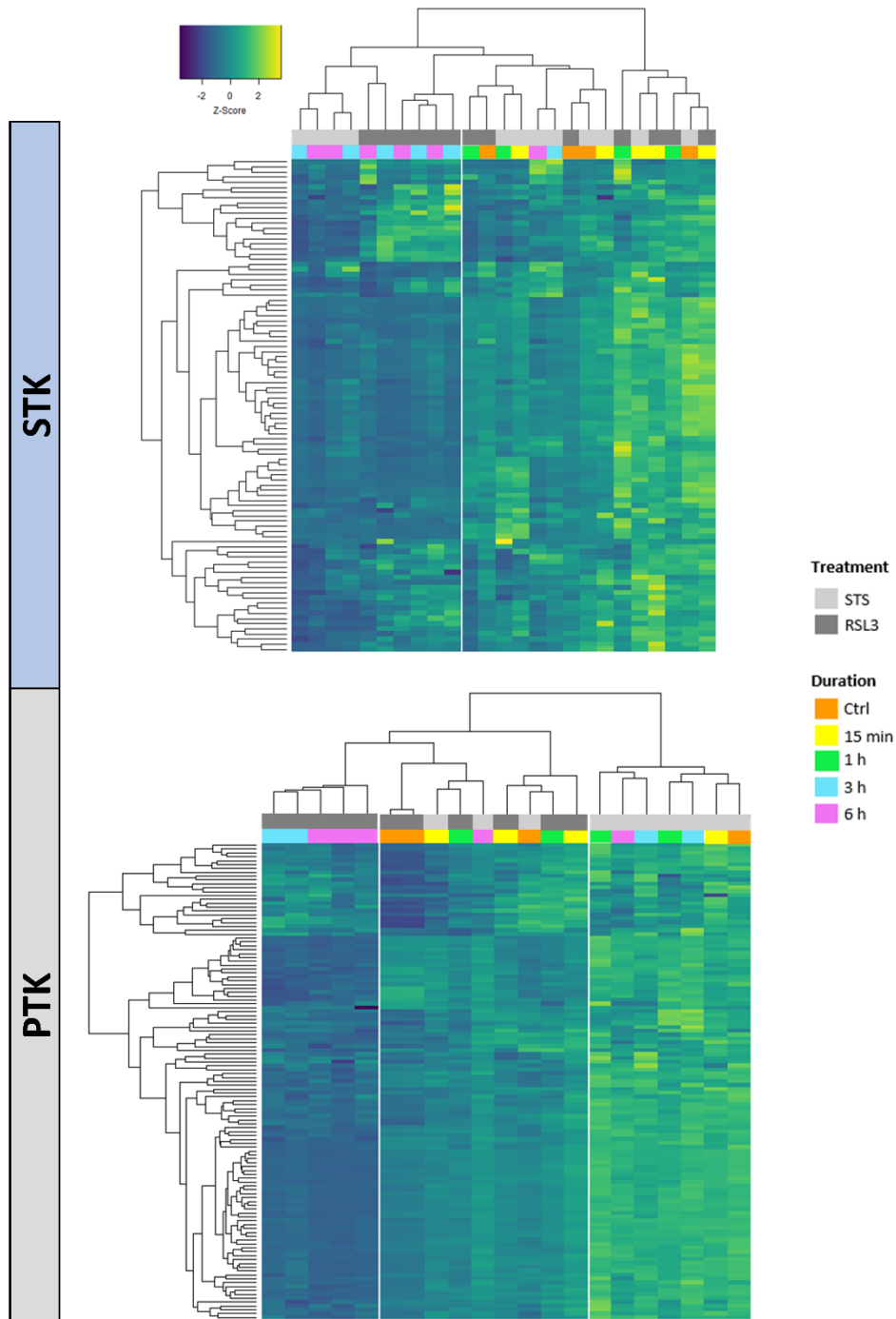## 4.2.2. RSL3 and STS Treatment of MM1R Cells Mainly Affects CMGC and AGC Protein Kinases

Based on the differential peptide phosphorylation pattern that indicated that apoptosis- and ferroptosis-mediated cell death are associated with protein kinase inhibition (Figure 2, Supplementary Figure S2), upstream kinase (UPK) analysis was performed to identify the top 10 downregulated protein kinases under apoptotic and ferroptotic conditions after ≥ 3 hours of treatment (i.e. the treatment time when a reduction in cell viability and inhibitory kinase effects are first observed, as described in section 2.1.). The final STK and PTK ranking per condition is represented in Figures 3 and 4, and is based on the mean final score of each kinase. Kinases with a mean final score of ≥ 1.3 and a kinase statistic of ≥ 0.5 were considered to be biologically relevant. Overall, kinase profiling revealed that both RSL3 and STS treatment of MM1R cells inhibits the activity of kinases involved in cell cycle regulation (PFTAIRE2, CK2α1, and CDK10), cytoskeletal reorganization (PKG1), cellular stress (MSK2), and inflammation (Srm, JAK1b) (Figures 2-3). Most of these UPKs belong to the AGC or CMGC kinase group, implying that these kinase families in particular are important in regulating cell death in MM1R cells. This was further confirmed by phylogenetic kinase mapping which showed that the majority of STS- and RSL3-mediated downregulated kinases were enriched in the CMGC and AGC kinase families (Figure 5). Both compounds also target kinases classified into the CAMK kinase family, including aurora kinases (AurA, AurB) and death-associated protein kinases (DAPK) that are known to play a vital role in cell death regulation [32-35]. Remarkably, within the CAMK group, RSL3 and STS can target different members within the same family. For instance, while RSL3 is able to significantly inhibit DAPK2 and AurA activity, STS preferentially inhibits DAPK3 and AurB. Further exploration of the synergistic interaction between apoptosis and ferroptosis inducers in multiple myeloma treatment might therefore help to identify effective combination therapies. A prior study in pancreatic tumor cells has revealed, for example, that ferroptotic agents can sensitize cells to TRAIL-induced apoptosis [36].

Although STS and RSL3 display similarities in their inhibitory kinase profiles in MM1R cells, key differences between both treatment conditions exist as well. Compared to RSL3, STS is able to inhibit a broader range of STKs, including kinases belonging to the CK1 (CK1α) , STE (COT), and Atypical (AlphaK1, ADCK3) families. Even within the AGC and CMG families, the number of kinases targeted by STS exceeds the number of RSL3-inhibited kinases (Figure 5). In contrast, RSL3 treatment has a more pronounced effect on PTKs and is able to inhibit several kinases that are involved in BCR signaling, which we previously reported to be hyperactivated in therapy-resistant MM cells [10]. Network interaction and functional enrichment analysis indeed demonstrates that kinase inhibitory changes mediated by RSL3, but not by STS, are enriched in regulation of BCR signaling activity (Figure 6). This might explain why some B-cell malignances, including diffuse large B-cell lymphoma, are more prone to ferroptosis-induced cell death in comparison to other solid tumors [37].
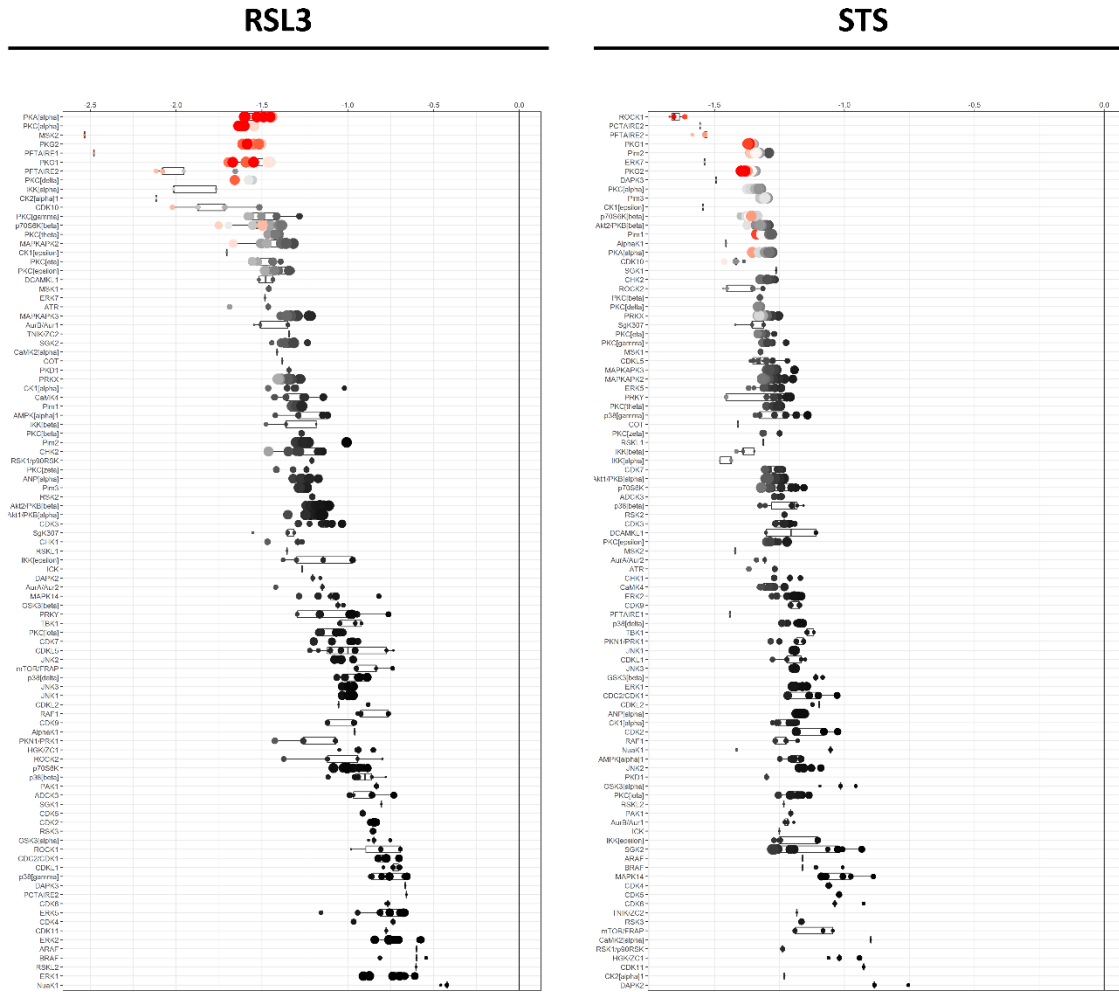
Kinase Name	Mean Final Score	Specificity Score	Mean Kinase Statistic
PKAα	4,20	2,34	-1,53
PKCα	3,82	1,96	-1,61
MSK2	3,69	1,83	-2,53
PKG2	3,63	1,77	-1,56
PKG1	3,60	1,75	-1,56
PFTAIRE1	3,59	1,71	-2,48
PFTAIRE2	3,22	1,36	-1,98
PKCδ	3,17	1,31	-1,58
CK2α1	2,93	1,07	-2,12
CDK10	2,90	1,04	-1,81

Kinase Name	Mean Final Score	Specificity Score	Mean Kinase Statistic
Pim2	3,66	1,93	-1,28
ROCK1	3,48	1,89	-1,58
PFTAIRE2	3,41	1,56	-1,49
CK2α1	3,20	1,34	-1,60
MSK2	3,14	1,28	-1,25
PKG1	2,97	1,35	-1,52
RSKL1	2,90	1,05	-1,21
Pim3	2,88	1,26	-1,38
MSK1	2,82	1,15	-1,40
CDK10	2,76	1,01	-1,22

Figure 3: Mean final score plots of serine/threonine kinase (**STK**) activity profiling in MM1R cells treated with 5 μM RSL3 (left) or 1μM STS (right) for 3 hours. Plots display the predicted upstream STK ranked by their final score. The x-axis indicates the values for the normalized kinase statistic, which reflects the activity difference after treatment (e.g. negative values represent inhibited kinase activity). The size of each dot visualizes the size of the peptide set used for the upstream kinase prediction analysis. The color of the points depicts the specificity score, which indicates the specificity of the normalized kinase statistic with respect to the amount of peptides used for predicting the corresponding kinase. Below each figure, a table displaying the top 10 ranked kinases and their kinase statistic and specificity score is presented. The final ranking of the kinases is based on the mean final score.

Figure 4: Mean final score plots of tyrosine kinase (**PTK**) activity profiling in MM1R cells treated with 5 µM RSL3 (left) or 1µM STS (right) for 3 hours. Plots display the predicted upstream STK ranked by their final score. The x-axis indicates the values for the normalized kinase statistic, which reflects the activity difference after treatment (e.g. negative values represent inhibited kinase activity). The size of each dot visualizes the size of the peptide set used for the upstream kinase prediction analysis. The color of the points depicts the specificity score, which indicates the specificity of the normalized kinase statistic with respect to the amount of peptides used for predicting the corresponding kinase. Below each figure, a table displaying the top 10 ranked kinases and their kinase statistic and specificity score is presented. The final ranking of the kinases is based on the mean final score.
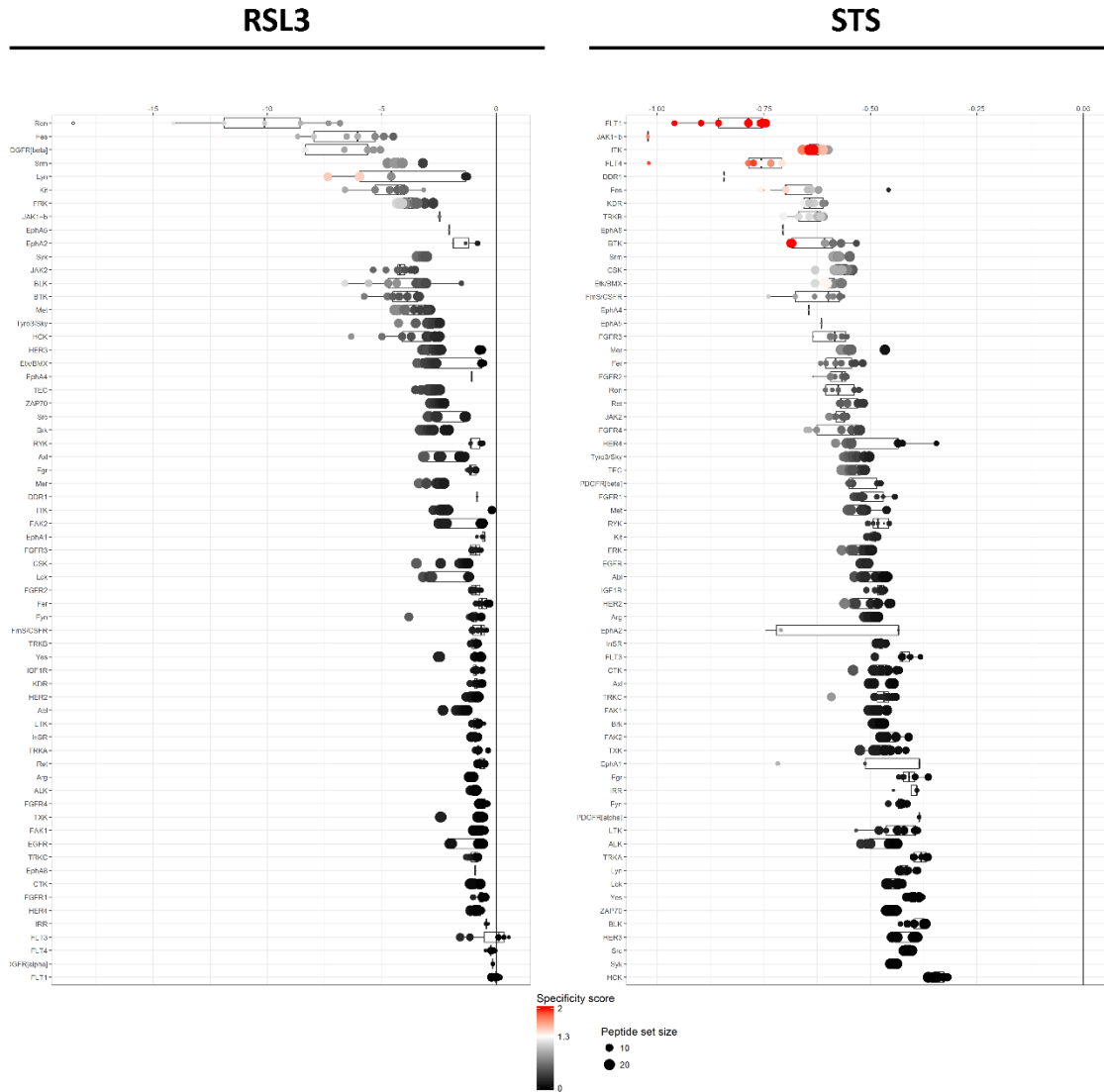
Kinase Name	Mean Final Score	Specificity Score	Mean Kinase Statistic
Ron	1,98	1,02	-10,67
Fes	1,84	0,87	-6,60
PDGFRβ	1,93	0,96	-6,55
Srm	1,72	0,75	-4,29
Lyn	1,79	0,82	-3,90
Kit	1,66	0,69	-4,52
FRK	1,68	0,71	-3,65
JAK1b	1,57	0,60	-2,477
EphA5	1,57	0,60	-2,06
EphA2	1,33	0,43	-1,55

Kinase Name	Mean Final Score	Specificity Score	Mean Kinase Statistic
JAK1b	2,92	2,70	-0,42
ITK	1,97	1,89	-0,24
BTK	1,94	1,85	-0,26
Srm	1,58	1,49	-0,23
CSFR	1,39	1,36	-0,28
DDR1	1,34	1,19	-0,33
FLT1	1,34	1,34	-0,26
FLT4	1,31	1,31	-0,26
CSK	1,12	1,03	-0,22
JAK2	1,05	1,01	-0,24

Figure 5: KinMap [38] phylogenetic kinome tree. Kinases inhibited by RSL3 treatment are indicated by red squares (■), kinases inhibited by STS treatment are marked as blue triangles (▲), kinases inhibited by both compounds are indicated as black circles (●). Only kinases with a mean final score ≥ 1.3 are included in the graph. Abbreviations: TK, tyrosine kinase group ;TKL, tyrosine kinase-like group; STE, serine/threonine kinase group; CK1, casein kinase 1 group; AGC, protein kinase A, G, and C group; CAMK, Ca^{2+}/calmodulin-dependent kinase group; CMGC, cyclin-dependent kinase, mitogen-activated protein kinase, glycogen synthase kinase, and CDC-like kinase group.
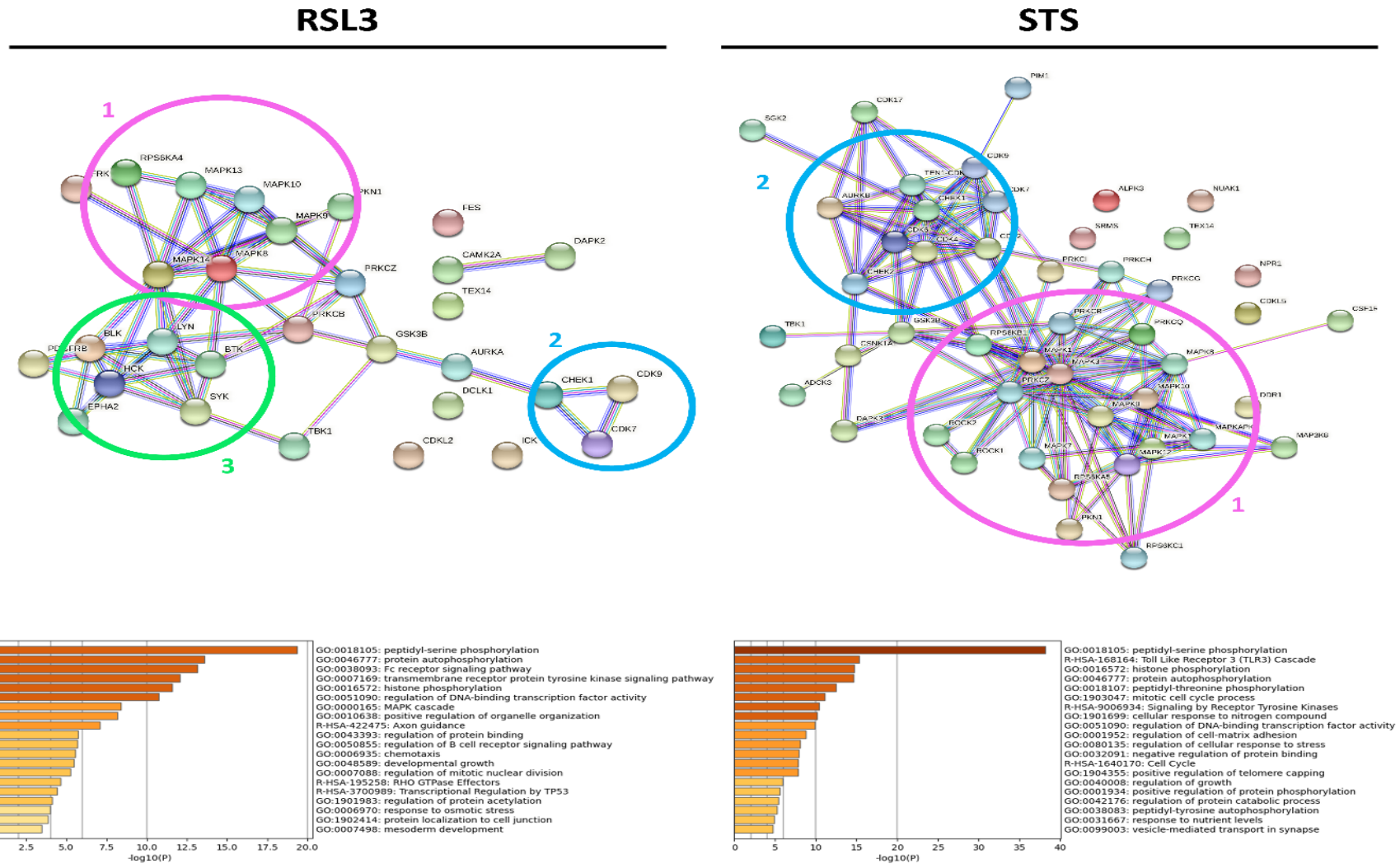
Figure 6: Network interaction and functional enrichment analysis of predicted kinases inhibited by RSL3 (left) or STS (right) in MM1R cells. The top panel visualizes the protein interaction networks of kinases with a mean final score ≥ 1.3, generated with String (v11) [39]. The clusters visible in the network are marked by a circle and include a MAPK signaling cluster (pink circle, number 1), CDK signaling (blue circle, number 2), and B-cell receptor signaling (green circle, number 3). The lower panel shows the Metascape [40] functional enrichment analysis of the included protein kinases.

4.2.3. Predicting the Cell Death Modality of Withaferin A Based on Kinome Profiling

After characterizing the kinase changes taking place in apoptotic STS-treated and ferroptotic RSL3-treated MM1R cells, we wondered whether the kinase inhibitory profile of these compounds can be used to predict the cell death modality of other anti-cancer agents. Our findings from a previous study demonstrate that the natural steroidal lactone WA effectively kills GC-resistant MM1R cells and that the induced cell death is, in part, orchestrated by WA-mediated inhibition of Bruton tyrosine kinase (BTK), a key player in BCR signaling [10]. However, whether this WA-mediated BTK-inhibition promotes apoptosis, ferroptosis, or other cell death modalities in MM1R cells has not been elucidated yet. To this end, we treated MM1R cells with WA and compared its kinase profile with STS and RSL3. Similar to STS and RSL3, a time-dependent decrease in cell viability could be observed in MM1R cells treated with 1 μM WA (Supplementary Figure S1) and was associated with a decrease in peptide phosphorylation after ≥ 3 hours of treatment (Supplementary Figure S2).

Further UPK analysis revealed that the top 10 WA-inhibited STKs and PTKs include PKα, PFTAIRE1, PKG2, PKCδ, and FRK (Figure 7), which are mainly targeted by RSL3, but not STS. Likewise, network interaction and functional enrichment analysis demonstrated that WA resembles RSL3 in its ability to inhibit B-cell receptor signaling by inhibiting BTK and other PTKs (Figure 8a-b), which is in line with our previous observations [10]. On the other hand, phylogenetic kinome mapping showed that WA is also able to target a broad range of STKs, especially those classified into the AGC kinase family, suggesting that the inhibitory kinome profile of WA is reminiscent of the STS profile as well (Figure 9). PKCη, PKCε, PKCγ, p70S6K, and SGK2 are all AGC kinases that are inhibited by both WA and STS. Based on the duality of its kinome profile, WA seems to be able to both induce apoptotic and ferroptotic cell death. In agreement with this observation, previous studies have reported that WA is able to trigger different cell death modalities based on the cellular context and concentration range used [41, 42].

Despite its similarities with RSL3, we observed no increase in lipid peroxidation in MM1R cells after treatment with WA (data not shown). WA-induced cell death could also not be reversed by pre-treatment of MM1R cells with ferrostatin-1, an inhibitor of ferroptosis (Supplementary Figure S2). In contrast, apoptosis inhibitor zVAD-FMK was able to partially rescue WA-mediated cell death, suggesting that WA triggers apoptosis rather than ferroptosis in MM1R cells (Supplementary Figure S3). Indeed, and increase in PARP-1 could also be observed in MM1R cells upon prolonged WA exposure (Supplementary Figure S4). Taken together, our results indicate that the inhibitory kinome profile of WA is similar to apoptotic and ferroptotic kinome profiles, suggesting that WA is able to promote both of these cell death mechanisms. Although WA and RSL3 are both able to inhibit BTK and BCR signaling, WA seems to trigger apoptosis rather than ferroptosis in MM1R cells. Most likely, other WA-targeted pathways, including NF-κB signaling [43], proteasome-mediated protein degradation [44], and heat shock-regulated stress signaling [45], tip the cell death balance towards apoptosis. It therefore remains important that kinase activity changes are interpreted within a broader biological kinome context.
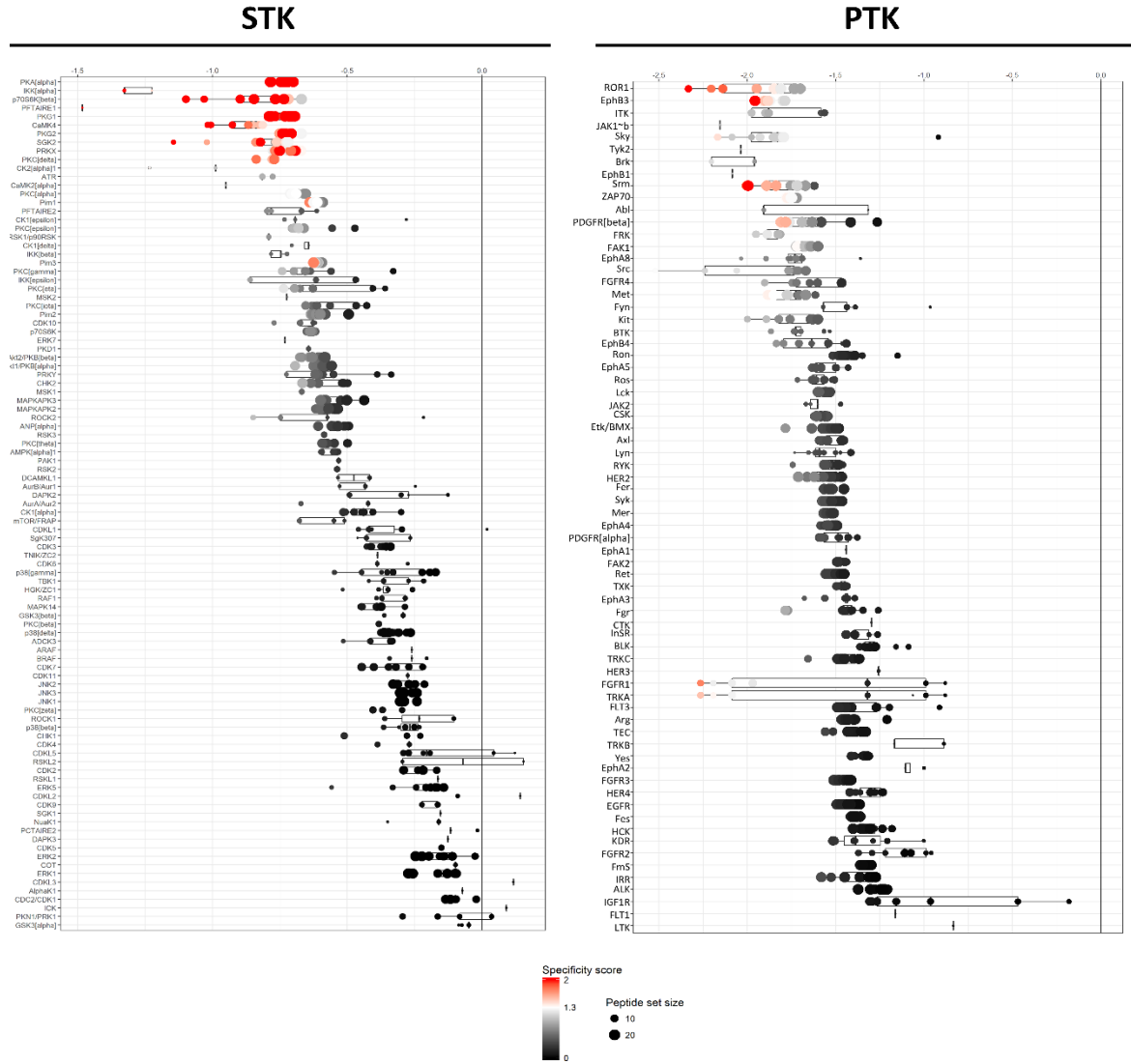
Kinase Name	Mean Final Score	Specificity Score	Mean Kinase Statistic
PKAα	3,70	2,70	-0,74
PFTAIRE1	3,50	2,3	-1,48
IKKα	3,49	1,86	-1,29
PKG1	3,40	2,28	-0,74
P70S6Kβ	3,40	2,15	-0,85
CAMK4	3,03	1,72	-0,89
PKG2	2,88	1,84	-,72
SGK2	2,83	1,46	-0,84
PKCδ	2,72	1,67	-0,79
PRKX	2,52	1,55	-0,99

Kinase Name	Mean Final Score	Specificity Score	Mean Kinase Statistic
ROR1	3,13	1,61	-0,76
EphB3	2,77	1,18	-0,63
Sky	2,72	1,82	-0,44
JAK1b	2,48	1,14	-0,57
ITK	2,45	1,78	-0,46
Tyk2	2,36	0,95	-0,57
FRK	1,91	1,18	-0,41
EphB1	1,90	1,02	-0,61
Srm	1,86	1,02	-0,41
Brk	1,83	0,93	-0,38

Figure 7: Mean final score plots of serine/threonine (STK) and tyrosine kinase (PTK) activity profiling in MM1R cells treated with 1 µM Withaferin a (WA) 3 hours. Plots display the predicted upstream STK ranked by their final score. The x-axis indicates the values for the normalized kinase statistic, which reflects the activity difference after treatment (e.g. negative values represent inhibited kinase activity). The size of each dot visualizes the size of the peptide set used for the upstream kinase prediction analysis. The color of the points depicts the specificity score, which indicates the specificity of the normalized kinase statistic with respect to the amount of peptides used for predicting the corresponding kinase. Below each figure, a table displaying the top 10 ranked kinases and their kinase statistic and specificity score is presented. The final ranking of the kinases is based on the mean final score.
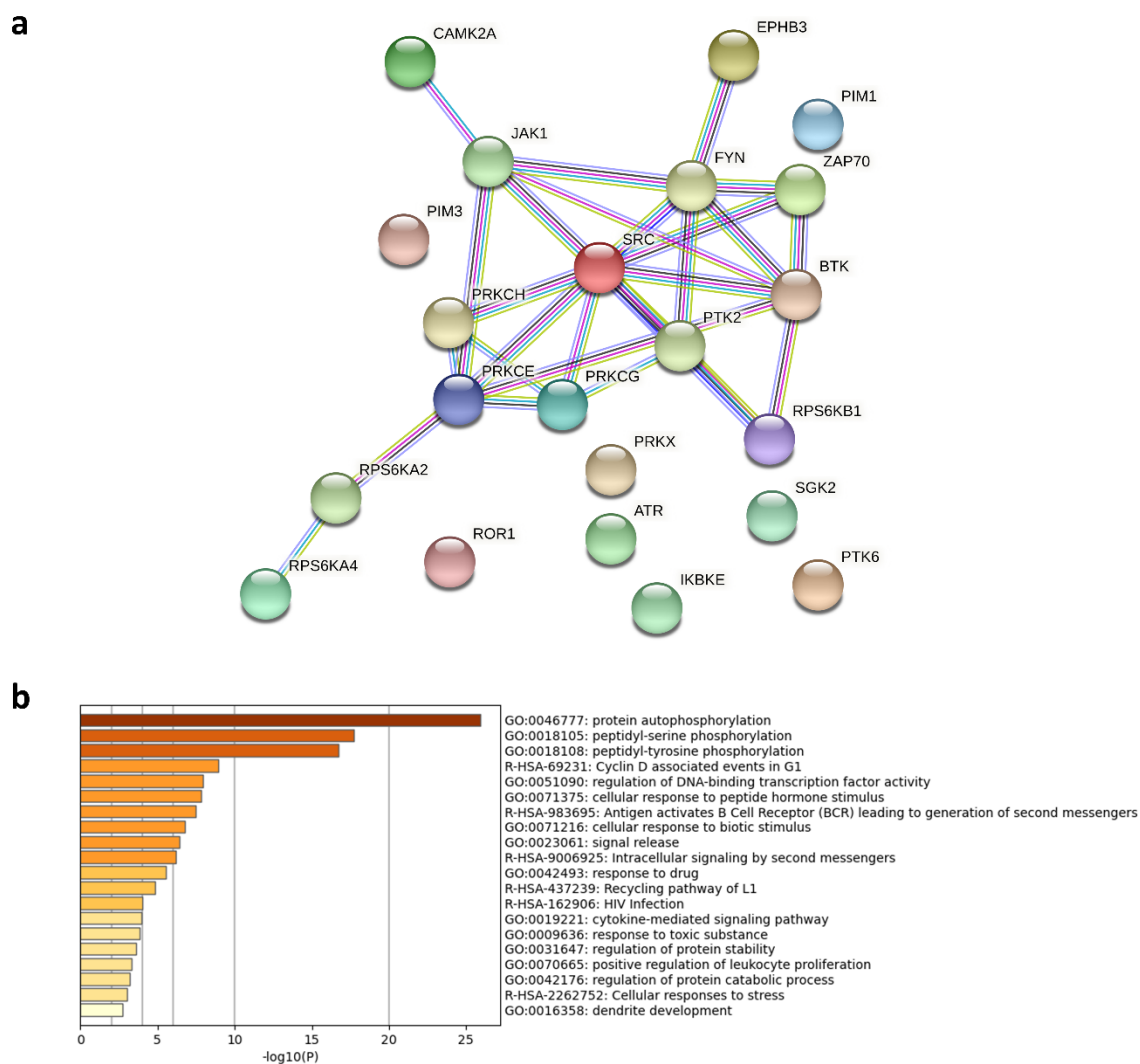
a

b

Figure 8: (**a**) Network interaction analysis of predicted kinases inhibited by 1 µM Withaferin a (WA) in MM1R cells. The protein interaction network (generated with String (v11) [39]) includes all kinases inhibited by WA with a mean final score ≥ 1.3. (**b**) Metascape [40] functional enrichment analysis of the protein kinases included in the protein interaction network.

4.3. Discussion

It is estimated that one quarter of all drug discovery efforts aim to target PKs, making them the largest group of clinical drug targets in the field of oncology [17]. Although several PKIs have reached phase II of clinical trials for treatment of MM, none have reached the market yet [46]. This is somewhat remarkable given that both myelomagenesis and development of therapy resistance are, at least in part, associated with perturbations in protein phosphorylation [47]. Both hyperactivation of the PI3K/AKT/mTOR and JAK/STAT signaling pathways, for example, are associated with poor prognosis and MM tumor proliferation, and are actively being explored in preclinical drug research as potential drug targets [48, 49]. However, since neither AKT or STAT inhibitors have been FDA-approved for clinical use in MM, identifying other targetable PKs crucial in MM tumorigenesis might contribute to developing novel anti-MM compounds. Because accumulating evidence suggest that B-cell
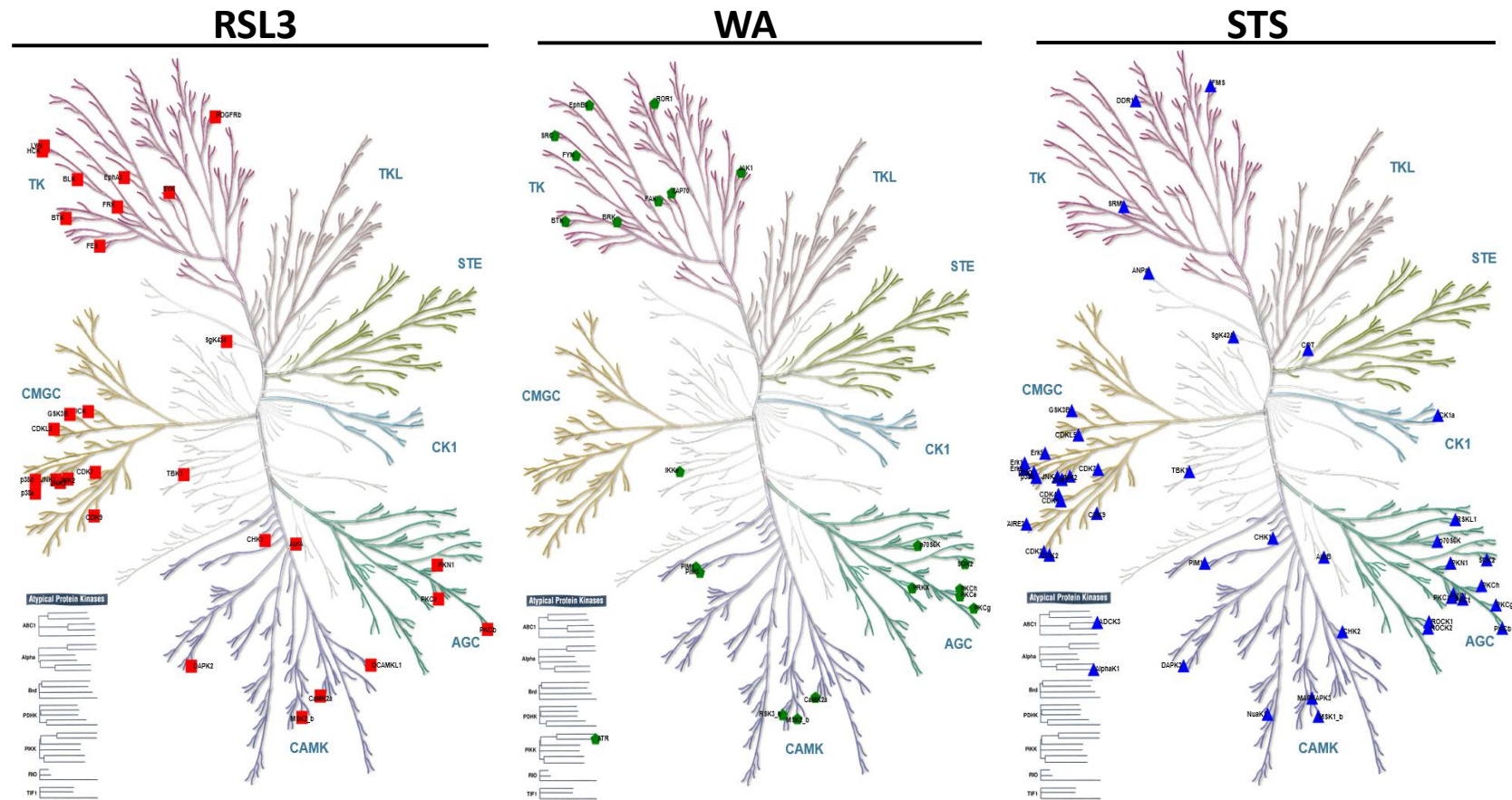
Figure 9: KinMap [38] phylogenetic kinome tree. Kinases inhibited by RSL3 treatment are indicated by red squares (■) (left), kinases inhibited by STS treatment are marked as blue triangles (▲) (right), kinases inhibited by WA are indicated as green hexagons (⬢). Only kinases with a mean final score ≥ 1.3 are included in the graph. Abbreviations: TK, tyrosine kinase group ;TKL, tyrosine kinase-like group; STE, serine/threonine kinase group; CK1, casein kinase 1 group; AGC, protein kinase A, G, and C group; CAMK, Ca^{2+}/calmodulin-dependent kinase group; CMGC, cyclin-dependent kinase, mitogen-activated protein kinase, glycogen synthase kinase, and CDC-like kinase group.

malignancies, including DLBCL and MM, are sensitive to ferroptotic cell death [37], finding kinases essential for ferroptotic cell death may offer translational potential for MM treatment by FDA approved kinase inhibitors. To this end, we applied phosphopeptidome kinome activity profiling of RSL3-treated GC-resistant MM1R cells to identify kinases inhibited by ferroptosis. We also compared these ferroptosis kinase signatures with those of STS-treated apoptotic MM1R cells to determine to which end each cell death modality has its own kinome profile. Our analysis revealed that prolonged treatment (≥ 3 hours) with either STS or RSL3 resulted in an overall decrease in STK activity, which was associated with a time-dependent increase in cell death. A similar inhibitory effect on PTKs was observed only in MM1R cells exposed to RSL3 exposure, implying that PTKs are more crucial in ferroptosis signaling compared to apoptosis signaling. This was also observed in our UPK analysis of the differential peptide phosphorylation patterns, where the mean kinase statistic score of top predicted RSL3 inhibited kinases was much higher compared to the score of STS inhibited kinases. Remarkably, functional enrichment analysis indicated that the majority of RSL3-targeted PTK kinases are involved in BCR, crucial for proliferation and survival of B-cells. This could possibly explain why B-cell cancers are more prone to ferroptotic cell death, as they heavily rely on BCR-related kinases for mediation of therapy resistance and tumor proliferation [13, 50, 51]. Although inhibition of BCR signaling is typically associated with apoptosis induction in several B-cell malignancies [52-54], this has only been sporadically explored in MM and deserves further investigation [55]. Alternatively, most BCR-related kinases are known to play a variety of different functions depending on their cellular context. Syk, for example, also orchestrates TNFα and NF-κB signaling in MM and other, non-hematological cells [55-57]. By inhibiting Syk, GPX4-inhibitor RSL3 potentially triggers MM cell death through inactivation of these two oncogenic pathways. In line with this hypothesis, a recent genetic-based kinome screening against ferroptosis in MDA-MB-231 breast cancer cells, revealed an important role for Syk and other TNFα/NF-κB kinase players suggesting that Syk-mediated inhibition by ferroptotic agents might be a universal phenomenon [29]. Indeed, a study in mucosal samples from ulcerative colitis patients revealed that NF-κB inhibition promotes ferroptotic cell death, albeit that the involvement of Syk was not investigated in this experimental setup [58]. Finally, another plausible explanation is that especially inhibition of PDGFRβ, in this study predicted to be the third most significant inhibited PTK by RSL3, is important to induce ferroptosis in MM. PDGFRβ is one of the major targets of sorafenib [59], a clinically approved PKI for treatment of hepatocellular and advanced renal cancer [60] that has been reported to induce ferroptosis in a variety of different human cell lines [30]. Although the correlation between ferroptosis and sorafenib has primarily been linked to non-kinase related events [61, 62], the role of PDGFRβ in RSL3-dependent cell death has not been explored. Intriguingly, overexpression of PDGFRβ is typically associated with worse prognosis in leukemia and myeloma patients [63, 64]

Compared to RSL3, the inhibitory effect of STS on STKs is considerably larger. As revealed by phylogenetic mapping STS targets STKs from different kinase families, including the STE, CK1, Atypical, CAMK, AGC, and CMGC families. This is in line with previous studies that have identified an extensive range of STS-inhibited kinases in HepG2 liver cells, such as PGK1,

AurB, PKAs, PKCs, and CDKs [65-67]. However, a subset of these kinases are also significantly inhibited by RSL3, highlighting that different cell death modalities can have overlapping kinome profiles. Most of the common kinases belong to the CMGC and AGC kinase families and include PFTAIRE2, CK2α1, CDK10, PKG1, and MSK2. Taking into account that the CMGC and AGC kinases mainly regulate cell cycle progression, proliferation, and survival, apoptosis- and ferroptosis mediated inhibition of these kinases seems crucial in promoting cell death. Both STS and RSL3 also impact CAMK kinases, which are involved in crucial cellular functions as well. Some CAMKs, such as CAMKK2 and CAMK4, have recently been associated with ferroptotic cell death [68, 69]. Although these kinases were not significantly inhibited by RSL3 in our setup, we did reveal that CAMK2A activity was considerably lower in ferroptotic MM1R cells, hinting that a larger CAMK-signaling network may be involved in ferroptosis signaling. Again, these observations are in line with the aforementioned genetic-based kinase screen, which also revealed CAMK2A to be one of the most crucial ferroptosis-dependent kinases [29]. However, results from the genetic-based screen also identified ATM and ATR as key ferroptosis regulators. Our phosphopeptidome screening did also point towards a RSL3-mediated inhibition of ATR, although this inhibition was found not to be biologically relevant as the threshold of mean kinase score ≥ 1.3 was not reached (0.55). Similarly, we did not find a strong association between RSL3-induced ferroptosis and AMPK activity (0.24) although this kinase has been previously been associated with ferroptotic cell death [28]. These discrepancies can partly be explained by differences in experimental setup, as various cell lines, ferroptosis inducers, and treatment times have been used throughout the listed studies. As kinase expression and kinase-phosphatase interplay is highly dependent on cellular context, repeating the current study in other (MM) cell lines or tissues with similar experimental conditions is therefore vital to further determine which kinase are truly essential for RSL3-mediated ferroptosis. Furthermore, the predicted kinome activity profiles identified here should be further experimentally validated by means of Western blotting, phosphoproteomics, NanoBRET kinase assays, and silencing approaches to further support their biological relevance.

To preliminary determine whether the obtained ferroptosis and apoptosis kinome activity profiles can be applied to predict therapeutic efficacy and/or characterize cell death properties of novel anti-cancer agents, we also treated MM1R cells with WA, a compound reported to inhibit several PKs (reviewed in [70]). Remarkably, WA is able to trigger different pro-apoptotic and pro-ferroptotic signaling pathways in a dose- and cell context-dependent manner [41, 71-74]. We found that these promiscuous anti-cancer properties of WA were also mirrored in its differential phosphopeptidome and kinome activity profile, which portrayed similarities to both the apoptosis and ferroptosis signatures. Functional enrichment and UPK analysis showed that the top WA-inhibited kinases mostly overlapped with RSL3-targeted kinases and that these were also enriched in regulation of BCR signaling. However, phylogenetic tree visualization also demonstrated that, like STS, WA is able to target a broad range of ACG kinases, including PKCη, PKCε, PKCγ, p70S6K, and SGK2. These results are in agreement with previous studies reporting WA-mediated inhibition of BCR-related kinases [10], PKC kinases [75], and p70S6K [76]. WA also targets a subset of kinases,

including IKK, that are not affected by STS or RSL3 treatment, revealing that WA also has unique inhibitor effects on kinase signaling in MM. This might explain why, despite its similarities with RSL3, WA triggers apoptosis and not ferroptosis in MM1R cells, as indicated by cell viability, Western blot, and lipid peroxidation analysis. For example, inhibition of IKK by WA in DLBCL is described to promote apoptosis [77] and might favor the WA-triggered cell death modality in MM1R cells towards apoptotic cell death. Likewise, WA-mediated targeting of non-kinase signaling pathways, such as proteasome degradation and unfolded protein stress responses [78, 79], might further impact cell death faith. Alternatively, the occurrence of lipid peroxidation might be crucial for some of the ferroptosis-driven promiscuous inhibitory effects observed in MM1R cells. Lipid peroxidation directly impacts the cellular redox status and can, in turn, inhibit tyrosine kinases by (reversible) cysteine oxidation [80-82]. Thus, although both WA and RSL3 possess chemical moieties that can interact with proteins harboring nucleophilic active sites, including (seleno)cysteine sites [10, 37], lipid peroxidation does not take place in WA-treated cells and might be the main explanation why apoptosis, rather than ferroptosis, is the main WA cell death modality in MM cells.

In conclusion, ferroptosis and apoptosis inducers both elicit a broad spectrum PK inhibitor signaling profile in MM1R cells. Although both cell death modalities display similarities in their inhibitory kinome activity profile, unique signatures in PK targeting could also be detected. These unique peptide-based kinase activity profiles might aid in identifying novel (ferroptosis-based) kinase targets in MM treatment or might help stratification of other apoptosis or ferroptosis sensitizing anti-cancer compounds. Moreover, multi-targeting of apoptosis- and ferroptosis-specific kinases might prove to be more efficient in treating multifactorial (therapy-resistant) diseases, such as cancer.

4.4. **Materials and Methods**

4.4.1. **Cell Culture and Cell Viability Assays**
Human MM1R cells (CRL-2975) were purchased from ATCC and grown in RPMI-1640 medium supplemented with 10% FBS (E.U Approved; South American Origin) and 1% Pen-Strep solution (Invitrogen, Carlsbad, CA, USA) at 37°C in 5% CO_2. Cell viability was measured with the colorimetric 3-(4, 5-dimethylthiozol-2-yl)-2, 5-diphenyltetrazolium bromide (MTT) assay (Sigma Aldrich, St. Louis, MO, US) as previously described [83].

4.4.2. **Antibodies and Reagents**
STS and RSL3 were purchased from Selleckchem (Houston, USA), dissolved in DMSO and stored as 50 mM stocks at -20°C. Antibodies targeting cleaved PARP-1 (sc-7150) and GAPDH (2118S) were obtained from Santa Cruz Biotechnology (Dallas, TX, USA) and Cell Signaling Technology (Danvers, MA, USA), respectively.

4.4.3. **Lipid Peroxidation Assay**
Cellular lipid reactive oxygen species were measured using the Image-iT™ Lipid Peroxidation Kit (C10445, ThermoFisher Scientific, Waltham, MA, USA) according to the

manufacturer's protocol. In short, cells were seeded in 6 well plates at a density of 5 x 10^5 cells/well and treated the next day with 5µM RSL3 (with or without pre-treatment with 2 µM Fer-1) or 100µM cumene hydroperoxide (positive control). Cells were subsequently incubated for 30 min with 10µM Image-iT™ Lipid Peroxidation Sensor at 37 °C. After incubation, cells were collected by trypsinization with TrypLE Express Enzyme (ThermoFisher Scientific, Waltham, MA, USA). Cells were washed 3 times with pre-warmed PBS and fluorescence shift from 590 nm to 510 nm was measured with the CytoFlex flow cytometer (Beckman Coulter Life Sciences, Indianapolis, IN, USA). Finally, the 510/590 ratio was calculated and visualized as a % of lipid peroxide positive cells.

4.4.4. Protein Extraction and Western blot Analysis

Cellular protein extraction occurred by resuspending cell pellets in 0.5 mL RIPA buffer (150 mM NaCl, 0.1% Triton X-100, 1% SDS, 50 mM Tris-HCl pH 8) supplemented with PhosphataseArrest (G-Biosciences, Saint-Louis, MO, USA) and protease inhibitors (Complete Mini®, Roche). After 15 min incubation on ice with regular vortexing, samples were briefly sonicated (1 min, amplitude 30 kHz, pulse 1s) and centrifuged at 13 200 rpm for 20 min at 4°C. Solubilized proteins were transferred to new Eppendorf tubes and stored at -20 °C. Protein lysates were separated using Bis-Tris SDS-PAGE with a high-MW MOPS running buffer, and transferred onto nitrocellulose membranes (Hybond C, Amersham) using the Power Blotter System (Thermofisher, MA, USA). Blocking the membranes for 1 hour with blocking buffer (20 mM Tris-HCl, 140 mM NaCl, 5% BSA, pH 7,5) at RT was followed by overnight incubation with the primary antibody at 4°C. Blots were then incubated for 1 hr with the secondary, HRP dye-conjugated antibody (Dako, Glostrup, Denmark) after which chemiluminescent signals were detected with the Amersham Imager 680 (Cytiva, MA, USA) and quantified with the ImageJ software (v1.53j) [84].

4.4.5. Kinase Activity Profiling using PamChip® Peptide Microarrays

Kinase activity profiling was performed as previously described [10]. In short, MM1R cells were treated with 1 µM STS or 5 µM RSL3 for increasing time periods (*n* = 3 biologically independent samples per time point) and lysed in M-PER lysis buffer (Mammalian Extraction Buffer) containing 1:100 Halt protease and phosphatase inhibitor cocktail (78440, Thermofisher, MA, USA). Protein yield was determined using the Pierce™ BCA Protein Assay method (23225, Thermo Scientific) [85]. Tyrosine and serine-/threonine kinase profiles were determined by employing the PamChip® peptide microarray system (Pamgene, BJ' s-Hertogenbosch, The Netherlands) according to the manufacturer's instructions. UPK analysis was automatically performed by the BioNavigator Analysis software tool (Pamgene) based on the tyrosine and serine/threonine kinase phosphorylation patterns. Each predicted kinases is scored with a mean kinase statistic, a specificity score and a mean final score. The mean kinase statistic score depicts the effect size (values) and direction (+ or -) between the group difference, while the specificity score indicates the specificity of the normalized kinase statistics with respect to the amount of peptides used for predicting the corresponding kinase. The mean final score is typically

used to generate the ranked predictive list of kinases and is a combination of the specificity score and the group difference.

Kinase interaction networks and phylogenetic trees were generated using the String database (v11) [39] and the KinMap web-based tool [38], respectively. These visualizations were performed with all kinases with a mean final score of ≥ 1.3, as recommended by Pamgene. Functional enrichment analysis was performed with Metascape using the default settings [40].

4.4.6. Statistical Analysis

Statistical tests were performed in GraphPad Prism (v7.0) (GraphPad Software, San Diego, CA, USA) unless otherwise stated in the main text. Results were considered to be statistically significant when p-values < 0.05 were obtained.

4.5. Supplementary Material
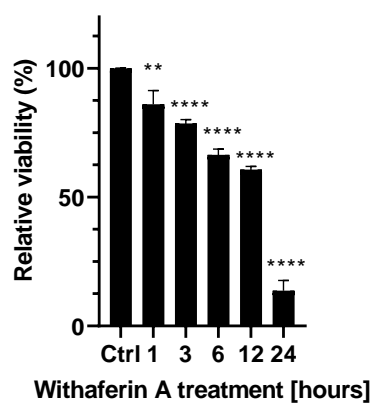
Figure S1: Relative cell viability (%) of MM1R cells treated with 1 µM WA. Data are presented as the mean ± s.d., *n*=3 biologically independent samples per treatment (**p < 0.01, ****p < 0.0001, ANOVA).
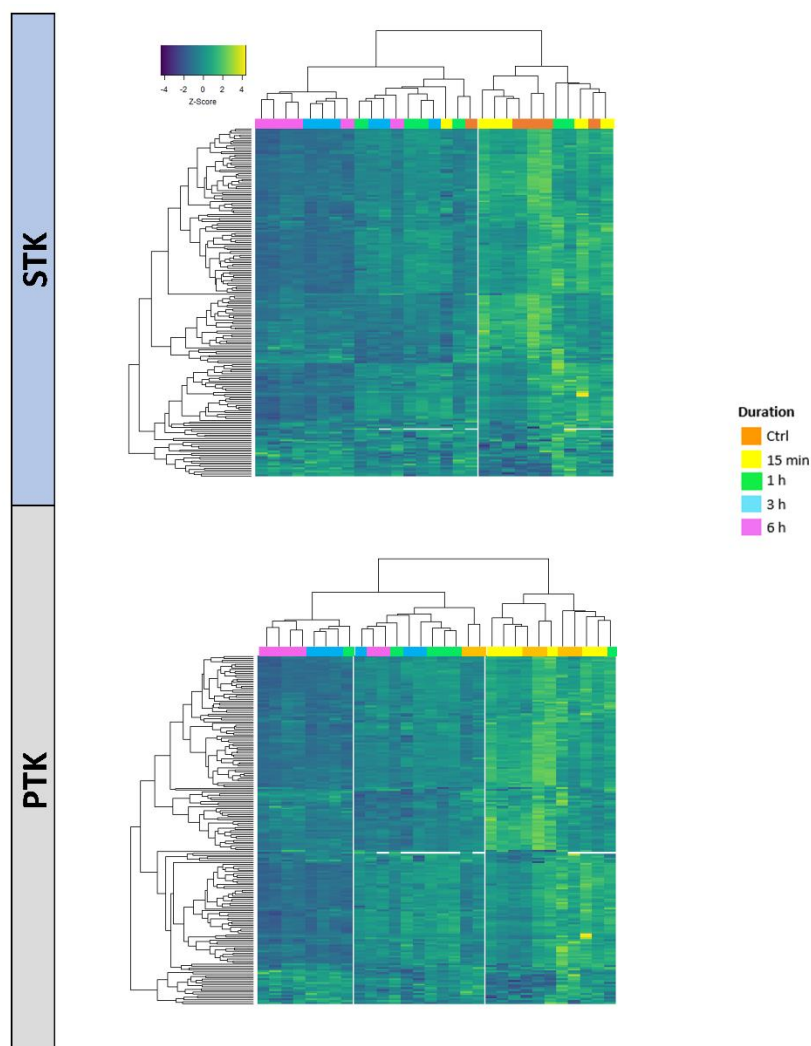
Figure S2: Heatmap visualization of individual phosphorylation intensities, represented as normalized z-scores, of peptides on serine/threonine kinase (STK) (upper panel) or tyrosine kinase (PTK) (lower panel) chips which serve as

substrates for serine/threonine or tyrosine kinases, respectively. Higher z-scores (yellow) indicate kinase activation while lower z-scores (dark blue) indicate kinase inhibition. MM1R cells were treated with 1 µM WA for increasing timepoints, as indicated by the figure legend.
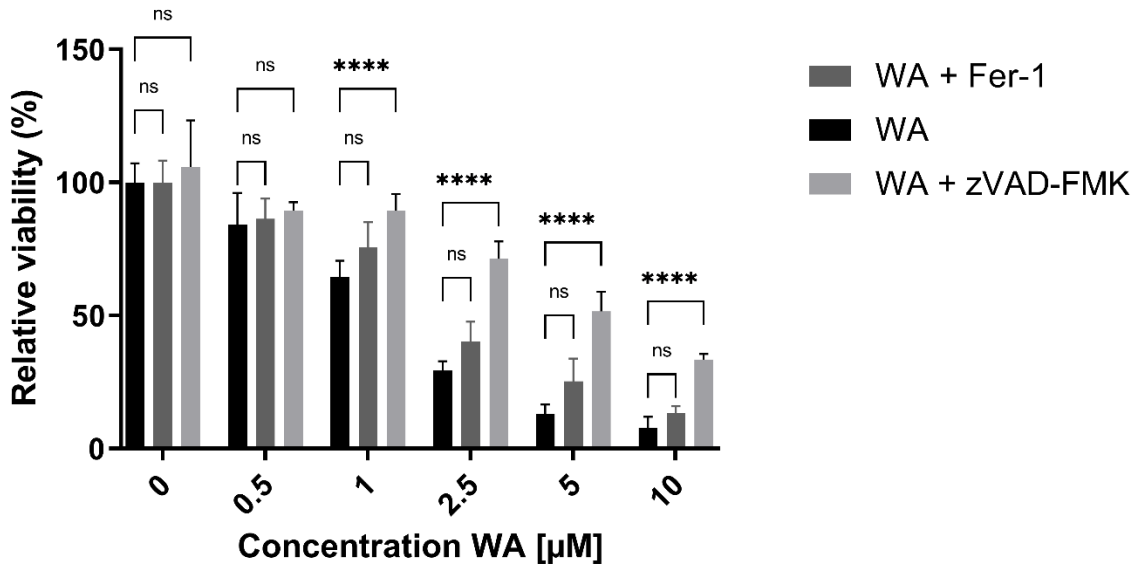
Figure S3: Relative cell viability (%) of MM1R cells treated with 1 µM WA for 24 hours with or without 2 hour pre-treatment with 2 µM ferrostatin-1 (Fer-1) or 50 µM zVAD-FMK. Data are presented as the mean ± s.d., *n*=3 biologically independent samples per treatment (ns p > 0.05, ****p < 0.0001, ANOVA).
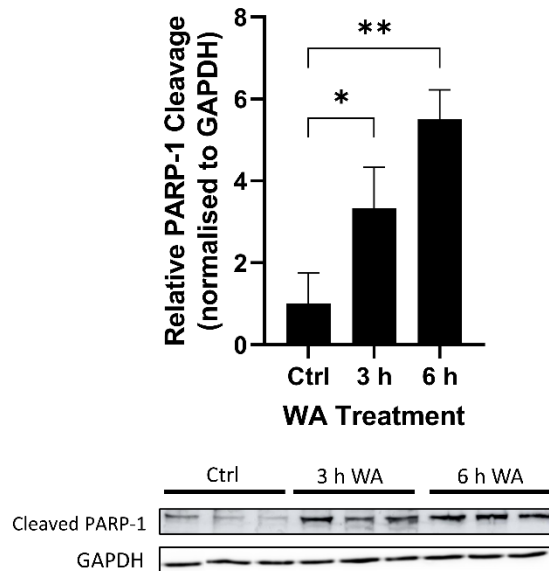
Figure S4: Western blot detection and quantification of PARP-1 cleavage and GAPDH expression levels in MM1R cells treated with 1 µM Withaferin a (WA) for 3 and 6 hrs. All data are presented as the mean ± s.d., *n*=3 biologically independent samples per treatment (*p < 0.05, **p < 0.01, ANOVA).

4.6. References

1. Towler MC, Hardie DG. AMP-activated protein kinase in metabolic control and insulin signaling. Circ Res. 2007;100(3):328-41.
2. Beharry Z, Mahajan S, Zemskova M, Lin YW, Tholanikunnel BG, Xia Z, Smith CD, Kraft AS. The Pim protein kinases regulate energy metabolism and cell growth. Proc Natl Acad Sci U S A. 2011;108(2):528-33.
3. Malumbres M. Cyclin-dependent kinases. Genome Biol. 2014;15(6):122.
4. Black AR, Black JD. Protein kinase C signaling and cell cycle regulation. Front Immunol. 2012;3:423.
5. Yu FX, Zhang Y, Park HW, Jewell JL, Chen Q, Deng Y, Pan D, Taylor SS, Lai ZC, Guan KL. Protein kinase A activates the Hippo pathway to modulate cell proliferation and differentiation. Genes Dev. 2013;27(11):1223-32.
6. Kinehara M, Kawamura S, Tateyama D, Suga M, Matsumura H, Mimura S, Hirayama N, Hirata M, Uchio-Yamada K, Kohara A, et al. Protein kinase C regulates human pluripotent stem cell self-renewal. PLoS One. 2013;8(1):e54122.
7. Wada T, Penninger JM. Mitogen-activated protein kinases in apoptosis regulation. Oncogene. 2004;23(16):2838-49.
8. Declercq W, Vanden Berghe T, Vandenabeele P. RIP kinases at the crossroads of cell death and survival. Cell. 2009;138(2):229-32.
9. Singh P, Ravanan P, Talwar P. Death Associated Protein Kinase 1 (DAPK1): A Regulator of Apoptosis and Autophagy. Front Mol Neurosci. 2016;9:46.
10. Logie E, Chirumamilla CS, Perez-Novo C, Shaw P, Declerck K, Palagani A, Rangarajan S, Cuypers B, De Neuter N, Mobashar Hussain Urf Turabe F, et al. Covalent Cysteine Targeting of Bruton's Tyrosine Kinase (BTK) Family by Withaferin-A Reduces Survival of Glucocorticoid-Resistant Multiple Myeloma MM1 Cells. Cancers (Basel). 2021;13(7).
11. Wang L, Lin N, Li Y. The PI3K/AKT signaling pathway regulates ABCG2 expression and confers resistance to chemotherapy in human multiple myeloma. Oncol Rep. 2019;41(3):1678-90.
12. Liu R, Chen Y, Liu G, Li C, Song Y, Cao Z, Li W, Hu J, Lu C, Liu Y. PI3K/AKT pathway as a key link modulates the multidrug resistance of cancers. Cell Death Dis. 2020;11(9):797.
13. Shain KH, Tao J. The B-cell receptor orchestrates environment-mediated lymphoma survival and drug resistance in B-cell malignancies. Oncogene. 2014;33(32):4107-13.
14. de Boussac H, Bruyer A, Jourdan M, Maes A, Robert N, Gourzones C, Vincent L, Seckinger A, Cartron G, Hose D, et al. Kinome expression profiling to target new therapeutic avenues in multiple myeloma. Haematologica. 2020;105(3):784-95.
15. Richardson PG, Bensinger WI, Huff CA, Costello CL, Lendvai N, Berdeja JG, Anderson LD, Jr., Siegel DS, Lebovic D, Jagannath S, et al. Ibrutinib alone or with dexamethasone for relapsed or relapsed and refractory multiple myeloma: phase 2 trial results. Br J Haematol. 2018;180(6):821-30.
16. Kannaiyan R, Mahadevan D. A comprehensive review of protein kinase inhibitors for cancer therapy. Expert Rev Anticancer Ther. 2018;18(12):1249-70.
17. Roskoski R, Jr. Properties of FDA-approved small molecule protein kinase inhibitors: A 2021 update. Pharmacol Res. 2021;165:105463.
18. Lind J, Czernilofsky F, Vallet S, Podar K. Emerging protein kinase inhibitors for the treatment of multiple myeloma. Expert Opin Emerg Drugs. 2019;24(3):133-52.
19. Dixon SJ, Lemberg KM, Lamprecht MR, Skouta R, Zaitsev EM, Gleason CE, Patel DN, Bauer AJ, Cantley AM, Yang WS, et al. Ferroptosis: an iron-dependent form of nonapoptotic cell death. Cell. 2012;149(5):1060-72.
20. Bebber CM, Muller F, Prieto Clemente L, Weber J, von Karstedt S. Ferroptosis in Cancer Cell Biology. Cancers (Basel). 2020;12(1).
21. Poltorack CD, Dixon SJ. Understanding the role of cysteine in ferroptosis: progress & paradoxes. FEBS J. 2021.

143

22. Yang WS, Kim KJ, Gaschler MM, Patel M, Shchepinov MS, Stockwell BR. Peroxidation of polyunsaturated fatty acids by lipoxygenases drives ferroptosis. Proc Natl Acad Sci U S A. 2016;113(34):E4966-75.

23. Dixon SJ, Stockwell BR. The role of iron and reactive oxygen species in cell death. Nat Chem Biol. 2014;10(1):9-17.

24. Torti SV, Torti FM. Iron and Cancer: 2020 Vision. Cancer Res. 2020;80(24):5435-48.

25. Combs JA, DeNicola GM. The Non-Essential Amino Acid Cysteine Becomes Essential for Tumor Proliferation and Survival. Cancers (Basel). 2019;11(5).

26. Fang J, Seki T, Maeda H. Therapeutic strategies by modulating oxygen stress in cancer and inflammation. Adv Drug Deliv Rev. 2009;61(4):290-302.

27. Hassannia B, Vandenabeele P, Vanden Berghe T. Targeting Ferroptosis to Iron Out Cancer. Cancer Cell. 2019;35(6):830-49.

28. Lee H, Zandkarimi F, Zhang Y, Meena JK, Kim J, Zhuang L, Tyagi S, Ma L, Westbrook TF, Steinberg GR, et al. Energy-stress-mediated AMPK activation inhibits ferroptosis. Nat Cell Biol. 2020;22(2):225-34.

29. Chen PH, Wu J, Ding CC, Lin CC, Pan S, Bossa N, Xu Y, Yang WH, Mathey-Prevot B, Chi JT. Kinome screen of ferroptosis reveals a novel role of ATM in regulating iron metabolism. Cell Death Differ. 2020;27(3):1008-22.

30. Lachaier E, Louandre C, Godin C, Saidak Z, Baert M, Diouf M, Chauffert B, Galmiche A. Sorafenib induces ferroptosis in human cancer cell lines originating from different solid tumors. Anticancer Res. 2014;34(11):6417-22.

31. Bahlis NJ, Miao Y, Koc ON, Lee K, Boise LH, Gerson SL. N-benzoylstaurosporine (PKC412) inhibits Akt kinase inducing apoptosis in multiple myeloma cells. Leuk Lymphoma. 2005;46(6):899-908.

32. Yuan CX, Zhou ZW, Yang YX, He ZX, Zhang X, Wang D, Yang T, Wang NJ, Zhao RJ, Zhou SF. Inhibition of mitotic Aurora kinase A by alisertib induces apoptosis and autophagy of human gastric cancer AGS and NCI-N78 cells. Drug Des Devel Ther. 2015;9:487-508.

33. Zekri A, Ghaffari SH, Yaghmaie M, Estiar MA, Alimoghaddam K, Modarressi MH, Ghavamzadeh A. Inhibitor of Aurora Kinase B Induces Differentially Cell Death and Polyploidy via DNA Damage Response Pathways in Neurological Malignancy: Shedding New Light on the Challenge of Resistance to AZD1152-HQPA. Mol Neurobiol. 2016;53(3):1808-23.

34. Geering B. Death-associated protein kinase 2: Regulator of apoptosis, autophagy and inflammation. Int J Biochem Cell Biol. 2015;65:151-4.

35. Kake S, Usui T, Ohama T, Yamawaki H, Sato K. Death-associated protein kinase 3 controls the tumor progression of A549 cells through ERK MAPK/c-Myc signaling. Oncol Rep. 2017;37(2):1100-6.

36. Hong SH, Lee DH, Lee YS, Jo MJ, Jeong YA, Kwon WT, Choudry HA, Bartlett DL, Lee YJ. Molecular crosstalk between ferroptosis and apoptosis: emerging role of ER stress-induced p53-independent PUMA expression. Oncotarget. 2017;8(70):115164-78.

37. Yang WS, SriRamaratnam R, Welsch ME, Shimada K, Skouta R, Viswanathan VS, Cheah JH, Clemons PA, Shamji AF, Clish CB, et al. Regulation of ferroptotic cancer cell death by GPX4. Cell. 2014;156(1-2):317-31.

38. Eid S, Turk S, Volkamer A, Rippmann F, Fulle S. KinMap: a web-based tool for interactive navigation through human kinome data. BMC Bioinformatics. 2017;18(1):16.

39. Szklarczyk D, Franceschini A, Wyder S, Forslund K, Heller D, Huerta-Cepas J, Simonovic M, Roth A, Santos A, Tsafou KP, et al. STRING v10: protein-protein interaction networks, integrated over the tree of life. Nucleic Acids Res. 2015;43(Database issue):D447-52.

40. Zhou Y, Zhou B, Pache L, Chang M, Khodabakhshi AH, Tanaseichuk O, Benner C, Chanda SK. Metascape provides a biologist-oriented resource for the analysis of systems-level datasets. Nat Commun. 2019;10(1):1523.

41. Hassannia B, Wiernicki B, Ingold I, Qu F, Van Herck S, Tyurina YY, Bayir H, Abhari BA, Angeli JPF, Choi SM, et al. Nano-targeted induction of dual ferroptotic mechanisms eradicates high-risk neuroblastoma. J Clin Invest. 2018;128(8):3341-55.

42. Hassannia B, Logie E, Vandenabeele P, Vanden Berghe T, Vanden Berghe W. Withaferin A: From ayurvedic folk medicine to preclinical anti-cancer drug. Biochem Pharmacol. 2020;173:113602.

43. Heyninck K, Lahtela-Kakkonen M, Van der Veken P, Haegeman G, Vanden Berghe W. Withaferin A inhibits NF-kappaB activation by targeting cysteine 179 in IKKbeta. Biochem Pharmacol. 2014;91(4):501-9.

44. Yang H, Wang Y, Cheryan VT, Wu W, Cui CQ, Polin LA, Pass HI, Dou QP, Rishi AK, Wali A. Withaferin A inhibits the proteasome activity in mesothelioma in vitro and in vivo. PLoS One. 2012;7(8):e41214.

45. Yu Y, Hamza A, Zhang T, Gu M, Zou P, Newman B, Li Y, Gunatilaka AA, Zhan CG, Sun D. Withaferin A targets heat shock protein 90 in pancreatic cancer cells. Biochem Pharmacol. 2010;79(4):542-51.

46. Abramson HN. Kinase inhibitors as potential agents in the treatment of multiple myeloma. Oncotarget. 2016;7(49):81926-68.

47. John L, Krauth MT, Podar K, Raab MS. Pathway-Directed Therapy in Multiple Myeloma. Cancers (Basel). 2021;13(7).

48. Chong PSY, Chng WJ, de Mel S. STAT3: A Promising Therapeutic Target in Multiple Myeloma. Cancers (Basel). 2019;11(5).

49. Keane NA, Glavey SV, Krawczyk J, O'Dwyer M. AKT as a therapeutic target in multiple myeloma. Expert Opin Ther Targets. 2014;18(8):897-915.

50. Von Suskil M, Sultana KN, Elbezanti WO, Al-Odat OS, Chitren R, Tiwari AK, Challagundla KB, Srivastava SK, Jonnalagadda SC, Budak-Alpdogan T, et al. Bruton's Tyrosine Kinase Targeting in Multiple Myeloma. Int J Mol Sci. 2021;22(11).

51. Young RM, Phelan JD, Wilson WH, Staudt LM. Pathogenic B-cell receptor signaling in lymphoid malignancies: New insights to improve treatment. Immunol Rev. 2019;291(1):190-213.

52. Su L, David M. Inhibition of B cell receptor-mediated apoptosis by IFN. J Immunol. 1999;162(11):6317-21.

53. Mouhamad S, Besnault L, Auffredou MT, Leprince C, Bourgeade MF, Leca G, Vazquez A. B cell receptor-mediated apoptosis of human lymphocytes is associated with a new regulatory pathway of Bim isoform expression. J Immunol. 2004;172(4):2084-91.

54. Wiestner A. The role of B-cell receptor inhibitors in the treatment of patients with chronic lymphocytic leukemia. Haematologica. 2015;100(12):1495-507.

55. Rushworth SA, Bowles KM, Barrera LN, Murray MY, Zaitseva L, MacEwan DJ. BTK inhibitor ibrutinib is cytotoxic to myeloma and potently enhances bortezomib and lenalidomide activities through NF-kappaB. Cell Signal. 2013;25(1):106-12.

56. Takada Y, Aggarwal BB. TNF activates Syk protein tyrosine kinase leading to TNF-induced MAPK activation, NF-kappaB activation, and apoptosis. J Immunol. 2004;173(2):1066-77.

57. Wang S, Ma Y, Wang X, Jiang J, Zhang C, Wang X, Jiang Y, Huang H, Hong L. IL-17A Increases Multiple Myeloma Cell Viability by Positively Regulating Syk Expression. Transl Oncol. 2019;12(8):1086-91.

58. Xu M, Tao J, Yang Y, Tan S, Liu H, Jiang J, Zheng F, Wu B. Ferroptosis involves in intestinal epithelial cell death in ulcerative colitis. Cell Death Dis. 2020;11(2):86.

59. Wilhelm SM, Adnane L, Newell P, Villanueva A, Llovet JM, Lynch M. Preclinical overview of sorafenib, a multikinase inhibitor that targets both Raf and VEGF and PDGF receptor tyrosine kinase signaling. Mol Cancer Ther. 2008;7(10):3129-40.

60. Iyer R, Fetterly G, Lugade A, Thanavala Y. Sorafenib: a clinical and pharmacologic review. Expert Opin Pharmacother. 2010;11(11):1943-55.

61. Sun X, Niu X, Chen R, He W, Chen D, Kang R, Tang D. Metallothionein-1G facilitates sorafenib resistance through inhibition of ferroptosis. Hepatology. 2016;64(2):488-500.

62. Sun X, Ou Z, Chen R, Niu X, Chen D, Kang R, Tang D. Activation of the p62-Keap1-NRF2 pathway protects against ferroptosis in hepatocellular carcinoma cells. Hepatology. 2016;63(1):173-84.

63. Ho CL, Hsu LF, Phyliky RL, Li CY. Autocrine expression of platelet-derived growth factor B in B cell chronic lymphocytic leukemia. Acta Haematol. 2005;114(3):133-40.

64. Bilalis A, Pouliou E, Roussou M, Papanikolaou A, Tassidou A, Economopoulos T, Terpos E. Increased expression of platelet derived growth factor receptor beta on trephine biopsies correlates with advanced myeloma. J BUON. 2017;22(4):1032-7.

65. Lawrie AM, Noble ME, Tunnah P, Brown NR, Johnson LN, Endicott JA. Protein kinase inhibition by staurosporine revealed in details of the molecular interaction with CDK2. Nat Struct Biol. 1997;4(10):796-801.

66. Shi H, Cheng X, Sze SK, Yao SQ. Proteome profiling reveals potential cellular targets of staurosporine using a clickable cell-permeable probe. Chem Commun (Camb). 2011;47(40):11306-8.

67. Fischer JJ, Graebner Baessler OY, Dalhoff C, Michaelis S, Schrey AK, Ungewiss J, Andrich K, Jeske D, Kroll F, Glinski M, et al. Comprehensive identification of staurosporine-binding kinases in the hepatocyte cell line HepG2 using Capture Compound Mass Spectrometry (CCMS). J Proteome Res. 2010;9(2):806-17.

68. Wang S, Yi X, Wu Z, Guo S, Dai W, Wang H, Shi Q, Zeng K, Guo W, Li C. CAMKK2 defines ferroptosis sensitivity of melanoma cells by regulating AMPK-Nrf2 pathway. J Invest Dermatol. 2021.

69. Kumar N, Perez-Novo C, Shaw P, Logie E, Privat-Maldonado A, Dewilde S, Smits E, Berghe WV, Bogaerts A. Physical plasma-derived oxidants sensitize pancreatic cancer cells to ferroptotic cell death. Free Radic Biol Med. 2021;166:187-200.

70. Chirumamilla CS, Perez-Novo C, Van Ostade X, Vanden Berghe W. Molecular insights into cancer therapeutic effects of the dietary medicinal phytochemical Withaferin A. Proc Nutr Soc. 2017;76(2):96-105.

71. Mayola E, Gallerne C, Esposti DD, Martel C, Pervaiz S, Larue L, Debuire B, Lemoine A, Brenner C, Lemaire C. Withaferin A induces apoptosis in human melanoma cells through generation of reactive oxygen species and down-regulation of Bcl-2. Apoptosis. 2011;16(10):1014-27.

72. Stan SD, Hahm ER, Warin R, Singh SV. Withaferin A causes FOXO3a- and Bim-dependent apoptosis and inhibits growth of human breast cancer cells in vivo. Cancer Res. 2008;68(18):7661-9.

73. Hahm ER, Moura MB, Kelley EE, Van Houten B, Shiva S, Singh SV. Withaferin A-induced apoptosis in human breast cancer cells is mediated by reactive oxygen species. PLoS One. 2011;6(8):e23354.

74. Sanchez-Martin M, Ambesi-Impiombato A, Qin Y, Herranz D, Bansal M, Girardi T, Paietta E, Tallman MS, Rowe JM, De Keersmaecker K, et al. Synergistic antileukemic therapies in NOTCH1-induced T-ALL. Proc Natl Acad Sci U S A. 2017;114(8):2006-11.

75. Sen N, Banerjee B, Das BB, Ganguly A, Sen T, Pramanik S, Mukhopadhyay S, Majumder HK. Apoptosis is induced in leishmanial cells by a novel protein kinase inhibitor Withaferin A and is facilitated by apoptotic topoisomerase I-DNA complex. Cell Death Differ. 2007;14(2):358-67.

76. Guo B, Liu J, Wang B, Zhang C, Su Z, Zhao M, Zheng R. Withaferin A promotes white adipose browning and prevents obesity through sympathetic nerve-activated Prdm16-FATP1 axis. bioRxiv. 2021:2021.02.25.432705.

77. Jackson SS, Oberley C, Hooper CP, Grindle K, Wuerzberger-Davis S, Wolff J, McCool K, Rui L, Miyamoto S. Withaferin A disrupts ubiquitin-based NEMO reorganization induced by canonical NF-kappaB signaling. Exp Cell Res. 2015;331(1):58-72.

78. Dom M, Offner F, Vanden Berghe W, Van Ostade X. Proteomic characterization of Withaferin A-targeted protein networks for the treatment of monoclonal myeloma gammopathies. J Proteomics. 2018;179:17-29.

79. Issa ME, Cuendet M. Withaferin A induces cell death and differentiation in multiple myeloma cancer stem cells. Medchemcomm. 2017;8(1):112-21.

80. Kemble DJ, Sun G. Direct and specific inactivation of protein tyrosine kinases in the Src and FGFR families by reversible cysteine oxidation. Proc Natl Acad Sci U S A. 2009;106(13):5070-5.

81. Paulsen CE, Carroll KS. Orchestrating redox signaling networks through regulatory cysteine switches. ACS Chem Biol. 2010;5(1):47-62.

82. Fowler NJ, Blanford CF, de Visser SP, Warwicker J. Features of reactive cysteines discovered through computation: from kinase inhibition to enrichment around protein degrons. Sci Rep. 2017;7(1):16338.

83. Palagani A, Op de Beeck K, Naulaerts S, Diddens J, Sekhar Chirumamilla C, Van Camp G, Laukens K, Heyninck K, Gerlo S, Mestdagh P, et al. Ectopic microRNA-150-5p transcription sensitizes glucocorticoid therapy response in MM1S multiple myeloma cells but fails to overcome hormone therapy resistance in MM1R cells. PLoS One. 2014;9(12):e113842.

84. Rueden CT, Schindelin J, Hiner MC, DeZonia BE, Walter AE, Arena ET, Eliceiri KW. ImageJ2: ImageJ for the next generation of scientific image data. BMC Bioinformatics. 2017;18(1):529.

85. Smith PK, Krohn RI, Hermanson GT, Mallia AK, Gartner FH, Provenzano MD, Fujimoto EK, Goeke NM, Olson BJ, Klenk DC. Measurement of protein using bicinchoninic acid. Anal Biochem. 1985;150(1):76-85.

CHAPTER 5

Ferroptosis Induction in Multiple Myeloma Cells Triggers DNA Methylation and Histone Modification Changes Associated with Cellular Senescence

Chapter 5

Ferroptosis Induction in Multiple Myeloma Cells Triggers DNA Methylation and Histone Modification Changes Associated with Cellular Senescence

Emilie Logie[1], Bart Van Puyvelde[2], Bart Cuypers[3], Anne Schepers[4], Jelle Verdonck[5], Kris Laukens[3],Guy Van Camp[4], Lode Godderis[5,6], Dieter Deforce[2], Maarten Dhaenens[2], Wim Vanden Berghe[1]*

1. Laboratory of Protein Science, Proteomics and Epigenetic Signaling (PPES) and Integrated Personalized and Precision Oncology Network (IPPON), Department of Biomedical Sciences, University of Antwerp, Campus Drie Eiken, Universiteitsplein 1, Wilrijk, Belgium
2. Laboratory of Pharmaceutical Biotechnology, Proteomics and Mass Spectrometry Department, Ghent University, Ghent, Belgium
3. Biomedical Informatics Network Antwerp (Biomina), Department of Computer Science, University of Antwerp, Wilrijk, Belgium
4. Center of Medical Genetics, University of Antwerp & Antwerp University Hospital, Edegem, Belgium
5. Center for Environment and Health, Department of Public Health and Primary Care, KU Leuven, Leuven, Belgium
6. IDEWE, External Service for Prevention and Protection at Work, Heverlee, Belgium

* Corresponding author: wim.vandenberghe@uantwerpen.be

Conflict of Interest: The authors declare no conflict of interest.

Abstract

Disease relapse and therapy resistance remain key challenges in treating multiple myeloma. Underlying (epi-)mutational events can promote myelomagenesis and contribute to multi-drug and apoptosis resistance. Therefore, compounds inducing ferroptosis, a form of iron and lipid peroxidation regulated cell death, are appealing alternative treatment strategies for multiple myeloma and other malignancies. Both ferroptosis and the epigenetic machinery are heavily influenced by reactive oxygen species (ROS) and iron metabolism changes. Yet, only a limited number of epigenetic enzymes and modifications have been identified as ferroptosis regulators. In this study, we found that MM1 multiple myeloma cells are sensitive to ferroptosis induction and epigenetic reprogramming by RSL3-mediated inhibition of glutathione peroxidase 4 (GPX4), irrespective of their glucocorticoid-sensitivity status. LC-MS/MS analysis revealed the formation of non-heme iron-histone complexes and altered expression of histone modifications associated with DNA repair and cellular senescence. In line with this observation, EPIC BeadChip measurements of significant DNA methylation changes in ferroptotic myeloma cells demonstrated an enrichment of CpG probes located in genes associated with cell cycle progression and senescence, such as NR4A2. Overall, our data show that ferroptotic cell death is associated with an epigenomic stress response that might advance the therapeutic applicability of ferroptotic compounds.

Keywords: Ferroptosis; multiple myeloma; DNA methylation; iron; histone post-translational modifications; epigenome; RSL3
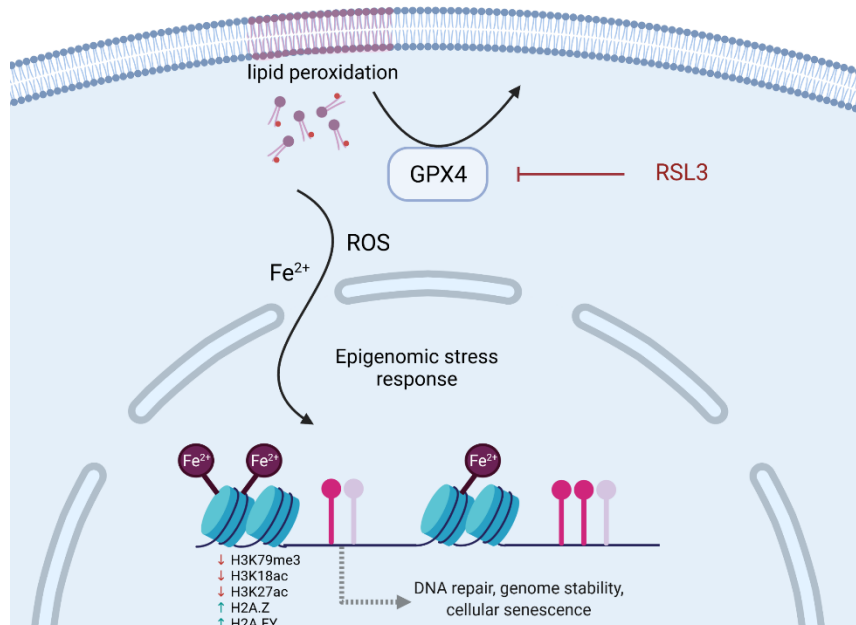
5.1. Introduction

Multiple myeloma (MM) is an incurable adult blood cancer characterized by uncontrolled growth of plasma cells within the bone marrow. More than 30.000 adults are diagnosed with MM every year, making it the second most common hematological malignancy after non-Hodgkin lymphoma [1]. Although therapeutic advancements over the last few decades have significantly improved the prognosis and progression-free survival of MM patients [2], the high-relapse rate remains a major challenge to improve treatment outcome. In most cases, the disease is characterized by a repeating pattern of remission and relapse periods during which patients receive multiple different treatment regimens, ultimately resulting in complete treatment failure. The need for finding alternative therapeutic strategies to overcome (acquired and primary) therapy resistance therefore remains a pressing matter. Myelomagenesis is frequently promoted by primary and secondary (epi)mutational events. Besides the well catalogued genetic alterations, including chromosomal translocations and hyperdiploidy, epigenetic aberrations, such as changes in DNA methylation [3, 4], histone modifications [5, 6], and abnormal microRNA (miRNA) expression [7, 8] have been linked to MM pathogenesis. Interestingly, several studies have shown that epigenetic alterations can mediate drug resistance [9-11] and that rewriting the abnormal epigenetic code in MM, i.e. by epigenetic drugs, might offer novel therapeutic options [12, 13]. Epigenetic compounds, including decitabine, 5-aza-2'-cytidine, and vorinostat have indeed demonstrated potent anti-myeloma activity [14-16].

Ferroptosis is a form of regulated cell death (RCD) that is currently being explored as a therapeutic strategy for treatment of malignant tumors, including B-cell malignancies [17-19]. In contrast to other modes of RCD, such as apoptosis, ferroptosis relies on intracellular increases in free iron levels and lipid peroxidation to promote cell death [20]. Given that most tumors already exhibit high basal oxidative stress levels and an altered iron metabolism due to their increased proliferation capacity, ferroptosis induction might further be exploited to exhaust the tumoral anti-oxidant defense mechanisms and overcome multi-drug resistance [21]. Intriguingly, although several genes (e.g. SLC7A11, GPX4, HMOX1, ACSL4) have already been identified as key players in ferroptotic cell death, the involvement of nuclear events and epigenetic regulatory mechanisms remain largely unexplored. Only a handful of epigenetic enzymes and - modifications, including KDM3B, LSH, and monoubiquitination of H2A-B, have been described as regulators of ferroptosis [22-28]. This is surprising since, similar to ferroptosis, the epigenetic machinery is heavily influenced by oxidative stress and the iron metabolism. Indeed, the activity of many epigenetic enzymes, including JmjC-domain-containing histone demethylases (JHDMs) and ten eleven translocation (TET) DNA demethylases, is highly dependent on the availability of iron [29-31]. Similarly, hydroxyl radicals, produced during Fe^{2+}-dependent Haber-Weiss reactions taking place in ferroptotic cells [32], can produce methyl radicals and cause non-enzymatic methylation of cytosine and guanidine residues in the DNA and directly impact methylome changes [33]. Finally, inhibition of cystine import by ferroptosis inducer erastin triggers the activation of the transsulfuration pathway [34], and might limit the availability of methyl donors required for DNA and histone methylation [35, 36]. Because epigenetic

alterations often contribute to the development of therapy resistance and malignant transformation of cancer cells, a better understanding of the interplay between ferroptotic cell death and epigenomic changes might further elucidate the therapeutic potential of ferroptotic compounds. In this study, we therefore combined RNA sequencing, LC-MS/MS, pyrosequencing, and EPIC BeadChip analysis to characterize the epigenetic changes taking place in therapy-resistant and -sensitive MM1 cells.

5.2. Results

5.2.1. Glucocorticoid-Sensitive and -Resistant MM1 Cells Exhibit a Similar Transcriptome Stress Response Upon Ferroptotic Cell Death Induction

Acquired and primary therapy resistance remain a major hurdle in clinical treatment of MM. Despite the availability of broad spectrum anti-cancer drugs, including glucocorticoids (GCs), proteasome inhibitors (PIs), and immunomodulatory drugs (IMiDs), most MM patients eventually relapse and become refractory to current treatments [37]. Therefore, we explored whether therapy-resistant MM cells are sensitive to ferroptosis induction, an iron-catalyzed mode of cell death associated with increased lipid peroxidation. In this study, we exposed GC-resistant (MM1R) and GC-sensitive (MM1S) MM1 cells to different ferroptosis inducers, including RSL3, ML162, erastin, and Withaferin A (WA), and evaluated their effect on cell viability (Figure 1a). Although both cell lines have the same origin, MM1R cells are known to be resistant to GC-mediated apoptosis due to their defective GC receptor (GR) and lack of GR expression. We observed that all compounds successfully induced cell death in both cell lines and that GPX4 inhibitor RSL3 was most potent, with IC_{50} values ranging between 2.82 µM and 6.31 µM (Figure 1b). RSL3-induced cell death could be fully prevented by pre-treatment with ferroptosis inhibitor ferrostatin-1 (Fer-1), but not by pre-treatment with necrostatin-1 (Nec) or ZVAD-FMK, necroptosis and apoptosis inhibitors respectively (Figure 1c). Of note, pre-treatment with Fer-1 does not impact or reverse dexamethasone sensitivity of MM1 cells and indicates that other modes of RCD are involved in mediating GC-triggered cell death (Supplementary Figure S1). Similarly, only ZVAD-FMK was able to partially rescue cell death induced by WA (Figure 1d), a natural steroidal lactone that has previously been reported to display both apoptotic- and ferroptotic-mediated anti-cancer properties [38-40]. This suggests that in our MM cell model, WA promotes apoptotic rather than ferroptotic cell death. Indeed, while flow cytometry analysis revealed that RSL3-induced cell death was accompanied by an increase in lipid peroxidation after 3 hours of treatment (Supplementary Figure S2a-b), this was not observed in cells incubated with WA (data not shown). The cell death modality induced by WA might therefore be highly dependent on cell type and – context.

To characterize transcriptional changes taking place in ferroptotic MM1 cells, RNA sequencing analysis of RSL3-treated MM1 cells was performed, and compared to untreated controls. For this RNAseq experiment, RSL3-treated MM1 cells were exposed to 5 µM RSL3 for 3 hours as this concentration and incubation time effectively initiate lipid peroxidation (Supplementary Figure S2b) without substantially lowering cell viability (Supplementary

Figure S2a). This to ensure that mostly early ferroptotic cells are included in the analysis, and that the transcriptome response to ferroptosis induction can be thoroughly assessed. Using selection criteria of FDR <0.05 and logFC > | 1 |, changes in gene expression patterns in both MM1S and MM1R cells were shown to be highly similar (Figure 2a-b). A total of 616 common significant differentially expressed genes (DEGs) could be identified, the majority of which (540 DEGs) were found to be upregulated upon ferroptosis induction (including FTH1, FTL, CHAC1, HSPB1, SLC7A11, and HMOX [40-43] (Supplementary Figure S3a-b)). Metascape pathway analysis of DEGs revealed an enrichment in inflammation, kinase signaling, cellular stress, and cell death related pathways (Figure 2c). Remarkably, altered expression of 95 of the 616 identified DEGs could completely be reverted by pre-treatment with Fer-1 (FDR < 0.05, logFC | 1 |), suggesting that these genes in particular are crucial for ferroptosis induction (Figure 2d). The most significant genes within this subset are involved in metal binding (including metallothioneins [MT1s] and zinc finger proteins [ZNF]), nuclear receptor signaling (orphan nuclear receptor 1-3 (NR4A1-3)), chromatin remodeling (NR4A2, FOXA1, KDM6B), and gene transcription (ZNFs, NR4A1-3) (Figure 2d). Taken together, these findings suggest that ferroptosis effectively targets MM1 cells and that RSL3-mediated ferroptosis triggers similar oxidative stress and cell death pathways in both MM1R and MM1S cells, irrespective of their GC-sensitivity status. Moreover, genes involved in metal binding and chromatin remodeling seem to be crucial for mediating ferroptotic cell death.

5.2.2. RSL3-Mediated GPX4 inhibition Triggers the Formation of non-heme Iron-Histone Complexes and Double-Stranded DNA Breaks

Because RNAseq data revealed the involvement of chromatin remodelers, including FOXA1, NR4A2, and KDM6B, in ferroptotic cell death, we next utilized a LC-MS/MS approach to investigate whether RSL3-induced oxidiative stress signals propagate to the nucleus and alter histone post-translational modifications (Supplementary Figure S4a) [44]. First, LC-MS compatible cell lysis and histone extraction protocols were optimized to obtain pure histone extracts (Supplementary Figure 4b). Overall, direct acid extraction of histones from the whole cell pellet resulted in higher protein yield compared to the hypotonic lysis protocol where nuclei are isolated prior to acid extraction (Supplementary Figure 4c).

After optimization, quantification of histone modification levels was performed using an untargeted, data-dependent acquisition (DDA) MS-based screening method [44]. Briefly, MM1 cells were treated with 5 µM RSL3 for increasing time periods (1hr-2hr-4hr-8hr) after which histones were extracted, propionylated and trypsinized. Next, MS1 and MS2 spectra were obtained by HPLC-MS/MS analysis and raw data was analyzed with the Progenesis QIP 3.0 software (Waters). Ultimately, relative abundances of histone PTMs were obtained and statistical analysis was performed to identify significantly altered PTMs (Supplementary Table S1). Overall, we observed that cells treated with RSL3 for increasing time periods showed a progressive increase and decrease in several histone PTMs (Figure 3). In line with our RNAseq data, where most genes were found to be upregulated upon RSL3 induction, ferroptotic cells portrayed a genome-wide, time-dependent decrease in repressive histone mark H3K37me3 [45]. However, loss of active marks, including H3K18ac,

H3K79me3, and H3K27ac was also detected upon continued RSL3 treatment (Supplementary Figure S5a). Remarkably, H3K79me3, H3K18ac, and H3K27ac have all been associated with DNA damage, cellular senescence, and genome instability (Table 1), suggesting that RSL3-mediated oxidative stress might drive these processes in MM1 cells. This is also reflected by the increased detection of histone variants H2A.Z and H2A.FY (macroH2A1), which are known to regulate DNA repair and cellular senescence (Table 1).
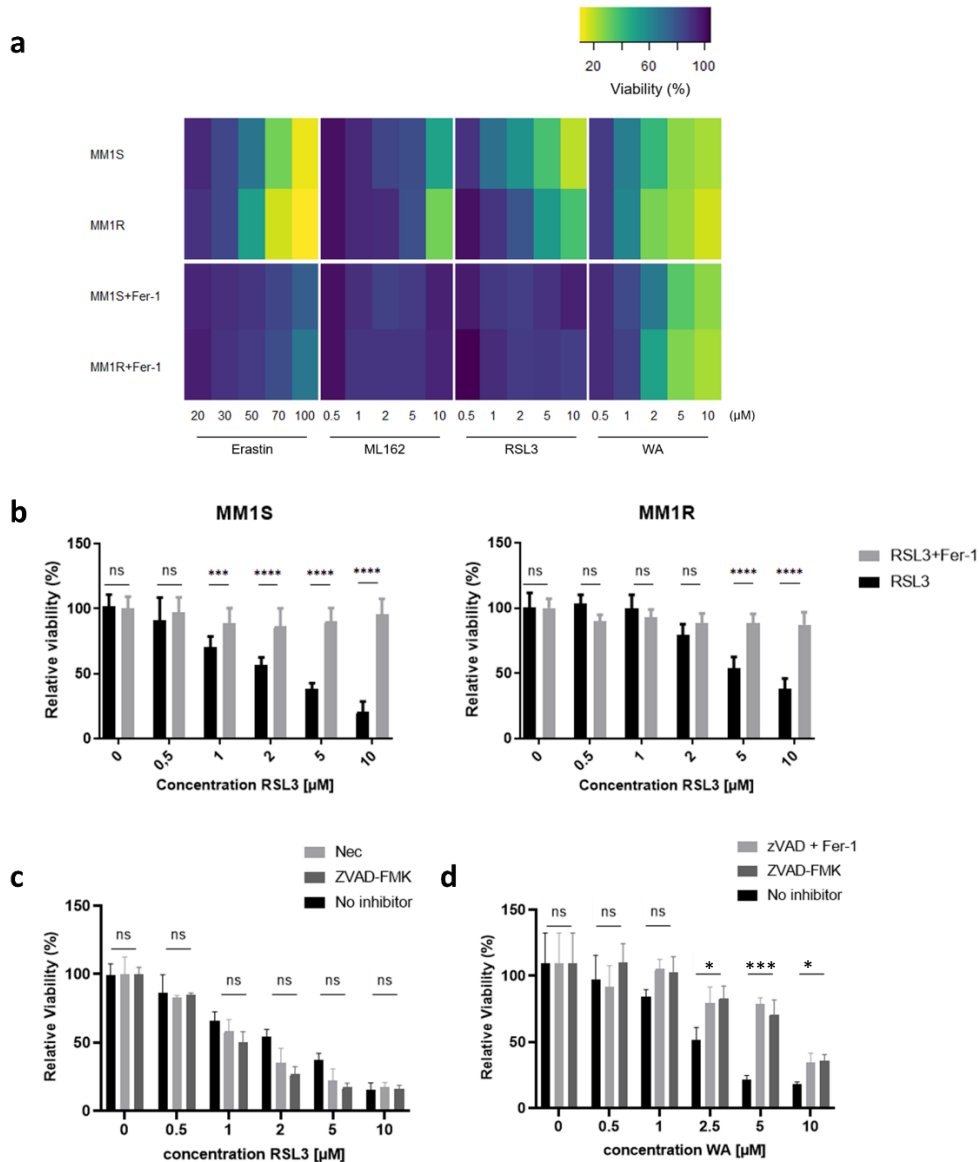
Figure 10: MM1 multiple myeloma cell lines are susceptible to ferroptosis induction. (**a**) Heatmap representing relative cell viability of MM1 cells upon 24 h exposure to increasing concentrations of Erastin, ML162, RSL3, and Withaferin A (WA). (**b**) Relative cell viability of MM1S (left) and MM1R (right) cells upon 24 h exposure to increasing concentrations of RSL3 with or without pretreatment with 2 μM ferrostatin-1 (Fer-1). Data are plotted as the mean ± s.d., *n*=3 biologically independent replicates (ns= p > 0.05, ***p < 0.001, ****p < 0.0001, ANOVA). (**c**) Relative viability of MM1 cells upon 24 exposure to increasing concentrations of RSL3 with or without pretreatment with 10 μM necrostatin-1 (Nec) or 50 μM caspase inhibitor ZVAD-FMK. Data are plotted as the mean ± s.d., *n*=3 biologically independent replicates. (**d**) Relative viability of MM1 cells upon 24 exposure to increasing concentrations of WA with or without pretreatment with 2 μM Fer-1 and/or

50 µM caspase inhibitor ZVAD-FMK. Data are plotted as the mean ± s.d., *n*=3 biologically independent replicates (*p < 0.05, ***p < 0.001, ANOVA).

Moreover, Western blot analysis revealed that prolonged exposure (>12 hours) to RSL3 resulted in a significant increase in pH2AX, a key maker for double-stranded DNA damage (Supplementary Figure S5b). Next to histone PTMs associated with DNA damage and cellular senescence, we found a significant increase in histone acylation modifications, including succinylation, crotonylation, and (hydroxyiso)butyrylation (Figure 3, Supplementary Table S1). Although the functional effects of these PTMs are far less characterized compared to those of histone acetylations, several studies highlight they are heavily influenced by the fatty acid metabolism (reviewed in [46]). Depending on the cellular metabolic state, crucial metabolic intermediates (e.g. crotonate) are increased or decreased, impacting their availability for acyl-transferase-mediated histone modifications. Given that ferroptosis is hallmarked by lipid peroxidation and overall changes in the lipid metabolism [47], these histone acylation changes might directly reflect the altered metabolic state of ferroptotic cells and regulate gene expression accordingly [48-50]. Suprisingly, we found that the altered iron metabolism during ferroptosis directly affects histone PTMs as well. Specifically, several glumate (E) and aspartate (D) residues in H2A, H3, and H4 histone tails were significantly enriched in Fe^{2+} binding (Figure 3, Supplementary Table S1). To the best of our knowledge, we are the first research group to describe Fe^{2+} binding to histone proteins. The biological relevance of the formation of non-heme iron histone complexes needs to be further explored, but might include a role in iron chelation in response to the ferroptosis-driven intracelullar increases in labile iron, regulation of gene expression, DNA damage, DNA damage protection, or even reflect the oxidoreductase activity of H3-H4 tetramers as previously reported for Cu^{2+} [52]. To further investigate the iron-binding properties of histone proteins, commercial H3-H4 tetramers were incubated with $FeSO_4$ and separated by gel filtration, after which absorbance at 280 nm was measured. Similar to the absorbance signal measured in the $CuSO_4$ positive control, H3-H4 tetramers incubated with $FeSO_4$ demonstrated an increased absorbance at 280 nm (Figure 4). Furthermore, FeSO4 incubated resulted in a small shift in H3-H4 protein size, suggesting that Fe^{2+} binding affects the structural organization of the tetramer complex. Overall, our data suggests that histone proteins and - PTMs are sensitive to altered oxidative stress, and fatty acid and iron metabolism changes mediated by GPX4 inhibition.

Figure 2 (next page): RNAseq analysis reveals RSL3-induced transcriptional changes in MM1 cells. (**a**) Heatmap representation of rlog gene counts of differentially expressed genes (FDR < 0.05, logFC > | 1 |) in MM1 cells. Gene counts are represented as Z-scores, *n*=3 biologically independent replicates per cell line. (**b**) Scatter plot displaying the correlation between the logFC of significant DEGS identified in MM1R and MM1S cells. The strength of the correlation is indicated by the regression line (with 95 % confidence interval indicated in light blue) and corresponding coefficient of determination (R). Significance of the correlation was calculated by pearson correlation and is represented by the pearson correlation coefficient (p). (**c**) Metascape pathway analysis [51] of RNAseq data displaying the top 20 significantly enriched pathways of RSL3-treated MM1 cells compared to untreated controls. (**d**) Heatmap representation (left) and protein interaction network (right) of differentially expressed genes in RSL3-treated MM1 cells of which the expression change could be completely

reverted by ferrostatin (Fer-1) pre-treatment. The most significant genes are indicated with * and included in the interaction network.
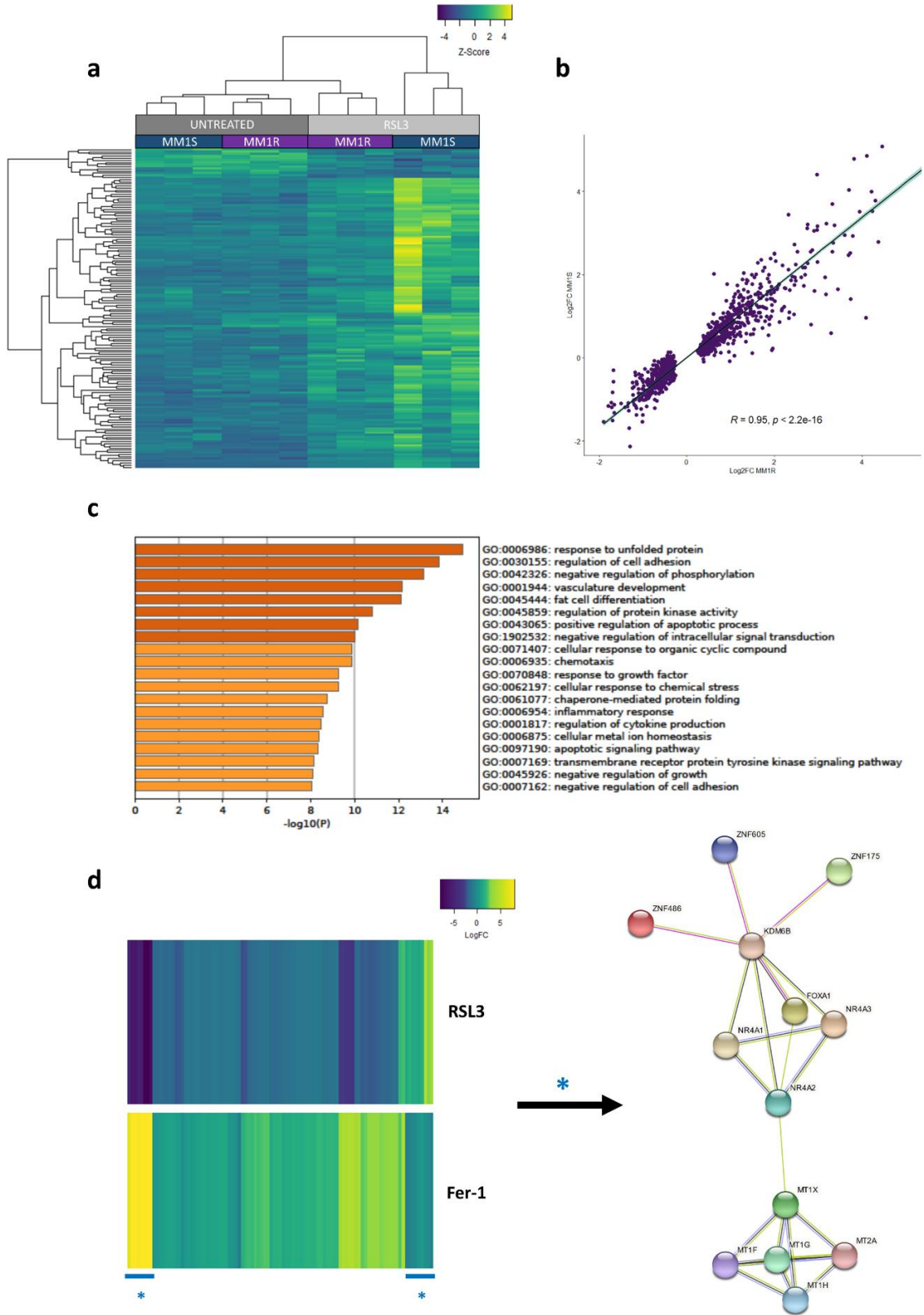
Table 1: Overview of RSL3-induced changes in histone PTMs linked to DNA repair and cellular senescence

Histone PTM or variant	Expression after RSL3 treatment	Biological process	Functional role	References
H3K79me3	↓	Genome stability	Enriched in heterochromatic centromeric & telomeric regions; Prevents spreading of hetero-chromatin	[53-55]
		DNA repair	Controls DNA resection at damaged sites during homologous recombination; Crucial in repairing UV-induced DNA damage	[56, 57]
H3K18ac	↓	DNA repair	Regulates the expression of anti-oxidant genes; Recruits DNA repair enzymes to damaged sites; Regulates expression of nucleotide excision repair-related genes	[58-61]
		Cellular senescence	H3K18 deacetylation protects cells against mitotic errors and cellular senescence	[62]
		Genome stability	Maintains pericentric hetero-chromatin silencing	[62]
H3K27ac	↓	DNA repair	Regulates the expression of nucleotide excision repair-related genes	[61, 63]
		Cellular senescence	Enriched in enhancers of senescence-associated secretory phenotype (SASP) genes	[64-66]
H2A.Z	↑	DNA repair	Facilitates chromatin decondensation to allow for loading of DNA repair proteins to DNA breaks	[67-69]
		Genome stability	Required for chromosome segregation and cytokinesis; Prevents spreading of hetero-chromatin; Preserves integrity of centromeres and telomeres	[70-73]
		Cellular senescence	Overexpression alters regulation of cell cycle and DNA damage repair enzymes and suppresses cellular senescence	[74]
H2A.FY	↑	Cellular senescence	Regulates downstream acetylation to regulate senescence transcription programs	[75, 76]
		DNA repair	Alters the kinetics of PAR polymerases during DNA damage responses	[77]

5.2.3. Prolonged exposure of MM1 Cells to RSL3 Results in Local DNA Methylation Changes and Promotes Expression of DNA Damage Repair Protein NR4A2

Taking into account that ferroptotic stress directly affects expression of chromatin remodelers and histone PTMs, we wondered whether DNA methylation changes also occur upon RSL3 induction in MM1 cells. Given that prior studies have reported significant global DNA methylation alterations upon intracellular increases in reactive oxygen species (ROS) and iron [33, 78, 79], we first evaluated changes in global DNA methylation levels (i.e. levels of 5mC content relative to the total cytosine) in MM1S and MM1R cells treated with 1 µM RSL3 for 72 h. Three independent methods, namely LINE-1 pyrosequencing, Infinium

Methylation EPIC BeadChip analysis, and HPLC-MS/MS analysis, revealed no significant shifts in DNA (hydroxy)methylation after chronic GPX4 inhibition (Figure 5a-c). All methods did show, however, that basal DNA methylation levels in MM1S cells were consistently higher compared to MM1R cells (Figure 5a-c).

Next, local CpG-dependent changes in DNA methylation were explored through Infinium Methylation EPIC BeadChip analysis, which measures mean methylation levels of 866.836 genome-wide CpG sites. CpG loci of RSL3-treated cells were compared to cells treated with Fer-1 and RSL3 and were considered to be differentially methylated if a difference of ≥ 10 % methylation and FDR < 0.05 could be detected. Overall, RSL3 treatment resulted in a large number of differentially methylated probes (DMPs) in both MM1R (51 168 CpG probes corresponding to 487 genes) and MM1S cells (32 813 CpG probes corresponding to 408 genes). The majority of DMPs in both cell lines were located in open sea regions located > 4 kb from CpG islands (Figure 6a). Remarkably, when comparing the top significant probes (FDR < 0.01) between both cell lines, the beta values of ferroptotic MM1R cells clustered with the beta values of Fer-1 treated MM1S cells and ferroptotic MM1S cells clustered with Fer-1 treated MM1R cells, suggesting that both cell lines converge towards a similar methylation profile under ferroptotic conditions (Figure 6b). In line with this observation, genes associated with the significant DMPs (FDR < 0.05 & beta value > 0.1) were distinct in both cell lines but were enriched in several common pathways, including cell cycle, autophagy, and insulin signaling (Table 2, Supplementary Figures S6-S7).

Ferroptosis induction by RSL3 also resulted in specific hyper- and hypomethylation of a subset of probes in both cell lines (indicated by arrowheads in Figure 6b). Genes associated with these probes were mainly enriched in cell adhesion, inflammation, DNA replication, mitochondrial organization, cell death, and cellular senescence (Figure 7a). Of note, one of these genes included NR4A2, which we previously identified as a top significant DEG in our RNAseq data (see section 5.2.1.). Both Infinium Methylation EPIC BeadChip analysis and pyrosequencing analysis demonstrated that one of the probes associated with NR4A2 (cg2285933 – located in the S shelf region of NR4A2) was significantly hypermethylated upon RSL3 treatment (Figure 7b) and that this hypermethylation was linked with increased mRNA and protein expression (Figure 7c-d). Similar observations have previously been made for another nuclear receptor gene, NR3C1, where hypermethylation outside of the CpG island led to an increase in gene expression [80].
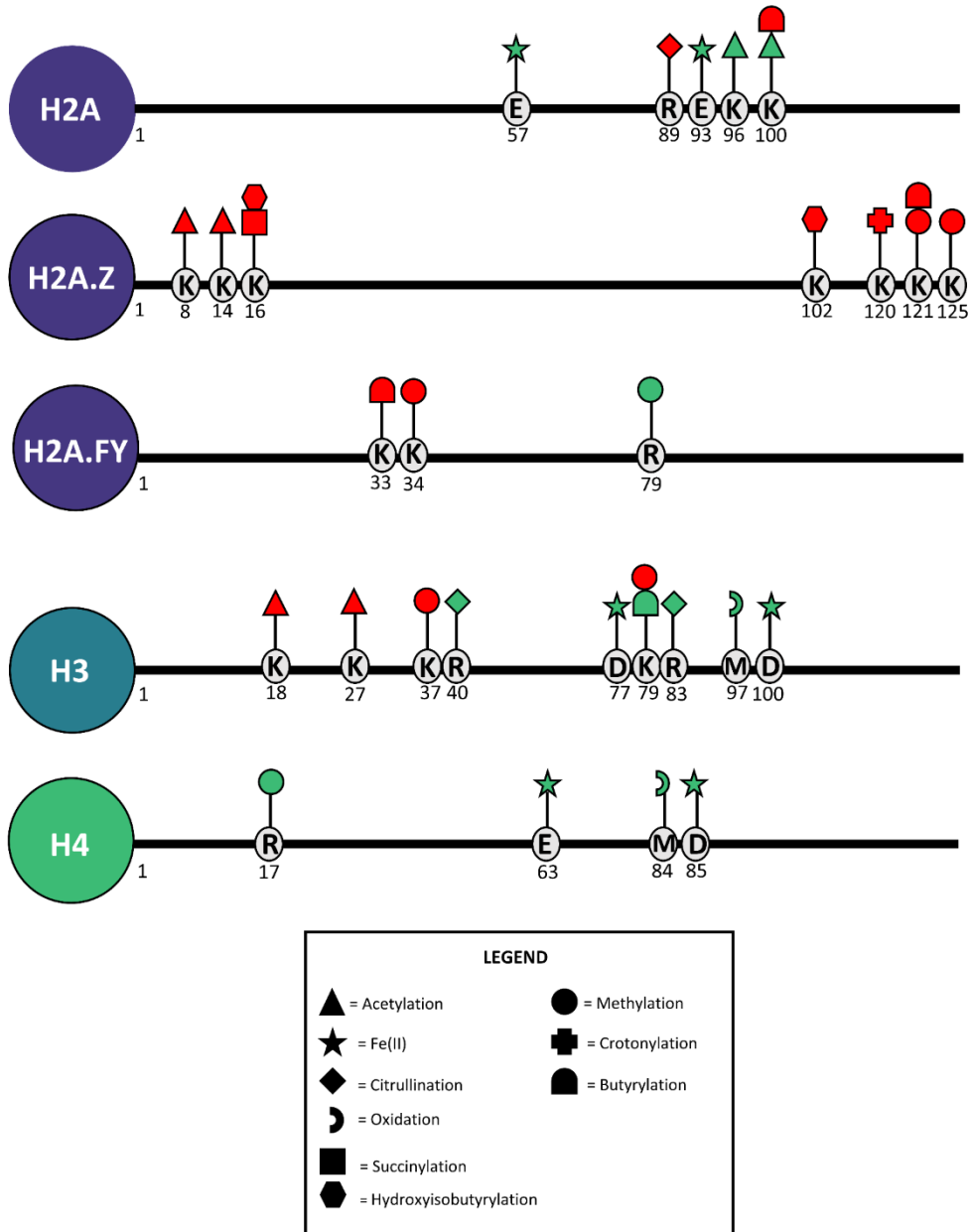
Figure 3: Overview of progressive significant (p < 0.05) changes in histone post-transcriptional modifications (PTMs) in MM1 cells after RSL3 treatment compared to untreated controls. Each symbol depicts a different PTM on N-terminal histone tails. Red symbols represent downregulated modifications while green symbols represent upregulation. The position of each PTM is indicated by the amino acid (AA) single letter code and its AA position within the corresponding histone protein sequence.
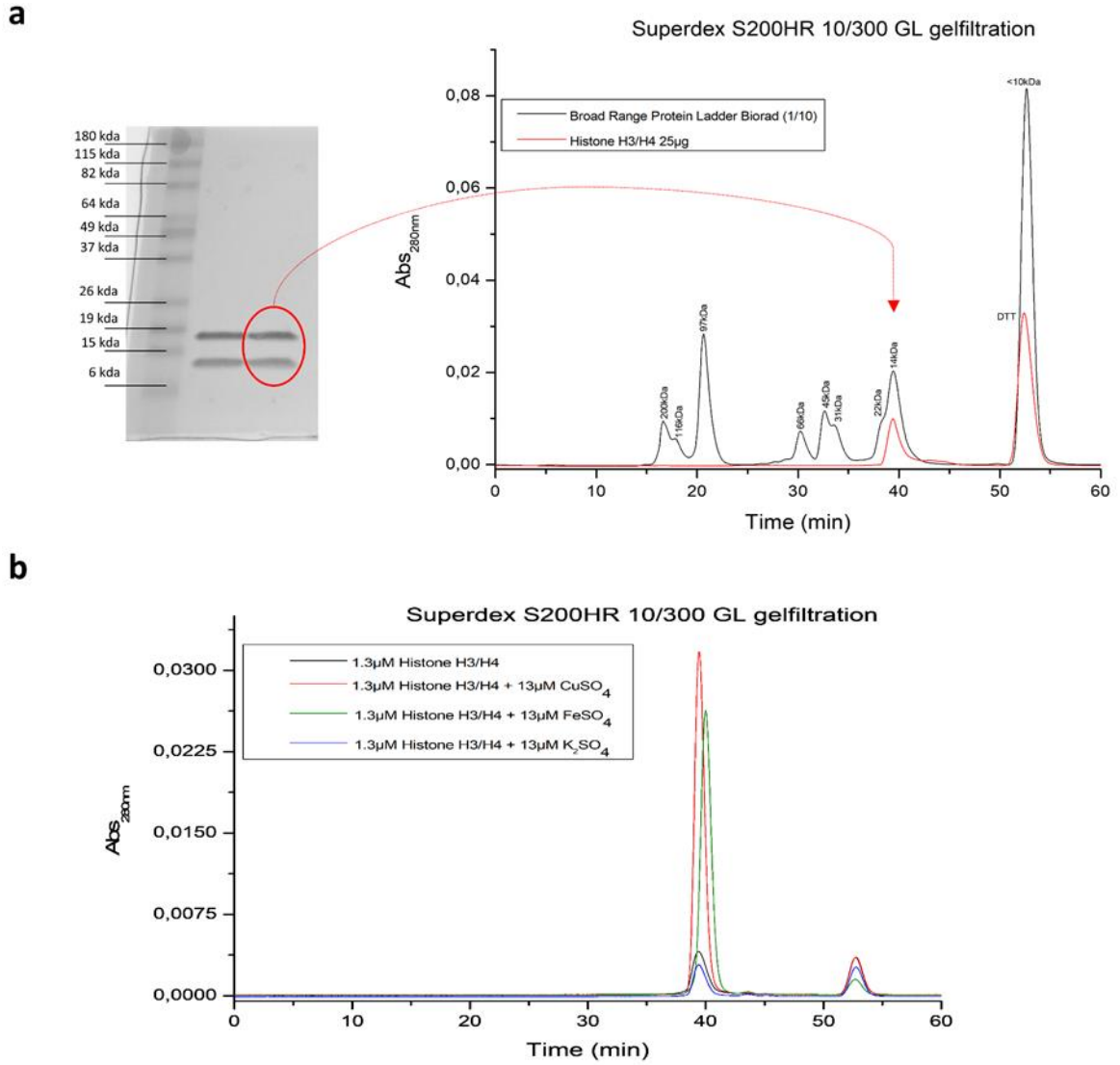
Figure 4: Purified H3-H4 tetramers display an increase in 280 nm absorbance after addition of FeSO₄. (**a**) Purity of commercial H3-H4 tetramers was evaluated by SDS-PAGE Coomassie staining (left) and gelfiltration (right). (**b**) Absorbance spectrum at 280 nm of H3-H4 tetramers incubated with a 10-fold excess of CuSO₄ (positive control), K₂SO₄ negative control), and FeSO₄.

Table 2: Common Enriched Pathways of Significant DMP-related Genes between RSL3-treated MM1S and MM1R cells

Common Pathway	GO term MM1S cells		GO term MM1R cells	
	GO term	*-log p.value*	*GO term*	*-log p.value*
Cell cycle	Negative regulation of cell cycle process	10	DNA replication	5
	Negative regulation of nuclear division	8	Meiotic cell cycle	3.8
	S Phase	4.5	Cell Cycle	2.4
	Negative regulation of meiotic nuclear division	3.8	Regulation of transcription involved in G1/S transition of mitotic cell cycle	2.1
Autophagy	Regulation of autophagy	4.4	Autophagy	2.2
Insulin Signaling Pathway	Insulin Signaling Pathway	3.8	Insulin processing	2.4
			Insulin-like growth factor receptor signaling pathway	2.0
CtBP core complex	CtBP complex	3.7	CtBP core complex	3.9
VEGF Signaling	VEGFA-VEGFR2 Signaling Pathway	2.3	VEGFA-VEGFR2 Signaling Pathway	4.6
Rett syndrome	Rett syndrome causing genes	3.1	Rett syndrome causing genes	2.5
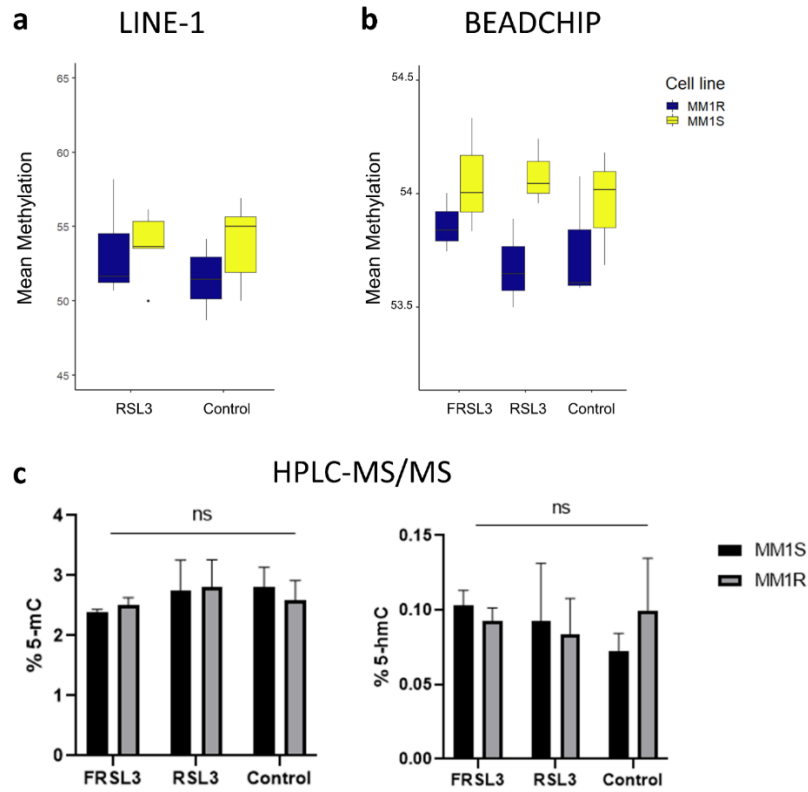
Figure 5: Global DNA methylation changes in MM1 cells after RSL3 treatment (with or without pre-treatment of ferrostatin-1 (FRSL3)). (**a**) Mean methylation levels (%) of 3 CpGs located in long interspersed nuclear elements 1 (LINE-1). *N=3* biologically independent replicates. (**b**) Mean methylation levels (%) of 866.836 genome-wide CpG sites analyzed with the Illumina Infinium Methylation EPIC BeadChip. *N=3* biologically independent replicates. (**c**) Mean % of 5-methylcytosine (left) and 5-hydroxymethylcytosine (right) residues present in MM1 samples. Data is represented as the mean ± s.d. (ns p > 0.05, ANOVA), *n*=3 biologically independent replicates.

Figure 6 (previous page): Local DNA methylation changes in MM1 cells after RSL3 treatment (with or without pre-treatment with Ferrostatin-1 (FRSL3)). (**a**) Bar chart visualization of 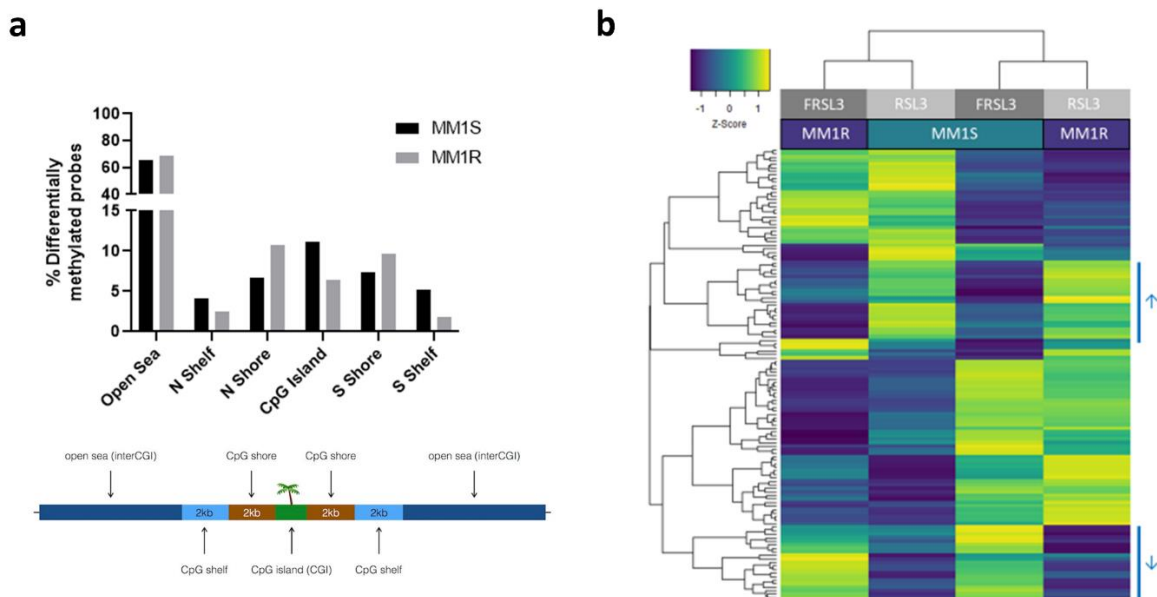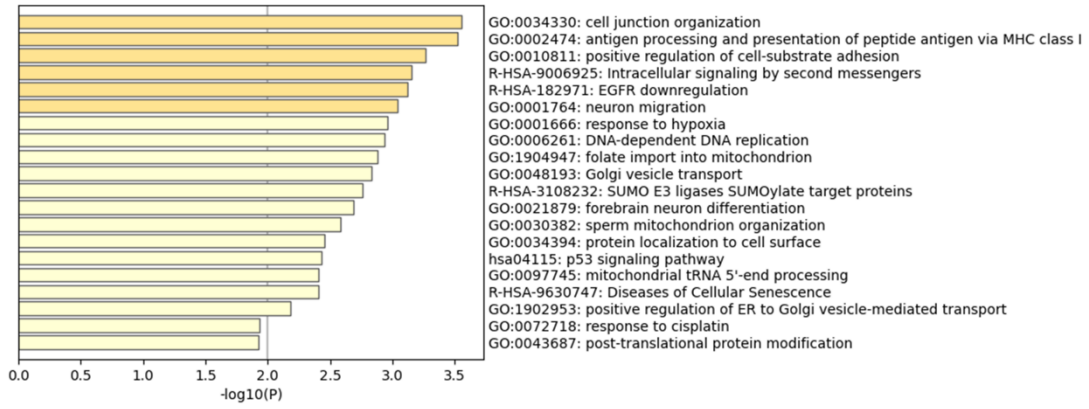the percentage of significantly differentially methylated (FDR <0.05, Δβ difference > 0.10) CpG loci (y-axis) between RSL3 and Ferrostatin-1 pre-treated RSL3 MM1 cells and their corresponding genomic compartments (x-axis). (**b**) Heatmap representation of the methylation level (β-values) of the top common DMP CpG sites of MM1 cells treated with RSL3 (with or without pre-treatment with Ferrostatin-1). β-values are represented as Z-scores, where the lowest methylation value is indicated in blue and the highest in yellow.
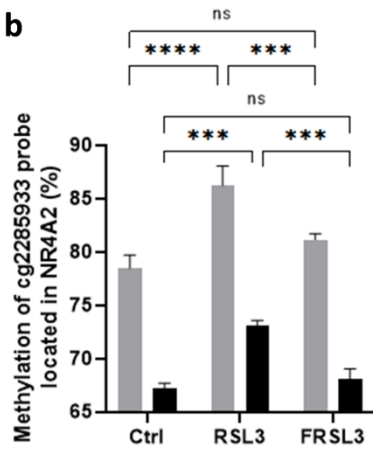
5.3. Discussion

The majority of available anti-myeloma drugs, including GCs, PIs, and IMiDs, aim to eradicate tumors cells through induction of apoptosis [81]. However, most myeloma cells acquire resistance to this mode of cell death by upregulating anti-apoptotic proteins and downregulating pro-apoptotic signals, which is often driven by (epi)mutational changes [82, 83]. For that reason, we explored whether induction of ferroptotic cell death might be an effective alternative to eliminate GC-resistant myeloma cells. Our data show that GPX4 inhibitor RSL3 successfully targets MM1 cells, irrespective of their GC sensitivity status, and that induction of ferroptosis is linked to a common transcriptional response. Specifically, ferroptotic myeloma cells upregulate a significant number of genes involved in cellular stress and cell death pathways, inflammation, and fatty acid metabolism. Among these genes, chromatin remodelers, such as NR4A2, FOXA1, and KDM6B, seem to be pivotal in triggering ferroptosis. To this end, we further explored the epigenetic changes in ferroptotic myeloma cells and found that ferroptosis is associated with significant changes in several histone modifications and variants, most of which have previously been linked with DNA damage and cellular senescence pathways. Interestingly, RSL3 treatment also caused an increased binding of Fe^{2+} ions to glutamate and aspartate residues of H2, H3, and H4, suggesting that the ferroptosis-driven changes in intracellular iron concentrations are propagated to the nucleus. The formation of non-heme iron-histone complexes could be confirmed in gel filtration chromatography experiments, where H3-H4 tetramers showed an increased absorption upon Fe^{2+} incubation. Whether this phenomenon is unique to MM cells or occurs universally in ferroptotic cells needs to be explored in other ferroptosis cell models, such as the HT-1080 cell line. Additionally, further validation with other biochemical techniques, including isothermal titration calorimetry, circular dichroism spectrometry, or microscale thermophoresis is required to determine whether the observed increase in Fe^{2+} binding to histone proteins is a biologically relevant process. If this is the case, the biological relevance of iron-histone complexes needs to be explored as well. Possibly, histone proteins mediate a genoprotective role by chelating iron and preventing DNA damage [84]. Because earlier experiments revealed a cupper binding-dependent reductase activity of H3-H4 tetramer complexes [52], Fe^{2+} binding to histones might also fuel an enzymatic function of histone proteins which has yet to be uncovered. Alternatively, histones are known to function as oxygen and nutrient sensors and the observed iron-binding might be a reflection of this role [85, 86]. In line with this latter hypothesis, significant changes in different histone acylation marks, which are known to respond to metabolic perturbations [87], were detected in ferroptotic myeloma cells as well.

a

GO:0034330: cell junction organization
GO:0002474: antigen processing and presentation of peptide antigen via MHC class I
GO:0010811: positive regulation of cell-substrate adhesion
R-HSA-9006925: Intracellular signaling by second messengers
R-HSA-182971: EGFR downregulation
GO:0001764: neuron migration
GO:0001666: response to hypoxia
GO:0006261: DNA-dependent DNA replication
GO:1904947: folate import into mitochondrion
GO:0048193: Golgi vesicle transport
R-HSA-3108232: SUMO E3 ligases SUMOylate target proteins
GO:0021879: forebrain neuron differentiation
GO:0030382: sperm mitochondrion organization
GO:0034394: protein localization to cell surface
hsa04115: p53 signaling pathway
GO:0097745: mitochondrial tRNA 5'-end processing
R-HSA-9630747: Diseases of Cellular Senescence
GO:1902953: positive regulation of ER to Golgi vesicle-mediated transport
GO:0072718: response to cisplatin
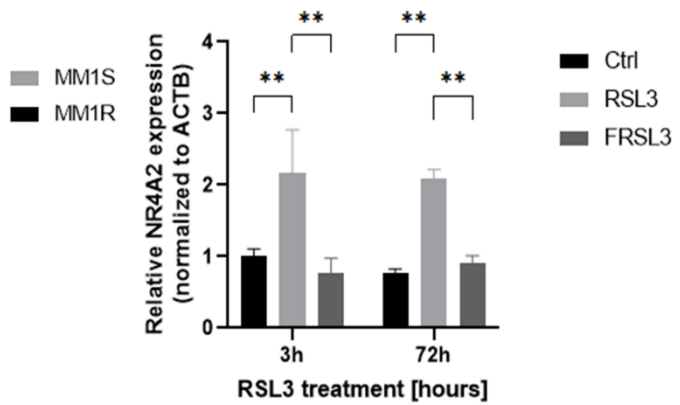GO:0043687: post-translational protein modification
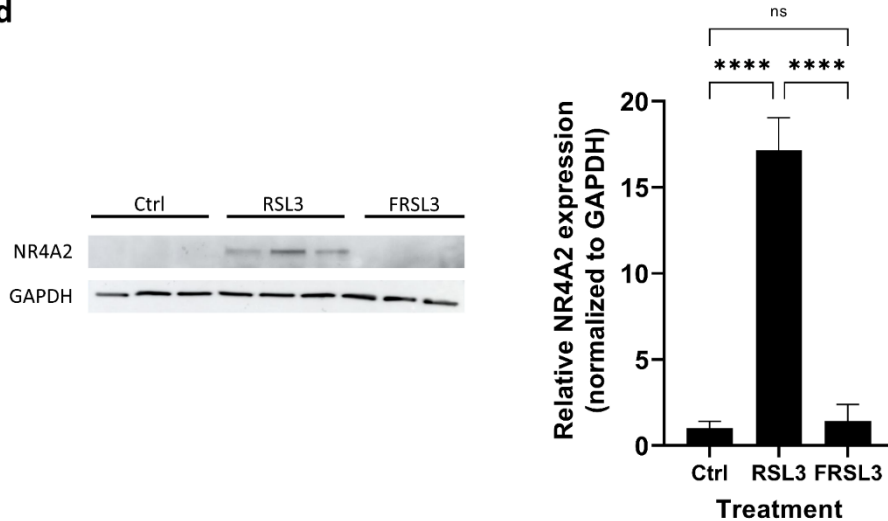
b

c

d

Figure 7: Ferroptosis induction results in significant methylation changes in genes associated with DNA repair and cellular senescence. (**a**) Metascape pathway analysis [51] of genes associated with the top significant (FDR < 0.01) differentially methylated CpG probes in MM1 cells after RSL3 treatment. (**b**) Mean methylation levels (%) of CpG probe cg2285933 located in the S shelf of the NR4A2 gene as determined by pyrosequencing. Data are represented as mean methylation levels ± s.d., *n=3* biologically independent replicates per cell line ((***p < 0.001, **** p < 0.0001). (**c**) Relative NR4A2 mRNA expression in MM1 cells after treatment with RSL3 with or without pre-treatment with 2 μM ferrostatin-1 (FRSL3). NR4A2 expression was normalized against the β-actin (ACTB) housekeeping gene. Data are plotted as the mean ± s.d., *n*=3 biologically independent replicates (**p <0.01). (**d**) Western blot detection and quantification of NR4A2 and GAPDH expression levels after RSL3 treatment in MM1 cells. Data are plotted as the mean ± s.d., *n*=3 biologically independent replicates per cell line. (ns p > 0.05, ****p <0.0001 ANOVA).

Since alterations in oxidative stress and intracellular iron concentration are known to directly impact DNA methylation [31, 33, 78, 79], we next investigated whether ferroptosis impacts DNA methylation levels in MM1 myeloma cells. Although ten-eleven translocation (TET) DNA demethylation enzymes are known to be sensitive to changes in labile iron [88, 89], no significant changes in global DNA (hydroxy)methylation in RSL3-treated cells could be observed by LINE-1 pyrosequencing, HPLC-MS/MS analysis, or BeadChip EPIC methylation arrays, indicating that the overall activity of these TET enzymes is not altered during ferroptosis. In contrast, BeadChip EPIC methylation analysis did uncover local DNA methylation changes of numerous DMPs in both GC-sensitive MM1S and GC-resistant MM1R ferroptotic cells. Clustering analysis of the top significant DMPs (FDR < 0.01) revealed two major trends in the methylation data. First, RSL3-mediated GPX4 inhibition drives MM1S and MM1R cells towards a similar methylation profile, indicating that ferroptosis triggers a common stress epigenome response in cells with different epigenetic backgrounds. This implies that ferroptosis signaling either differentially methylates DMPs located in MM1S but not in MM1R (or vice versa) or that both cell lines undergo methylation changes in opposite directionalities (i.e. hypermethylated in MM1R, hypomethylated in MM1S). Nevertheless, both cell lines portray similar RSL3-dependent transcriptional changes and sensitivities to ferroptotic compounds, suggesting that most of these DNA methylation changes are epigenetically redundant. Second, similar to the histone proteomics data, ferroptotic cell death induction resulted in specific hyper- and hypomethylation of a genes involved in DNA repair, cellular senescence and cell death pathways. Of note, NR4A2 expression was found to be upregulated upon methylation of its S shore region. NR4A2, also known as Nurr1, is involved in mediating DNA damage repair responses induced by genotoxic triggers [90, 91] and has been identified as a potential target for anti-aging interventions (reviewed in [92]).

Although we did not directly assess expression of senescent markers of ferroptotic myeloma cells in this study, both our histone proteomics and DNA methylation data suggest cellular senescence pathways are altered during ferroptosis. Generally, cellular senescence is described as a state of permanent growth arrest that can be induced by cellular stress or DNA damage [93]. Western blot analysis of pH2AX, a marker of double stranded DNA breaks, indeed shows an increase in DNA damage upon prolonged RSL3 stimulation in MM1 cells. Other proteins involved in the DNA damage response (DDR), including p53 and ATM/ATR kinases, have recently also been linked to ferroptotic cell death

[94]. In agreement with our observations, studies in neuronal and retina epithelial cells have revealed that ferroptotic compounds are able to promote cellular senescence [95-97]. Whether cellular senescence promotes sensitization [96, 98] or resistance [99] to ferroptosis is currently still under debate. Ferroptosis-driven epigenetic changes characterized in this study seem to suggest that RSL3-mediated oxidative stress orchestrates DNA damage and genomic instability, which induces premature cell senescence and prompts activation of DNA repair genes, such as NR4A2 (summarized in Figure 8). Interestingly, prior research reported that drug-induced senescence promoted MM cell recognition by natural killer cells and elimination of tumor cells [100]. Similarly, ferroptosis-mediated senescence might provide new insights for the exploitation of senolytic drugs in cancer therapies that specifically target senescent cells [101].
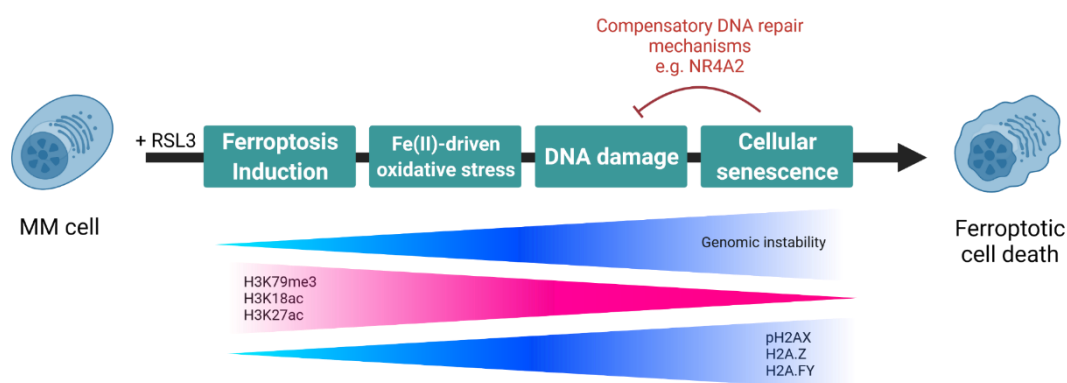
Figure 8: Ferroptosis induction in multiple myeloma (MM) cells triggers oxidative stress mediated changes in epigenetic modifications, DNA damage, and cellular senescence. Figure created with BioRender.com.

5.4. Materials and Methods

5.4.1. Antibodies and Reagents

Ferroptosis inducers erastin (S7242) and RSL3 (S8155), and cell death inhibitors ferrostatin-1 (S7243) and necrostatin (S8037) were purchased from Selleckchem (Houston, TX, USA). ML162 (SML2561) and ZVAD-FMK (V166) were purchased from Sigma-Aldrich (Saint Louis, MO, USA). WA was obtained from Alta Vista Phytochemicals (Hyderabad, India). All compounds were dissolved in DMSO at a stock concentration of 20 or 50 mM.

Primary antibodies targeting pH2AX (ab81299), H3K27ac (ab4729), H3K36me3 (ab9050), and GAPDH (ab9485) were obtained from abcam (Cambridge, UK). The NR4A2 antibody (Nurr1 monoclonal antibody, MA1-195) was purchased from ThermoFisher Scientific (Waltham, MA, USA).

5.4.2. Cell Culture and Cell Viability Assays

MM1R and MM1S cells were cultured in RPMI 1640 medium supplemented with 10% fetal bovine serum (E.U. Approved; South American Origin), 1 % MEM non-essential amino acids (Invitrogen, Carlsbad, CA, USA), 1 % sodium pyruvate (Invitrogen, Carlsbad, CA, USA), and 1 % penicillin/streptomycin solution (Invitrogen, Carlsbad, CA, USA). Cell viability was

assessed by the MTT colorimetric assay (Sigma Aldrich, St. Louis, MO, US) as previously described [102].

5.4.3. Lipid Peroxidation Assay

Cellular lipid reactive oxygen species were measured using the Image-iT™ Lipid Peroxidation Kit (C10445, ThermoFisher Scientific, Waltham, MA, USA) according to the manufacturer's protocol. In short, cells were seeded in 6 well plates at a density of 5 x 10^5 cells/well and treated the next day with 5µM RSL3 (with or without pre-treatment with 2 µM Fer-1) or 100µM cumene hydroperoxide (positive control). Cells were subsequently incubated for 30 min with 10µM Image-iT™ Lipid Peroxidation Sensor at 37 °C. After incubation, cells were collected by trypsinization with TrypLE Express Enzyme (ThermoFisher Scientific, Waltham, MA, USA). Cells were washed 3 times with pre-warmed PBS and fluorescence shift from 590 nm to 510 nm was measured with the CytoFlex flow cytometer (Beckman Coulter Life Sciences, Indianapolis, IN, USA).

5.4.4. RNA Extraction and RNA Sequencing

Total RNA from control and RSL3-treated (5 µM RSL3, 3 hour treatment) MM1 cells was isolated using the RNeasy Mini Kit (Qiagen, Venlo, Netherlands) according to the manufacturer's protocol. Isolated RNA was quantified and qualified using the Epoch™ Microplate Spectrophotometer (BioTek, Winooski, VT, USA) and sent to BGI (BGI Group, Bejing, China) for RNA sequencing analysis. Briefly, RNA integrity (RNA content > 80 ng/µL, 28s/18s ≥ 1.0 and RIN ≥ 7.0) was determined using the 2100 Bioanalyzer system (Agilent Technologies, Santa Clara, CA, USA) after which library preparation was initiated. 2 X 50 bp pair-end RNA sequencing was subsequently performed on the BGISEQ-500 platform (BGI Group, Bejing, China). RNAseq data have been deposited in the NCBI GEO database with accession number (awaiting accession number).

Quality of the sequencing reads was evaluated using FastQC (v0.11.5) [103] and subsequent alignment to the human reference genome build 37 (hg19) was performed with the STAR (v.2.7.3a) tool [104]. Differential gene expression and Metascape pathway analysis were performed in R with the DESeq2 R (v1.30.1) [105] and the online Metascape web tool [51], respectively. Correlation of differentially expressed genes between MM1S and MM1R cells was visualized using the ggscatter function of the gplots R package (v3.1.1) [106]. Protein interaction networks were generated using the STRING database (v11) [107].

5.4.5. cDNA Synthesis and qPCR Analysis

Total extracted RNA (500 ng) was converted into cDNA using the GoScript™ Reverse Transcriptase System (Promega, Madison, WI , USA) according to the manufacturer's instructions. cDNA was subsequently used as input for qPCR analysis using the GoTaq® qPCR Master Mix (Promega, Madison, WI , USA) as previously described [102]. ΔΔCt-values were calculated using ACTB as housekeeping gene. Primers sequences are listed in Supplementary Table S2.

5.4.6. **Histone Extraction and MS Sample Preparation**

Extraction of histone proteins was performed as previously described [44, 108]. In short, two extraction protocols, namely hypotonic lysis (protocol A) and direct acid lysis (protocol B), were explored. In protocol A, 2 x 10^6 cells were resuspended in hypotonic lysis buffer (10 mM Tris-HCl pH 8.0, 1 mM KCl, 1.5 mM $MgCl_2$) supplemented with 1 mM DTT, 1 mM PMSF, Halt Protease and Phosphatase Inhibitor Cocktail 100x (ThermoFisher Scientific, Waltham, MA, USA), and phosphatase inhibitor cocktails II and III (Sigma-Aldrich, Saint-Louis, MO, USA). Lysates were incubated for 30 min at 4 °C on a rotator, after which nuclei were pelleted by 10 min centrifugation at 10 000 g and 4 °C. Pellets were then resuspended in 0.4 N HCl and incubated again at 4 °C for 30 min on a rotator. In protocol B, 2 x 10^6 cells were lysed directly in 0.4 N HCl and incubated at 4 °C on a rotator for 2 hours. For both protocols, lysates were subsequently centrifuged (16 000 g, 10 min, 4 °C) and supernatant was transferred to new Protein LoBind Eppendorf tubes. A final concentration of 25 % trichloroacetic acid was slowly added to the histone solution, after which samples were inverted several times and incubated on ice for 30 min. Pelleted (16 000 g, 10 min, 4 °C) histones were washed twice with ice-cold acetone and air-dried in a fume hood at RT. Part of the extracted histones (corresponding to 4 x 10^5 cells) were used to assess purity and quantity by gel electrophoresis. Dried histones were resuspended in 2X Laemmli buffer (2.14% SDS, 26.3 % glycerol, and 10 % 2-mercaptoethanol in 65.8 mM Tris-HCl pH 6.8) and separated on 8-16 % Criterion TGX™ gradient gels (Bio-Rad Laboratories, Hercules, CA, USA). Gels were stained with the Sypro Ruby fluorescent gel stain (ThermoFisher Scientific, Waltham, MA, USA) and visualized with the VersaDoc 3000 imager (Bio-Rad Laboratories, Hercules, CA, USA). Quantity One software (Bio-Rad Laboratories, Hercules, CA, USA) was used for purity analysis. Remaining purified histones were propionylated and trypsin digested as previously described [108]. Proprionylated histones were dissolved in 0.1 % formic acid in UPLC-grade water, sonicated and centrifuged to remove insoluble aggregates prior to injection onto the LC-MS system. Equal fractions of all samples were pooled to generate quality control (QC) samples, which were run in fixed intervals in between the other samples. All samples were spiked with digested beta-galactosidase (20 fmole on column; Sciex) to monitor chromatographic quality and variation between LC-MS runs.

5.4.7. **LC-MS Method and Data Analysis**

All samples were acquired in Data-Dependent Acquisition (DDA) using a TripleTOF 5600 mass spectrometer (Sciex, Concord, Ontario, Canada) coupled to a NanoLC 400 HPLC system (Eksigent, Dublin, CA). Histone samples were loaded onto a YMC TriArt C18 trap column (id 500μm, length 5mm, particle size 3 μm) at a flow rate of 5 μL/min for 5 min in 0.1% trifluoroacetic acid (TFA) in water. Afterwards, histone peptides were transferred to a microLC YMC TriArt C18 column (id 300 μm, length 15 cm, particle size 3 μm) and separated at a flow rate of 5 μL/min using a gradient of 60 min going from 3 to 45 % mobile phase B. Mobile phase A consisted of UPLC-grade water spiked with 0.1% (v/v) FA and 3% (v/v) DMSO, while mobile phase B consisted of UPLC-grade ACN spiked with 0.1% (v/v) FA. The 10 most intense precursors ions from 400-1250 m/z with charge states 2-5 that exceed

300 counts per second were selected for fragmentation, and the corresponding fragmentation MS2 spectra were collected between 65-2000 m/z for 200 ms. After the fragmentation event, the precursor ions were dynamically excluded from reselection for 10 s. Progenesis QI for Proteomics (Progenesis QIP v4.1, Nonlinear Dynamics, Waters) was used to process the raw LC–MS data as described before [108]. In short, raw data was imported and aligned in the Progenesis software, after which the detected peptide spectra were annotated to histone PTMs using Mascot (Matrix Science) with the same settings as described in [44]. Once histone PTMs were identified, relative abundances of each PTM were calculated by dividing the area under the curve (AUC) of each peptidoform containing the PTM by the sum of AUCs for all observed forms of that peptide. Significant ($p < 0.05$) differences in PTM relative abundance between treatment groups and the untreated controls were identified by performing two-tailed student t-tests.

5.4.8. Protein extraction and Western blot analysis

To validate and quantify histone PTMs, 6 µg of purified histone extracts were resuspended in 4 X Laemmli buffer diluted in high-purity water. Protein separation and Western blot detection were performed as previously described [102]. Whole cell lysates of RSL3-treated cells were obtained by lysing cell pellets (1×10^6 cells) in 0.5 ml RIPA buffer (150 mM NaCl, 0.1% Triton X-100, 0.1% SDS, 50 mM Tris-HCl pH 8) supplemented with protease inhibitors (Complete Mini®, Roche). Soluble protein extracts were obtained after 15 min incubation on ice followed by brief sonication and centrifugation at 16 g for 20 min at 4°C. All blots were blocked for 1 hour at RT in 5 % BSA blocking buffer and incubated overnight with primary antibody at 4 °C. After 2 hour incubation at RT with dye-conjugates secondary antibody (Dako, Glostrup, Denmark), signal intensities were measured with the Amersham Imager 680 (Cytiva) and quantified with Image J software.

5.4.9. Gel Filtration Chromatography

Commercially available H3-H4 tetramers (Epicypher, Durham, NC, USA) were incubated for 30 min with a tenfold excess of $FeSO_4$, $CuSO_4$ (positive control), or K_2SO_4 (negative control). After 15 min centrifugation at 13 400 rpm, samples were loaded on a Superdex 200 HR 10/300 GL gelfiltration column (Cytiva, MA, USA) equilibarated with running buffer (500 mM NaCl, pH 7.2) at a flow rate of 0,5 ml/min. Absorbance was measured at 280 nm and retention times were compared to those of the Biorad Broad Range Standard (Biorad, CA, USA).

5.4.10. DNA Extraction and Bisulfite Conversion

Total DNA from MM1 cells was isolated using the QIAmp DNA mini kit (Qiagen, Venlo, Netherlands) according to the manufacturer's instructions. Subsequent bisulfite conversion of 1 µg isolated DNA was performed using the EpiTect Fast Bisulfite Conversion kit (Qiagen, Venlo, Netherlands) and the EZ DNA Methylation Kit (Zymo Research, Irvine, CA, USA) for pyrosequencing and Infinium MethylationEPIC analysis, respectively. To confirm successful bisulfite conversion, a PCR using bisulfite-specific primers was executed

with the PyroMark PCR kit (Qiagen, Venlo, Netherlands) and the resulting PCR product was visualized on a 2 % agarose gel to which GelRed™ staining (Biotium, Fremont, CA, USA) was added. Primers sequences are listed in Supplementary Table S2.

5.4.11. LINE-1 Pyrosequencing

Methylation of LINE-1 in MM1 cells was analyzed by Pyrosequencing, as previously described [109]. Briefly, all required primers (i.e. forward, biotinylated-reverse, and sequencing primers) were designed using the PyroMaker Assay Design 2.0 software (Qiagen, Venlo, Netherlands) and sequences are provided in Supplementary Table S2X. Bisulfite converted LINE-1 DNA fragments were PCR amplified using the PyroMark PCR kit (Qiagen, Venlo, Netherlands). Successful PCR amplification was assessed by TBE electrophoresis at 2 % agarose gel as described above after which the PyroMark Q24 Instrument (Qiagen, Venlo, Netherlands) was used to perform Pyrosequencing. Biotinylated PCR products were immobilized on streptavidin-coated Sepharose beads (High Performance, GE Healthcare, Chicago, IL, USA), captured by the PyroMark vacuum Q24 workstation, washed and denatured. Single-stranded PCR products were then released into a 24-well plate and annealed to the sequencing primer for 2 min at 80 °C. After completion of the pyrosequencing run, results were analyzed using the PyroMark Q24 software (Qiagen, Venlo, Netherlands).

5.4.12. Infinium Methylation EPIC BeadChip Analysis

Genome-wide DNA methylation was analyzed on the Infinium Methylation EPIC BeadChip platform (Illumina, San Diego, CA, USA) at the Center for Medical Genetics (UZA, University of Antwerp). 500 ng of bisulfite-converted DNA from MM1S and MM1R cells left untreated, treated with 1 µM RSL3 or treated with 2 µM Fer-1 and 1 µM RSL3 was used for whole genome amplification, enzymatic fragmentation, precipitation and resuspension as described in the manufacturer's protocol. EPIC chips were analyzed using the Illumina Hi-Scan system and DNA methylation was measured at 866.836 CpG sites.

DNA methylation data was processed using the minfi (v1.36.0) [110] and limma (v3.46.0) [111] R packages as described by Maksimovic and colleagues [112]. Quality control of all samples occurred by evaluating whether < 95 % of the CpG probes had a detection p-value of < 0.05. Data was subsequently corrected for background signal and normalized using quantile normalization. Finally, cross-reactive and SNP-proximal probes were removed from the data [112]. Normalized data was subsequently analyzed for target selection with a cut-off of 10 % differential methylation and FDR < 0.05. Methylation intensities for each probe are represented as β-values [113]. Heatmap visualization of differentially methylated probes was generated using the heatmap.2 R package (v3.1.1). Pathway enrichment of differentially methylated probes was performed using the Metascape online tool [51]. Methylation data have been deposited in the NCBI GEO database (awaiting accession number).

5.4.13. Global DNA Methylation by LC-MS/MS

DNA was analyzed by LC-MS/MS as previously described [114]. In short, 0.5 µg of isolated DNA was enzymatically hydrolyzed to individual deoxyribonucleosides by a one-step DNA hydrolysis procedure consisting of a digest mix prepared by adding phosphodiesterase I, alkaline phosphatase and benzonase nuclease to Tris-HCl buffer (Sigma-Aldrich, Saint Louis, MO, USA). Global genomic DNA (hdyroxy)methylation was measured using ultrapressure liquid-chromatography combined with tandem mass spectrometry. Absolute concentrations of cytosine (C), 5-methylcytosine (5-mC), and 5-hydroxymethylcytosine (5-hmC) were calculated by interpolation the results onto a calibration curve. The results are expressed as DNA methylation in percentage (%) [calculated as 5-mC/(5-mC + 5-hmC + C)], and DNA hydroxymethylation (%) [calculated as 5-hmC/(5-mC +5-hmC + C)].

5.5. Supplementary Material
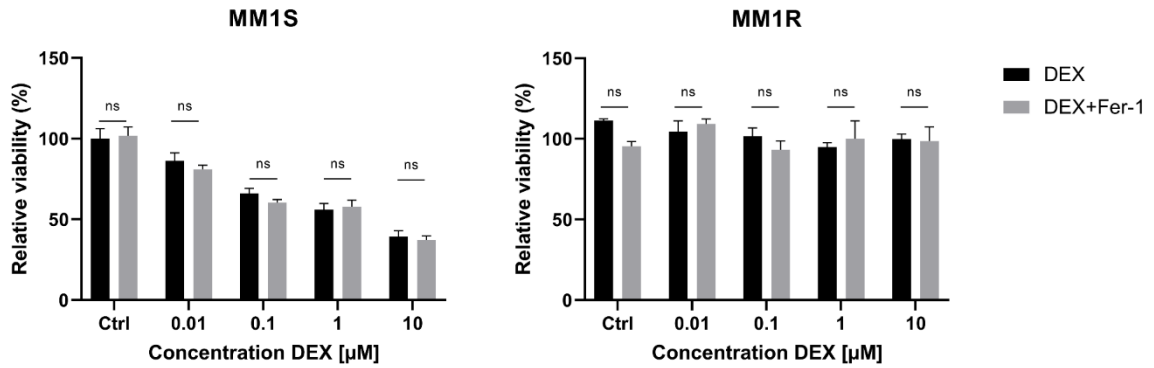
Figure S1: Relative viability of MM1S (left) and MM1R (right) cells upon 24 h exposure to increasing concentrations of dexamethasone (DEX) with or without pretreatment with ferrostatin-1 (Fer-1). Data are plotted as the mean ± s.d., *n*=3 biologically independent replicates (ns p < 0.05, ANOVA).
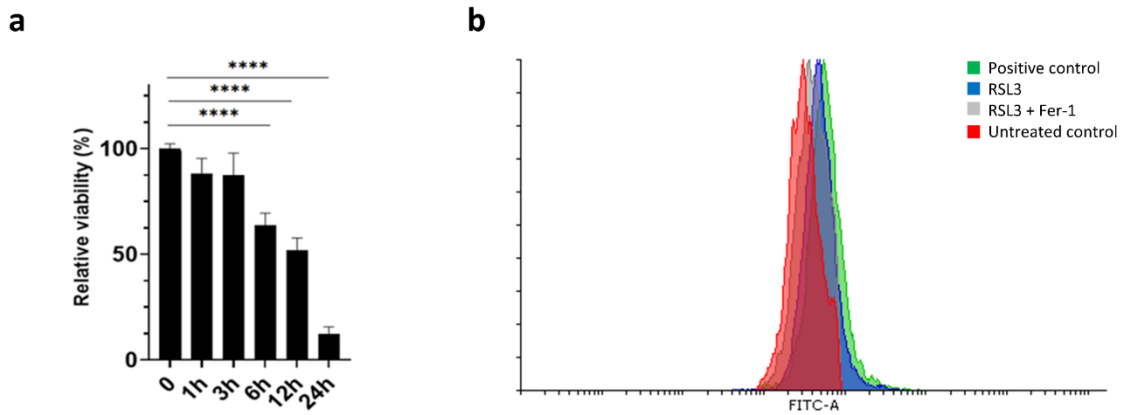
Figure S2: (**a**) Time-dependent relative viability of MM1 cells after 5 µM RSL3 treatment. Data are plotted as the mean ± s.d., *n*=3 biologically independent replicates (****p < 0.0001, ANOVA). (**b**) Flow cytometric analysis of the lipid peroxidation sensor (C11-BODIPY-581/591 dye) on live MM1R cells after 3h treatment with 5µM RSL3 with or without pre-treatment with 2 µM ferrostatin-1 (Fer-1) or 100 µM cumene hydroxide (positive control).
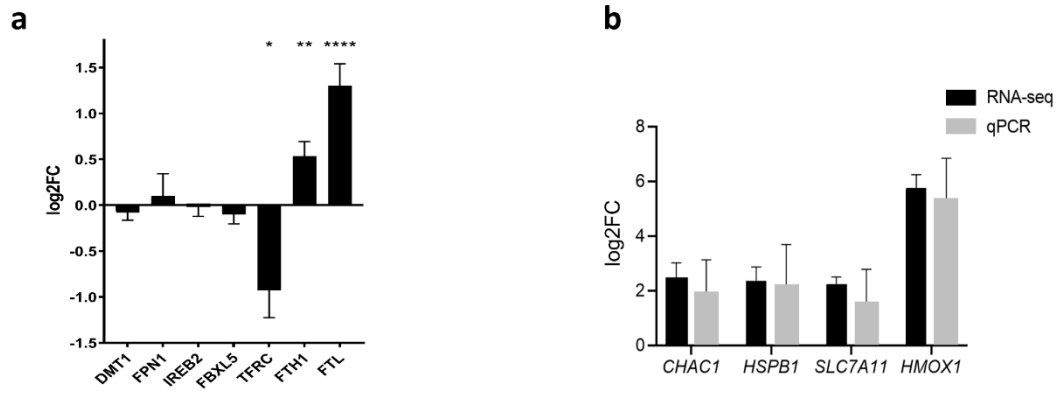
Figure S3: (**a**) LogFC of iron-responsive genes in RSL3-treated MM1 cells versus untreated controls as determined by RNAseq. Data are plotted as the mean logFC ± SEM, *n*=3 biologically independent replicates per cell line (*p < 0.05, **p < 0.01, ****p < 0.0001, ANOVA). (**b**) Comparison of log2FC of RNAseq and qPCR analysis of 4 ferroptosis-related genes. Data are plotted as the mean ± s.d., *n*=3 biologically independent replicates per cell line.
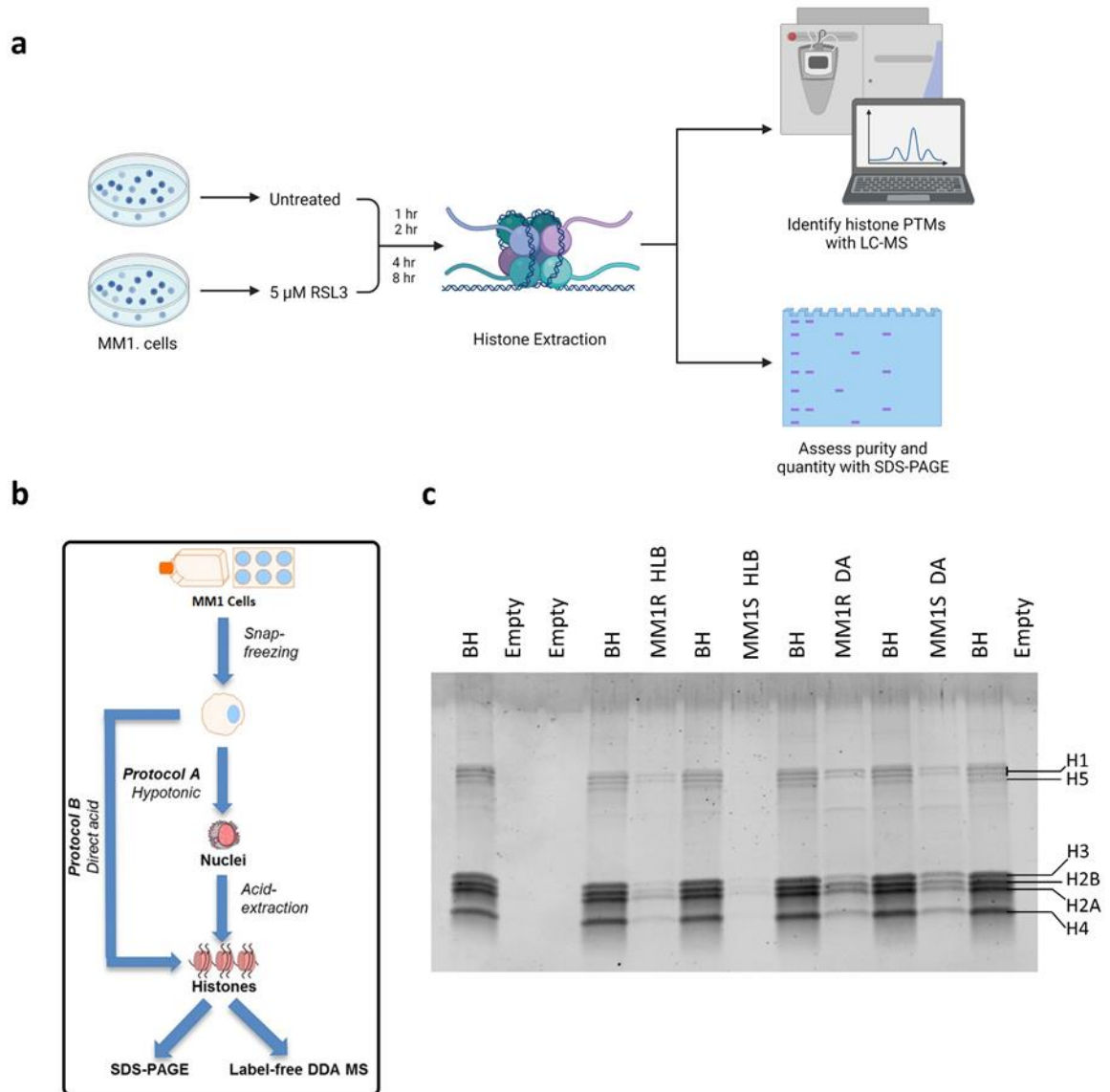
Figure S4: Histone extraction optimization from MM1 cells for LC-MS analysis of post-translational modifications (PTMs). (**a**) Experimental pipeline for identification of histone PTMs with liquid chromatography-mass spectrometry (LC-MS). Prior to LC-MS analysis, purity and quantity of histone extracts is assessed with polyacrylamide gel electrophoresis (PAGE). Figure created with BioRender.com. (**b**) Lysis protocols that were explored for histone extraction from MM1 cells. Adapted from [108]. (**c**) Purity of MM1 histone extracts obtained with either hypotonic lysis buffer (HLB) or direct acid lysis (DA). Extracts from 4 x 10^5 cells were loaded onto a 8-16 % gradient gel and compared to a 2 µg bovine histone (BH) commercial standard.
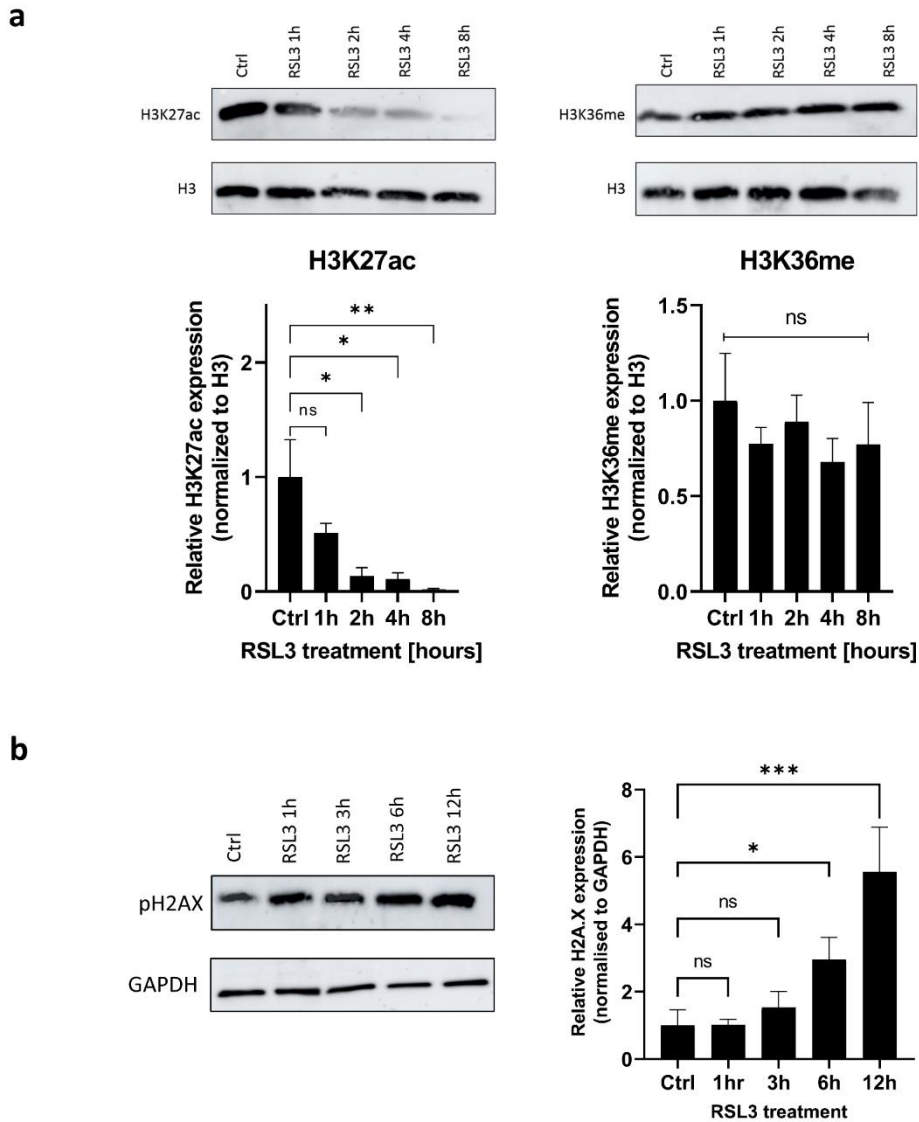
Figure S5: (**a**) Western blot validation of histone proteomics LC-MS data. H3K27ac (left) was significantly upregulated upon RSL3 treatment in MM1 cells while H3K36me3 (right) levels remained unchanged, both in LC-MS and Western blot analysis. (**b**) Western blot detection and quantification of pH2AX and GAPDH expression levels after RSL3 treatment in MM1 cells. Data are plotted as the mean ± s.d., *n*=3 biologically independent replicates. (ns p > 0.05, *p < 0.05, **p < 0.01, ***p <0.001 ANOVA).
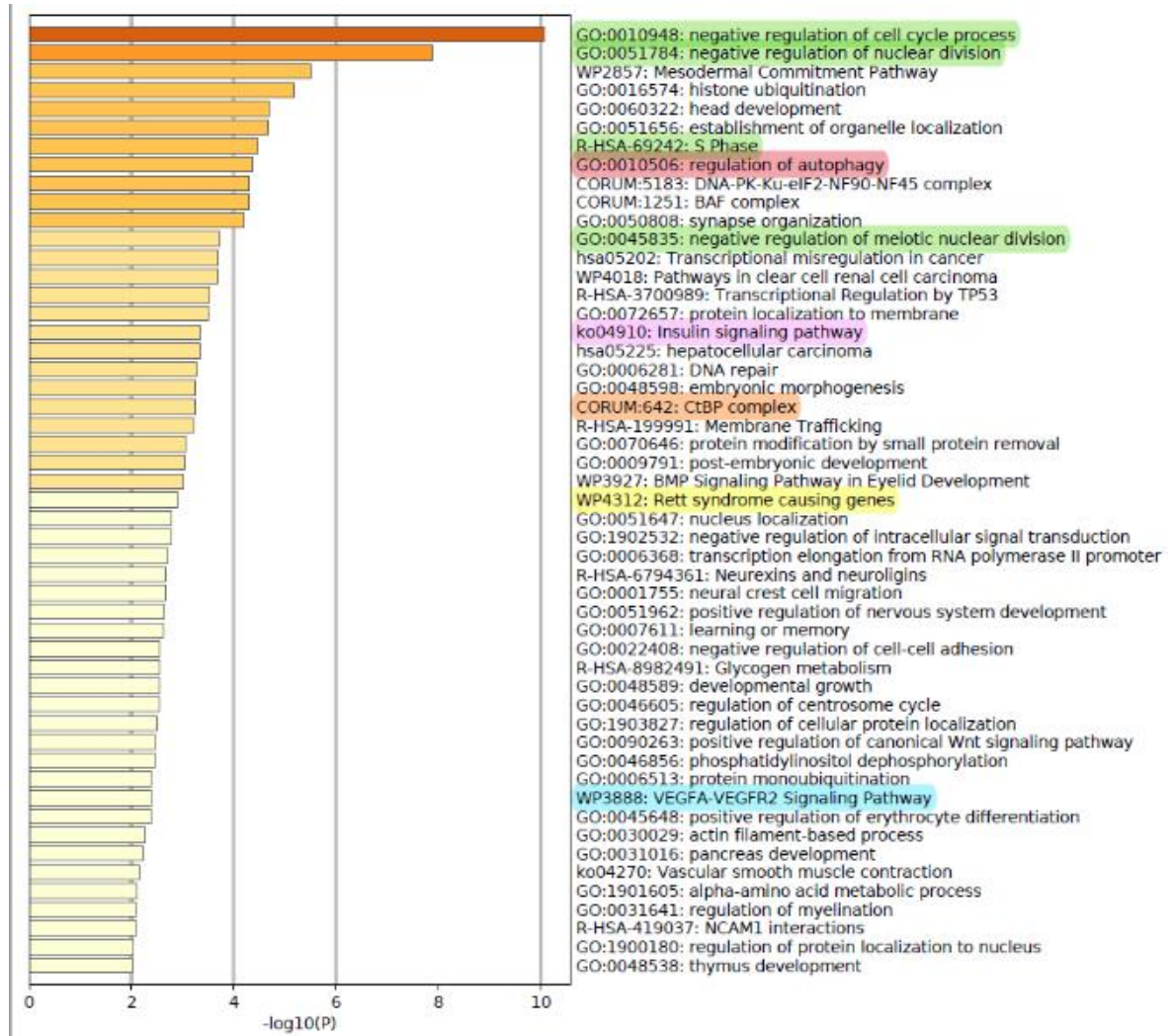
Figure S6: Metascape pathway enrichment of significantly differentially methylated CpG probes (FDR <0.05 & Δβ differences > 0.1) in RSL3-treated **MM1S** cells compared to Ferrostatin-1 pre-treated, RSL3-treated MM1S cells. Terms marked in color are common pathways between MM1S and MM1R cells (see Supplementary Figure S6).
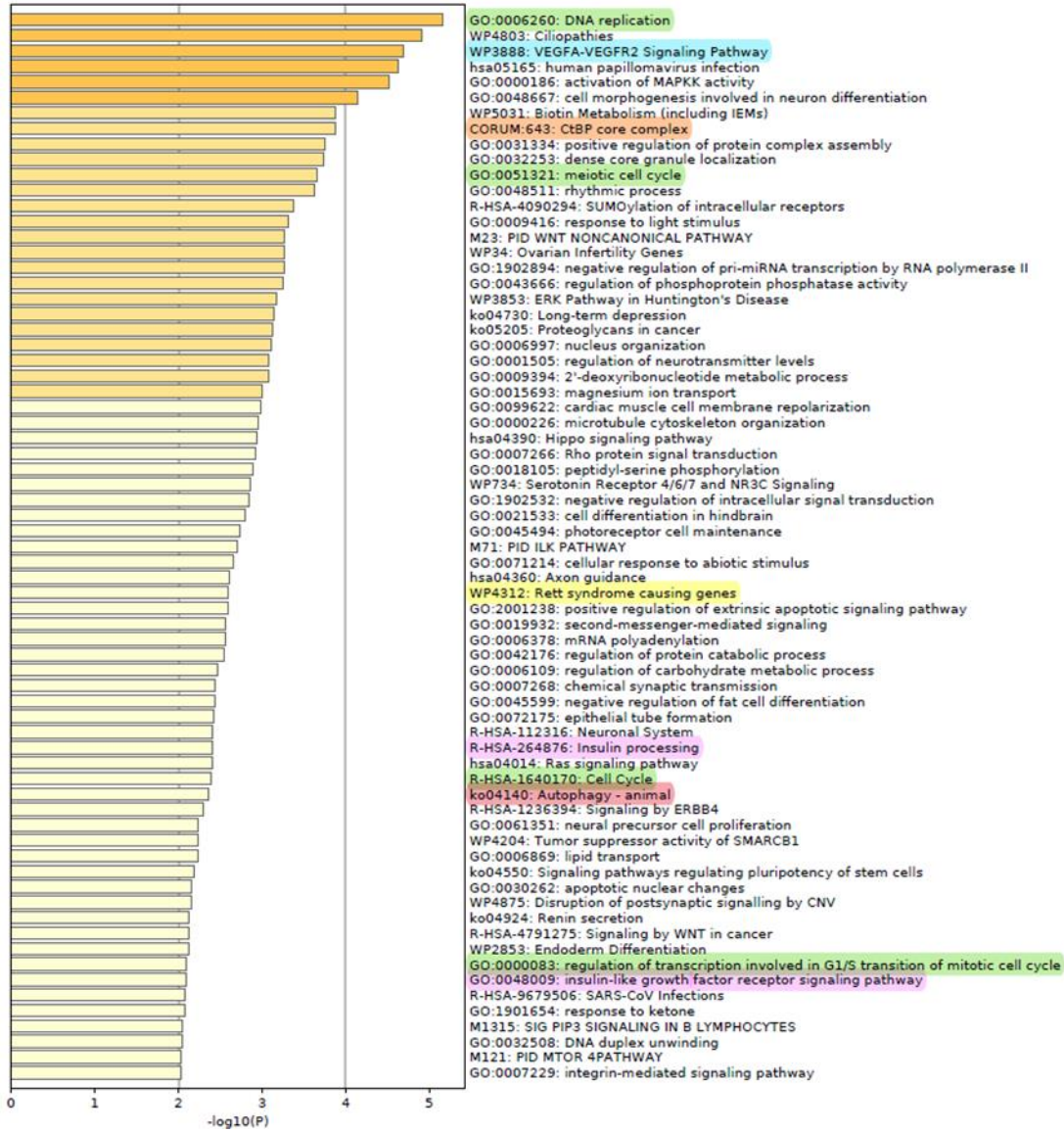
Figure S7: Metascape pathway enrichment of significantly differentially methylated CpG probes (FDR <0.05 & Δβ differences > 0.1) in RSL3-treated **MM1R** cells compared to Ferrostatin-1 pre-treated, RSL3-treated MM1S cells. Terms marked in color are common pathways between MM1S and MM1R cells (see Supplementary Figure S5).

Table S1: Overview of significantly altered histone PTMs in RSL3-treated MM1 cells compared to untreated controls.

Histone	PTM	Sequence	Log2FC				p.value			
			1 h	2 h	4 h	8 h	1 h	2 h	4 h	8 h
H2A	E57Fe	VGAGAPVYMAAVLEYLTAEILELAGNAAR	0,20	0,61	0,69	0,56	3,70E-01	1,46E-03	1,75E-04	5,90E-03
	R89Cit	HLQLAIRNDEELNKLLGR	-0,15	-0,63	-0,47	-0,53	4,51E-01	1,27E-02	5,28E-02	3,54E-02
	E93Fe	NDEELNKLLGR	0,32	0,63	0,80	0,90	1,21E-01	6,33E-04	1,93E-05	1,84E-04
	K96Ac	HLQLAIRNDEELNKLLGK	0,52	2,26	2,86	1,93	2,99E-01	5,55E-03	1,37E-03	1,17E-02
	K100Ac	HLQLAIRNDEELNKLLGK	0,52	2,26	2,86	1,93	2,99E-01	5,55E-03	1,37E-03	1,17E-02
	K100But	HLQLAIRNDEELNKLLGK	0,52	2,26	2,86	1,93	2,99E-01	5,55E-03	1,37E-03	1,17E-02
H2A.Z	K8Ac	AGGKAGKDSGKAKAKAVSR	0,08	-0,14	-0,23	-0,61	6,84E-01	4,78E-01	2,78E-01	1,68E-02
	K14Ac	AGGKAGKDSGKAKAKAVSR	-0,77	-2,49	-2,32	-2,08	2,29E-01	1,36E-02	1,61E-02	2,81E-02
	K16Suc	AGGKAGKDSGKAKAKAVSR	-0,77	-2,49	-2,32	-2,08	2,29E-01	1,36E-02	1,61E-02	2,81E-02
	K16Hib	AGGKAGKDSGKAKAKAVSR	-0,43	-3,28	-2,15	-2,15	5,66E-01	3,18E-02	6,74E-02	8,32E-02
	K102Hib	HLQLAIRGDEELDSLIKATIAGGGVIPHIHKSLIGKKGQQKTA	-0,08	-0,56	-0,98	-0,84	8,10E-01	1,21E-01	1,94E-02	4,04E-02
	K120Cro	HLQLAIRGDEELDSLIKATIAGGGVIPHIHKSLIGKKGQQKTA	-0,08	-0,56	-0,98	-0,84	8,10E-01	1,21E-01	1,94E-02	4,04E-02

	K121Me3	HLQLAIRGDEELDSLIKATIAGGGVIPHIHKSLIGKKGQQKTA	-0,08	-0,56	-0,98	-0,84	8,10E-01	1,21E-01	1,94E-02	4,04E-02
	K121But	HLQLAIRGDEELDSLIKATIAGGGVIPHIHKSLIGKKGQQKTA	-0,20	-1,55	-0,87	-0,63	5,91E-01	2,93E-03	4,95E-02	0,14E-01
	K125Me3	HLQLAIRGDEELDSLIKATIAGGGVIPHIHKSLIGKKGQQKTA	-0,08	-0,56	-0,98	-0,84	8,10E-01	1,21E-01	1,94E-02	4,04E-02
H2A.FY	K33But	YIKKGHPKYR	-0,04	-0,90	-1,32	0,56	8,36E-01	1,72E-03	5,90E-05	0,38E-01
	K34Me3	YIKKGHPKYR	-0,04	-0,90	-1,32	0,56	8,36E-01	1,72E-03	5,90E-05	0,38E-01
	R79Me	VTPRHILLAVANDEELNQLLKGVTIASGGVLPNIHPELLAKKR	0,09	0,55	0,62	0,73	8,19E-01	9,05E-02	7,74E-02	2,34E-02
H3	K18Ac	KQLATKAAR	-0,61	-5,01	-2,99	-3,30	4,03E-01	1,67E-02	3,11E-02	3,31E-02
	K27Ac	KSAPATGGVKKPHR	-0,40	-0,56	-0,72	-0,56	1,38E-01	6,21E-02	2,19E-02	8,62E-02
	K37Me3	KSAPATGGVKKPHR	-0,91	-2,79	-2,80	-2,03	7,09E-02	8,88E-04	9,00E-04	5,21E-03
	K37Bu	KSAPSTGGVKKPHR	-0,11	0,19	0,17	0,34	3,94E-01	1,27E-01	1,91E-01	2,02E-03
	R40Cit	KSAPATGGVKKPHR	0,12	0,45	0,31	0,66	4,46E-01	5,00E-04	6,95E-02	3,99E-05
	D77Fe	EIAQDFKTDLR	0,25	0,73	0,78	0,62	2,73E-01	1,79E-04	6,56E-05	5,31E-03
	K79But	EIAQDFKTDLR	0,04	0,25	0,11	0,74	7,54E-01	4,46E-02	3,66E-01	2,48E-04
	K79Me3	EIAQDFKTDLR	-0,27	-0,84	-0,80	-1,07	4,76E-02	1,14E-06	2,40E-06	1,45E-07

	R83Cit	EIAQDFKTDLR	0,01	0,22	-0,08	0,94	9,72E-01	3,56E-01	7,61E-01	3,99E-03
	M97Ox	VTIMPKDIQLAR	0,57	1,43	1,39	1,32	1,36E-02	2,49E-02	2,46E-02	2,48E-02
	D100Fe	VTIMPKDIQLAR	0,56	1,57	2,25	1,38	1,43E-01	2,83E-01	0,35E-01	0,27E-01
H4	R17Me	GKGGKGLGKGGAKRHR	-0,17	0,47	0,02	0,53	5,09E-01	2,53E-02	9,31E-01	1,02E-02
	E63Fe	GVLKVFLENVIR	0,37	0,88	0,96	0,60	4,50E-01	2,32E-02	1,51E-02	0,18E-01
	M84Ox	KTVTAMDVVYALKR	0,12	0,29	0,29	0,28	2,46E-01	3,92E-03	3,81E-03	7,12E-03
	D85Fe	KTVTAMDVVYALKR	0,09	0,57	0,54	0,52	5,36E-01	1,56E-05	1,23E-04	4,66E-04

Table S2: Overview of primers used in this study

Target		Primer Sequence	Gene accession number
qPCR primers			
CHAC1	Forward	ATG CCT GGC CGT GTG G	ENSG00000128965
	Reverse	GCT TAC CTG CTC CCC TTG C	
HSPB1	Forward	AGG ATG GCG TGG TGG AGA T	ENSG00000106211
	Reverse	GAT GTA GCC ATG CTC GTC CTG	
SLC7A11	Forward	CAC ATG CCT CTT CAT GGT TG	ENSG00000151012
	Reverse	AGT GAT GAC GAA GCC AAT CC	
HMOX1	Forward	CCA GCG GGC CAG CAA CAA AGT GC	ENSG00000100292
	Reverse	AAG CCT TCA GTG CCC ACG GTA AGG	
ACTB	Forward	CTG GAA CGG TGA AGG TGA CA	ENSG00000075624
	Reverse	AAG GGA CTTC CTG TAA CAA TGC A	
NR4A2	Forward	GGT CCC TTT TGC CTG TCC A	ENSG00000153234
	Reverse	TGG CTT CAG CCG AGT TAC AG	
Methylation-specific PCR primers			
SALL3	Forward	GTT TGG GTT TGG TTT TTG TT	ENSG00000263310
	Reverse	ACC CTT TAC CAA TCT CTT AAC TTT C	
Pyrosequencing primers			
LINE-1	Forward	TTT TTT GAG TTA GGT GTG GG	
	Reverse	TCT CAC TAA AAA ATA CCA AAC AA	
	Sequencing	GGG TGG GAG TGA T	

5.6. References

1. Kazandjian D. Multiple myeloma epidemiology and survival: A unique malignancy. Semin Oncol. 2016;43(6):676-81.
2. Nunnelee J, Zhao QH, Benson DM, Rosko AE, Chaudhry M, Bumma N, Khan AM, Devarakonda S, Efebera YA, Sharma N. Improvement in Survival of Multiple Myeloma Patients: A Long-Term Institutional Experience. Blood. 2019;134.
3. Martinez-Banos D, Sanchez-Hernandez B, Jimenez G, Barrera-Lumbreras G, Barrales-Benitez O. Global methylation and promoter-specific methylation of the P16, SOCS-1, E-cadherin, P73 and SHP-1 genes and their expression in patients with multiple myeloma during active disease and remission. Exp Ther Med. 2017;13(5):2442-50.
4. Li J, Hu WX, Luo SQ, Xiong DH, Sun S, Wang YP, Bu XF, Liu J, Hu J. Promoter methylation induced epigenetic silencing of DAZAP2, a downstream effector of p38/MAPK pathway, in multiple myeloma cells. Cell Signal. 2019;60:136-45.
5. Popovic R, Martinez-Garcia E, Giannopoulou EG, Zhang Q, Zhang Q, Ezponda T, Shah MY, Zheng Y, Will CM, Small EC, et al. Histone methyltransferase MMSET/NSD2 alters EZH2 binding and reprograms the myeloma epigenome through global and focal changes in H3K36 and H3K27 methylation. PLoS Genet. 2014;10(9):e1004566.
6. Ren Z, Ahn JH, Liu H, Tsai YH, Bhanu NV, Koss B, Allison DF, Ma A, Storey AJ, Wang P, et al. PHF19 promotes multiple myeloma tumorigenicity through PRC2 activation and broad H3K27me3 domain formation. Blood. 2019;134(14):1176-89.
7. Handa H, Murakami Y, Ishihara R, Kimura-Masuda K, Masuda Y. The Role and Function of microRNA in the Pathogenesis of Multiple Myeloma. Cancers (Basel). 2019;11(11).
8. Tatekawa S, Chinen Y, Ri M, Narita T, Shimura Y, Matsumura-Kimoto Y, Tsukamoto T, Kobayashi T, Kawata E, Uoshima N, et al. Epigenetic repression of miR-375 is the dominant mechanism for constitutive activation of the PDPK1/RPS6KA3 signalling axis in multiple myeloma. Br J Haematol. 2017;178(4):534-46.
9. Dimopoulos K, Sogaard Helbo A, Fibiger Munch-Petersen H, Sjo L, Christensen J, Sommer Kristensen L, Asmar F, Hermansen NEU, O'Connel C, Gimsing P, et al. Dual inhibition of DNMTs and EZH2 can overcome both intrinsic and acquired resistance of myeloma cells to IMiDs in a cereblon-independent manner. Mol Oncol. 2018;12(2):180-95.
10. Hentati-Kallel M, Le Jan S, Bernard P, Antonicelli F, Trussardi-Regnier A. Histone deacetylases meet microRNA-associated MMP-9 expression regulation in glucocorticoid-sensitive and -resistant cell lines. Int J Oncol. 2017;50(2):717-26.
11. Qin Y, Zhang S, Deng S, An G, Qin X, Li F, Xu Y, Hao M, Yang Y, Zhou W, et al. Epigenetic silencing of miR-137 induces drug resistance and chromosomal instability by targeting AURKA in multiple myeloma. Leukemia. 2017;31(5):1123-35.
12. Issa ME, Takhsha FS, Chirumamilla CS, Perez-Novo C, Vanden Berghe W, Cuendet M. Epigenetic strategies to reverse drug resistance in heterogeneous multiple myeloma. Clin Epigenetics. 2017;9:17.
13. Herviou L, Kassambara A, Boireau S, Robert N, Requirand G, Muller-Tidow C, Vincent L, Seckinger A, Goldschmidt H, Cartron G, et al. PRC2 targeting is a therapeutic strategy for EZ score defined high-risk multiple myeloma patients and overcome resistance to IMiDs. Clin Epigenetics. 2018;10(1):121.
14. Zhou J, Shen Q, Lin H, Hu L, Li G, Zhang X. Decitabine shows potent anti-myeloma activity by depleting monocytic myeloid-derived suppressor cells in the myeloma microenvironment. J Cancer Res Clin Oncol. 2019;145(2):329-36.
15. Che F, Chen J, Dai J, Liu X. Inhibition of Multiple Myeloma Using 5-Aza-2'-Deoxycytidine and Bortezomib-Loaded Self-Assembling Nanoparticles. Cancer Manag Res. 2020;12:6969-76.

16. Gao X, Shen L, Li X, Liu J. Efficacy and toxicity of histone deacetylase inhibitors in relapsed/refractory multiple myeloma: Systematic review and meta-analysis of clinical trials. Exp Ther Med. 2019;18(2):1057-68.

17. Yang WS, SriRamaratnam R, Welsch ME, Shimada K, Skouta R, Viswanathan VS, Cheah JH, Clemons PA, Shamji AF, Clish CB, et al. Regulation of ferroptotic cancer cell death by GPX4. Cell. 2014;156(1-2):317-31.

18. Wang N, Zeng GZ, Yin JL, Bian ZX. Artesunate activates the ATF4-CHOP-CHAC1 pathway and affects ferroptosis in Burkitt's Lymphoma. Biochem Biophys Res Commun. 2019;519(3):533-9.

19. Zhang Y, Tan H, Daniels JD, Zandkarimi F, Liu H, Brown LM, Uchida K, O'Connor OA, Stockwell BR. Imidazole Ketone Erastin Induces Ferroptosis and Slows Tumor Growth in a Mouse Lymphoma Model. Cell Chem Biol. 2019;26(5):623-33 e9.

20. Dixon SJ, Lemberg KM, Lamprecht MR, Skouta R, Zaitsev EM, Gleason CE, Patel DN, Bauer AJ, Cantley AM, Yang WS, et al. Ferroptosis: an iron-dependent form of nonapoptotic cell death. Cell. 2012;149(5):1060-72.

21. Cort A, Ozben T, Saso L, De Luca C, Korkina L. Redox Control of Multidrug Resistance and Its Possible Modulation by Antioxidants. Oxid Med Cell Longev. 2016;2016:4251912.

22. Wang Y, Yang L, Zhang X, Cui W, Liu Y, Sun QR, He Q, Zhao S, Zhang GA, Wang Y, et al. Epigenetic regulation of ferroptosis by H2B monoubiquitination and p53. EMBO Rep. 2019;20(7):e47563.

23. Jiang Y, Mao C, Yang R, Yan B, Shi Y, Liu X, Lai W, Liu Y, Wang X, Xiao D, et al. EGLN1/c-Myc Induced Lymphoid-Specific Helicase Inhibits Ferroptosis through Lipid Metabolic Gene Expression Changes. Theranostics. 2017;7(13):3293-305.

24. Zhang Y, Koppula P, Gan B. Regulation of H2A ubiquitination and SLC7A11 expression by BAP1 and PRC1. Cell Cycle. 2019;18(8):773-83.

25. Wang Y, Zhao Y, Wang H, Zhang C, Wang M, Yang Y, Xu X, Hu Z. Histone demethylase KDM3B protects against ferroptosis by upregulating SLC7A11. FEBS Open Bio. 2020;10(4):637-43.

26. Huang D, Li Q, Sun X, Sun X, Tang Y, Qu Y, Liu D, Yu T, Li G, Tong T, et al. CRL4(DCAF8) dependent opposing stability control over the chromatin remodeler LSH orchestrates epigenetic dynamics in ferroptosis. Cell Death Differ. 2021;28(5):1593-609.

27. Rroji O, Kumar A, Karuppagounder SS, Ratan RR. Epigenetic regulators of neuronal ferroptosis identify novel therapeutics for neurological diseases: HDACs, transglutaminases, and HIF prolyl hydroxylases. Neurobiol Dis. 2021;147:105145.

28. Wang M, Mao C, Ouyang L, Liu Y, Lai W, Liu N, Shi Y, Chen L, Xiao D, Yu F, et al. Long noncoding RNA LINC00336 inhibits ferroptosis in lung cancer by functioning as a competing endogenous RNA. Cell Death Differ. 2019;26(11):2329-43.

29. Cyr AR, Domann FE. The redox basis of epigenetic modifications: from mechanisms to functional consequences. Antioxid Redox Signal. 2011;15(2):551-89.

30. Wang Y, Yu L, Ding J, Chen Y. Iron Metabolism in Cancer. Int J Mol Sci. 2018;20(1):95.

31. Cao LL, Liu H, Yue Z, Liu L, Pei L, Gu J, Wang H, Jia M. Iron chelation inhibits cancer cell growth and modulates global histone methylation status in colorectal cancer. Biometals. 2018;31(5):797-805.

32. Shi Z, Zhang L, Zheng J, Sun H, Shao C. Ferroptosis: Biochemistry and Biology in Cancers. Front Oncol. 2021;11:579286.

33. Kawai K, Li YS, Song MF, Kasai H. DNA methylation by dimethyl sulfoxide and methionine sulfoxide triggered by hydroxyl radical and implications for epigenetic modifications. Bioorg Med Chem Lett. 2010;20(1):260-5.

34 .Liu N, Lin X, Huang C. Activation of the reverse transsulfuration pathway through NRF2/CBS confers erastin-induced ferroptosis resistance. Br J Cancer. 2020;122(2):279-92.

35. Lertratanangkoon K, Wu CJ, Savaraj N, Thomas ML. Alterations of DNA methylation by glutathione depletion. Cancer Lett. 1997;120(2):149-56.

36. Ulrey CL, Liu L, Andrews LG, Tollefsbol TO. The impact of metabolism on DNA methylation. Hum Mol Genet. 2005;14 Spec No 1:R139-47.

37. Pinto V, Bergantim R, Caires HR, Seca H, Guimaraes JE, Vasconcelos MH. Multiple Myeloma: Available Therapies and Causes of Drug Resistance. Cancers (Basel). 2020;12(2).

38. Hassannia B, Logie E, Vandenabeele P, Vanden Berghe T, Vanden Berghe W. Withaferin A: From ayurvedic folk medicine to preclinical anti-cancer drug. Biochem Pharmacol. 2020;173:113602.

39. Rai M, Jogee PS, Agarkar G, dos Santos CA. Anticancer activities of Withania somnifera: Current research, formulations, and future perspectives. Pharm Biol. 2016;54(2):189-97.

40. Hassannia B, Wiernicki B, Ingold I, Qu F, Van Herck S, Tyurina YY, Bayir H, Abhari BA, Angeli JPF, Choi SM, et al. Nano-targeted induction of dual ferroptotic mechanisms eradicates high-risk neuroblastoma. J Clin Invest. 2018;128(8):3341-55.

41. Chen MS, Wang SF, Hsu CY, Yin PH, Yeh TS, Lee HC, Tseng LM. CHAC1 degradation of glutathione enhances cystine-starvation-induced necroptosis and ferroptosis in human triple negative breast cancer cells via the GCN2-eIF2alpha-ATF4 pathway. Oncotarget. 2017;8(70):114588-602.

42. Sun X, Ou Z, Xie M, Kang R, Fan Y, Niu X, Wang H, Cao L, Tang D. HSPB1 as a novel regulator of ferroptotic cancer cell death. Oncogene. 2015;34(45):5617-25.

43. Dixon SJ, Patel DN, Welsch M, Skouta R, Lee ED, Hayano M, Thomas AG, Gleason CE, Tatonetti NP, Slusher BS, et al. Pharmacological inhibition of cystine-glutamate exchange induces endoplasmic reticulum stress and ferroptosis. Elife. 2014;3:e02523.

44. Verhelst S, De Clerck L, Willems S, Van Puyvelde B, Daled S, Deforce D, Dhaenens M. Comprehensive histone epigenetics: A mass spectrometry based screening assay to measure epigenetic toxicity. MethodsX. 2020;7:101055.

45. Licht JD. Epigenetic Regulation and Therapeutic Targeting in Myeloma Blood. 2018.

46. Dutta A, Abmayr SM, Workman JL. Diverse Activities of Histone Acylations Connect Metabolism to Chromatin Function. Mol Cell. 2016;63(4):547-52.

47. Lee JY, Kim WK, Bae KH, Lee SC, Lee EW. Lipid Metabolism and Ferroptosis. Biology (Basel). 2021;10(3).

48. Flynn EM, Huang OW, Poy F, Oppikofer M, Bellon SF, Tang Y, Cochran AG. A Subset of Human Bromodomains Recognizes Butyryllysine and Crotonyllysine Histone Peptide Modifications. Structure. 2015;23(10):1801-14.

49. Goudarzi A, Zhang D, Huang H, Barral S, Kwon OK, Qi S, Tang Z, Buchou T, Vitte AL, He T, et al. Dynamic Competing Histone H4 K5K8 Acetylation and Butyrylation Are Hallmarks of Highly Active Gene Promoters. Mol Cell. 2016;62(2):169-80.

50. Tan M, Luo H, Lee S, Jin F, Yang JS, Montellier E, Buchou T, Cheng Z, Rousseaux S, Rajagopal N, et al. Identification of 67 histone marks and histone lysine crotonylation as a new type of histone modification. Cell. 2011;146(6):1016-28.

51. Zhou Y, Zhou B, Pache L, Chang M, Khodabakhshi AH, Tanaseichuk O, Benner C, Chanda SK. Metascape provides a biologist-oriented resource for the analysis of systems-level datasets. Nat Commun. 2019;10(1):1523.

52. Attar N, Campos OA, Vogelauer M, Cheng C, Xue Y, Schmollinger S, Salwinski L, Mallipeddi NV, Boone BA, Yen L, et al. The histone H3-H4 tetramer is a copper reductase enzyme. Science. 2020;369(6499):59-64.

53. Ontoso D, Kauppi L, Keeney S, San-Segundo PA. Dynamics of DOT1L localization and H3K79 methylation during meiotic prophase I in mouse spermatocytes. Chromosoma. 2014;123(1-2):147-64.

54. Altaf M, Utley RT, Lacoste N, Tan S, Briggs SD, Cote J. Interplay of chromatin modifiers on a short basic patch of histone H4 tail defines the boundary of telomeric heterochromatin. Mol Cell. 2007;28(6):1002-14.

55. Ng HH, Feng Q, Wang H, Erdjument-Bromage H, Tempst P, Zhang Y, Struhl K. Lysine methylation within the globular domain of histone H3 by Dot1 is important for telomeric silencing and Sir protein association. Genes Dev. 2002;16(12):1518-27.

56. Lazzaro F, Sapountzi V, Granata M, Pellicioli A, Vaze M, Haber JE, Plevani P, Lydall D, Muzi-Falconi M. Histone methyltransferase Dot1 and Rad9 inhibit single-stranded DNA accumulation at DSBs and uncapped telomeres. EMBO J. 2008;27(10):1502-12.

57. Bostelman LJ, Keller AM, Albrecht AM, Arat A, Thompson JS. Methylation of histone H3 lysine-79 by Dot1p plays multiple roles in the response to UV damage in Saccharomyces cerevisiae. DNA Repair (Amst). 2007;6(3):383-95.

58. Zhang AL, Chen L, Ma L, Ding XJ, Tang SF, Zhang AH, Li J. Role of H3K18ac-regulated nucleotide excision repair-related genes in arsenic-induced DNA damage and repair of HaCaT cells. Hum Exp Toxicol. 2020;39(9):1168-77.

59. Zhang PY, Li G, Deng ZJ, Liu LY, Chen L, Tang JZ, Wang YQ, Cao ST, Fang YX, Wen F, et al. Dicer interacts with SIRT7 and regulates H3K18 deacetylation in response to DNA damaging agents. Nucleic Acids Res. 2016;44(8):3629-42.

60. Ma L, Li J, Zhan Z, Chen L, Li D, Bai Q, Gao C, Li J, Zeng X, He Z, et al. Specific histone modification responds to arsenic-induced oxidative stress. Toxicol Appl Pharmacol. 2016;302:52-61.

61. Banerjee DR, Deckard CE, 3rd, Zeng Y, Sczepanski JT. Acetylation of the histone H3 tail domain regulates base excision repair on higher-order chromatin structures. Sci Rep. 2019;9(1):15972.

62. Tasselli L, Xi Y, Zheng W, Tennen RI, Odrowaz Z, Simeoni F, Li W, Chua KF. SIRT6 deacetylates H3K18ac at pericentric chromatin to prevent mitotic errors and cellular senescence. Nat Struct Mol Biol. 2016;23(5):434-40.

63. Schick S, Fournier D, Thakurela S, Sahu SK, Garding A, Tiwari VK. Dynamics of chromatin accessibility and epigenetic state in response to UV damage. J Cell Sci. 2015;128(23):4380-94.

64. .Ito T, Teo YV, Evans SA, Neretti N, Sedivy JM. Regulation of Cellular Senescence by Polycomb Chromatin Modifiers through Distinct DNA Damage- and Histone Methylation-Dependent Pathways. Cell Rep. 2018;22(13):3480-92.

65. Zhou J, So KK, Li Y, Li Y, Yuan J, Ding Y, Chen F, Huang Y, Liu J, Lee W, et al. Elevated H3K27ac in aged skeletal muscle leads to increase in extracellular matrix and fibrogenic conversion of muscle satellite cells. Aging Cell. 2019;18(5):e12996.

66. Guan Y, Zhang C, Lyu G, Huang X, Zhang X, Zhuang T, Jia L, Zhang L, Zhang C, Li C, et al. Senescence-activated enhancer landscape orchestrates the senescence-associated secretory phenotype in murine fibroblasts. Nucleic Acids Res. 2020;48(19):10909-23.

67. Nishibuchi I, Suzuki H, Kinomura A, Sun J, Liu NA, Horikoshi Y, Shima H, Kusakabe M, Harata M, Fukagawa T, et al. Reorganization of damaged chromatin by the exchange of histone variant H2A.Z-2. Int J Radiat Oncol Biol Phys. 2014;89(4):736-44.

68. Kalocsay M, Hiller NJ, Jentsch S. Chromosome-wide Rad51 spreading and SUMO-H2A.Z-dependent chromosome fixation in response to a persistent DNA double-strand break. Mol Cell. 2009;33(3):335-43.

69. Xu Y, Ayrapetov MK, Xu C, Gursoy-Yuzugullu O, Hu Y, Price BD. Histone H2A.Z controls a critical chromatin remodeling step required for DNA double-strand break repair. Mol Cell. 2012;48(5):723-33.

70. Rangasamy D, Berven L, Ridgway P, Tremethick DJ. Pericentric heterochromatin becomes enriched with H2A.Z during early mammalian development. EMBO J. 2003;22(7):1599-607.

71. Meneghini MD, Wu M, Madhani HD. Conserved histone variant H2A.Z protects euchromatin from the ectopic spread of silent heterochromatin. Cell. 2003;112(5):725-36.

72. Hou H, Wang Y, Kallgren SP, Thompson J, Yates JR, 3rd, Jia S. Histone variant H2A.Z regulates centromere silencing and chromosome segregation in fission yeast. J Biol Chem. 2010;285(3):1909-18.

73. Greaves IK, Rangasamy D, Ridgway P, Tremethick DJ. H2A.Z contributes to the unique 3D structure of the centromere. Proc Natl Acad Sci U S A. 2007;104(2):525-30.

74. Avila-Lopez PA, Guerrero G, Nunez-Martinez HN, Peralta-Alvarez CA, Hernandez-Montes G, Alvarez-Hilario LG, Herrera-Goepfert R, Albores-Saavedra J, Villegas-Sepulveda N, Cedillo-Barron L, et al. H2A.Z overexpression suppresses senescence and chemosensitivity in pancreatic ductal adenocarcinoma. Oncogene. 2021;40(11):2065-80.

75. Ruiz PD, Gamble MJ. MacroH2A1 chromatin specification requires its docking domain and acetylation of H2B lysine 20. Nat Commun. 2018;9(1):5143.

76. Lo Re O, Vinciguerra M. Histone MacroH2A1: A Chromatin Point of Intersection between Fasting, Senescence and Cellular Regeneration. Genes (Basel). 2017;8(12).

77. Ruiz PD, Hamilton GA, Park JW, Gamble MJ. MacroH2A1 Regulation of Poly(ADP-Ribose) Synthesis and Stability Prevents Necrosis and Promotes DNA Repair. Mol Cell Biol. 2019;40(1).

78. Pogribny IP, Tryndyak VP, Pogribna M, Shpyleva S, Surratt G, Gamboa da Costa G, Beland FA. Modulation of intracellular iron metabolism by iron chelation affects chromatin remodeling proteins and corresponding epigenetic modifications in breast cancer cells and increases their sensitivity to chemotherapeutic agents. Int J Oncol. 2013;42(5):1822-32.

79. Ye Q, Trivedi M, Zhang Y, Bohlke M, Alsulimani H, Chang J, Maher T, Deth R, Kim J. Brain iron loading impairs DNA methylation and alters GABAergic function in mice. FASEB J. 2019;33(2):2460-71.

80. Bockmuhl Y, Patchev AV, Madejska A, Hoffmann A, Sousa JC, Sousa N, Holsboer F, Almeida OF, Spengler D. Methylation at the CpG island shore region upregulates Nr3c1 promoter activity after early-life stress. Epigenetics. 2015;10(3):247-57.

81. Pistritto G, Trisciuoglio D, Ceci C, Garufi A, D'Orazi G. Apoptosis as anticancer mechanism: function and dysfunction of its modulators and targeted therapeutic strategies. Aging (Albany NY). 2016;8(4):603-19.

82. Löffler D, Brocke-Heidrich K, Pfeifer G, Stocsits C, Hackermüller J, Kretzschmar AK, Burger R, Gramatzki M, Blumert C, Bauer K, et al. Interleukin-6 dependent survival of multiple myeloma cells involves the Stat3-mediated induction of microRNA-21 through a highly conserved enhancer. Blood. 2007;110(4):1330-3.

83. Hurt EM, Thomas SB, Peng B, Farrar WL. Reversal of p53 epigenetic silencing in multiple myeloma permits apoptosis by a p53 activator. Cancer Biol Ther. 2006;5(9):1154-60.

84. Enright HU, Miller WJ, Hebbel RP. Nucleosomal histone protein protects DNA from iron-mediated damage. Nucleic Acids Res. 1992;20(13):3341-6.

85. Gallipoli P, Huntly BJP. Histone modifiers are oxygen sensors. Science. 2019;363(6432):1148-9.

86. Campit SE, Meliki A, Youngson NA, Chandrasekaran S. Nutrient Sensing by Histone Marks: Reading the Metabolic Histone Code Using Tracing, Omics, and Modeling. BioEssays. 2020;42(9):2000083.

87. .Jo C, Park S, Oh S, Choi J, Kim EK, Youn HD, Cho EJ. Histone acylation marks respond to metabolic perturbations and enable cellular adaptation. Exp Mol Med. 2020;52(12):2005-19.

88. Camarena V, Sant DW, Huff TC, Mustafi S, Muir RK, Aron AT, Chang CJ, Renslo AR, Monje PV, Wang G. cAMP signaling regulates DNA hydroxymethylation by augmenting the intracellular labile ferrous iron pool. Elife. 2017;6.

89. Schachtschneider KM, Liu Y, Rund LA, Madsen O, Johnson RW, Groenen MA, Schook LB. Impact of neonatal iron deficiency on hippocampal DNA methylation and gene transcription in a porcine biomedical model of cognitive development. BMC Genomics. 2016;17(1):856.

90. Smith AG, Luk N, Newton RA, Roberts DW, Sturm RA, Muscat GE. Melanocortin-1 receptor signaling markedly induces the expression of the NR4A nuclear receptor subgroup in melanocytic cells. J Biol Chem. 2008;283(18):12564-70.

91. Beard JA, Tenga A, Hills J, Hoyer JD, Cherian MT, Wang YD, Chen T. The orphan nuclear receptor NR4A2 is part of a p53-microRNA-34 network. Sci Rep. 2016;6:25108.

92. Paillasse MR, de Medina P. The NR4A nuclear receptors as potential targets for anti-aging interventions. Med Hypotheses. 2015;84(2):135-40.

93. Sharpless NE, Sherr CJ. Forging a signature of in vivo senescence. Nat Rev Cancer. 2015;15(7):397-408.

94. Chen PH, Tseng WH, Chi JT. The Intersection of DNA Damage Response and Ferroptosis-A Rationale for Combination Therapeutics. Biology (Basel). 2020;9(8).

95. Li S, Wang M, Wang Y, Guo Y, Tao X, Wang X, Cao Y, Tian S, Li Q. p53-mediated ferroptosis is required for 1-methyl-4-phenylpyridinium-induced senescence of PC12 cells. Toxicol In Vitro. 2021;73:105146.

96. Wei Z, Hao C, Huangfu J, Srinivasagan R, Zhang X, Fan X. Aging lens epithelium is susceptible to ferroptosis. Free Radic Biol Med. 2021;167:94-108.

97. .Sun Y, Zheng Y, Wang C, Liu Y. Glutathione depletion induces ferroptosis, autophagy, and premature cell senescence in retinal pigment epithelial cells. Cell Death Dis. 2018;9(7):753.

98. Huang Y, Wu B, Shen D, Chen J, Yu Z, Chen C. Ferroptosis in a sarcopenia model of senescence accelerated mouse prone 8 (SAMP8). Int J Biol Sci. 2021;17(1):151-62.

99. Masaldan S, Clatworthy SAS, Gamell C, Meggyesy PM, Rigopoulos AT, Haupt S, Haupt Y, Denoyer D, Adlard PA, Bush AI, et al. Iron accumulation in senescent cells is coupled with impaired ferritinophagy and inhibition of ferroptosis. Redox Biol. 2018;14:100-15.

100. Borrelli C, Ricci B, Vulpis E, Fionda C, Ricciardi MR, Petrucci MT, Masuelli L, Peri A, Cippitelli M, Zingoni A, et al. Drug-Induced Senescent Multiple Myeloma Cells Elicit NK Cell Proliferation by Direct or Exosome-Mediated IL15 Trans-Presentation. Cancer Immunol Res. 2018;6(7):860-9.

101. Go S, Kang M, Kwon SP, Jung M, Jeon OH, Kim BS. The Senolytic Drug JQ1 Removes Senescent Cells via Ferroptosis. Tissue Eng Regen Med. 2021.

102. Logie E, Chirumamilla CS, Perez-Novo C, Shaw P, Declerck K, Palagani A, Rangarajan S, Cuypers B, De Neuter N, Mobashar Hussain Urf Turabe F, et al. Covalent Cysteine Targeting of Bruton's Tyrosine Kinase (BTK) Family by Withaferin-A Reduces Survival of Glucocorticoid-Resistant Multiple Myeloma MM1 Cells. Cancers (Basel). 2021;13(7).

103. .Andrews S. FastQC: a quality control tool for high throughput sequence data. Babraham Bioinformatics, Babraham Institute, Cambridge, United Kingdom; 2010

104. Dobin A, Davis CA, Schlesinger F, Drenkow J, Zaleski C, Jha S, Batut P, Chaisson M, Gingeras TR. STAR: ultrafast universal RNA-seq aligner. Bioinformatics. 2013;29(1):15-21.

105. Love MI, Huber W, Anders S. Moderated estimation of fold change and dispersion for RNA-seq data with DESeq2. Genome Biol. 2014;15(12):550.

106. R. Warnes, Ben Bolker, Lodewijk Bonebakker, Robert Gentleman, Wolfgang Huber, Andy Liaw, Thomas Lumley, Martin Maechler, Arni Magnusson, Steffen Moeller, et al. gplots: Various R Programming Tools for Plotting Data. 2020.

107. Szklarczyk D, Gable AL, Lyon D, Junge A, Wyder S, Huerta-Cepas J, Simonovic M, Doncheva NT, Morris JH, Bork P, et al. STRING v11: protein-protein association networks with increased coverage, supporting functional discovery in genome-wide experimental datasets. Nucleic Acids Res. 2019;47(D1):D607-D13.

108. Govaert E, Van Steendam K, Scheerlinck E, Vossaert L, Meert P, Stella M, Willems S, De Clerck L, Dhaenens M, Deforce D. Extracting histones for the specific purpose of label-free MS. PROTEOMICS. 2016;16(23):2937-44.

109. Szarc Vel Szic K, Declerck K, Crans RAJ, Diddens J, Scherf DB, Gerhauser C, Vanden Berghe W. Epigenetic silencing of triple negative breast cancer hallmarks by Withaferin A. Oncotarget. 2017;8(25):40434-53.

110. Aryee MJ, Jaffe AE, Corrada-Bravo H, Ladd-Acosta C, Feinberg AP, Hansen KD, Irizarry RA. Minfi: a flexible and comprehensive Bioconductor package for the analysis of Infinium DNA methylation microarrays. Bioinformatics. 2014;30(10):1363-9.

111. Ritchie ME, Phipson B, Wu D, Hu Y, Law CW, Shi W, Smyth GK. limma powers differential expression analyses for RNA-sequencing and microarray studies. Nucleic Acids Res. 2015;43(7):e47.

112. Maksimovic J, Phipson B, Oshlack A. A cross-package Bioconductor workflow for analysing methylation array data. F1000Res. 2016;5:1281.

113. Du P, Zhang X, Huang CC, Jafari N, Kibbe WA, Hou L, Lin SM. Comparison of Beta-value and M-value methods for quantifying methylation levels by microarray analysis. BMC Bioinformatics. 2010;11:587.

114. Godderis L, Schouteden C, Tabish A, Poels K, Hoet P, Baccarelli AA, Van Landuyt K. Global Methylation and Hydroxymethylation in DNA from Blood and Saliva in Healthy Volunteers. Biomed Res Int. 2015;2015:845041.

CHAPTER 6

Investigating the Role of Chromatin Remodeler FOXA1 in Ferroptotic Cell Death

Chapter 6

Investigating the Role of Chromatin Remodeler FOXA1 in Ferroptotic Cell Death

Emilie Logie[1], Louis Maes[1], Joris Van Meenen[2], Peter De Rijk[3], Mojca Strazisar[3], Geert Joris[3], Bart Cuypers[4], Kris Laukens[4], Wim Vanden Berghe[1]*

1. Laboratory of Protein Science, Proteomics and Epigenetic Signaling (PPES) and Integrated Personalized and Precision Oncology Network (IPPON), Department of Biomedical Sciences, University of Antwerp, Campus Drie Eiken, Universiteitsplein 1, Wilrijk, Belgium
2. Antwerp Research Group for Ocular Science (ARGOS), Department of Translational Neurosciences, University of Antwerp, Wilrijk, Belgium
3. Center for Molecular Neurology, Applied and Translational Neurogenomics Research Group, VIB, Wilrijk, Belgium
4. Biomedical Informatics Network Antwerp (Biomina), Department of Informatics, University of Antwerp, Wilrijk, Belgium

* Corresponding author: wim.vandenberghe@uantwerpen.be

Conflict of Interest: The authors declare no conflict of interest.

Abstract

Ferroptosis is a lipid peroxidation-dependent mechanism of regulated cell death known to suppress tumor proliferation and progression. Although several genetic and protein hallmarks have been identified in ferroptotic cell death, it remains challenging to fully characterize ferroptosis signaling pathways and to find suitable biomarkers. Moreover, changes taking place in the epigenome of ferroptotic cells remain poorly studied. In this context, we aimed to investigate the role of chromatin remodeler forkhead box protein A1 (FOXA1) in RSL3-treated multiple myeloma cells because, similar to ferroptosis, this transcription factor has been associated with changes in the lipid metabolism, DNA damage, and epithelial-to-mesenchymal transition (EMT). RNA sequencing and Western blot analysis revealed that FOXA1 expression is consistently upregulated upon ferroptosis induction in different *in vitro* and *in vivo* disease models. *In silico* motif analysis and transcription factor enrichment analysis further suggested that ferroptosis-mediated FOXA1 expression is orchestrated by specificity protein 1 (Sp1), a transcription factor known to be influenced by lipid peroxidation. Remarkably, FOXA1 upregulation in ferroptotic myeloma cells did not alter hormone signaling or EMT, two key downstream signaling pathways of FOXA1. CUT&RUN genome-wide transcriptional binding site profiling showed that GPX4-inhibition by RSL3 triggered loss of binding of FOXA1 to pericentromeric regions in multiple myeloma cells, suggesting that this transcription factor is possibly involved in genomic instability, DNA damage, or cellular senescence under ferroptotic conditions.

Keywords: FOXA1; forkhead box; ferroptosis; multiple myeloma; perichromatin
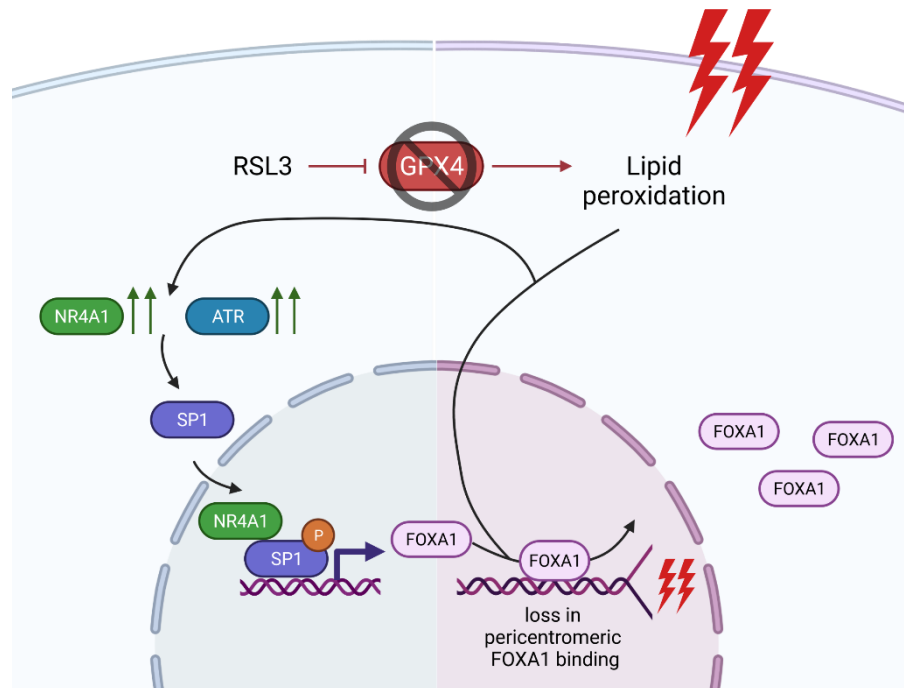
6.1. Introduction

Ferroptosis is a non-apoptotic mode of regulated cell death (RCD) characterized by an iron-dependent rise in reactive oxygen species (ROS) that propagate lipid peroxidation reactions [1]. Mechanistically, intracellular increases in labile ferrous iron (Fe^{2+}) challenge the cellular anti-oxidant defense systems by triggering the formation of toxic hydroxyl radicals through Fenton and Fenton-like chemistry [2]. Should enzymatic anti-oxidants, such as superoxide dismutase or glutathione peroxidases, fail to eliminate these toxic by-products, excessive peroxidation of polyunsaturated fatty acids (PUFAs) will ensue and ultimately cause detrimental loss of membrane integrity [3]. Several pathologies, including neurodegenerative diseases, cardiovascular diseases, ischemia-reperfusion injuries, and diabetes, have already been associated with ferroptotic cell death [4-8]. Small molecules targeting ferroptosis signaling pathways have therefore gained considerable clinical interest in the past couple of years [9]. Interestingly, the induction of ferroptosis has also demonstrated to offer therapeutic potential, especially in the field of oncology. One of the major hallmarks of cancer cells includes evasion of apoptotic cell death due to (acquired) therapy resistance mechanisms [10]. Provoking non-apoptotic modes of cell death, such as ferroptosis or necroptosis, might therefore help in eliminating therapy-resistant cancer (stem) cells [11]. Additionally, compared to healthy tissue, malignant tumors heavily rely on an increased iron metabolism to sustain their augmented proliferation capacity, exposing them to higher basal levels of oxidative stress [12]. Further elevating intracellular Fe^{2+} concentrations with ferroptotic compounds might further disturb their precarious redox balance and efficiently promote cell death [13]. For example, several B-cell malignancies, including multiple myeloma (MM) and B-cell lymphomas, portray an increased iron uptake and display sensitivity to ferroptosis inducers [14-20].

On a molecular level, genetic and protein hallmarks of ferroptosis have been identified and are mainly involved in oxidative stress pathways (NRF2, GPX4, CHAC1) [17, 21, 22], iron metabolism (TFRC, FTH1) [23, 24], inflammation (PTGS2) [17], and lipid metabolism (ACSL4) [25]. The overexpression or downregulation of these genes have been considered as potential biomarkers of ferroptosis cell death, yet it remains challenging to find ferroptosis-specific markers [26]. ACSL4, for instance, is currently considered to be a specific driver for ferroptotic cell death as it is involved in enhancing PUFA content in phospholipid bilayers, which are most susceptible to lipid peroxidation [25, 27]. However, a recent study by Chu and colleagues has demonstrated that even ACSL4-depleted cells can undergo p53-mediated ferroptosis [28]. Thus, there is an unmet need for finding more precise and specific contributors of ferroptotic cell death. A (combination of) suitable ferroptosis biomarker(s) might not only offer new insights in designing novel therapies for iron-related diseases, but might also aid in early detection of ferroptotic cells [29]. Moreover, it could help identify ferroptosis-resistant cancers, which, unfortunately, have already been identified as well [30-33].

In the present study, we investigated the role of chromatin remodeler forkhead box A1 (FOXA1) in MM cells undergoing ferroptotic cell death. FOXA1 belongs to a large family of FOX pioneer TFs that, unlike most TFs, can access target sequences located on nucleosomes and on some forms of compacted chromatin [34]. It is believed that members of the FOXA

subfamily stably bind to genomic regions prior to activation and prior to binding of other TFs, and promote ATP-independent chromatin opening to allow binding of other TFs, nucleosome remodelers, or chromatin modifiers [34]. In case of FOXA1, it is suggested that chromatin opening is promoted by simultaneous DNA- and core histone binding (through a C-terminal domain), which disrupts local internucleosomal interactions required for stability of higher-order chromatin structure [35]. Depending on its chromatin recruitment sites, FOXA1 plays a role in embryonic development [35], hormone regulation [36, 37], lipid metabolism [38, 39], epithelial-to-mesenchymal transition (EMT) [40, 41], and DNA damage [42]. Given that the three latter processes have directly been linked to ferroptosis sensitivity or ferroptotic cell death [27, 43, 44], we combined RNA and CUT&RUN sequencing to characterize FOXA1 expression profiles and downstream targets in different ferroptosis models.

6.2. Results

6.2.1. Ferroptotic Cell Death Promotes FOXA1 expression in Different Disease Models

Although inhibition and induction of ferroptotic cell death is extensively being studied as a therapeutic strategy in several disease models, finding suitable ferroptosis biomarkers remains challenging [26]. To identify key genetic hallmarks of ferroptosis signaling pathways, we compared publicly available RNAseq data (GSE104462) of erastin-treated HEPG2 liver cancer cells to our own RNAseq data of RSL3-treated MM1 myeloma cancer cells (GSE22309570). More specifically, the ferroptotic conditions (i.e. erastin treatment or RLS3 treatment, respectively) in each dataset were compared to their corresponding untreated controls. Significant differentially expressed genes (DEGs) of the erastin dataset were subsequently compared to the significant DEGs of the RSL3 dataset to evaluate similarities between both datasets. Despite considerable differences in experimental design and starting material (Table 1), we found 23 common significant (FDR < 0.05 & |log2FC > 1|) differentially expressed genes (DEGs) that displayed a similar pattern in gene expression upon ferroptosis induction (Figure 1a). These genes are mainly involved in metal binding (YPEL5, ZBTB10, MT2A, MT1F, MT1X), DNA binding (BHLHE41, FOXA1, MAFF, KLF2, NR4A2), protein ubiquitination (HERPUD, PELI1, FBXO32), calcium ion binding (STX11, JAG1), and protein dephosphorylation (DUSP4, DUSP5). Interestingly, we could identify the ATP-independent chromatin remodeler FOXA1 as one of the common genes between both RNAseq datasets. FOXA1 is a 473 amino acid long TF that belongs to the family of FOX pioneer TFs. Through its winged forkhead domain (FKHD), it is able to open chromatin by disrupting internucleosomal interactions (Figure 1b). In agreement with the RNAseq data, qPCR and Western blot analysis revealed a time-dependent upregulation of FOXA1 expression in therapy-resistant and – sensitive MM1 cells treated with RSL3, a class II ferroptosis inducer (Figure 2a-c). As prolonged treatment with RSL3 results in decreased cell viability, these data suggest that FOXA1 expression is tied to severity of ferroptotic cell death and GPX4 inhibition (Figure 2b).

Given that we detected ferroptosis-mediated FOXA1 induction in two different cell types

(i.e. MM1 and HEPG2), we questioned whether similar observations could be made in *in vivo* ferroptosis models. To this end, we performed Western blot analysis on liver samples isolated from GPX4 liver-specific inducible knockout mice (Supplementary Figure S1). LoxP-GPX4 homozygous mice carrying the *cre* transgene (Cre Tg/+) demonstrated an increased, yet not significant, FOXA1 protein expression compared to their healthy controls (Cre +/+) (Figure 2d). Taken together, these findings suggest that FOXA1 upregulation may be a universal phenomenon in different ferroptotic (disease) models and that FOXA1 might be a central regulator in ferroptosis signaling.

Table 1: Overview of experimental design differences in public RNAseq data vs own RNAseq data

Feature	Public RNAseq data (GSE104462)	Our RNAseq data
Cell line	HEPG2	MM1S & MM1R
Tissue of origin	Liver	Peripheral blood
Ferroptosis inducer	10 µM erastin (inhibits Xc⁻ system)	5 µM RSL3 (inhibits GPX4)
Duration ferroptosis treatment	24 hr	3 hr
Ferroptosis inhibitor	1 µM ferrostatin-1	2 µM ferrostatin-1

Abbreviations: Xc⁻ system, Cystine/glutamate transporter; GPX4, Glutathione peroxidase 4.
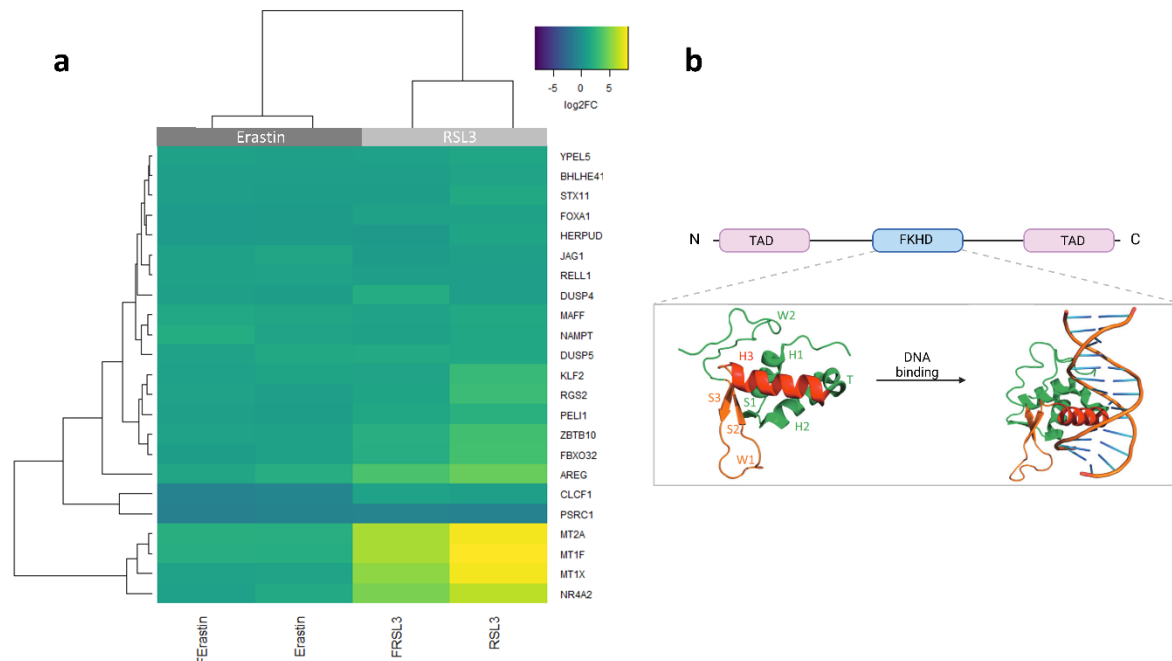
Figure 1: (**a**) Heatmap representation of common differentially expressed genes (FDR < 0.05, logFC > | 1 |) between erastin-treated HEPG2 cells (publicly available data GSE104462) and RSL3-treated MM1 cells. *N*=3 biologically independent replicates per cell line. (**b**) Schematic overview of Forkhead box A1 (FOXA1) protein domains. The forkhead domain (FKHD) is crucial for DNA binding and consists of 3 α-helices (H1-3) and 3 β-sheets (S1-3) organized in a helix-turn-helix motif. This motif is flanked on both sides by polypeptide chain "wings" (W1-2) that interact with the minor DNA groove.
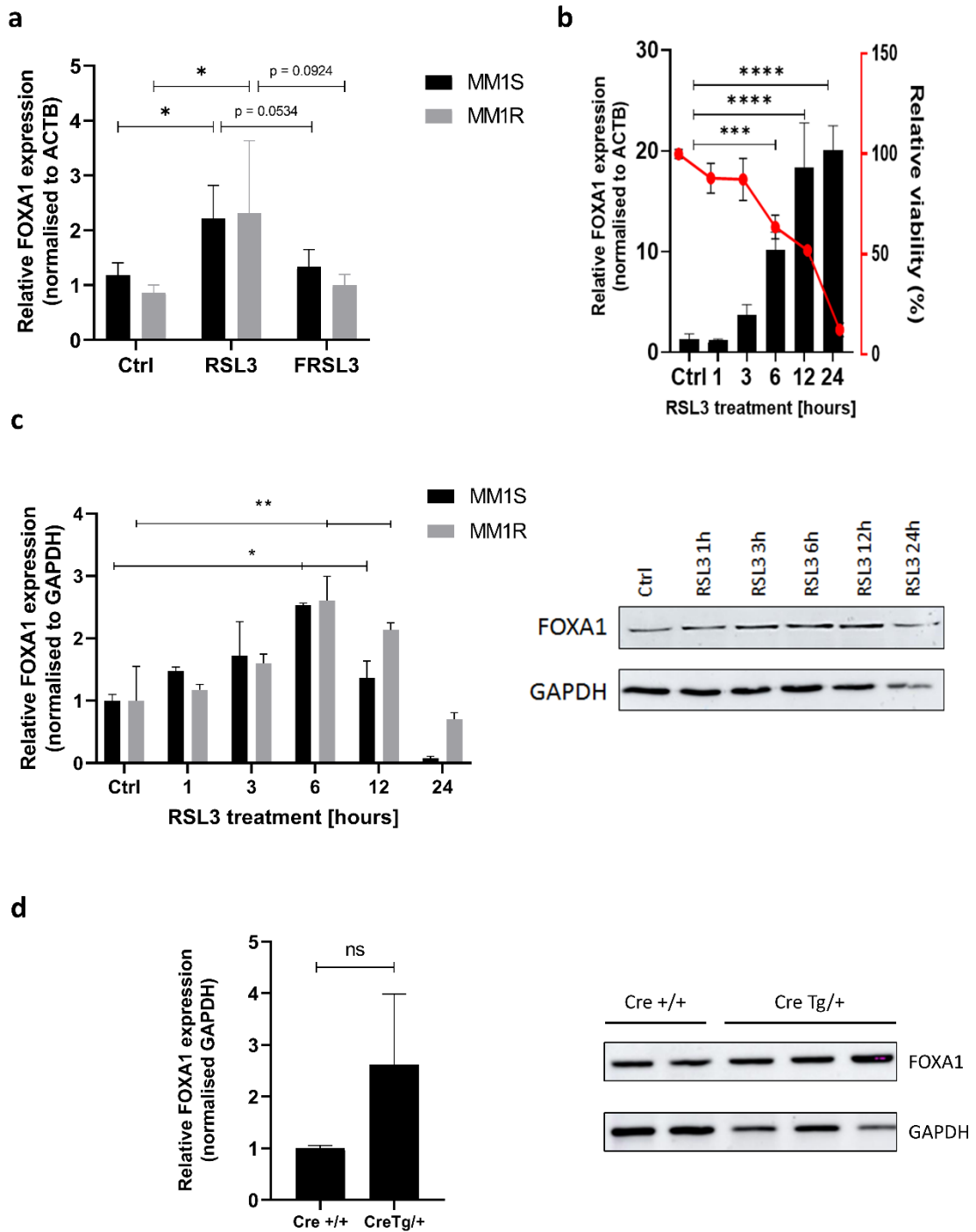
Figure 2: (**a**) Relative FOXA1 mRNA expression in MM1R and MM1S cells treated with 5 µM RSL3 for 3 hrs with (FRSL3) or without (RSL3) 2 hr pre-treatment with 2 µM ferrostatin-1 compared to untreated controls. FOXA1 expression is normalized against the β-actin (ACTB) housekeeping gene. Data are plotted as the mean ± s.d., *n*=3 biologically independent samples per cell line (*p < 0.05), ANOVA. (**b**) Relative mRNA FOXA1 expression and cell viability (%) in MM1 cells after RSL3 treatment. FOXA1 expression is normalized against ACTB mRNA expression. Data are plotted as the mean ± s.d., *n*=3 biologically independent samples per cell line (***p < 0.001, ****p < 0.0001, ANOVA). (**c**) Western blot detection and quantification of FOXA1 and GAPDH expression levels in MM1 cells treated with RSL3. Data are plotted as the mean ± s.d., *n*=3 biologically independent samples. (**d**) Western blot detection and quantification of FOXA1 and GAPDH expression levels in liver samples from healthy Cre +/+ mice versus sick Cre Tg/+ mice. Data are plotted as the mean ± s.d., *n*= 2 Cre +/+ mice and 3 Cre Tg/+ mice (ns = p > 0.05, two-tailed t-test).

6.2.2. FOXA1 Binding to Pericentromeric DNA Regions is Reduced Under Ferroptotic Conditions

A PubMed search of all articles featuring the FOXA1 transcription factor revealed that FOXA1 expression is mostly associated with hormone signaling in prostate, breast and testis cancer (Supplementary Figure S2). Therefore, RNAseq data was further explored to assess whether expression of nuclear hormone receptors is significantly altered in ferroptotic MM1 cells. Supplementary Figure S3 demonstrates that most hormone receptors, including estrogen (ESR), glucocorticoid (NR3C1), retinoid X (RXR), and peroxisome proliferator-activated receptors (PPAR) remain largely unaltered upon RSL3 treatment. Similarly, we could not detect significant differences in ferroptosis sensitivity in glucocorticoid-sensitive MM1S cells, expressing NR3C1, versus glucocorticoid-resistant MM1R cells, lacking functional NR3C1 expression. In contrast, an increase in mRNA expression of lipid and oxidative metabolism sensing orphan nuclear receptors NR4A1, NR4A2, and NR4A3 could be observed in RSL3-treated cells compared to untreated controls, and was partly validated by Western blot (Supplementary Figure S4). The interplay between FOXA1 and orphan nuclear receptors has only poorly been characterized, mostly in context of dopaminergic neurons [45, 46]. Interestingly, important tumor suppressor roles for NR4A TFs have recently been described (reviewed in [47]), and NR4A defects are reported to promote formation of blood-tumors (e.g. leukemia, lymphoma) and T-cell immunity dysfunctions [48-51]. As such, possible anti-tumor functions of NR4A TFs in ferroptotic cells deserves further investigation.

We next explored whether FOXA1 might play a role in epithelial-to-mesenchymal transition (EMT) as reported in previous studies [40, 41, 52]. Correlation analysis of the RNAseq data indeed demonstrated that genes highly correlated with FOXA1 expression were enriched in cytoskeleton organization, epithelial cell differentiation, and regulation of EMT (Figure 3a-c). Interestingly, the EMT status is known to directly affect ferroptosis sensitivity, with mesenchymal cells being more susceptible to ferroptotic cell death compared to epithelial cells [43]. Ferroptosis-mediated upregulation of FOXA1 might subsequently drive MM1 cells towards a mesenchymal profile and promote cell death by RSL3. To this end, qPCR analysis of four key EMT markers was performed on MM1 cells treated with RSL3 for increasing timepoints (Supplementary Figure S5). Overall, no significant expression differences of epithelial marker E-cadherin (E-CAD) or mesenchymal markers N-cadherin (N-CAD), Twist-related protein 1 (TWIST1) or Snail Family transcriptional repressor 2 (SLUG) could be observed in ferroptotic cells. These preliminary results indicate that FOXA1 does not orchestrate trans-differentiation of MM1 cells into a mesenchymal phenotype.

Since our targeted approaches did not further elucidate the role of FOXA1 in ferroptosis signaling, we aimed to characterize the downstream effects of FOXA1 by performing CUT&RUN sequencing. This technique allows for genome-wide profiling of chromatin binding sites of transcription factors, similar to ChIP-Seq [53]. In short, MM1R cells were treated for 3 hours with 5 µM RSL3, after which FOXA1-bound DNA fragments were collected and purified for downstream analysis. After completing library preparation and DNA sequencing, enriched regions were called using the sparse enrichment analysis for CUT&RUN (SEARC) [54].

a

b

R-HSA-5661231: Metallothioneins bind metals
GO:0043435: response to corticotropin-releasing hormone
GO:0030855: epithelial cell differentiation
GO:0071407: cellular response to organic cyclic compound
GO:0038066: p38MAPK cascade
GO:0030865: cortical cytoskeleton organization
GO:0071363: cellular response to growth factor stimulus

c

GOBP:regulation of epithelial to mesenchymal transition (G

NES- 1.9
q- 0.001

Gene	Rho	Title
FOXA1	1,00	forkhead box A1
LDLRAD4	0,71	low density lipoprotein receptor class A domain-containing protein 4
TGFB2	0,67	transforming growth factor beta 2
SDCBP	0,67	syndecan binding protein
COL1A1	0,67	collagen type I alpha 1 chain
SMAD7	0,65	SMAD family member 7
TGFBR1	0,65	transforming growth factor beta receptor 1
BMP2	0,56	bone morphogenetic protein 2
BAMBI	0,52	BMP and activin membrane bound inhibitor
CTNNB1	0,45	catenin beta 1
PPP2CA	0,42	protein phosphatase 2 catalytic subunit alpha
SMAD3	0,41	SMAD family member 3
TGFB3	0,36	transforming growth factor beta 3
STRAP	0,34	serine/threonine kinase receptor associated protein

Figure 3: (**a**) Histogram plot displaying the top correlated genes in respect to FOXA1. The height of the bars correspond to the Pearson correlation value. Figure was generated using the Omics Playground tool (v2.7.18). (**b**) Metascape pathway analysis [57] of RNAseq data displaying the top 20 significantly enriched pathways of RSL3-treated MM1 cells compared to untreated controls. (**c**) Functional GSEA enrichment of genes correlated with FOXA1 expression (left). The green curve corresponds to the normalized enrichment score (NES). Black vertical bars indicate the rank of genes in the gene set in the sorted correlation metric. FDR is represented by the q-value in the figure. Figure was generated using the Omics Playground tool (v2.7.18). The leading-edge table (right) reports the leading edge genes as reported by GSEA corresponding to the selected geneset. The 'Rho' columns report the correlation with respect to FOXA1.

Only a limited number of genomic regions (n = 43) were identified to be differentially altered in FOXA1 binding after RSL3 treatment (Supplementary Table S2). Although we previously measured higher FOXA1 expression in ferroptotic cells, untreated controls displayed higher FOXA1 binding compared to RSL3-treated cells (Supplementary Table S2). Remarkably, all identified regions were located in pericentromeric DNA (Figure 4a),

suggesting that a ferroptosis-mediated loss of FOXA1 binding to pericentromeric hetero-chromatin takes place upon RSL3 induction. Given that FOXA1 is a pioneer TF that is able to bind compact DNA, these observations could indicate that DNA decondensation (of pericentromeric regions) triggers genome-wide loss of FOXA1 binding. In line with these results, we previously reported (Chapter 5 of this thesis) that ferroptosis might induce early cellular senescence in MM1 cells, a process which has been associated with defective pericentric silencing and decondensation [55, 56]. However, CUT&RUN sequencing experiments need to be repeated before definitive conclusions can be made. In our setup, signal-to noise ratios in the treatment groups were rather low as compared to negative IgG controls (Figure 4b), which indicates rather limited enrichment of FOXA1 binding sites in our samples. Nonetheless, when looking at the identified enriched regions in closer detail, a significant loss of FOXA1 binding could consistently be observed (Figure 4b). Preliminary Western blot analysis of RSL3-treated MM1R cells confirmed the observed loss of FOXA1 expression in chromatin-bound cellular protein fractions (Figure 5). In parallel, cytoplasmic protein expression of FOXA1 was slightly increased upon RSL3 exposure, indicating that chromatin-free FOXA1 is transported toward the cytoplasmic compartment (Figure 5).

6.2.3. Sp1 is a Possible Driver of FOXA1 Expression

Taking into account that FOXA1 is upregulated under different ferroptotic conditions in different cell lines, we investigated whether a common transcription factor drives expression of FOXA1. To this end, we generated a list of potential FOXA1 driver genes by identifying transcription factor binding sites located in the FOXA1 promotor region obtained from the SwissRegulon database [58]. Next, a target list of each of the candidate drivers was constructed using three different databases, namely IFTP, TRRUSR, and Marbach2016, employed in the tftarget R package [59]. Finally, an overlap between candidate driver target genes and significant DEGs identified in the two RNAseq studies (cfr. Section 6.2.1) was performed. Our analysis showed that transcription factor Sp1 is the most probable driver in FOXA1 expression, both in MM1R cells and HEPG2 cells (Table 2).

Table 2: Top 5 candidate drivers of FOXA1 expression in ferroptotic cells.

Candidate driver	# DEGs in RNAseq data regulated by candidate driver	% DEGs in RNAseq regulated by candidate driver
Sp1	46	82.14
SPI1	36	64.29
TFAP2A	33	58.93
TFAP2C	31	55.36
RREB1	30	55.57

Abbreviations: Sp1, Sp1 transcription factor; SPI1, Spi-1 proto-oncogene; TFAP2A, Transcription factor AP-2 alpha; TFAP2C, Transcription factor AP-2 gamma; RREB1, Ras responsive element binding protein 1

Although other studies have reported a ferroptosis-dependent increase in Sp1 expression [7, 60, 61], we did not find significant alterations in Sp1 mRNA levels in RSL3-treated MM1 cells compared to untreated controls (Figure 6a). Nonetheless, preliminary experiments demonstrate that siRNA silencing of Sp1 abolishes ferroptosis-driven FOXA1 upregulation (Figure 2a, Figure 6b), suggesting that Sp1 (partly) drives FOXA1 upregulation in MM1 cells.

Possibly, ferroptotic triggers regulate Sp1 transcriptional activity through alternative mechanisms and subsequently promote downstream FOXA1 expression. In agreement with this hypothesis, a recent kinome screen has revealed that Sp-1 upstream ATR damage response serine/threonine kinase directly impacts ferroptosis sensitivity [62]. Sp1 phosphorylation is known to directly impact Sp-1 dependent transcription [63] and might be increased in ferroptotic cells. Alternatively, ferroptosis signaling pathways could increase expression of Sp1 cofactors and promote Sp1 target site binding. NR4A1 is a cofactor of Sp1 that has recently been described in ferroptotic cell death [64] and was also found to be upregulated in this study. Through its interaction with Sp1, NR4A1 might recruit Sp1 more efficiently to its GC-ich gene targets and promote transcription [65]. Further research exploring the Sp1-FOXA1 signaling axis during ferroptosis are needed to fully confirm the role of Sp1 in RSL3-dependent FOXA1 expression.

6.3. Discussion

In the past decade, RCD and ferroptosis research has grown rapidly, especially in the field of neurological diseases and oncology [66]. Several morphological, biochemical, genetic, and protein hallmarks of ferroptotic cell death have been identified over the last years, but the exact executioner signals of ferroptosis remain largely unknown (reviewed in [29]). Identification of specific ferroptosis contributors may therefore provide novel opportunities for creating anti-cancer therapies. Consequently, we compared RNAseq data of ferroptotic MM and HEPG2 cells to explore whether common expression signatures could be found in these different experimental setups. Our analysis revealed that genes involved in metal binding, DNA binding, protein ubiquitination, and protein phosphorylation were shared in both ferroptosis models. Of particular interest, we identified ATP-independent chromatin remodeler FOXA1 to be specifically upregulated upon RSL3 and erastin treatment. FOXA1 levels were also found to be upregulated in liver tissue obtained from liver-specific GPX4 inducible knock-out mice, suggesting that increased FOXA1 mRNA and protein expression might be a universal trigger in various ferroptosis disease models. Further *in silico* motif and TF enrichment analysis predicted that Sp1 is the most likely driver of ferroptosis-driven FOXA1 expression. Sp1 has previously been described in context of lipid peroxidation and ferroptotic cell death, and is hypothesized to play a dual role in the regulation of tissue injury [7, 60, 61]. However, our qPCR data demonstrate that Sp1 expression remains unaltered in RSL3-treated MM1 cells, implying that transcriptional activity of Sp1 is orchestrated through other upstream mechanisms. Post-translational modifications (PTMs), such as protein phosphorylation, are reported to directly influence Sp1 activity and might be altered in ferroptotic conditions [67]. Indeed, several upstream kinases responsible for Sp1 phosphorylation, including p38 and ATM/ATR are known to be involved in ferroptosis signaling as well [62, 68-70]. Alternatively, transcription activity of Sp1 may be stimulated through improved recruitment to its DNA target binding sites by cofactor proteins that are differentially expressed in the presence of ferroptotic stimuli. NR4A1, for example, has recently been identified as a modulator of ferroptotic cell death and is also reported to act as a cofactor of Sp1 [64, 65]. Follow-up proteomics, Western blot, and immunoprecipitation experiments will undoubtedly reveal to which extend PTMs and cofactor-recruitment of Sp1 are crucial for FOXA1 expression.
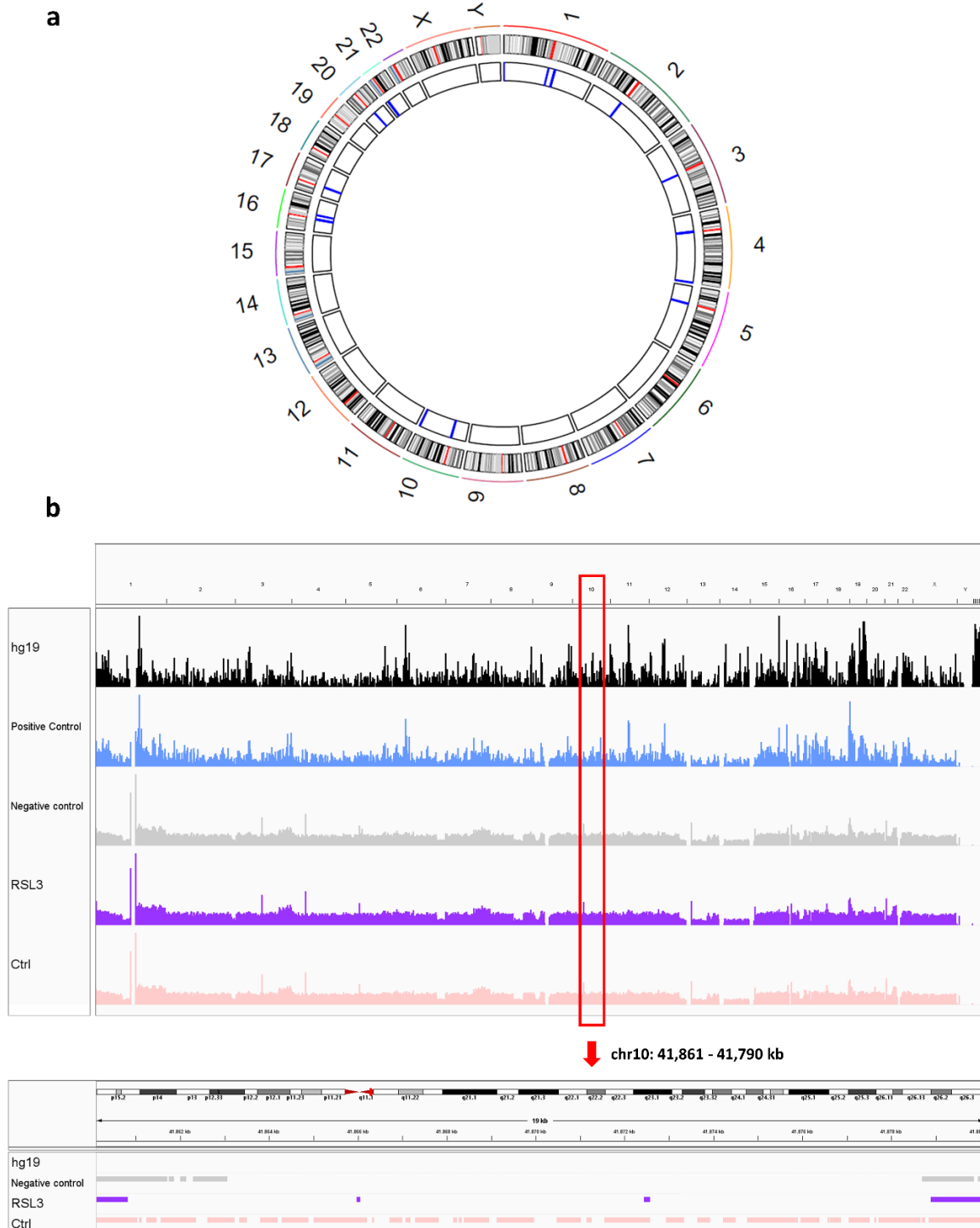
Figure 4: (**a**) Circos plot displaying chromosome ideograms (outer ring) with centromeric regions marked in red. Blue markings on the inner ring show the differentially enriched FOXA1-bound DNA regions in untreated control cells compared to RSL3-treated cells. (**b**) Overview of genomic regions sequenced in each CUT&RUN treatment condition (upper panel). The hg19 panel represents the reference genome and displays known mapped genes. The lower panel represents a close-up visualization of chr10: 41,861 – 41,790 kb highlighting the loss of FOXA1 binding to perichromatin in RSL3-treated cells compared to controls. Figures were generated with Integrative Genomics Viewer (v2.9.4).
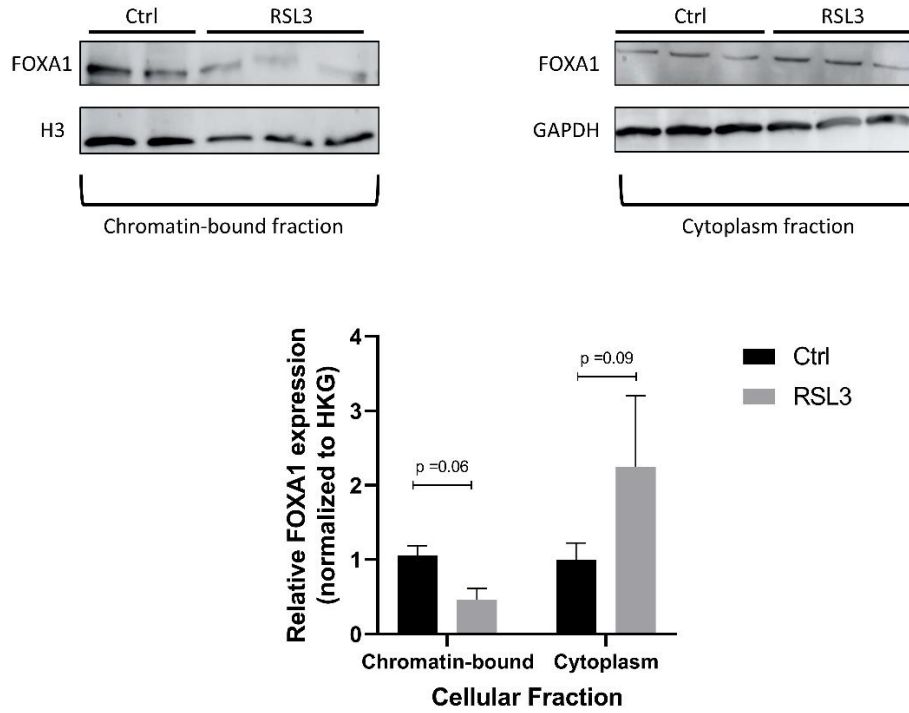
Figure 5: Relative FOXA1 protein expression of different cellular protein fractions in MM1R cells treated with 5 µM RSL3 compared to untreated controls. Data are plotted as the mean ± s.d., *n*= 3 independent samples per treatment (indicated p-values are outcomes of unpaired, two-tailed t-test).
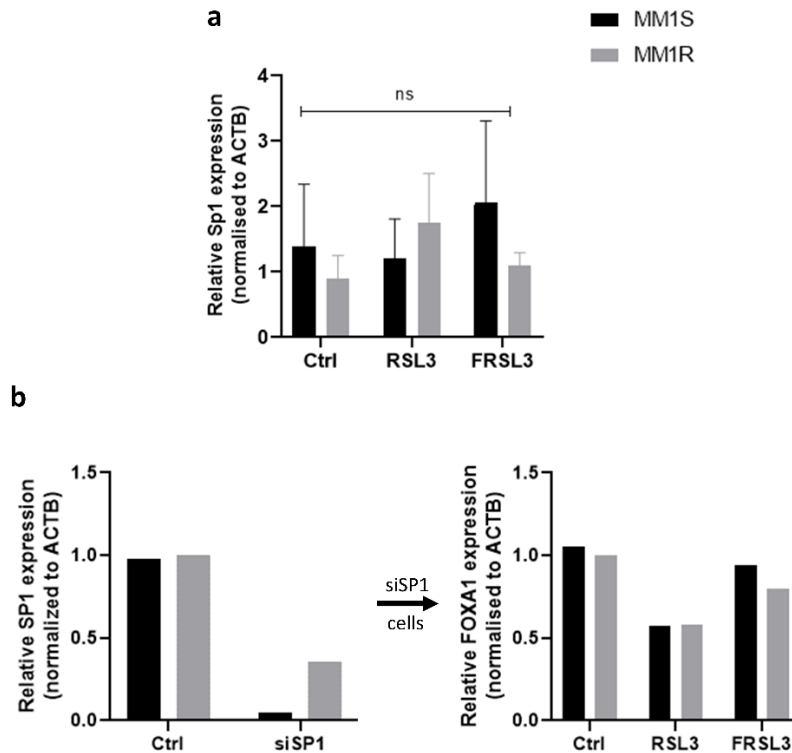
Figure 6: (**a**) Relative mRNA Sp1 expression in MM1 cells after 3 hr treatment with 5 µM RSL3, with (FRSL3) or without pre-treatment with ferrostatin. Data are plotted as the mean ± s.d., *n*=3 biologically independent samples per cell line (ns = p > 0.05, ANOVA). (**b**) Relative mRNA SP1 (left) and FOXA1 (right) expression in MM1 cells transfected with siRNA targeting SP1. Data are plotted as the mean ± s.d., *n*=1 biological independent sample per cell line

Two independent studies have recently reported that nuclear hormone receptor activity is highly correlated with ferroptosis sensitivity [71, 72]. Presumably, cells with higher endocrine activity are subjected to hormone-dependent ROS production, which promotes lipid peroxidation through activation of Fenton reactions [73]. Because FOXA1 is a critical interacting partner of several nuclear receptors [74], we wondered whether ferroptosis induction in MM1 cells is associated with an increase in hormone receptor activity. A preliminary screening of hormone receptor expression mRNA changes in RSL3-treated MM1 cells showed that the expression of the majority of nuclear receptors remain unchanged. Only a subset of orphan nuclear receptors, NR4A1-3, are specifically upregulated upon RSL3 induction. Although FOXA1 has been reported to regulate NR4A2 expression in immature midbrain dopaminergic neurons [45], the interplay between both proteins needs to be explored further. Possibly, NR4A receptors mediate ferroptotic cell death by influencing the cellular energy and lipid metabolism [64, 75]. On the other hand, these orphan receptors might orchestrate ferroptosis signaling pathways by recruiting other ferroptosis-dependent proteins to their target site, as previously explained. NR4A orphan receptors have also been associated with tumor suppressor functions, and mutations in NR4A1-3 have been linked with the formation of blood cancers, including leukemia and lymphoma [48, 49]. RSL3-driven upregulation of NR4A TFs might therefore drive elimination of MM cancer cells by regulating key cancer pathways (reviewed in [47]. Intriguingly, both ferroptosis and NR4A proteins are known to be regulated by the p53 tumor suppressor [76, 77] and indicates that an GPX4-NR4A-p53 signaling network may drive MM cell death. Further research about the anti-cancer effects of NR4A TFs in ferroptotic cells could potentially offer new therapeutic insights for MM and other hematological malignancies. Regardless, based on assessing expression changes, FOXA1 does not seem to primarily target (steroid) hormone receptors during ferroptosis. A direct measurement of hormone receptor activity, by evaluating nuclear translocation or by performing ChIP for example, might aid in fully characterizing the effects of FOXA1 in hormone signaling. Furthermore, evaluating FOXA1-dependent changes on nuclear receptors in more endocrine active cell systems, such as breast or pancreas cancer cell lines, might reveal cell type-dependent effects of FOXA1.

Because both FOXA1 and ferroptosis have been associated with EMT [40, 43, 52], we also investigated whether RSL3 treatment triggers significant changes in EMT markers. Generally, (tumor) cells harboring a more mesenchymal profile are considered to portray an increased ferroptosis sensitivity because they heavily rely on GPX4 activity compared to their epithelial counterparts [78]. Mesenchymal-state cells also exhibit more dysregulated antioxidant programs, explaining why ferroptotic compounds are more potent in these cells [78, 79]. In this regard, ferroptosis-dependent reprogramming of the epithelial-mesenchymal state through FOXA1 upregulation, might promote ferroptosis sensitivity. While our RNAseq data revealed a correlation of FOXA1 expression with several other drivers of EMT, including TRIB1, N-CAD, E-CAD, SLUG, and TWIST1 mRNA expression was not significantly altered upon RSL3 incubation. This suggests that MM1 cells do not shift toward a more epithelial – or mesenchymal-like state under ferroptotic conditions.

Given that neither hormone signaling or EMT seem to be direct downstream targets of FOXA1 in ferroptotic MM1 cells, genome-wide transcription site profiling was performed

by CUT&RUN. Similar to ChIP-Seq, this technique combines ChIP with parallel DNA sequencing to identify binding sites of DNA-associated proteins, such as FOXA1. Unfortunately, signal-to-noise signals were quite low in our treatment setups, with signal intensities being similar to the negative IgG control. Further optimization of the experimental setup is therefore required before biologically relevant interpretations can be finalized. Increasing the starting amount of MM1 cells or addition of an extra cross-linking step might improve experimental outcome, especially since FOXA1 has been reported to transiently bind to its DNA sites [80]. Taking this into account, we could still identify 43 genome regions wherein FOXA1 binding was significantly altered in RSL3-treated MM1 cells compared to their untreated controls. Remarkably, all these regions were located in pericentromeric chromatin and FOXA1 binding was significantly lower in RSL3 conditions, despite the earlier observed transcriptional and translational FOXA1 upregulation in MM1 cells. Pericentric (satellite) DNA is typically considered to be void of functional genes and transcriptionally silent since they are confined in transcriptionally inert heterochromatin [81]. However, mounting evidence suggests that pericentric transcripts are crucial in maintaining genome stability (reviewed in [82] and [83]). To this end, loss of FOXA1 binding in ferroptotic cells could potentially promote genome instability and DNA double strand breakage. Another possibility is that ferroptotic stress triggers defective pericentric transcription due to dramatic DNA decondensation, as is also observed when cells are exposed to UV (i.e. DNA damage), cadmium toxicity or cellular senescence [56, 84-86]. Given that FOXA1, as a pioneer TF, mainly binds to heterochromatin regions, genome-wide DNA decondensation might promote overall loss of FOXA1 pericentromeric DNA binding and uncontrolled pericentric transcription. Our previous work (see Chapter 5 of this PhD thesis) has indeed suggested that ferroptosis is associated with an epigenomic stress response linked to oxidative stress and cellular senescence, suggesting that DNA decondensation might occur in ferroptotic cells. Intriguingly, FOXA1 expression has been reported to increase with cellular senescence [87]. Possibly, loss binding to heterochromatin pericentromeric DNA promotes recruitment of FOXA1 to other target sites that trigger cellular senescence [87]. Repeating the CUT&RUN experiments under optimized experimental conditions should help in investigating this hypothesis further. Alternatively, "DNA-free" FOXA1 might localize to the cytoplasm and inhibit nuclear translocation of other TFs to promote cell death [88]. This seems to occur in our experimental setup as well, given that Western blot analysis revealed an RSL3-dependent increase in FOXA1 expression in cytoplasmic protein fractions.

Taken together, our data suggest that ferroptosis triggers a time-dependent upregulation of FOXA1 expression in different experimental models, which could be orchestrated by transcriptional activation of Sp1. The downstream effects of this FOXA1 expression surge in MM1 cells remain somewhat elusive but do not seem to include steroid hormone signaling or EMT. In contrast, preliminary data imply that ferroptotic stress might trigger uncontrolled pericentric transcription and genome instability, due to loss of FOXA1-binding to pericentromeric DNA. Moreover, relocalization of pericentric-free FOXA1 to secondary target sites or the cytoplasm might further promote cellular stress responses, such as cellular senescence or cell death.

6.4. Materials and Methods

6.4.1. Cell Culture and Cell Viability Assays

Human MM1S cells (CRL-2974) and MM1R cells (CRL-2975) were purchased from ATCC. RPMI-1640 medium, supplemented with 10% FBS (E.U Approved; South American Origin) and 1% Pen-Strep solution (Invitrogen, Carlsbad, CA, USA), was used to sustain the cells. The cells were cultivated at 37°C in 5% CO2 and 95% air atmosphere and 95-98% humidity. To assess cell viability, the colorimetric assay with 3-(4, 5-dimethylthiozol-2-yl)-2, 5-diphenyltetrazolium bromide (MTT) was used (Sigma Aldrich, St. Louis, MO, US) as previously described [89].

6.4.2. Antibodies and Reagents

RSL3 was purchased from Selleckchem (Houston, USA), dissolved in DMSO and stored as 50 mM stocks at -20°C. siRNA targeting Sp1 (1299001) was purchased from ThermoFisher Scientific (Waltham, MA, USA)). Antibodies FOXA1 (ab23738) and GAPDH (2118S) were obtained from Abcam (Cambridge, UK) and Cell Signaling Technology (Danvers, MA, USA), respectively.

6.4.3. RNA Extraction and Sequencing

After cell harvest, total RNA from untreated or RSL3-treated (with or without 2 hr pre-treatment with 2 µM Ferrostatin-1) MM1S and MM1R cells was extracted using the RNeasy Mini Kit (Qiagen, Venlo, the Netherlands) according to the manufacturer's protocol. Once isolated, quantification was performed with the Qubit RNA BR Assay Kit (ThermoFisher, MA, USA) and RNA was stored at -80°C. Extracted RNA was used as input for RNA sequencing as previously described [90]. In brief, RNA was shipped to BGI (BGI Group, Bejing, China) where quality checks were performed using the 2100 Bioanalyzer system (Agilent Technologies, USA) and sequencing took place using the BGISE-500 platform (BGI Group, Beijing, China). Quality control, genome mapping and differential gene expression analysis was performed using the R- packages FastQC (v0.11.5) [91], STAR (v2.7.3a) [92], and DESeq2 (v3.12) [93]. DEGs were considered to be significant when FDR < 0.05 and |log2FC|> 1. Raw gene counts from the GSE104462 dataset [94] were extracted from the Gene Expression Omnibus (GEO) database and used as input for the same RNAseq analysis pipeline as described above.

6.4.4. cDNA Synthesis and Quantitative Real-time PCR

Extracted RNA from RSL3-treated cells was converted into cDNA using the Go-Script reverse transcription system (Promega, Madison, Wisconsin, USA) according to the manufacturer's protocol. Subsequently, qPCR analysis was carried out using the GoTag qPCR Master Mix (Promega, Madison, Wisconsin, USA) as explained by manufacturer's protocol. In short, 1µL cDNA was added to a master mix comprising SYBR green, nuclease-free water, and 0.4 µM forward and reverse primers. The following PCR program was applied on the Rotor-Gene Q qPCR machine (Qiagen, Venlo, the Netherlands): 95°C for 2 min, 40 cycli denaturation (95°C, 15 s) and annealing/extension (60°C, 30 s), and dissociation (60–95°C). Each sample was run in triplicate and the median

value was used to determine the ΔΔCt-values using β-actin (BACT) as the normalization gene. Primer sequences are listed in Supplementary Table S1.

6.4.5. Protein Extraction and Western blot Analysis

Cellular protein extraction occurred by resuspending cell pellets in 0.5 mL RIPA buffer (150 mM NaCl, 0.1% Triton X-100, 1% SDS, 50 mM Tris-HCl pH 8) supplemented with PhosphataseArrest (G-Biosciences, Saint-Louis, MO, USA) and protease inhibitors (Complete Mini®, Roche). After 15 min incubation on ice with regular vortexing, samples were briefly sonicated (1 min, amplitude 30 kHz, pulse 1s) and centrifuged at 13 200 rpm for 20 min at 4°C. Solubilized proteins were transferred to new Eppendorf tubes and stored at -20 °C. To extract proteins from mouse liver tissue, RIPA buffer containing 2% SDS was added to the tissue. Sample homogenisation was performed with the TissueRuptor, followed by 1 hour incubation at 4°C on a rotor. Sonication (5 min, low amplitude 1 kHz and 20 Hz burst rate) was used to shear DNA and debris was removed by centrifugation for 8 min at 13 000 g.

Using standard protocols, all protein samples were separated using Bis-Tris SDS-PAGE with a high-MW MOPS running buffer, and transferred onto nitrocellulose membranes (Hybond C, Amersham) using the Power Blotter System (Thermofisher, MA, USA). Blocking the membranes for 1 hour with blocking buffer (20 mM Tris-HCl, 140 mM NaCl, 5% BSA, pH 7,5) at RT was followed by overnight incubation with the primary antibody at 4°C. Blots were then incubated for 1 hr with the secondary, HRP dye-conjugated antibody (Dako, Glostrup, Denmark) after which chemiluminescent signals were detected with the Amersham Imager 680 (Cytiva, MA, USA) and quantified with the ImageJ software (v1.53j) [95].

6.4.6. Liver Samples of Cre-lox Liver-Specific GPX4 Knockout Mice

Liver samples from Cre-lox liver-specific inducible GPX4 kockout mice were kindly provided by Ines Goetschalckx and Prof. Dr. Tom Vanden Berghe (Laboratory of Pathophysiology, University of Antwerp). GPX4 knockout mice were generated by crossing homozygous GPX4-floxed mice with heterozygous GPX4 conditional knockout mice (Supplementary Figure S1).

6.4.7. Nucleofection of MM cells

MM1 cells were transfected using the Nucleofector IIb device (Lonza Amaxa, Switzerland) as described by the manufacturer's protocol. Briefly, 1 million cells were resuspended in 100 μL supplemented nucleofector solution. Next, 300 nM siSp1 was added to resuspended cells. To assess transfection efficiency, an additional pmaxGFP Vector (Lonza, Bazel, Switserland) was included in each nucleofection reaction (average transfection efficiency = 51.3 ± 2.4 %). Cell suspensions were transferred to a provided cuvettes and nucleofection was performed using the O-020 program. 48 hours after transfection, cells were harvested and used as input for qPCR analysis.

6.4.8. **Motif Analysis and Transcription Factor Enrichment Analysis**

To search for a potential driver of FOXA1, a list of candidate drivers was composed using transcription factor binding sites from the SwissRegulon database located at the *FOXA1* promoter [58, 96]. Using that list, a list of targets of these candidate drivers was composed using data from three different databases – IFTP, TRRUST and Marbach2016 – provided via the tftargets package in R [59]. Targets of each candidate driver were matched to DEGs common to both datasets and two metrics for overlap were calculated: the number of overlapping genes and the percentage of overlap with respect to the number of DEGs. As an additional control, the X2Kweb tool was further used to identify putative enriched transcription factors through Transcription factor enrichment analysis (TFEA) [97]. Results from TFEA were compared with results from IFTP, TRRUST and Marbach2016.

6.4.9. **CUTANA Cut&Run to Identify Chromatin-Associated Proteins**

Downstream targets of FOXA1 were identified using the EpiCypher CUTANA ChIC CUT&RUN Kit (23614-1048, EpiCypher, USA) as previously described [53, 98]. In short, 5 x 10^5 MM1R were plated into 6-well plates and either treated with 5 μM RSL3 (3 hours) or left untreated. For each treatment condition, 4 biological replicates were included. Cells were washed and bound to concanavalin A-coated magnetic beads and permeabilized with wash buffer (20 mM HEPES pH 7.5, 150 mM NaCl, 0,5 mM spermidine and protease inhibitors) supplemented with 0,05% digitonin. After overnight incubation at 4°C with the primary FOXA1 antibody (13-2001, Epicypher), cell-bead slurry was washed twice more after which pA-MNase digestion was activated by placing samples on an ice-cold block and incubated with digitonin wash buffer containing 2 mM CaCl2. Each CUT&RUN experiment also featured a positive (anti-H3K4me3) and negative (anti-Rabbit IgG) antibody control. After 2 hours, the cleavage reaction was stopped with stop buffer (340 mM NaCl, 20 mM EDTA, 4 mM EGTA, 0.05% digitonin, 0.05 mg/mL glycogen, 5 μg/mL RNase A, 2 pg/mL *E. coli* spike-in DNA) and fragments were released by 30 minute incubation at 37°C. Samples were centrifuged and DNA-containing supernatant was collected. DNA extraction was performed with a DNA extraction kit supplied with the CUTANA Kit. Resulting DNA was used as input for library preparation using the Kapa HyperPrep Kit (792363001, Roche) and barcoding using xGen UDI-UMI barcodes (10005903,IDT) following manufacturers protocols. Barcoded libraries of ten samples (4 treated, 4 untreated and two controls) were equimolarly pooled and sequenced on MiSeq (Illumina) using MiSeq v3 150 reagent kit (MS-102-3001, illumina) according to manufacturer's protocol. The run ended in obtaining 4.16 Gb, 56.66 million reads (Q30 92.09%, 3.86 Gb).

Sequencing data were aligned to the UCSC h38 reference genome using the Burrows-Wheeler Aligner [99] and peaks were called using SEARC[54]. Mapped reads were converted to paired-end BED files containing coordinates for the termini of each read pair, and then converted to bedgraph files. Differential analysis was performed using the DESeq2 package (v3.12) [93], where gene counts were normalized to *E.coli* spike-in counts. Differentially enriched regions were visualized with the RCircos R package (v1.2.1) [100] and IGV (v2.9.4) (BroadInstitute, Cambridge, MA, USA).

6.4.10. **Subcellular Protein Fractionation**

The subcellular protein fractionation kit (# 78840, Thermofisher, MA, USA) was used to fractionate proteins into nuclear and cytoplasmic fractions according to the manufacturer's instructions. The yield of obtained chromatin-bound nuclear proteins and cytoplasmic proteins was determined by the BCA method. Finally, 20 µg of protein from each cellular fraction was used to perform SDS-PAGE and Western blot analysis, as described in section 6.4.5.

6.4.11. **Statistical Analysis**

Statistical tests were performed in GraphPad Prism (v7.0) (GraphPad Software, San Diego, CA, USA) unless otherwise stated in the main text. Results were considered to be statistically significant when p-values < 0.05 were obtained.

6.5. Supplementary Material

Cre-lox Tissue-Specific Knockout, cont.

Figure S1: Generation of liver-specific, inducible GPX4 knockout mice. Heterozygous GPX4-floxed mice carrying the *cre* transgene are crossed with homozygous GPX4-floxed mice to obtain homozygous loxP-flanked GPX4 mice that are heterozygous for the *cre* transgene. Figure adapted from https://www.jax.org/news-and-insights/jax-blog/2011/september/cre-lox-breeding#

.

Figure S2: Word cloud displaying word associations with FOXA1 obtained from PubMed abstracts and free PubMed full-length articles. The strength of the association is represented by the word size. Word cloud was generated using the online webtools Textrous! and Jason Davies word cloud generator.

Figure S3: Heatmap representation of expression changes (log2FC) of nuclear receptors in RSL3-treated cells (with or without Ferrostatin-1 pre-treatment (FRSL3)) and untreated controls. Heatmap was generated using Omics Playground Tool (v2.7.18).
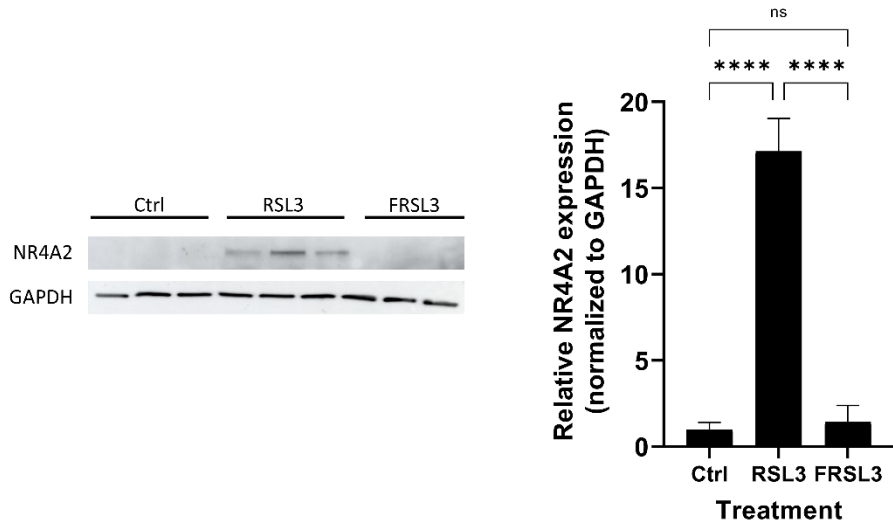
Figure S4: Relative NR4A2 protein expression in MM1S cells treated with 5 µM RSL3 (with or without Ferrostatin-1 pre-treatment (FRSL3)) compared to untreated controls. Data are plotted as the mean ± s.d., *n*= 3 independent samples per treatment (ns p > 0.05, ****p < 0.0001), ANOVA).
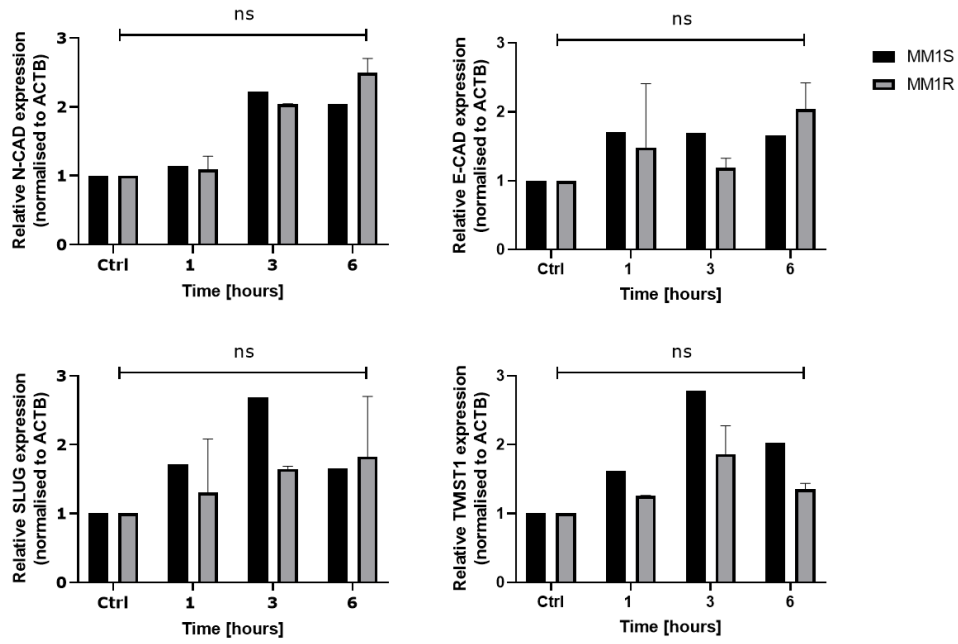
Figure S5: Relative mRNA expression of different EMT markers in MM1R and MM1S cells treated with 5 μM RSL3 compared to untreated controls. Data are plotted as the mean ± s.d., *n*=1 or 2 (indicated by presence of error bar) biologically independent samples per cell line (ns p > 0.05), ANOVA). Abbreviations: N-CAD = N-cadherin, E-CAD = E-cadherin, SLUG = snail family transcriptional repressor 2, TWIST1 = twist family BHLH transcription factor 1.

Table S1: Overview of primers used in this study

Target		Primer Sequence	Gene accession number
qPCR primers			
FOXA1	Forward	AGG TGT GTA TTC CAG ACC CG	ENSG00000129514
	Reverse	TTG ACG GTT TGG TTT GTG TG	
Sp1	Forward	TTG AAA AAG GAG TTG GTG GC	ENSG00000185591
	Reverse	TGC TGG TTC TGT AAG TTG GG	
ACTB	Forward	CTG GAA CGG TGA AGG TGA CA	ENSG00000075624
	Reverse	AAG GGA CTTC CTG TAA CAA TGC A	
E-CAD	Forward	TGC CCA GAA AAT GAA AAA GG	ENSG00000039068
	Reverse	GTG TAT GTG GCA ATG CGT TC	
N-CAD	Forward	GAC AAT GCC CCT CAA GTG TT	ENSG00000170558
	Reverse	TCA CAC GCA GGA TGG AAA TA	
SLUG	Forward	CTT TTT CTT GCC CTC ACT GC	ENSG00000019549
	Reverse	GCT TCG GAG TGA AGA AAT GC	
TWIST1	Forward	AGT CCG CAG TCT TAC GAG GA	ENSG00000122691
	Reverse	CAT CTT GGA GTC CAG CTC GT	

Table S2: Overview of significantly enriched genome regions bound to FOXA1 in ferroptotic cells compared to untreated controls

Chromosome	Start	End	Width	Log2FoldChange	pvalue	padj
chr1	125177010	125184585	7576	-1,194	0,002	0,006
chr1	143189543	143196164	6622	-1,163	0,003	0,006
chr1	143211365	143224006	12642	-1,203	0,002	0,005
chr1	143227041	143228185	1145	-1,166	0,003	0,006
chr1	143249564	143250811	1248	-1,335	0,004	0,006
chr1	143261455	143267803	6349	-1,206	0,002	0,005
chr1_KI270709v1_random	3587	8994	5408	-1,167	0,002	0,005
chr2	89830889	89834065	3177	-1,050	0,003	0,006
chr2	89835550	89837865	2316	-1,337	0,009	0,012
chr3	93470359	93470801	443	-1,328	0,001	0,005
chr4	49091387	49093922	2536	-1,070	0,008	0,010
chr4	49094532	49100149	5618	-1,232	0,002	0,005
chr4	49143075	49146670	3596	-1,147	0,004	0,006
chr4	49153138	49155368	2231	-1,050	0,003	0,006
chr4	49632314	49635881	3568	-1,118	0,003	0,006
chr4	49636565	49641731	5167	-1,097	0,012	0,015
chr4	190177041	190180141	3101	-1,058	0,004	0,006
chr5	49656292	49661874	5583	-1,208	0,002	0,005
chr5	49666169	49667431	1263	-1,330	0,000	0,005
chr10	41859110	41860822	1713	-1,227	0,003	0,006
chr10	41879171	41879681	511	-1,230	0,001	0,005
chr10	41881948	41884082	2135	-1,142	0,020	0,022
chr10	133687126	133690435	3310	-1,141	0,004	0,006
chr16	34571516	34576751	5236	-1,260	0,001	0,005
chr16	34584655	34587633	2979	-1,291	0,002	0,005
chr16	34587798	34589011	1214	-1,175	0,003	0,006
chr16	34589077	34596197	7121	-1,233	0,002	0,005

|						
chr16	46383894	46396853	12960	-1,226	0,002	0,005
chr17	26603527	26604747	1221	-1,108	0,007	0,009
chr17	26619202	26620327	1126	-1,278	0,005	0,006
chr17_KI270729v1_random	2108	6136	4029	-1,141	0,004	0,006
chr17_KI270729v1_random	20501	23628	3128	-1,133	0,004	0,006
chr20	31056797	31070093	13297	-1,162	0,002	0,005
chr21	8217544	8220689	3146	-0,890	0,047	0,050
chr21	8224769	8232425	7657	-1,168	0,002	0,005
chr21	8239285	8246018	6734	-1,199	0,002	0,005
chr21	8450219	8456017	5799	-1,135	0,004	0,006
chr21	8460222	8464400	4179	-1,001	0,017	0,020
chr22_KI270733v1_random	133817	136973	3157	-0,827	0,026	0,028
chrUn_GL000216v2	5261	7418	2158	-1,362	0,000	0,000
chrUn_KI270333v1	93	2683	2591	-0,965	0,020	0,022
chrUn_KI270337v1	0	1020	1021	-1,049	0,013	0,016

6.6. References

1. Dixon SJ, Lemberg KM, Lamprecht MR, Skouta R, Zaitsev EM, Gleason CE, Patel DN, Bauer AJ, Cantley AM, Yang WS, et al. Ferroptosis: an iron-dependent form of nonapoptotic cell death. Cell. 2012;149(5):1060-72.

2. Stockwell BR, Friedmann Angeli JP, Bayir H, Bush AI, Conrad M, Dixon SJ, Fulda S, Gascon S, Hatzios SK, Kagan VE, et al. Ferroptosis: A Regulated Cell Death Nexus Linking Metabolism, Redox Biology, and Disease. Cell. 2017;171(2):273-85.

3. Yan B, Ai Y, Sun Q, Ma Y, Cao Y, Wang J, Zhang Z, Wang X. Membrane Damage during Ferroptosis Is Caused by Oxidation of Phospholipids Catalyzed by the Oxidoreductases POR and CYB5R1. Mol Cell. 2021;81(2):355-69 e10.

4. Kupershmidt L, Amit T, Bar-Am O, Weinreb O, Youdim MB. Multi-target, neuroprotective and neurorestorative M30 improves cognitive impairment and reduces Alzheimer's-like neuropathology and age-related alterations in mice. Mol Neurobiol. 2012;46(1):217-20.

5. Yan N, Zhang J. Iron Metabolism, Ferroptosis, and the Links With Alzheimer's Disease. Front Neurosci. 2019;13:1443.

6. Fang X, Wang H, Han D, Xie E, Yang X, Wei J, Gu S, Gao F, Zhu N, Yin X, et al. Ferroptosis as a target for protection against cardiomyopathy. Proc Natl Acad Sci U S A. 2019;116(7):2672-80.

7. Li Y, Feng D, Wang Z, Zhao Y, Sun R, Tian D, Liu D, Zhang F, Ning S, Yao J, et al. Ischemia-induced ACSL4 activation contributes to ferroptosis-mediated tissue injury in intestinal ischemia/reperfusion. Cell Death Differ. 2019;26(11):2284-99.

8. Li S, Zheng L, Zhang J, Liu X, Wu Z. Inhibition of ferroptosis by up-regulating Nrf2 delayed the progression of diabetic nephropathy. Free Radic Biol Med. 2021;162:435-49.

9. Han C, Liu Y, Dai R, Ismail N, Su W, Li B. Ferroptosis and Its Potential Role in Human Diseases. Front Pharmacol. 2020;11:239.

10. Fernald K, Kurokawa M. Evading apoptosis in cancer. Trends Cell Biol. 2013;23(12):620-33.

11. Hassannia B, Vandenabeele P, Vanden Berghe T. Targeting Ferroptosis to Iron Out Cancer. Cancer Cell. 2019;35(6):830-49.

12. Torti SV, Torti FM. Iron and Cancer: 2020 Vision. Cancer Res. 2020;80(24):5435-48.

13. Trachootham D, Alexandre J, Huang P. Targeting cancer cells by ROS-mediated mechanisms: a radical therapeutic approach? Nat Rev Drug Discov. 2009;8(7):579-91.

14. VanderWall K, Daniels-Wells TR, Penichet M, Lichtenstein A. Iron in multiple myeloma. Crit Rev Oncog. 2013;18(5):449-61.

15. Steegmann-Olmedillas JL. The role of iron in tumour cell proliferation. Clin Transl Oncol. 2011;13(2):71-6.

16. Wang F, Lv H, Zhao B, Zhou L, Wang S, Luo J, Liu J, Shang P. Iron and leukemia: new insights for future treatments. J Exp Clin Cancer Res. 2019;38(1):406.

17. Yang WS, SriRamaratnam R, Welsch ME, Shimada K, Skouta R, Viswanathan VS, Cheah JH, Clemons PA, Shamji AF, Clish CB, et al. Regulation of ferroptotic cancer cell death by GPX4. Cell. 2014;156(1-2):317-31.

18. Bordini J, Morisi F, Cerruti F, Cascio P, Camaschella C, Ghia P, Campanella A. Iron Causes Lipid Oxidation and Inhibits Proteasome Function in Multiple Myeloma Cells: A Proof of Concept for Novel Combination Therapies. Cancers (Basel). 2020;12(4).

19. Zhong Y, Tian F, Ma H, Wang H, Yang W, Liu Z, Liao A. FTY720 induces ferroptosis and autophagy via PP2A/AMPK pathway in multiple myeloma cells. Life Sci. 2020;260:118077.

20. Kinowaki Y, Kurata M, Ishibashi S, Ikeda M, Tatsuzawa A, Yamamoto M, Miura O, Kitagawa M, Yamamoto K. Glutathione peroxidase 4 overexpression inhibits ROS-induced cell death in diffuse large B-cell lymphoma. Lab Invest. 2018;98(5):609-19.

21. Abdalkader M, Lampinen R, Kanninen KM, Malm TM, Liddell JR. Targeting Nrf2 to Suppress Ferroptosis and Mitochondrial Dysfunction in Neurodegeneration. Front Neurosci. 2018;12:466.

22. Dixon SJ, Patel DN, Welsch M, Skouta R, Lee ED, Hayano M, Thomas AG, Gleason CE, Tatonetti NP, Slusher BS, et al. Pharmacological inhibition of cystine-glutamate exchange induces endoplasmic reticulum stress and ferroptosis. Elife. 2014;3:e02523.

23. Feng H, Schorpp K, Jin J, Yozwiak CE, Hoffstrom BG, Decker AM, Rajbhandari P, Stokes ME, Bender HG, Csuka JM, et al. Transferrin Receptor Is a Specific Ferroptosis Marker. Cell Reports. 2020;30(10):3411-23.e7.

24. Park E, Chung SW. ROS-mediated autophagy increases intracellular iron levels and ferroptosis by ferritin and transferrin receptor regulation. Cell Death Dis. 2019;10(11):822.

25. Yuan H, Li X, Zhang X, Kang R, Tang D. Identification of ACSL4 as a biomarker and contributor of ferroptosis. Biochem Biophys Res Commun. 2016;478(3):1338-43.

26. Tang D, Chen X, Kang R, Kroemer G. Ferroptosis: molecular mechanisms and health implications. Cell Res. 2021;31(2):107-25.

27. Doll S, Proneth B, Tyurina YY, Panzilius E, Kobayashi S, Ingold I, Irmler M, Beckers J, Aichler M, Walch A, et al. ACSL4 dictates ferroptosis sensitivity by shaping cellular lipid composition. Nat Chem Biol. 2017;13(1):91-8.

28. Chu B, Kon N, Chen D, Li T, Liu T, Jiang L, Song S, Tavana O, Gu W. ALOX12 is required for p53-mediated tumour suppression through a distinct ferroptosis pathway. Nat Cell Biol. 2019;21(5):579-91.

29. Chen X, Comish PB, Tang D, Kang R. Characteristics and Biomarkers of Ferroptosis. Front Cell Dev Biol. 2021;9:637162.

30. Brown CW, Amante JJ, Chhoy P, Elaimy AL, Liu H, Zhu LJ, Baer CE, Dixon SJ, Mercurio AM. Prominin2 Drives Ferroptosis Resistance by Stimulating Iron Export. Dev Cell. 2019;51(5):575-86 e4.

31. Doll S, Freitas FP, Shah R, Aldrovandi M, da Silva MC, Ingold I, Goya Grocin A, Xavier da Silva TN, Panzilius E, Scheel CH, et al. FSP1 is a glutathione-independent ferroptosis suppressor. Nature. 2019;575(7784):693-8.

32. Brown CW, Amante JJ, Goel HL, Mercurio AM. The alpha6beta4 integrin promotes resistance to ferroptosis. J Cell Biol. 2017;216(12):4287-97.

33. Sun X, Niu X, Chen R, He W, Chen D, Kang R, Tang D. Metallothionein-1G facilitates sorafenib resistance through inhibition of ferroptosis. Hepatology. 2016;64(2):488-500.

34. Zaret KS, Carroll JS. Pioneer transcription factors: establishing competence for gene expression. Genes Dev. 2011;25(21):2227-41.

35. Cirillo LA, Lin FR, Cuesta I, Friedman D, Jarnik M, Zaret KS. Opening of compacted chromatin by early developmental transcription factors HNF3 (FoxA) and GATA-4. Mol Cell. 2002;9(2):279-89.

36. Nakshatri H, Badve S. FOXA1 as a therapeutic target for breast cancer. Expert opinion on therapeutic targets. 2007;11(4):507-14.

37. Gao N, Zhang J, Rao MA, Case TC, Mirosevich J, Wang Y, Jin R, Gupta A, Rennie PS, Matusik RJ. The role of hepatocyte nuclear factor-3 alpha (Forkhead Box A1) and androgen receptor in transcriptional regulation of prostatic genes. Mol Endocrinol. 2003;17(8):1484-507.

38. Moya M, Benet M, Guzman C, Tolosa L, Garcia-Monzon C, Pareja E, Castell JV, Jover R. Foxa1 reduces lipid accumulation in human hepatocytes and is down-regulated in nonalcoholic fatty liver. PLoS One. 2012;7(1):e30014.

39. Slebe F, Rojo F, Vinaixa M, Garcia-Rocha M, Testoni G, Guiu M, Planet E, Samino S, Arenas EJ, Beltran A, et al. FoxA and LIPG endothelial lipase control the uptake of extracellular lipids for breast cancer growth. Nat Commun. 2016;7:11199.

40. BenAyed-Guerfali D, Dabbeche-Bouricha E, Ayadi W, Trifa F, Charfi S, Khabir A, Sellami-Boudawara T, Mokdad-Gargouri R. Association of FOXA1 and EMT markers (Twist1 and E-cadherin) in breast cancer. Mol Biol Rep. 2019;46(3):3247-55.

41. Anzai E, Hirata K, Shibazaki M, Yamada C, Morii M, Honda T, Yamaguchi N, Yamaguchi N. FOXA1 Induces E-Cadherin Expression at the Protein Level via Suppression of Slug in Epithelial Breast Cancer Cells. Biol Pharm Bull. 2017;40(9):1483-9.

42. Zhang Y, Zhang D, Li Q, Liang J, Sun L, Yi X, Chen Z, Yan R, Xie G, Li W, et al. Nucleation of DNA repair factors by FOXA1 links DNA demethylation to transcriptional pioneering. Nat Genet. 2016;48(9):1003-13.

43. Lee J, You JH, Kim MS, Roh JL. Epigenetic reprogramming of epithelial-mesenchymal transition promotes ferroptosis of head and neck cancer. Redox Biol. 2020;37:101697.

44. Chen PH, Tseng WH, Chi JT. The Intersection of DNA Damage Response and Ferroptosis-A Rationale for Combination Therapeutics. Biology (Basel). 2020;9(8).

45. Ferri AL, Lin W, Mavromatakis YE, Wang JC, Sasaki H, Whitsett JA, Ang SL. Foxa1 and Foxa2 regulate multiple phases of midbrain dopaminergic neuron development in a dosage-dependent manner. Development. 2007;134(15):2761-9.

46. Pristera A, Lin W, Kaufmann AK, Brimblecombe KR, Threlfell S, Dodson PD, Magill PJ, Fernandes C, Cragg SJ, Ang SL. Transcription factors FOXA1 and FOXA2 maintain dopaminergic neuronal properties and control feeding behavior in adult mice. Proc Natl Acad Sci U S A. 2015;112(35):E4929-38.

47. Beard JA, Tenga A, Chen T. The interplay of NR4A receptors and the oncogene-tumor suppressor networks in cancer. Cell Signal. 2015;27(2):257-66.

48. Mullican SE, Zhang S, Konopleva M, Ruvolo V, Andreeff M, Milbrandt J, Conneely OM. Abrogation of nuclear receptors Nr4a3 and Nr4a1 leads to development of acute myeloid leukemia. Nat Med. 2007;13(6):730-5.

49. Ramirez-Herrick AM, Mullican SE, Sheehan AM, Conneely OM. Reduced NR4A gene dosage leads to mixed myelodysplastic/myeloproliferative neoplasms in mice. Blood. 2011;117(9):2681-90.

50. Sekiya T, Kashiwagi I, Yoshida R, Fukaya T, Morita R, Kimura A, Ichinose H, Metzger D, Chambon P, Yoshimura A. Nr4a receptors are essential for thymic regulatory T cell development and immune homeostasis. Nat Immunol. 2013;14(3):230-7.

51. Odagiu L, Boulet S, Maurice De Sousa D, Daudelin JF, Nicolas S, Labrecque N. Early programming of CD8(+) T cell response by the orphan nuclear receptor NR4A3. Proc Natl Acad Sci U S A. 2020;117(39):24392-402.

52. Wang H, Meyer CA, Fei T, Wang G, Zhang F, Liu XS. A systematic approach identifies FOXA1 as a key factor in the loss of epithelial traits during the epithelial-to-mesenchymal transition in lung cancer. BMC Genomics. 2013;14:680.

53. Skene PJ, Henikoff S. An efficient targeted nuclease strategy for high-resolution mapping of DNA binding sites. Elife. 2017;6.

54. Meers MP, Tenenbaum D, Henikoff S. Peak calling by Sparse Enrichment Analysis for CUT&RUN chromatin profiling. Epigenetics Chromatin. 2019;12(1):42.

55. De Cecco M, Criscione SW, Peckham EJ, Hillenmeyer S, Hamm EA, Manivannan J, Peterson AL, Kreiling JA, Neretti N, Sedivy JM. Genomes of replicatively senescent cells undergo global epigenetic changes leading to gene silencing and activation of transposable elements. Aging Cell. 2013;12(2):247-56.

56. Tasselli L, Xi Y, Zheng W, Tennen RI, Odrowaz Z, Simeoni F, Li W, Chua KF. SIRT6 deacetylates H3K18ac at pericentric chromatin to prevent mitotic errors and cellular senescence. Nat Struct Mol Biol. 2016;23(5):434-40.

57. Zhou Y, Zhou B, Pache L, Chang M, Khodabakhshi AH, Tanaseichuk O, Benner C, Chanda SK. Metascape provides a biologist-oriented resource for the analysis of systems-level datasets. Nat Commun. 2019;10(1):1523.

58. Pachkov M, Balwierz PJ, Arnold P, Ozonov E, van Nimwegen E. SwissRegulon, a database of genome-wide annotations of regulatory sites: recent updates. Nucleic Acids Res. 2013;41(Database issue):D214-20.

59. Human transcription factor target genes. https://github.com/slowkow/tftargets. Date accessed: 18th May 2021

60. Alim I, Caulfield JT, Chen Y, Swarup V, Geschwind DH, Ivanova E, Seravalli J, Ai Y, Sansing LH, Ste Marie EJ, et al. Selenium Drives a Transcriptional Adaptive Program to Block Ferroptosis and Treat Stroke. Cell. 2019;177(5):1262-79 e25.

61. Ayala A, Munoz MF, Arguelles S. Lipid peroxidation: production, metabolism, and signaling mechanisms of malondialdehyde and 4-hydroxy-2-nonenal. Oxidative medicine and cellular longevity. 2014;2014:360438.

62. Chen PH, Wu J, Ding CC, Lin CC, Pan S, Bossa N, Xu Y, Yang WH, Mathey-Prevot B, Chi JT. Kinome screen of ferroptosis reveals a novel role of ATM in regulating iron metabolism. Cell Death Differ. 2020;27(3):1008-22.

63. Tan NY, Khachigian LM. Sp1 phosphorylation and its regulation of gene transcription. Mol Cell Biol. 2009;29(10):2483-8.

64. Ye Z, Zhuo Q, Hu Q, Xu X, Mengqi L, Zhang Z, Xu W, Liu W, Fan G, Qin Y, et al. FBW7-NRA41-SCD1 axis synchronously regulates apoptosis and ferroptosis in pancreatic cancer cells. Redox Biol. 2021;38:101807.

65. Safe S, Shrestha R, Mohankumar K. Orphan nuclear receptor 4A1 (NR4A1) and novel ligands. Essays Biochem. 2021.

66. Wu H, Wang Y, Tong L, Yan H, Sun Z. Global Research Trends of Ferroptosis: A Rapidly Evolving Field With Enormous Potential. Front Cell Dev Biol. 2021;9:646311.

67. Chu S. Transcriptional regulation by post-transcriptional modification--role of phosphorylation in Sp1 transcriptional activity. Gene. 2012;508(1):1-8.

68. Hattori K, Ishikawa H, Sakauchi C, Takayanagi S, Naguro I, Ichijo H. Cold stress-induced ferroptosis involves the ASK1-p38 pathway. EMBO Rep. 2017;18(11):2067-78.

69. Li L, Hao Y, Zhao Y, Wang H, Zhao X, Jiang Y, Gao F. Ferroptosis is associated with oxygen-glucose deprivation/reoxygenation-induced Sertoli cell death. Int J Mol Med. 2018;41(5):3051-62.

70. Yu Y, Xie Y, Cao L, Yang L, Yang M, Lotze MT, Zeh HJ, Kang R, Tang D. The ferroptosis inducer erastin enhances sensitivity of acute myeloid leukemia cells to chemotherapeutic agents. Mol Cell Oncol. 2015;2(4):e1054549.

71. Kwon OS, Kwon EJ, Kong HJ, Choi JY, Kim YJ, Lee EW, Kim W, Lee H, Cha HJ. Systematic identification of a nuclear receptor-enriched predictive signature for erastin-induced ferroptosis. Redox Biol. 2020;37:101719.

72. Weigand I, Schreiner J, Rohrig F, Sun N, Landwehr LS, Urlaub H, Kendl S, Kiseljak-Vassiliades K, Wierman ME, Angeli JPF, et al. Active steroid hormone synthesis renders adrenocortical cells highly susceptible to type II ferroptosis induction. Cell Death Dis. 2020;11(3):192.

73. Belavgeni A, Bornstein SR, Linkermann A. Stress will kill you anyway! Cell Death Dis. 2020;11(4):218.

74. Augello MA, Hickey TE, Knudsen KE. FOXA1: master of steroid receptor function in cancer. EMBO J. 2011;30(19):3885-94.

75. Hertz R, Magenheim J, Berman I, Bar-Tana J. Fatty acyl-CoA thioesters are ligands of hepatic nuclear factor-4alpha. Nature. 1998;392(6675):512-6.

76. Kang R, Kroemer G, Tang D. The tumor suppressor protein p53 and the ferroptosis network. Free Radic Biol Med. 2019;133:162-8.

77. Fedorova O, Petukhov A, Daks A, Shuvalov O, Leonova T, Vasileva E, Aksenov N, Melino G, Barlev NA. Orphan receptor NR4A3 is a novel target of p53 that contributes to apoptosis. Oncogene. 2019;38(12):2108-22.

78. Viswanathan VS, Ryan MJ, Dhruv HD, Gill S, Eichhoff OM, Seashore-Ludlow B, Kaffenberger SD, Eaton JK, Shimada K, Aguirre AJ, et al. Dependency of a therapy-resistant state of cancer cells on a lipid peroxidase pathway. Nature. 2017;547(7664):453-7.

79. Hangauer MJ, Viswanathan VS, Ryan MJ, Bole D, Eaton JK, Matov A, Galeas J, Dhruv HD, Berens ME, Schreiber SL, et al. Drug-tolerant persister cancer cells are vulnerable to GPX4 inhibition. Nature. 2017;551(7679):247-50.

80. Metzakopian E, Bouhali K, Alvarez-Saavedra M, Whitsett JA, Picketts DJ, Ang SL. Genome-wide characterisation of Foxa1 binding sites reveals several mechanisms for regulating neuronal differentiation in midbrain dopamine cells. Development. 2015;142(7):1315-24.

81. Smurova K, De Wulf P. Centromere and Pericentromere Transcription: Roles and Regulation ... in Sickness and in Health. Front Genet. 2018;9:674.

82. Eymery A, Callanan M, Vourc'h C. The secret message of heterochromatin: new insights into the mechanisms and function of centromeric and pericentric repeat sequence transcription. Int J Dev Biol. 2009;53(2-3):259-68.

83. Hall LE, Mitchell SE, O'Neill RJ. Pericentric and centromeric transcription: a perfect balance required. Chromosome Res. 2012;20(5):535-46.

84. Jolly C, Metz A, Govin J, Vigneron M, Turner BM, Khochbin S, Vourc'h C. Stress-induced transcription of satellite III repeats. J Cell Biol. 2004;164(1):25-33.

85. Valgardsdottir R, Chiodi I, Giordano M, Rossi A, Bazzini S, Ghigna C, Riva S, Biamonti G. Transcription of Satellite III non-coding RNAs is a general stress response in human cells. Nucleic Acids Res. 2008;36(2):423-34.

86. Rizzi N, Denegri M, Chiodi I, Corioni M, Valgardsdottir R, Cobianchi F, Riva S, Biamonti G. Transcriptional activation of a constitutive heterochromatic domain of the human genome in response to heat shock. Mol Biol Cell. 2004;15(2):543-51.

87. Li Q, Zhang Y, Fu J, Han L, Xue L, Lv C, Wang P, Li G, Tong T. FOXA1 mediates p16(INK4a) activation during cellular senescence. EMBO J. 2013;32(6):858-73.

88. Hirata K, Takakura Y, Shibazaki M, Morii M, Honda T, Oshima M, Aoyama K, Iwama A, Nakayama Y, Takano H, et al. Forkhead box protein A1 confers resistance to transforming growth factor-beta-induced apoptosis in breast cancer cells through inhibition of Smad3 nuclear translocation. J Cell Biochem. 2018.

89. Palagani A, Op de Beeck K, Naulaerts S, Diddens J, Sekhar Chirumamilla C, Van Camp G, Laukens K, Heyninck K, Gerlo S, Mestdagh P, et al. Ectopic microRNA-150-5p transcription sensitizes glucocorticoid therapy response in MM1S multiple myeloma cells but fails to overcome hormone therapy resistance in MM1R cells. PLoS One. 2014;9(12):e113842.

90. Logie E, Chirumamilla CS, Perez-Novo C, Shaw P, Declerck K, Palagani A, Rangarajan S, Cuypers B, De Neuter N, Mobashar Hussain Urf Turabe F, et al. Covalent Cysteine Targeting of Bruton's Tyrosine Kinase (BTK) Family by Withaferin-A Reduces Survival of Glucocorticoid-Resistant Multiple Myeloma MM1 Cells. Cancers (Basel). 2021;13(7).

91. FastQC. 2015

92. Dobin A, Davis CA, Schlesinger F, Drenkow J, Zaleski C, Jha S, Batut P, Chaisson M, Gingeras TR. STAR: ultrafast universal RNA-seq aligner. Bioinformatics. 2013;29(1):15-21.

93. Love MI, Huber W, Anders S. Moderated estimation of fold change and dispersion for RNA-seq data with DESeq2. Genome Biol. 2014;15(12):550.

94. Zhang X, Du L, Qiao Y, Zhang X, Zheng W, Wu Q, Chen Y, Zhu G, Liu Y, Bian Z, et al. Ferroptosis is governed by differential regulation of transcription in liver cancer. Redox Biol. 2019;24:101211.

95. Rueden CT, Schindelin J, Hiner MC, DeZonia BE, Walter AE, Arena ET, Eliceiri KW. ImageJ2: ImageJ for the next generation of scientific image data. BMC Bioinformatics. 2017;18(1):529.

96. Pachkov M, Erb I, Molina N, van Nimwegen E. SwissRegulon: a database of genome-wide annotations of regulatory sites. Nucleic Acids Res. 2007;35(Database issue):D127-31.

97. Chen EY, Xu H, Gordonov S, Lim MP, Perkins MH, Ma'ayan A. Expression2Kinases: mRNA profiling linked to multiple upstream regulatory layers. Bioinformatics. 2012;28(1):105-11.

98. Skene PJ, Henikoff JG, Henikoff S. Targeted in situ genome-wide profiling with high efficiency for low cell numbers. Nat Protoc. 2018;13(5):1006-19.

99. Li H. Aligning sequence reads, clone sequences and assembly contigs with BWA-MEM. 2013.

100. Zhang H, Meltzer P, Davis S. RCircos: an R package for Circos 2D track plots. BMC Bioinformatics. 2013;14:244.
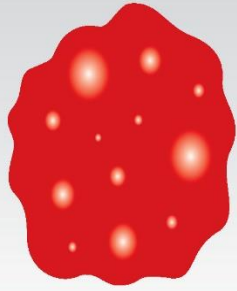
General Discussion

&

Future Perspectives

General Discussion and Future Perspectives

The main focus of this thesis was to evaluate protein kinase (PK) and ferroptosis therapeutics for effective treatment of therapy-resistant multiple myeloma (MM). Which PKs are involved in regulating multi-drug resistance in MM? Can MM cells be eliminated when (a subset) of these kinases are targeted with chemical compounds? Can induction of ferroptotic cell death help in overcoming resistance to drug-induced apoptosis? To what extent are ferroptosis-dependent epigenetic changes involved in promoting cell death?

Do Protein Kinase Inhibitors Hold Promise in Treating Drug-Resistant Multiple Myeloma Cells?

The importance of B cell receptor signaling in drug-resistant MM cells: BTK as therapeutic target

The human immune system heavily relies on the humoral response system, which is responsible for the production of pathogen-specific antibodies. Antibody-secreting plasma cells (PCs) orchestrate antibody production in response to pathological triggers and are typically generated in secondary lymphoid organs either from naive B cells or memory B cells. In healthy individuals, the differentiation of B cells toward PCs is associated with the downregulation of proliferative signaling pathways, such as B cell receptor signaling (BCR), and the upregulation of genes required for antibody production [1, 2]. In MM, however, PCs regain their proliferative capacity and accumulate unlimitedly in the bone marrow. Previous studies have reported that this enhanced self-renewal is partly caused by elevated expression and activation of Bruton tyrosine kinase (BTK), a non-receptor tyrosine kinase involved in BCR signaling [3, 4]. BTK also promotes MM metastasis and survival, bone disease, and therapy resistance [4-6], indicating that BTK is a critical positive regulator of MM. In line with these findings, we demonstrated in chapter 3 that glucocorticoid (GC)-resistant MM cells show significant hyperactivation of BTK and other non-receptor tyrosine kinases involved in BCR signaling compared to their therapy-sensitive counterparts. Although MM cells typically lack active BCRs, these results suggest that activation of downstream mediators of the BCR signaling pathway are involved in regulating therapy resistance, irrespective of BCR expression. To this end, pharmacological inhibition of BCR kinases, such as BTK and Syk (reviewed in [7]), has gained growing clinical interest. Preclinical data indicates that (combination) treatment with the irreversible covalent BTK inhibitor ibrutinib (IBR) is a promising therapeutic strategy for MM [5, 8-10]. This is supported by results obtained in clinical phase I/II trials investigating the anti-MM activity of IBR in combination treatments [11-13]. However, IBR is currently only FDA-approved in chronic lymphoid leukemia, mantle cell lymphoma, Waldenstrom macroglobulinemia, and marginal zone lymphoma, and has yet to be evaluated in MM phase III clinical trials. Unfortunately, phase III approval for protein kinase inhibitors (PKIs) in MM remains a major bottle neck as most trials are prematurely terminated due to issues with therapy efficacy

[7]. It is also important to note that, although preliminary clinical data has revealed that IBR displays an acceptable safety profile in MM, studies in other B cell malignancies have linked IBR use to an increased occurrence of ventricular arrhythmias and sudden cardiac death [14, 15]. Moreover, many patients harboring B cell malignancies display primary resistance against IBR therapy, while others often acquire resistance over time [16]. These concerns have prompted the development of second and third generation BTK inhibitors, which are also currently being explored in MM clinical trials [17]. However, as both first and later generations of BTK inhibitors target the conserved ATP-binding site of BTK, they typically share structural similarities. Exploring novel, structurally different BTK inhibitors could aid in achieving improved clinical benefits for MM patients.

BTK inhibition by Withaferin A and other natural compounds

Knowing that many FDA-approved drugs are natural products and derivatives, the extensive arsenal of plant compounds could be further explored to identify novel BTK inhibitors. A recent study in a murine model of collagen-induced arthritis, for instance, showed that decursin, a major active component of the purple parsnip (*Angelica gigas*), effectively and irreversibly targets BTK [18]. Likewise, curcuminoid extracts of turmeric (i.e. demethoxycurcumin, bisdemethoxycurcumin, and cyclocurcumin) are reported to indirectly inhibit BTK activity by targeting the histone acetyltransferase protein EP300, which orchestrates BTK activity and expression through histone acetylation of lysine residues located in the BTK promotor region [19, 20]. In chapter 3 of this dissertation, we explored whether another natural compound, namely the preclinical phytochemical Withaferin A (WA), also displays BTK inhibitory effects, since its broad spectrum anti-tumor activities have previously been attributed to covalent binding of target proteins, including protein kinases (PKs) [21-25]. Our data revealed that the tyrosine kinase inhibitor profiles of WA and IBR show a degree of similarity and that, analogous to IBR, WA inhibits BTK activity by covalently targeting the Cys481 residue located in its active site. Despite these similarities, WA is significantly more potent in killing GC-resistant MM cells compared to IBR, indicating that both MM-targeting agents harbor differences in their mechanisms of action. Indeed, we demonstrated that WA displays redundant kinase inhibitory effects and is able to target several Hinge-6 domain type (tyrosine) kinases. In line with other studies, kinome data presented in chapter 4 further suggests that several serine/threonine kinases (STKs) are inhibited by WA exposure as well [26]. As a result, the therapeutic efficacy of WA against different cancer cell types may strongly depend on its promiscuous nucleophilic cysteine reactivity towards the cellular repertoire of hyperactivated cell survival kinases. Moreover, chemoproteomics strategies have identified additional WA non-kinase target proteins as well, further explaining why the therapeutic efficacy of WA is much higher compared to IBR in GC-resistant MM cells [27, 28]. Does this polypharmacological drug profile of WA hamper its therapeutic applicability in MM? Compared to synthetic drugs, characterization of the molecular targets and pharmacokinetic and safety profiles of natural products, such as WA, remains much more challenging [29]. Additionally, low affinity and/or low specificity protein interactions of natural compounds are often responsible for adverse effects and can obscure experimental results. An extensive

pharmacological and toxicological characterization of these herbal agents is therefore required before their therapeutic use in a pre-clinical setting can be considered. This is especially important in the development of protein kinase inhibitors (PKIs), which is often plagued by issues with drug toxicity due to an inadequate understanding of PKI selectivity [30]. So far, preliminary (pre)clinical toxicology studies of WA in different cancer models revealed that WA administration is generally well tolerated with limited to no adverse toxicity reported [31-33]. However, no toxicology data of WA have been collected in B-cell malignancies, such as MM.

A possible strategy to minimize potential WA-related side effects in MM might include optimization of drug formulation and drug delivery. (Non)-targeted nanoparticle drug delivery systems are currently widely explored in context of MM treatment and demonstrate promising results in both preclinical and clinical studies [34]. Similarly, nanoparticle and milk-derived exosome delivery of WA in neuroblastoma and lung cancer models greatly reduces adverse drugs reactions [35, 36]. Increasing evidence, however, suggest that improving drug selectivity can sometimes negatively impact the therapeutic efficacy of PKIs and that compounds targeting multiple kinase may even be less toxic compared to single-target drugs because of their low-affinity binding properties [37-40]. Moreover, PKIs with different substrates may even be more beneficial in overcoming therapy resistance in oncological settings [40-44]. IBR resistant cancers, for example, generally harbor Cys481Ser mutations that disrupt IBR binding and, by extension, WA covalent targeting [45]. Yet, we demonstrate that the anti-MM effects of WA only partially rely on Cys481 binding and that cells dominantly expressing the Cys481Ser mutation still undergo WA-induced cell death. In this regard, targeting the cancer kinome with promiscuous polypharmacological (natural) products might be the next paradigm in treating multi-drug resistant tumors.

Target versus multi-target pharmacology: which way to go?

Compared to other therapeutic areas, drug attrition rates in anti-cancer drug development is much higher, with over 95 % of tested phase I compounds not reaching market authorization [46]. Although this is a multifactorial issue with several causes, a possible explanation lies in the dominant concept in drug discovery that only maximally selective ligands acting on individual targets have acceptable therapeutic indices (i.e. 'one gene', 'one drug', 'one disease' concept). Despite this target specificity paradigm, data mining studies have estimated the average drug compound interacts with 2-7 targets [47, 48]. This observation has prompted a drug-design paradigm shift from target-specific drugs to multi-target drugs [48], especially in multifactorial diseases which often require a polypharmacological treatment, such as cancer. In practice, it remains challenging to design synthetic compound with the desired polypharmacological profile, explaining why primarily bioactive natural compounds are currently being explored as multi-target drugs [48] (Figure 1). However, our understanding of the molecular pharmacology of most natural drugs largely remains incomplete and negatively affects the rational design of compounds acting on multiple targets with optimal efficacy and minimal toxicity [49]. This is also reflected by the results presented in this dissertation, where WA treatment of MM impact

several (kinase) signaling pathways. Although we, and others, demonstrate that WA decreases BTK, proteasome [50], and NF-κB [21] activity – all crucial, pro-oncogenic pathways in (therapy-resistant) MM – new molecular substrates and promiscuous binding targets of WA in different cancer models and within different concentration ranges are still being identified to this day [51-53]. Further extensive pharmacological profiling of WA therefore remains pivotal before its multi-target profile can be optimized for clinical use in MM.

In favor of multi-target pharmacology, large-scale functional genomic studies have shown that knockouts of single genes only sporadically exhibit phenotypic effects [54]. This robustness of phenotype is caused by underlying compensatory and redundant signaling pathways and protein interaction networks [55]. According to network biology analysis, impacting only one node or protein has a negligible effect on disease networks, while multi-targeting promotes robust functional changes [56]. This is especially true for epigenetic heterogenic cancer cells, which can adopt different compensatory or resistance mechanisms to escape drug single-targeting. In case of PKIs, for example, tumor cells can easily upregulate the expression or activity of secondary PKs to substitute for the targeted PK (Figure 2).
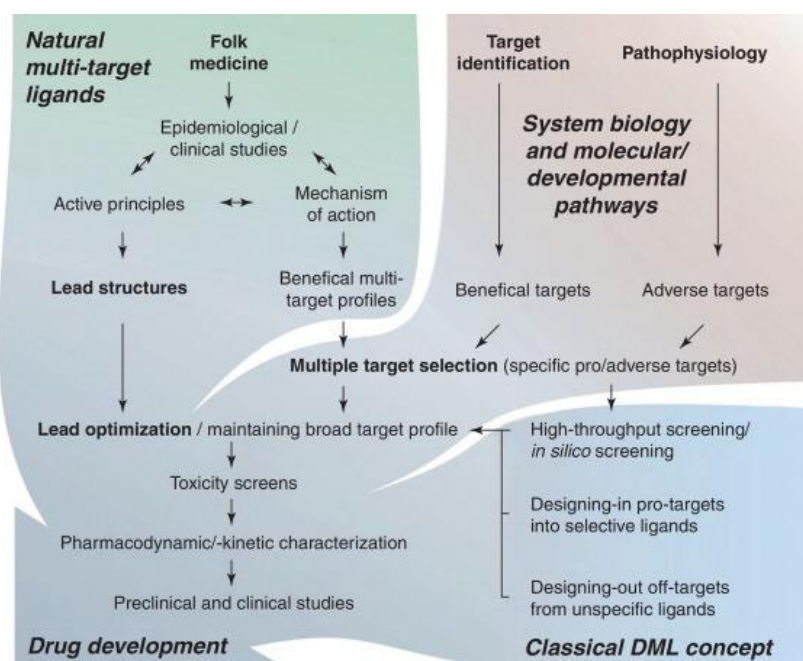
Figure 1: Multi-target approach for natural products. Figure copied from [49]. Abbreviations: DLM, designed multiple ligand.

For this reason, simultaneous targeting of different nodes within a kinase signaling network is being explored in several cancer types [57]. Combination treatments of PI3K inhibitors together with EGFR or ERBB2 inhibitors have been shown to be effective in different models and are currently being tested in clinical settings [58-60]. Similarly, dual inhibition of PI3K and mTOR by one or more PKIs have demonstrated to be more effective in glioma treatment than inhibition of either target alone [43]. These data imply that broad spectrum

kinase inhibitors hold promise in certain oncological settings, and might improve response rates in therapy resistant tumors, such as MM. In chapter 4, we further explored the potential of targeted polypharmacology in MM by performing a phosphopeptidome based kinase activity screening of apoptotic and ferroptotic GC-resistant MM cells. Our results show that both cell death modalities display unique signatures in PK inhibition, which could be further exploited by multi-targeting drugs. Although this requires further experimental validation, inhibition of ferroptosis- or apoptosis-specific kinases with (promiscuous) PKIs could potentially shape the mode of therapy-induced cell death and could even promote induction of mixed cell death types to completely eradicate all cancer subclones.

Although the biological rationale for considering polypharmacological drugs or promiscuous PKIs is compelling, multi-target compounds still face considerable challenges and still present a minority in the pharmaceutical industry [55]. The current lack of robust design tools that allow for efficient balancing of drug-like properties and unwanted adverse effects, make it extremely difficult to optimize the efficacy of multi-target drugs [55]. Moreover, even when polypharmaceutical agents of drug cocktails have been carefully designed, preclinical studies do not always predict their efficacy in humans. Failure of the preclinical model, misinterpretation of experimental data, or preexisting biases towards promising drug targets all limit the applicability of drug combinations [61]. For instance, preclinical studies supported the combination of cetuximab and bevacizumab in colorectal cancer [62], but failed in clinical trials and even reduced survival compared to single agents [63]. Another major obstacle is that it is often difficult to conduct clinical trials combining investigational (promiscuous) drugs if the two drugs originate from different pharmaceutical companies [61]. Because many companies fear about losing intellectual properties and the possibility of unforeseen off-target effects of the drug cocktails, they are often reluctant to participate in joint clinicals. Finally, investigating drug-drug interactions, drug toxicities, and pharmacokinetic properties of multi-target compounds is much more complex and labor-intensive, making the switch toward targeted polypharmacology considerably more demanding.
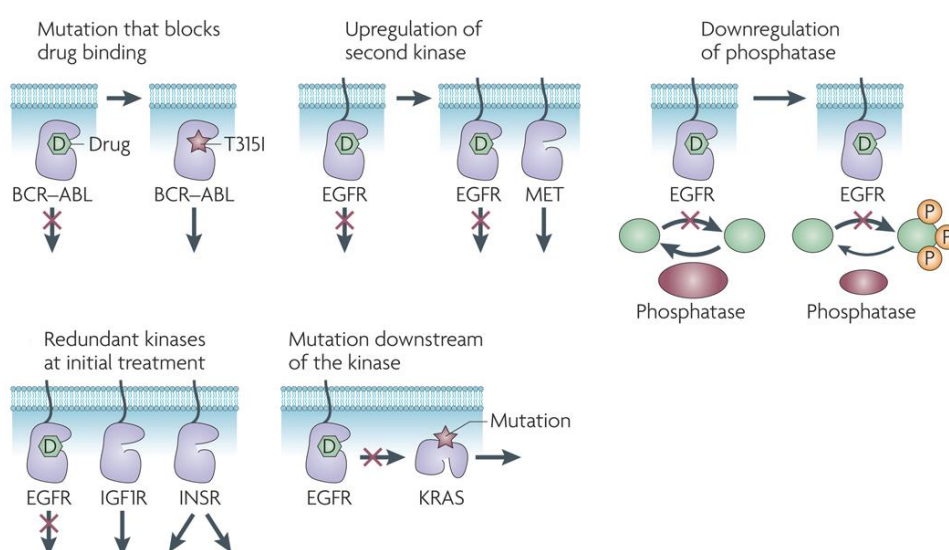
Figure 2 (previous page): Tumor cells can adopt several resistance or compensatory mechanisms to circumvent single protein kinase targeting by protein kinase inhibitors. First, treatment with single kinase inhibitors can result in the selection of a subpopulation of cancer cells that carry a mutation required for drug binding. Second, inhibition of a specific kinase can trigger the upregulation of second kinases that substitute for the drug target. Thirdly, cancer cells can respond to kinase inhibition by downregulating protein phosphatases responsible for dephosphorylating the substrates of that kinase. Alternatively, expression of multiple redundant oncogenic kinases can decrease the cellular potency of kinase inhibitors. Finally, mutational activation of downstream kinase pathway components can bypass the inhibitory effects of protein kinases. Figure copied from [61].

Can ferroptosis-induced epigenetic changes overcome therapy-resistance in multiple myeloma?

Differentiating between cell death modalities

Most anti-cancer compounds are reported to promote (regulated) cell death (RCD) of malignant cells by hijacking apoptosis signaling pathways. However, the expanding cell death research field has emphasized the importance of other RCD modalities, such as necroptosis and ferroptosis, in cancer therapeutic as well (reviewed in [64] and [65]). What is the therapeutical relevance of these cell death modalities in cancer research? Why is it important to discriminate between different modes of cell death when the main goal essentially remains to eradicate all malignant cells, regardless of how this is achieved? From an investigational and drug developmental point of view, quantification and identification of cell death modes provides crucial information for important physiological questions, such as cytotoxicity, dose- and time-dependency, and efficacy of anti-cancer compounds [66]. Different cell death modalities can also have distinct therapeutical and functional consequences. For example, most human cancers are able to evade apoptosis through various molecular mechanisms, which not only promotes tumor formation and progression but also enhances therapy resistance. Inducing other modes of RCD can therefore aid in overcoming drug-induced apoptosis resistance. In chapter 5, we explored the sensitivity of (GC-resistant) MM cells to ferroptosis and found that several ferroptosis inducers proved to be effective in killing myeloma cells. These results demonstrate that even MM cells resistant to GC-induced apoptosis are prone to ferroptotic cell death. In line with these findings, ferroptosis induction in pancreas cancer [67], DLBCL [68], and head and neck cancer [69], could overcome apoptosis-resistance, highlighting the importance of choosing the most effective cell death modulators for specific oncological settings. Furthermore, growing evidence suggests that, unlike apoptosis, ferroptosis promotes immunogenic cell death in early stages and promotes immune system recognition [70]. Since malignant cells often develop strategies to escape immune surveillance, this additional pro-immunogenic feature of ferroptotic compounds may help in targeting cancer-induced immune dysfunction. The choice of desired cell death modality can also be important for the implementation of combination treatment strategies. Due to the heterogeneity of the disease, MM patients are mainly treated with drug cocktails that include compounds targeting different oncogenic pathways (e.g. proteasome inhibitors, GCs, immunomodulatory drugs, etc.). In this context, the addition of agents that promote non-apoptotic cell death could increase the therapeutic efficacy of combination treatments.

Indeed, ferroptosis-mediated iron toxicity is reported to increase the therapeutic response of bortezomib-melphalan-prednisone regimens in MM [71]. A final aspect that can be considered when comparing different cell death inducers, is their tumor-targeting selectivity. Several apoptotic compounds, including imiquimod [72], leczyme [73], and K$_V$10.1-targeting antibodies [74], have been described to primarily target cancer cells without affecting healthy cells. So far, the tumor selectivity of ferroptotic compounds has not sufficiently been studied. However, as most ferroptotic inducers either target glutathione peroxidase 4 (GPX4) or the system Xc⁻ cystine/glutamate antiporter, two proteins that exhibit ubiquitous expression patterns, some adverse effects are to be expected. On the other hand, GPX4 and Xc⁻ expression generally is significantly higher in tumor cells due to their increased oxidative stress levels [75, 76], and optimizing delivery methods and dosage might improve tumor selectivity. In the same line, malignant cells, including cancer stem cells, typically display higher intracellular iron levels because of their increased proliferation capacity, which likely increases their sensitivity to ferroptosis agents [76]. All these examples illustrate that a more thorough understanding of the various cell death routes can have far-reaching implications for the pharmacological management of cancer and other diseases

Epigenetic changes of ferroptotic cancer cells: cause or consequence?

The involvement of nuclear and epigenetic signaling events in RCD often remains poorly studied, especially in context of ferroptotic cell death. Some would argue that it is rather irrelevant to study epigenetic regulatory mechanisms in cells that are dying anyway: to what extend are these cell death-induced epigenetic changes biologically relevant? Firstly, characterization of ferroptosis-mediated epigenetic alterations could have significant therapeutical implications and may provide an additional rationale for the use of epigenetic drugs for ferroptosis chemosensitization strategies. Typically, tumor cells show high epigenetic heterogeneity-plasticity in their microenvironment, which triggers clonal selection for therapy resistant clones upon exposure to chemotherapeutic drugs. In chapter 5 of this PhD work, we demonstrated that early and late ferroptotic cells display broad spectrum changes in epigenetic marks and display decreased expression of H3K18ac, H3K27ac, and H3K79me3, which are all associated with chromatin instability and DNA damage. Epigenetic drugs, which are already widely used for treatment of hematological cancers [77, 78], could be employed to enhance or disrupt ferroptosis-dependent epigenetic changes. For example, treatment with histone acetyltransferase (HAT) inhibitors could further decrease acetylation of key ferroptosis-driven histone marks and facilitate ferroptotic cell death in malignant cells [79-81]. Alternatively, in clinical settings where inhibition of ferroptosis is preferred, such as Alzheimer's disease or other neurodegenerative disorders, histone deacetylase inhibitors (HDACi) could possibly help in preventing ferroptosis-mediated loss of histone acetylation and genome instability. This hypothesis is in line with a recent study by Zille et al., which reported that class I HDACi selectively protect neurons while augmenting ferroptosis in cancer cells [82]. Thus, including HDACi in (combination) cancer and/or neurodegenerative treatment regimens could significantly impact ferroptosis sensitivity.

Characterization of ferroptotic-mediated epigenetic changes also helps in uncovering novel cell death signaling pathways. Western blot screening and chromatin immunoprecipitation (ChIP) experiments recently demonstrated that the tumor suppressor p53 negatively regulates H2B monoubiquitination, which leads to downregulation of the solute carrier family member 11 (SLC7A11), a key component of the Xc⁻ system and regulator of ferroptosis sensitivity [83]. These observations further expand the idea that p53 is a critical chromatin regulator [84, 85] and that chromatin remodeling plays an essential role in ferroptosis. In chapter 6, we reported that another chromatin regulator, forkhead box a1 (FOXA1), is significantly upregulated in ferroptotic cells and that its binding interactions with pericentromeric chromatin are disrupted upon RSL3 treatment. Therefore, the anti-cancer effects of ferroptotic compounds seem to rely on chromatin destabilization and aberrant transcription of pericentromeric satellite regions. Indeed, two hallmarks of ferroptosis, namely lipid peroxidation and increased labile iron levels, have previously been associated with genome instability [86, 87]. In this context, we found in chapter 5 that histone proteins display iron-binding properties and are able to form complexes with labile, non-heme iron, providing another possible explanation for iron-mediated genotoxicity in ferroptotic cells. Overall, the role of key epigenetic players, such as histones, in cell death modalities deserves further investigation as their oxidative stress and (iron) metabolic sensor abilities might be considerably more prominent in preserving genome integrity.

Despite these promising applications of epigenetic cell death research, it remains challenging to assess whether identified epigenetic alterations are a cause or consequence of ferroptosis induction. To this end, functional assays, animal studies, and longitudinal studies should be applied to independently prove the causality and functionality of specific epigenetic marks in ferroptotic cell death. Of particular interest, novel CRISPR/Cas9-based epigenetic editing techniques could help to investigate the causative relationship between ferroptosis induction and some of the epigenetic marks described in chapter 5 [88]. When these epigenetic marks prove to be non-causal, they could alternatively be used as predictive or prognostic markers for ferroptosis sensitivity as ferroptosis resistance has already been described in some cancer types [35, 89]. Given that cancer therapy-resistance is often orchestrated by epigenetic alterations, an epigenome comparison of ferroptosis-resistant and -sensitive might help to identify novel ferroptosis biomarkers and predict efficacy of ferroptosis inducers.

Ferrosenescence: eradicating MM tumor cells through premature aging?

Cellular senescence is a phenomenon wherein proliferation-competent cells undergo permanent growth arrest in response to genotoxic stress [90, 91]. This senescent state is accompanied by an acquired resistance to mitogenic or oncogenic stimuli and is implicated in a wide spectrum of age-related diseases [92]. Throughout chapters 5 and 6, we observed that ferroptosis induction is associated with significant alterations in expression of cellular senescence markers and with epigenetic and chromatin landscape remodeling. For instance, our histone proteomics analysis showed that RSL3-treated myeloma cells are depleted of H3K18ac compared to untreated controls. This histone modification has

previously been reported to drive progression of many cancer types [93] and is linked to cellular senescence protection by regulating expression of pericentric transcripts [94]. Proper regulation of pericentric gene expression is crucial for preventing cellular senescence seeing that aberrant pericentric satellite DNA decondensation and subsequent defective pericentric silencing promote genome instability and genotoxic stress, key triggers of senescence [95, 96]. Notably, we described in chapter 6 that heterochromatin-binding pioneer transcription factor (TF) FOXA1 is depleted in pericentromeric regions of ferroptotic MM cells despite its significant increase in mRNA and protein expression. This suggests that FOXA1 is no longer able to bind to pericentric DNA of ferroptotic cells, possibly due to increased DNA decondensation taking place in these repetitive regions, and indirectly indicates that ferroptosis inducers promote pericentric DNA decondensation in MM, similar as observed in senescent cells. In support of this hypothesis, increased FOXA1 expression [97], lipid peroxidation [98], iron [99], and ferroptotic cell death itself [99, 100] have been associated with the onset of senescent phenotypes.

This potential ferroptosis-induced cellular senescence of MM cells can have both beneficial as harmful clinical implications. In response to anti-cancer interventions, cancer cells can adopt a senescent state (also known as 'therapy induced senescence') [101]. In early stages of the disease, this promotes tumor suppression by blocking the proliferation of damaged/malignant cells and by enhancing immune clearance through higher secretion of inflammatory cytokines, growth factors, and proteases [102-104]. Accordingly, doxorubicin- and melphalan-induced senescent MM cells triggered natural killer cell activation, proliferation, and maturation, thus enhancing tumor immune surveillance [105]. However, when senescent cells are not cleared timely, they can facilitate the development of therapy-resistant cancer cells via upregulation of senescence-orchestrated upregulation of survival pathways [106, 107]. For example, several studies have reported that senescent MM cells can trigger a senescent phenotype in bone marrow mesenchymal stromal cells, which participate in disease progression and relapse by altering the tumor microenvironment [108-110]. To this end, ferroptosis-triggered senescence can have a dual impact on MM development. To circumvent the detrimental effects of cellular senescence, several research groups are currently investigating a 'one-two punch approach', wherein senescence-inducing cancer therapies are followed by treatments with senotherapeutics, which selectively targets senescent cells (reviewed in [111]). This combined regimen would allow for mitigation of unwanted effects of persistent senescent cells while optimally exploiting the senescence-dependent tumor suppressive effects. One of the senolytic therapies proposed for elimination of senescent myeloma cells includes chimeric antigen receptor T-cell (CAR-T) therapy targeting the urokinase-type plasminogen activator receptor, which is broadly induced during cellular senescence [112]. However, the lack of reliable senescence markers, especially *in vivo*, is one of the critical issues hampering the clinical implication of senolytic drugs in oncology [113].

Key Findings

Do protein kinase inhibitors hold promise in treating drug-resistant multiple myeloma cells?

- Glucocorticoid resistance in multiple myeloma is associated with hyperactivation of BTK-mediated B-cell receptor (BCR) signaling
- Withaferin A inhibits BCR-BTK kinase activity by Cys481-mediated covalent targeting of BTK
- Withaferin A is more potent in eliminating glucocorticoid-resistant multiple myeloma cells than FDA approved BTK inhibitor ibrutinib
- Similar to Withaferin A, ferroptotic compounds are able to inhibit kinases involved in B-cell receptor signaling, including BTK
- Different cell death mechanisms exhibit different kinase inhibitory profiles, highlighting that combination treatments of ferroptotic and apoptotic drugs may be beneficial for targeting multifactorial diseases, such as multiple myeloma
- Promiscuous inhibition of (multiple) BTK family tyrosine kinases by Withaferin A or ferroptotic agents represents a promising strategy to overcome glucocorticoid-therapy resistance in multiple myeloma

Can ferroptosis-induced epigenetic changes overcome therapy-resistance in multiple myeloma?

- Multiple myeloma cells are sensitive to ferroptosis cell death induction, irrespective of their glucocorticoid-sensitivity status
- Ferroptosis induction in multiple myeloma triggers a transcriptome stress response and promotes expression of several chromatin remodelers, including heterochromatin-binding pioneer transcription factor FOXA1
- Despite its significant upregulation in ferroptotic multiple myeloma cells, FOXA1 binding to pericentric DNA is lost, suggesting that global DNA decondensation of pericentric regions is triggered under ferroptotic conditions
- Ferroptotic stress signals propagate to the nuclei and initiate double-stranded DNA breaks, formation or iron-histone complexes, DNA methylation changes, and histone post-translational modification changes
- Ferroptosis-dependent remodeling of the epigenetic and chromatin landscape alters cellular senescence and DNA repair signaling pathways
- Combining ferroptotic, epigenetic, and senolytic drugs might prove to be an attractive strategy to eliminate multiple myeloma cells

Conclusions and future perspectives

The results presented in this dissertation highlight that, through interfering with therapy resistance pathways, remodeling of the epigenetic landscape, and promoting genomic instability, PKIs and ferroptosis agents demonstrate therapeutical potential in overcoming therapy resistance in MM. However, further validation studies are essential before compounds investigated in this study, including WA, IBR, and RSL3, can be applied in a clinical setting. In this PhD work, most experiments were performed on one cell model of GC-resistant MM cells. Follow-up studies will have to validate whether the research outcomes presented here are valid in other *in vitro* and *in vivo* models of MM therapy resistance, such as bortezomib-resistant or thalidomide-resistant MM models, as well.

The disease heterogeneity observed in MM and other (hematological) cancers provide one explanation for the high drug attrition rates of anti-cancer drugs. The exploration of combinational or multi-pharmacological drug targeting approaches might aid in overcoming the challenges that single-target drugs and the overall target-specificity paradigm in drug design currently face. The implication of (natural) kinase inhibitors that can simultaneously target several resistance- or disease-causing PKs might limit MM relapse and improve median overall survival. Similarly, a combined regimen of epigenetic drugs, ferroptosis inducers or senolytic agents could prevent the development of therapy resistance and enhance drug response rates. Nonetheless, the wanted versus unwanted effects of each of these polypharmaceutical drug cocktails will have to be carefully considered and balanced, and will continue to remain one of the key challenges that the pharmacological industry has to face. Extensive fundamental and preclinical studies aiming to further characterize the broad spectrum effects of (natural) cytotoxic compounds and to identify (ferroptotic) cell death and senescence markers will, therefore, be extremely valuable in developing novel anti-MM agents. To this end, the combination and integration of transcriptomics, proteomics, kinomics, and epigenomics data, as carried out in this PhD work, will prove to be indispensable to fully understand and overcome MM therapy resistance mechanisms.

References

1. Shaffer AL, Lin KI, Kuo TC, Yu X, Hurt EM, Rosenwald A, Giltnane JM, Yang L, Zhao H, Calame K, et al. Blimp-1 orchestrates plasma cell differentiation by extinguishing the mature B cell gene expression program. Immunity. 2002;17(1):51-62.
2. Reimold AM, Iwakoshi NN, Manis J, Vallabhajosyula P, Szomolanyi-Tsuda E, Gravallese EM, Friend D, Grusby MJ, Alt F, Glimcher LH. Plasma cell differentiation requires the transcription factor XBP-1. Nature. 2001;412(6844):300-7.
3. Yang Y, Shi J, Gu Z, Salama ME, Das S, Wendlandt E, Xu H, Huang J, Tao Y, Hao M, et al. Bruton tyrosine kinase is a therapeutic target in stem-like cells from multiple myeloma. Cancer Res. 2015;75(3):594-604.
4. Bam R, Venkateshaiah SU, Khan S, Ling W, Randal SS, Li X, Zhang Q, van Rhee F, Barlogie B, Epstein J, et al. Role of Bruton's tyrosine kinase (BTK) in growth and metastasis of INA6 myeloma cells. Blood Cancer J. 2014;4:e234.
5. Tai YT, Chang BY, Kong SY, Fulciniti M, Yang G, Calle Y, Hu Y, Lin J, Zhao JJ, Cagnetta A, et al. Bruton tyrosine kinase inhibition is a novel therapeutic strategy targeting tumor in the bone marrow microenvironment in multiple myeloma. Blood. 2012;120(9):1877-87.
6. Gu C, Peng H, Lu Y, Yang H, Tian Z, Yin G, Zhang W, Lu S, Zhang Y, Yang Y. BTK suppresses myeloma cellular senescence through activating AKT/P27/Rb signaling. Oncotarget. 2017;8(34):56858-67.
7. Lind J, Czernilofsky F, Vallet S, Podar K. Emerging protein kinase inhibitors for the treatment of multiple myeloma. Expert Opin Emerg Drugs. 2019;24(3):133-52.
8. Rushworth SA, Bowles KM, Barrera LN, Murray MY, Zaitseva L, MacEwan DJ. BTK inhibitor ibrutinib is cytotoxic to myeloma and potently enhances bortezomib and lenalidomide activities through NF-kappaB. Cell Signal. 2013;25(1):106-12.
9. Murray MY, Zaitseva L, Auger MJ, Craig JI, MacEwan DJ, Rushworth SA, Bowles KM. Ibrutinib inhibits BTK-driven NF-kappaB p65 activity to overcome bortezomib-resistance in multiple myeloma. Cell Cycle. 2015;14(14):2367-75.
10. Ma J, Gong W, Liu S, Li Q, Guo M, Wang J, Wang S, Chen N, Wang Y, Liu Q, et al. Ibrutinib targets microRNA-21 in multiple myeloma cells by inhibiting NF-κB and STAT3. Tumour biology : the journal of the International Society for Oncodevelopmental Biology and Medicine. 2018;40(1):1010428317731369.
11. Richardson PG, Bensinger WI, Huff CA, Costello CL, Lendvai N, Berdeja JG, Anderson LD, Jr., Siegel DS, Lebovic D, Jagannath S, et al. Ibrutinib alone or with dexamethasone for relapsed or relapsed and refractory multiple myeloma: phase 2 trial results. Br J Haematol. 2018;180(6):821-30.
12. Chari A, Cornell RF, Gasparetto C, Karanes C, Matous JV, Niesvizky R, Lunning M, Usmani SZ, Anderson LD, Jr., Chhabra S, et al. Final analysis of a phase 1/2b study of ibrutinib combined with carfilzomib/dexamethasone in patients with relapsed/refractory multiple myeloma. Hematol Oncol. 2020;38(3):353-62.
13. Hajek R, Pour L, Ozcan M, Martin Sanchez J, Garcia Sanz R, Anagnostopoulos A, Oriol A, Cascavilla N, Terjung A, Lee Y, et al. A phase 2 study of ibrutinib in combination with bortezomib and dexamethasone in patients with relapsed/refractory multiple myeloma. Eur J Haematol. 2020;104(5):435-42.
14. Guha A, Derbala MH, Zhao Q, Wiczer TE, Woyach JA, Byrd JC, Awan FT, Addison D. Ventricular Arrhythmias Following Ibrutinib Initiation for Lymphoid Malignancies. J Am Coll Cardiol. 2018;72(6):697-8.
15. Salem JE, Manouchehri A, Bretagne M, Lebrun-Vignes B, Groarke JD, Johnson DB, Yang T, Reddy NM, Funck-Brentano C, Brown JR, et al. Cardiovascular Toxicities Associated With Ibrutinib. J Am Coll Cardiol. 2019;74(13):1667-78.

16. George B, Chowdhury SM, Hart A, Sircar A, Singh SK, Nath UK, Mamgain M, Singhal NK, Sehgal L, Jain N. Ibrutinib Resistance Mechanisms and Treatment Strategies for B-Cell lymphomas. Cancers (Basel). 2020;12(5).

17. An Open-Label, Phase 1b Study of Acalabrutinib With and Without Dexamethasone in Subjects With Multiple Myeloma.

18. Cho H, Lee E, Kwon HA, Seul L, Jeon HJ, Yu JH, Ryu JH, Jeon R. Discovery of Tricyclic Pyranochromenone as Novel Bruton's Tyrosine Kinase Inhibitors with in Vivo Antirheumatic Activity. Int J Mol Sci. 2020;21(21).

19. Chen Y, Shu W, Chen W, Wu Q, Liu H, Cui G. Curcumin, both histone deacetylase and p300/CBP-specific inhibitor, represses the activity of nuclear factor kappa B and Notch 1 in Raji cells. Basic & clinical pharmacology & toxicology. 2007;101(6):427-33.

20. Liu Z, Mai A, Sun J. Lysine acetylation regulates Bruton's tyrosine kinase in B cell activation. Journal of immunology (Baltimore, Md : 1950). 2010;184(1):244-54.

21. Heyninck K, Lahtela-Kakkonen M, Van der Veken P, Haegeman G, Vanden Berghe W. Withaferin A inhibits NF-kappaB activation by targeting cysteine 179 in IKKbeta. Biochem Pharmacol. 2014;91(4):501-9.

22. Hahm ER, Lee J, Singh SV. Role of mitogen-activated protein kinases and Mcl-1 in apoptosis induction by Withaferin A in human breast cancer cells. Mol Carcinog. 2014;53(11):907-16.

23. Grogan PT, Sleder KD, Samadi AK, Zhang H, Timmermann BN, Cohen MS. Cytotoxicity of Withaferin A in glioblastomas involves induction of an oxidative stress-mediated heat shock response while altering Akt/mTOR and MAPK signaling pathways. Invest New Drugs. 2013;31(3):545-57.

24. Mandal C, Dutta A, Mallick A, Chandra S, Misra L, Sangwan RS, Mandal C. Withaferin A induces apoptosis by activating p38 mitogen-activated protein kinase signaling cascade in leukemic cells of lymphoid and myeloid origin through mitochondrial death cascade. Apoptosis. 2008;13(12):1450-64.

25. Oh JH, Lee TJ, Kim SH, Choi YH, Lee SH, Lee JM, Kim YH, Park JW, Kwon TK. Induction of apoptosis by Withaferin A in human leukemia U937 cells through down-regulation of Akt phosphorylation. Apoptosis. 2008;13(12):1494-504.

26. Chirumamilla CS, Perez-Novo C, Van Ostade X, Vanden Berghe W. Molecular insights into cancer therapeutic effects of the dietary medicinal phytochemical Withaferin A. Proc Nutr Soc. 2017;76(2):96-105.

27. Dom M, Offner F, Vanden Berghe W, Van Ostade X. Proteomic characterization of Withaferin A-targeted protein networks for the treatment of monoclonal myeloma gammopathies. J Proteomics. 2018;179:17-29.

28. Dom M, Vanden Berghe W, Van Ostade X. Broad-spectrum antitumor properties of Withaferin A: a proteomic perspective. RSC Med Chem. 2020;11:30-50.

29. Carlson EE. Natural products as chemical probes. ACS Chem Biol. 2010;5(7):639-53.

30. Noble ME, Endicott JA, Johnson LN. Protein kinase inhibitors: insights into drug design from structure. Science. 2004;303(5665):1800-5.

31. Pires N, Gota V, Gulia A, Hingorani L, Agarwal M, Puri A. Safety and pharmacokinetics of Withaferin-A in advanced stage high grade osteosarcoma: A phase I trial. J Ayurveda Integr Med. 2020;11(1):68-72.

32. Patel SB, Rao NJ, Hingorani LL. Safety assessment of Withania somnifera extract standardized for Withaferin A: Acute and sub-acute toxicity study. J Ayurveda Integr Med. 2016;7(1):30-7.

33. Thaiparambil JT, Bender L, Ganesh T, Kline E, Patel P, Liu Y, Tighiouart M, Vertino PM, Harvey RD, Garcia A, et al. Withaferin A inhibits breast cancer invasion and metastasis at sub-cytotoxic doses by inducing vimentin disassembly and serine 56 phosphorylation. Int J Cancer. 2011;129(11):2744-55.

34. de la Puente P, Azab AK. Nanoparticle delivery systems, general approaches, and their implementation in multiple myeloma. Eur J Haematol. 2017;98(6):529-41.

35. Hassannia B, Wiernicki B, Ingold I, Qu F, Van Herck S, Tyurina YY, Bayir H, Abhari BA, Angeli JPF, Choi SM, et al. Nano-targeted induction of dual ferroptotic mechanisms eradicates high-risk neuroblastoma. J Clin Invest. 2018;128(8):3341-55.

36. Munagala R, Aqil F, Jeyabalan J, Gupta RC. Bovine milk-derived exosomes for drug delivery. Cancer Lett. 2016;371(1):48-61.

37. Csermely P, Agoston V, Pongor S. The efficiency of multi-target drugs: the network approach might help drug design. Trends Pharmacol Sci. 2005;26(4):178-82.

38. Ogunleye L, Jester B, Riemen A, Badran A, Wang P, Ghosh I. When tight is too tight: Dasatinib and its lower affinity analogue for profiling kinase inhibitors in a three-hybrid split-luciferase system. MedChemComm. 2014(3).

39. Tang X, Orlicky S, Mittag T, Csizmok V, Pawson T, Forman-Kay JD, Sicheri F, Tyers M. Composite low affinity interactions dictate recognition of the cyclin-dependent kinase inhibitor Sic1 by the SCFCdc4 ubiquitin ligase. Proc Natl Acad Sci U S A. 2012;109(9):3287-92.

40. Apsel B, Blair JA, Gonzalez B, Nazif TM, Feldman ME, Aizenstein B, Hoffman R, Williams RL, Shokat KM, Knight ZA. Targeted polypharmacology: discovery of dual inhibitors of tyrosine and phosphoinositide kinases. Nat Chem Biol. 2008;4(11):691-9.

41. Copland M, Pellicano F, Richmond L, Allan EK, Hamilton A, Lee FY, Weinmann R, Holyoake TL. BMS-214662 potently induces apoptosis of chronic myeloid leukemia stem and progenitor cells and synergizes with tyrosine kinase inhibitors. Blood. 2008;111(5):2843-53.

42. Sergina NV, Rausch M, Wang D, Blair J, Hann B, Shokat KM, Moasser MM. Escape from HER-family tyrosine kinase inhibitor therapy by the kinase-inactive HER3. Nature. 2007;445(7126):437-41.

43. Fan QW, Knight ZA, Goldenberg DD, Yu W, Mostov KE, Stokoe D, Shokat KM, Weiss WA. A dual PI3 kinase/mTOR inhibitor reveals emergent efficacy in glioma. Cancer Cell. 2006;9(5):341-9.

44. Engelman JA, Chen L, Tan X, Crosby K, Guimaraes AR, Upadhyay R, Maira M, McNamara K, Perera SA, Song Y, et al. Effective use of PI3K and MEK inhibitors to treat mutant Kras G12D and PIK3CA H1047R murine lung cancers. Nat Med. 2008;14(12):1351-6.

45. Sharma S, Galanina N, Guo A, Lee J, Kadri S, Van Slambrouck C, Long B, Wang W, Ming M, Furtado LV, et al. Identification of a structurally novel BTK mutation that drives ibrutinib resistance in CLL. Oncotarget. 2016;7(42):68833-41.

46. Moreno L, Pearson AD. How can attrition rates be reduced in cancer drug discovery? Expert Opin Drug Discov. 2013;8(4):363-8.

47. Jasial S, Hu Y, Bajorath J. Determining the Degree of Promiscuity of Extensively Assayed Compounds. PLoS One. 2016;11(4):e0153873.

48. Ho TT, Tran QT, Chai CL. The polypharmacology of natural products. Future Med Chem. 2018;10(11):1361-8.

49. Koeberle A, Werz O. Multi-target approach for natural products in inflammation. Drug Discov Today. 2014;19(12):1871-82.

50. Khedgikar V, Kushwaha P, Gautam J, Verma A, Changkija B, Kumar A, Sharma S, Nagar GK, Singh D, Trivedi PK, et al. Withaferin A: a proteasomal inhibitor promotes healing after injury and exerts anabolic effect on osteoporotic bone. Cell Death Dis. 2013;4:e778.

51. Kumar R, Nayak D, Somasekharan SP. SILAC-based quantitative MS approach reveals Withaferin A regulated proteins in prostate cancer. J Proteomics. 2021;247:104334.

52. Kashyap D, Jakhmola S, Tiwari D, Kumar R, Moorthy N, Elangovan M, Bras NF, Jha HC. Plant derived active compounds as potential anti SARS-CoV-2 agents: an in-silico study. J Biomol Struct Dyn. 2021:1-22.

53. Tomita T, Wadhwa R, Kaul SC, Kurita R, Kojima N, Onishi Y. Withanolide Derivative 2,3-Dihydro-3beta-methoxy Withaferin-A Modulates the Circadian Clock via Interaction with RAR-Related Orphan Receptor alpha (RORa). J Nat Prod. 2021;84(7):1882-8.

54. Austin CP, Battey JF, Bradley A, Bucan M, Capecchi M, Collins FS, Dove WF, Duyk G, Dymecki S, Eppig JT, et al. The knockout mouse project. Nat Genet. 2004;36(9):921-4.

55. Hopkins AL. Network pharmacology: the next paradigm in drug discovery. Nat Chem Biol. 2008;4(11):682-90.
56. Barabasi AL, Oltvai ZN. Network biology: understanding the cell's functional organization. Nat Rev Genet. 2004;5(2):101-13.
57. Sun X, Ou Z, Chen R, Niu X, Chen D, Kang R, Tang D. Activation of the p62-Keap1-NRF2 pathway protects against ferroptosis in hepatocellular carcinoma cells. Hepatology. 2016;63(1):173-84.
58. Fan QW, Cheng CK, Nicolaides TP, Hackett CS, Knight ZA, Shokat KM, Weiss WA. A dual phosphoinositide-3-kinase alpha/mTOR inhibitor cooperates with blockade of epidermal growth factor receptor in PTEN-mutant glioma. Cancer Res. 2007;67(17):7960-5.
59. Eichhorn PJ, Gili M, Scaltriti M, Serra V, Guzman M, Nijkamp W, Beijersbergen RL, Valero V, Seoane J, Bernards R, et al. Phosphatidylinositol 3-kinase hyperactivation results in lapatinib resistance that is reversed by the mTOR/phosphatidylinositol 3-kinase inhibitor NVP-BEZ235. Cancer Res. 2008;68(22):9221-30.
60. Junttila TT, Akita RW, Parsons K, Fields C, Lewis Phillips GD, Friedman LS, Sampath D, Sliwkowski MX. Ligand-independent HER2/HER3/PI3K complex is disrupted by trastuzumab and is effectively inhibited by the PI3K inhibitor GDC-0941. Cancer Cell. 2009;15(5):429-40.
61. Knight ZA, Lin H, Shokat KM. Targeting the cancer kinome through polypharmacology. Nat Rev Cancer. 2010;10(2):130-7.
62. Tonra JR, Deevi DS, Corcoran E, Li H, Wang S, Carrick FE, Hicklin DJ. Synergistic antitumor effects of combined epidermal growth factor receptor and vascular endothelial growth factor receptor-2 targeted therapy. Clin Cancer Res. 2006;12(7 Pt 1):2197-207.
63. Tol J, Koopman M, Cats A, Rodenburg CJ, Creemers GJ, Schrama JG, Erdkamp FL, Vos AH, van Groeningen CJ, Sinnige HA, et al. Chemotherapy, bevacizumab, and cetuximab in metastatic colorectal cancer. N Engl J Med. 2009;360(6):563-72.
64. Su Z, Yang Z, Xie L, DeWitt JP, Chen Y. Cancer therapy in the necroptosis era. Cell Death Differ. 2016;23(5):748-56.
65. Bebber CM, Muller F, Prieto Clemente L, Weber J, von Karstedt S. Ferroptosis in Cancer Cell Biology. Cancers (Basel). 2020;12(1).
66. Koren E, Fuchs Y. Modes of Regulated Cell Death in Cancer. Cancer Discov. 2021;11(2):245-65.
67. Eling N, Reuter L, Hazin J, Hamacher-Brady A, Brady NR. Identification of artesunate as a specific activator of ferroptosis in pancreatic cancer cells. Oncoscience. 2015;2(5):517-32.
68. Yang WS, SriRamaratnam R, Welsch ME, Shimada K, Skouta R, Viswanathan VS, Cheah JH, Clemons PA, Shamji AF, Clish CB, et al. Regulation of ferroptotic cancer cell death by GPX4. Cell. 2014;156(1-2):317-31.
69. Roh JL, Kim EH, Jang HJ, Park JY, Shin D. Induction of ferroptotic cell death for overcoming cisplatin resistance of head and neck cancer. Cancer Lett. 2016;381(1):96-103.
70. Efimova I, Catanzaro E, Van der Meeren L, Turubanova VD, Hammad H, Mishchenko TA, Vedunova MV, Fimognari C, Bachert C, Coppieters F, et al. Vaccination with early ferroptotic cancer cells induces efficient antitumor immunity. J Immunother Cancer. 2020;8(2).
71. Bordini J, Morisi F, Cerruti F, Cascio P, Camaschella C, Ghia P, Campanella A. Iron Causes Lipid Oxidation and Inhibits Proteasome Function in Multiple Myeloma Cells: A Proof of Concept for Novel Combination Therapies. Cancers (Basel). 2020;12(4).
72. Schon M, Bong AB, Drewniok C, Herz J, Geilen CC, Reifenberger J, Benninghoff B, Slade HB, Gollnick H, Schon MP. Tumor-selective induction of apoptosis and the small-molecule immune response modifier imiquimod. J Natl Cancer Inst. 2003;95(15):1138-49.
73. Tatsuta T, Sugawara S, Takahashi K, Ogawa Y, Hosono M, Nitta K. Cancer-selective induction of apoptosis by leczyme. Front Oncol. 2014;4:139.
74. Hartung F, Stuhmer W, Pardo LA. Tumor cell-selective apoptosis induction through targeting of K(V)10.1 via bifunctional TRAIL antibody. Mol Cancer. 2011;10:109.

75. Stockwell BR, Jiang X. A Physiological Function for Ferroptosis in Tumor Suppression by the Immune System. Cell Metab. 2019;30(1):14-5.

76. Habib E, Linher-Melville K, Lin HX, Singh G. Expression of xCT and activity of system xc(-) are regulated by NRF2 in human breast cancer cells in response to oxidative stress. Redox Biol. 2015;5:33-42.

77. Chun P. Histone deacetylase inhibitors in hematological malignancies and solid tumors. Arch Pharm Res. 2015;38(6):933-49.

78. Gore SD. Combination therapy with DNA methyltransferase inhibitors in hematologic malignancies. Nat Clin Pract Oncol. 2005;2 Suppl 1:S30-5.

79. Balasubramanyam K, Altaf M, Varier RA, Swaminathan V, Ravindran A, Sadhale PP, Kundu TK. Polyisoprenylated benzophenone, garcinol, a natural histone acetyltransferase inhibitor, represses chromatin transcription and alters global gene expression. J Biol Chem. 2004;279(32):33716-26.

80. Gajer JM, Furdas SD, Grunder A, Gothwal M, Heinicke U, Keller K, Colland F, Fulda S, Pahl HL, Fichtner I, et al. Histone acetyltransferase inhibitors block neuroblastoma cell growth in vivo. Oncogenesis. 2015;4:e137.

81. Wang YM, Gu ML, Meng FS, Jiao WR, Zhou XX, Yao HP, Ji F. Histone acetyltransferase p300/CBP inhibitor C646 blocks the survival and invasion pathways of gastric cancer cell lines. Int J Oncol. 2017;51(6):1860-8.

82. Zille M, Kumar A, Kundu N, Bourassa MW, Wong VSC, Willis D, Karuppagounder SS, Ratan RR. Ferroptosis in Neurons and Cancer Cells Is Similar But Differentially Regulated by Histone Deacetylase Inhibitors. eNeuro. 2019;6(1).

83. Wang Y, Yang L, Zhang X, Cui W, Liu Y, Sun QR, He Q, Zhao S, Zhang GA, Wang Y, et al. Epigenetic regulation of ferroptosis by H2B monoubiquitination and p53. EMBO Rep. 2019;20(7):e47563.

84. Pfister NT, Prives C. Chromatin dysregulation by mutant p53. Oncotarget. 2016;7(21):29875-6.

85. Pfister NT, Fomin V, Regunath K, Zhou JY, Zhou W, Silwal-Pandit L, Freed-Pastor WA, Laptenko O, Neo SP, Bargonetti J, et al. Mutant p53 cooperates with the SWI/SNF chromatin remodeling complex to regulate VEGFR2 in breast cancer cells. Genes Dev. 2015;29(12):1298-315.

86. Winczura A, Zdzalik D, Tudek B. Damage of DNA and proteins by major lipid peroxidation products in genome stability. Free Radic Res. 2012;46(4):442-59.

87. Pra D, Franke SI, Henriques JA, Fenech M. Iron and genome stability: an update. Mutat Res. 2012;733(1-2):92-9.

88. Tost J. Engineering of the epigenome: synthetic biology to define functional causality and develop innovative therapies. Epigenomics. 2016;8(2):153-6.

89. Brown CW, Chhoy P, Mukhopadhyay D, Karner ER, Mercurio AM. Targeting prominin2 transcription to overcome ferroptosis resistance in cancer. EMBO Mol Med. 2021;13(8):e13792.

90. Sharpless NE, Sherr CJ. Forging a signature of in vivo senescence. Nat Rev Cancer. 2015;15(7):397-408.

91. Hernandez-Segura A, de Jong TV, Melov S, Guryev V, Campisi J, Demaria M. Unmasking Transcriptional Heterogeneity in Senescent Cells. Curr Biol. 2017;27(17):2652-60 e4.

92. Kaur J, Farr JN. Cellular senescence in age-related disorders. Transl Res. 2020;226:96-104.

93. Halasa M, Wawruszak A, Przybyszewska A, Jaruga A, Guz M, Kalafut J, Stepulak A, Cybulski M. H3K18Ac as a Marker of Cancer Progression and Potential Target of Anti-Cancer Therapy. Cells. 2019;8(5).

94. Tasselli L, Xi Y, Zheng W, Tennen RI, Odrowaz Z, Simeoni F, Li W, Chua KF. SIRT6 deacetylates H3K18ac at pericentric chromatin to prevent mitotic errors and cellular senescence. Nat Struct Mol Biol. 2016;23(5):434-40.

95. De Cecco M, Criscione SW, Peckham EJ, Hillenmeyer S, Hamm EA, Manivannan J, Peterson AL, Kreiling JA, Neretti N, Sedivy JM. Genomes of replicatively senescent cells undergo global epigenetic changes leading to gene silencing and activation of transposable elements. Aging Cell. 2013;12(2):247-56.

96. Rocha A, Dalgarno A, Neretti N. The functional impact of nuclear reorganization in cellular senescence. Brief Funct Genomics. 2021.

97. Li Q, Zhang Y, Fu J, Han L, Xue L, Lv C, Wang P, Li G, Tong T. FOXA1 mediates p16(INK4a) activation during cellular senescence. EMBO J. 2013;32(6):858-73.

98. Flor AC, Wolfgeher D, Wu D, Kron SJ. A signature of enhanced lipid metabolism, lipid peroxidation and aldehyde stress in therapy-induced senescence. Cell Death Discov. 2017;3:17075.

99. Cozzi A, Orellana DI, Santambrogio P, Rubio A, Cancellieri C, Giannelli S, Ripamonti M, Taverna S, Di Lullo G, Rovida E, et al. Stem Cell Modeling of Neuroferritinopathy Reveals Iron as a Determinant of Senescence and Ferroptosis during Neuronal Aging. Stem Cell Reports. 2019;13(5):832-46.

100. Sun Y, Zheng Y, Wang C, Liu Y. Glutathione depletion induces ferroptosis, autophagy, and premature cell senescence in retinal pigment epithelial cells. Cell Death Dis. 2018;9(7):753.

101. Myrianthopoulos V, Evangelou K, Vasileiou PVS, Cooks T, Vassilakopoulos TP, Pangalis GA, Kouloukoussa M, Kittas C, Georgakilas AG, Gorgoulis VG. Senescence and senotherapeutics: a new field in cancer therapy. Pharmacol Ther. 2019;193:31-49.

102. Kang TW, Yevsa T, Woller N, Hoenicke L, Wuestefeld T, Dauch D, Hohmeyer A, Gereke M, Rudalska R, Potapova A, et al. Senescence surveillance of pre-malignant hepatocytes limits liver cancer development. Nature. 2011;479(7374):547-51.

103. Wajapeyee N, Serra RW, Zhu X, Mahalingam M, Green MR. Oncogenic BRAF induces senescence and apoptosis through pathways mediated by the secreted protein IGFBP7. Cell. 2008;132(3):363-74.

104. Iannello A, Thompson TW, Ardolino M, Lowe SW, Raulet DH. p53-dependent chemokine production by senescent tumor cells supports NKG2D-dependent tumor elimination by natural killer cells. J Exp Med. 2013;210(10):2057-69.

105. Borrelli C, Ricci B, Vulpis E, Fionda C, Ricciardi MR, Petrucci MT, Masuelli L, Peri A, Cippitelli M, Zingoni A, et al. Drug-Induced Senescent Multiple Myeloma Cells Elicit NK Cell Proliferation by Direct or Exosome-Mediated IL15 Trans-Presentation. Cancer Immunol Res. 2018;6(7):860-9.

106. Soto-Gamez A, Quax WJ, Demaria M. Regulation of Survival Networks in Senescent Cells: From Mechanisms to Interventions. J Mol Biol. 2019;431(15):2629-43.

107. Coppe JP, Desprez PY, Krtolica A, Campisi J. The senescence-associated secretory phenotype: the dark side of tumor suppression. Annu Rev Pathol. 2010;5:99-118.

108. Andre T, Meuleman N, Stamatopoulos B, De Bruyn C, Pieters K, Bron D, Lagneaux L. Evidences of early senescence in multiple myeloma bone marrow mesenchymal stromal cells. PLoS One. 2013;8(3):e59756.

109. Berenstein R, Blau O, Nogai A, Waechter M, Slonova E, Schmidt-Hieber M, Kunitz A, Pezzutto A, Doerken B, Blau IW. Multiple myeloma cells alter the senescence phenotype of bone marrow mesenchymal stromal cells under participation of the DLK1-DIO3 genomic region. BMC Cancer. 2015;15:68.

110. Guo J, Zhao Y, Fei C, Zhao S, Zheng Q, Su J, Wu D, Li X, Chang C. Dicer1 downregulation by multiple myeloma cells promotes the senescence and tumor-supporting capacity and decreases the differentiation potential of mesenchymal stem cells. Cell Death Dis. 2018;9(5):512.

111. Liao C, Xiao Y, Liu L. The Dynamic Process and Its Dual Effects on Tumors of Therapy-Induced Senescence. Cancer Manag Res. 2020;12:13553-66.

112. Amor C, Feucht J, Leibold J, Ho YJ, Zhu C, Alonso-Curbelo D, Mansilla-Soto J, Boyer JA, Li X, Giavridis T, et al. Senolytic CAR T cells reverse senescence-associated pathologies. Nature. 2020;583(7814):127-32.

113. Hernandez-Segura A, Nehme J, Demaria M. Hallmarks of Cellular Senescence. Trends Cell Biol. 2018;28(6):436-53.

Academic CV

Academic Curriculum Vitae

Personal Details

Last name: Logie
First name: Emilie
Home address: Goudenregenlaan 4, bus 14
                   2610 Wilrijk
                   Belgium
Date of Birth: 21/01/1994
Nationality: Belgian
Email: emilie_l@hotmail.be

Career & Education Overview

October 2017 – October 2021

University of Antwerp, PPES laboratory
PhD in Biomedical Sciences
- PhD thesis entitled: 'Targeting multiple myeloma through protein kinase and ferroptosis therapeutics'.
  Promotor: Prof. Dr. Wim Vanden Berghe

September 2015 – June 2017

University of Antwerp
Master degree in Biomedical Sciences
- Major: Molecular and cellular biomedical sciences
- Minor: Research
- Master thesis entitled: 'Characterization of the 3' UTRs of transcripts localized in sympathetic neuron axons.'
  Promotor: Prof. Dr. Antonella Riccio
Graduated with greatest honors

September 2012 – June 2015

University of Antwerp
Bachelor degree in Biomedical Sciences
- Bachelor thesis entitled: 'Neuroglobine en zijn rol in neuroprotectie.'
  Promotor: Prof. Dr. Sylvia Dewilde
Graduated with great honors

September 2006 – June 2012   *Royal Athenaeum Mortsel*
                                Majors: Sciences, Latin
                                Graduated with great honors

International Research Stays

February 2019   Short-term scientific mission 'Epigenetic editing of PLAU dependent cancer metastasis'

                                University Medical Center Groningen
                                Groningen, The Netherlands
                                Department Medical Biology
                                Epigenetic Editing Research group of Prof. Dr. Marianne Rots

March 2018   Practical course 'Epigenetic Chemical Biology – Computational methods in drug design'.

                                Kadir Has University
                                Istanbul, Turkey

November 2017 – June 2018   Research stay abroad for the completion of my master thesis entitled 'Characterization of the 3'UTRs of transcripts localized in sympathetic neuron axons'.

                                University College London
                                London, United Kingdom
                                MRC Laboratory for Molecular Cell Biology
                                Research Group of Prof. Dr. Antonella Riccio

Educational Activities / Student Supervision

• Supervisor bachelor thesis of Zufaisa Van Cooten, titled: 'Evaluatie van epigenetische respons op UV blootstelling in huid keratinocyt cellen' – 'Evaluation of epigenetic responses to UV exposure in skin keratinocyte cells'. Academic year 2017-2018 (Biomedical sciences, University of Antwerp)

• Supervisor bachelor thesis of Ana de Abreu, titled: 'Evaluation of epigenetic response to ferroptosis modulator compounds in cancer cells'. Academic year 2017-2018 (Biomedical sciences, University of Antwerp)

- Supervisor bachelor thesis of Michelle Zurek, titled: 'Onderzoek naar epigenetische effecten van abiotische stress' - 'Investigating epigenetic effects of abiotic stress'. Academic year 2018-2019 (Biomedical sciences, University of Antwerp)

- Supervisor bachelor thesis of Jöran Melis, titled: 'Ferroptose-afhankelijke veranderingen in genexpressie van epigenetische enzymen in multiple myeloma'. Academic year 2019-2020 (Biomedical sciences, University of Antwerp)

- Supervisor bachelor thesis of Elise Vrebosch, titled: 'Bepalen van ferroptose-geïnduceerde veranderingen in globale DNA (hydroxy)methylatie'. Academic year 2019-2020 (Biomedical sciences, University of Antwerp)

- Supervision bachelor thesis Nele Pauwels and Anouk Peymen, titled: 'FOXA1 als mogelijke DNA-schade merker voor ferroptotische celdood in multiple myeloma' – 'FOXA1 as a potential DNA damage marker for ferroptotic cell death in multiple myeloma'. Academic year 2020-2021 (Biomedical sciences, University of Antwerp).

- Supervisor master research internship of Alexander Rdzen, titled: 'Experimental methods that validate ferroptotic stress in different cell lines.' Academic year 2018-2019 (Biochemistry and biotechnology, University of Antwerp)

- Supervisor master thesis of Niels Van Herck, titled: 'Determining LSD1-specific effects of Withaferin A treatment in breast cancer and multiple myeloma cell lines'. Academic year 2017-2018 (Biochemistry and biotechnology, University of Antwerp)

- Supervisor master thesis Joris Van Meenen, titled: 'Transcriptional regulation of ferroptosis in multiple myeloma: FOXA1 as a novel long-term biomarker for ferroptosis'. Academic year 2019-2020 (Biochemistry and biotechnology, University of Antwerp)

- Supervisor master thesis Louis Maes, titled: 'Characterization of the role of chromatin remodeler FOXA1 in ferroptotic cell death'. Academic year 2020-2021 (Biochemistry and biotechnology, University of Antwerp).

Teaching Experience

November 2018 – December 2018	Teaching assistant in 'Biostatistics' course for bachelor students

Educational Guidance / Popularization of Science

March 2018	Participation in PRESS>SPEAK competition aiming to popularize scientific communication

Additional Scientific Training & Certificates

2020	Creating a scientific poster University of Antwerp
2019	Writing academic papers in English University of Antwerp
2019	Introductory course to NGS data analysis University of Antwerp
2019	BePA Proteomics Workshop: What can proteomics do for you? University of Ghent
2018	Introduction to (u)HPLC and LC-MS University of Antwerp
2018	Data science using R and the Tidyverse University of Antwerp
2018	Computational methods in drug design Kadir Has University, Istanbul
2017	FELASA Category C attest University of Antwerp

Scientific Grants and Awards

2017 - 2021	FWO PhD Fellowship fundamental research
2019	COST STSM Travel Grant
2017	FBD Faculty Award of the University of Antwerp for top graduated master student

Conferences

June 2021	European Association for Cancer Research
	Poster Presentation
	Online
	'Withaferin A inhibits multiple myeloma survival by covalent targeting of BTK in glucocorticoid-resistant MM1 cells'
September 2019	Josep Carreras Leukaemia Research Institute (IJC)
	Poster presentation
	Barcelona, Spain
	'Multiple myeloma therapy response to GC involves epigenetic modulation of B-cell receptor signaling'
February 2019	Belgian Association for Cancer Research (BACR)
	Poster presentation
	Antwerp, Belgium
	'Polypharmacological sensitization of heterogenous multidrug resistant cancers by the steroidal withanolide Withaferin A'
November 2018	Systems Epigenetics
	Poster presentation
	Amsterdam, The Netherlands
	'Epigenetic modulation of B-cell receptor signaling in glucocorticoid-induced multiple myeloma resistant'

Publication list

1. **Logie, E.**; Perez-Novo C, Driesen A, Van Vlierberghe P, Vanden Berghe W. Phosphocatalytic Kinome Activity Profiling of Apoptotic and Ferroptotic Agents in Multiple Myeloma Cells. Int. J. Mol. Sci. - *In revision*

2. **Logie, E**; Van Puyvelde, B; Cuypers, B; Schepers, A; Berghmans, H; Verdonck, J; Laukens, K; Godderis, L; Dhaenens, M; Deforce, D; Vanden Berghe, W. Ferroptosis Induction in Multiple Myeloma Cells Triggers DNA Methylation and Histone Modification Changes Associated with Cellular Senescence. Int. J. Mol. Sci. Nov 2021, 22, 12234. doi: 10.3390/ijms222212234

3. **Logie E**, Chirumamilla CS, Perez-Novo C, Shaw P, Declerck K, Palagani A, Rangarajan S, Cuypers B, De Neuter N, Mobashar Hussain Urf Turabe F, Kumar Verma N, Bogaerts A, Laukens K, Offner F, Van Vlierberghe P, Van Ostade X, Berghe WV. Covalent Cysteine Targeting of Bruton's Tyrosine Kinase (BTK) Family by Withaferin-A Reduces Survival of Glucocorticoid-Resistant Multiple Myeloma MM1 Cells. Cancers (Basel). 2021 Mar 31;13(7):1618. doi: 10.3390/cancers13071618. PMID: 33807411; PMCID: PMC8037275.

4. Kumar N, Perez-Novo C, Shaw P, **Logie E**, Privat-Maldonado A, Dewilde S, Smits E, Berghe WV, Bogaerts A. Physical plasma-derived oxidants sensitize pancreatic cancer cells to ferroptotic cell death. Free Radic Biol Med. 2021 Apr;166:187-200. doi: 10.1016/j.freeradbiomed.2021.02.026. Epub 2021 Feb 23. PMID: 33636332.

5. **Logie E**, Vanden Berghe W. Tackling Chronic Inflammation with Withanolide Phytochemicals-A Withaferin a Perspective. Antioxidants (Basel). 2020 Nov 10;9(11):1107. doi: 10.3390/antiox9111107. PMID: 33182809; PMCID: PMC7696210.

6. Pintatum A, Maneerat W, **Logie E**, Tuenter E, Sakavitsi M, Pieters L, Vanden Berghe W, Sripisut T, Dechatai S, Laphookhieo S. In vitro anti-inflammatory, anti-oxidant, and cytotoxic activities of four *Curcuma* species and the isolation of compounds from *Curcuma aromatica* Rhizome, biomolecules (2020), doi: https://doi.org/10.3390/biom10050799.

7. Pintatum A, Laphookhieo S, **Logie E**, Vanden Berghe W, Maneerat W. Chemical Composition of Essential Oils from Different Parts of Zingiber kerrii Craib and Their Antibacterial, Antioxidant, and Tyrosinase Inhibitory Activities , biomolecules (2020), doi: https://doi.org/10.3390/biom10020228.

8. Delgado-Hernández R, Hernández-Balmaseda I, Rodeiro-Guerra I, Cesar Rodriguez Gonzalez J, De Wever O, **Logie E**, Declerck K, Pérez-Novo C, Vanden Berghe W. Anti-angiogenic effects of mangiferin and mechanism of action in metastatic melanoma, Melanoma Research (2020), doi: https://doi.org/10.1097/cmr.0000000000000647.

9. Hassannia B, **Logie E**, Vandenabeele P, Vanden Berghe T, Vanden Berghe W. Withaferin A: from Ayurvedic folk medicine to preclinical anti-cancer drug, Biochemical Pharmacology (2019), doi: https://doi.org/10.1016/j.bcp.2019.08.004.

10. Van Acker ZP, Van Raemdonck GA, **Logie E**, Baggerman G, Vanden Berghe W, Ponsaerts P, and Dewilde S. Connecting the dots in the neuroglobin-protein interaction network of an unstressed and ferroptotic cell death neuroblastoma model, Cells (2019), doi: https://doi.org/10.3390/cells8080873

11. Crerar H, Bodkin-Clarke C, Scott-Solomon E, Andreassi C, Hazbon M, **Logie E,** Cano-Jaimez M, Gaspari M, Kuruvilla Rejji, and Riccio A. Regulation of NGF signalling by an axonal non-coding mRNA, Neuron (2019), doi: https://doi.org/10.1016/j.neuron.2019.02.011.